University of Alberta

Experimental and Numerical Investigation of the Fast-SAGD Process

by

Hyundon   Shin   ©

A thesis
submitted to the Faculty of Graduate Studies and Research
in partial fulfillment of the requirements for the degree of

Doctor of Philosophy

in

Petroleum Engineering

Department of Civil and Environmental Engineering

Edmonton, Alberta

Spring 2006

Canada

University of Alberta

Library Release Form

Name of Author: Hyundon Shin

Title of Thesis: Experimental and Numerical Investigation of the Fast-SAGD Process

Degree: Doctor of Philosophy

Year this Degree Granted: 2006

Permission is hereby granted to the University of Alberta Library to reproduce single copies of this thesis and to lend or sell such copies for private, scholarly or scientific research purposes only.

The author reserves all other publication and other rights in association with the copyright in the thesis, and except as herein before provided, neither the thesis nor any substantial portion thereof may be printed or otherwise reproduced in any material form whatever without the author's prior written permission.

#201-2010 Ulster Road,
NW, Calgary, Alberta
Canada T2N 4C2

Date: _____

DEDICATION

To

my wife Hyeong-Mee and my daughter Erin

and

my families

ABSTRACT

The SAGD process has been tested in the field, and is now in a commercial stage in Western Canadian oil sands areas. The Fast-SAGD method can partly solve the drilling difficulty and reduce costs in a SAGD operation requiring paired parallel wells one above the other. This method also enhances the thermal efficiency in the reservoir.

In this research, the reservoir parameters and operating conditions for the SAGD and Fast-SAGD processes are investigated by numerical simulation in the three Alberta oil sands areas. Scaled physical model experiments, which are operated by an automated process control system, are conducted under high temperature and high pressure conditions.

The results of the study indicate that the shallow Athabasca-type reservoir, which is thick with high permeability (high k×h), is a good candidate for SAGD application, whereas Cold Lake- and Peace River-type reservoirs, which are thin with low permeability, are not as good candidates for conventional SAGD implementation.

The simulation results indicate improved energy efficiency and productivity in most cases for the Fast-SAGD process; in those cases, the project economics were enhanced compared to the SAGD process. Both Cold Lake- and Peace River-type reservoirs are good candidates for a Fast-SAGD application rather than a conventional SAGD application. This new process demonstrates improved efficiency and lower costs for extracting heavy oil from these important reservoirs.

A new economic indicator, called simple thermal efficiency parameter (STEP), was developed and validated to evaluate the performance of a SAGD project. STEP is based on cumulative steam-oil ratio (CSOR), calendar day oil rate (CDOR) and recovery factor (RF) for the time prior to the steam-oil ratio (SOR) attaining 4. STEP can be used as a financial metric quantitatively as well as qualitatively for this type of thermal project.

An automated process control system was set-up and validated, and has the capability of controlling and handling steam injection processes like the steam-assisted gravity drainage process.

The results of these preliminary experiments showed the overall cumulative oil production to be larger in the Fast-SAGD case, but end-point CSOR to be lower in the SAGD case. History matching results indicated that the steam quality was as low as 0.3 in the SAGD experiments, and even lower in the Fast-SAGD experiments after starting the CSS.

ACKNOWLEDGEMENTS

TABLE OF CONTENTS

LIST OF TABLES

LIST OF FIGURES

NOMENCLATURE

α Thermal diffusivity, $L^2 t^{-1}$

ν_s Kinematic viscosity of oil at steam temperature, $L^2 t^{-1}$

ϕ Fractional porosity

ρ Density, ML^{-3}

B_3 Dimensionless constant

c Kozeny constant

C Specific heat, $L^2 t^{-2} T^{-1}$

D Average particle diameter, L

g Gravity, Lt^{-2}

h Reservoir height, L

H Enthalpy, $L^2 t^{-2}$

K Permeability, L^2

m Parameter which depends on oil viscosity temperature curve T_R and T_S

ΔP Pressure drop, $ML^{-1} t^{-2}$

q Flow rate, $L^3 t^{-1}$

Q Heat, kJ

R Scaling factor

S_o Fractional oil saturation

S_{or} Residual oil saturation

ΔS_o $S_o - S_{or}$

T Temperature, T

t Time,   t

$t*$ Dimensionless time

V Volume, L^3

w Reservoir width, L

Subscripts

ac	accumulated
an	annulus
cn	contour
gl	glass bead
gn	generated
L	liquid
ls	lost
m	model
o	oil
p	prototype
pd	produced
s	steam
st	stainless steel
v	vapour
w	water

Abbreviations

SAGD	Steam-Assisted Gravity Drainage
CDOR	Calendar Day Oil Rate
C-NPV	Compensated-Net Present Value
CSF	Cyclic Steam Flooding
CSOR	Cumulative Steam-Oil Ratio
CSS	Cyclic Steam Stimulation
NCG	Non-Condensable Gas
NPV	Net Present Value
RF	Recovery Factor
ROR	Rate of Return

SF	Steam Flooding
SS	Steam Stimulation
STEP	Simple Thermal Efficiency Parameter
SOR	Steam-Oil Ratio
VW	Vertical Well
HW	Horizontal Well

1 INTRODUCTION

1.1 Overview

Alberta's oil sands contain the largest crude bitumen resource in the world, approximately 259 billion cubic meters of initial in-place and 27.7 billion cubic meters of remaining established reserves (AEUB, 2004). In situ recovery methods have to be used to recover over 80% of these reserves; therefore research to find more effective in situ recovery methods is encouraged.

The steam-assisted gravity drainage (SAGD) process has been tested in the field, and is now in a commercial stage in Western Canadian oil sands areas (Butler, 2001). Recent research studies have been conducted (Butler, 2002) not only for reducing the steam production costs but also for enhancing heat efficiency of the SAGD process.

The Fast-SAGD recovery process invented by Polikar et al. (2000), combining the SAGD and cyclic steam stimulation (CSS) processes, helps to propagate sideways the steam chamber formed by SAGD. As Fast-SAGD only requires additional single horizontal wells beside the SAGD well pair, this method can partly solve the difficulty of drilling two horizontal wells one exactly above the other thereby reducing costs, and also enhance the thermal efficiency in the reservoir.

1.2 Statement of Problem

The SAGD process is an attractive in-situ recovery method for oil sands development. The thick and high permeability clean sands are perfect conditions for SAGD application. Also, the reservoirs with no overburden gas cap, no over/under burden water zone, and a fining upward depositional environment which may reduce heat losses in the reservoir are ideal for a SAGD operation. Reservoir heterogeneity will affect negatively the SAGD performance.

1

The SAGD performance can be improved by reducing the number of horizontal wells and the injected steam quantity or by enhancing the thermal efficiency in the reservoir. The Fast-SAGD can partly solve the drilling difficulty, reduce costs in a SAGD operation requiring paired parallel wells one above the other, and also enhance the thermal efficiency in the reservoir (Polikar et al., 2000).

The success of the SAGD process in the field depends on two main factors: reservoir parameters and operating conditions. It is very important to find out the most favorable SAGD conditions under the various reservoir parameters.

Numerical simulation results show that the Fast-SAGD process performance is better than that of the conventional SAGD (Polikar et al., 2000). Physical model experiments using suitable scaling procedures are needed for verification of the numerical findings. Low-pressure models cannot scale high temperature and high pressure phenomena, such as rock-fluid interaction, fluid properties, and gas solubility; therefore high pressure and high temperature scaled models are better for explaining the steam injection process.

Conducting high pressure and high temperature scaled model experiments is very difficult as there are so many variables such as steam quality, injection rate, and pressure to be controlled. An automated process control system will operate these high temperature and high pressure experiments safely and in real time.

1.3 Objectives and Scope of Research

This study will investigate the Fast-SAGD process mechanisms both by numerical and experimental methods. Numerical simulation studies will provide the most favourable operating conditions by conducting sensitivity analysis. The main objectives of this research include:

1) Screening of the reservoir parameters and defining the most favourable operating conditions for the SAGD and the Fast-SAGD processes;

2

2) Development of an experimental facility using an automated control system for the steam injection processes; and

3) Investigation of SAGD and Fast-SAGD recovery mechanisms at high temperature and high pressure conditions.

For performing the sensitivity studies of the SAGD and Fast-SAGD processes, a simple economic indicator will be introduced to evaluate SAGD and Fast-SAGD performance.

To develop a high temperature and high pressure experimental apparatus having an automated process control system, validation experiments will be conducted under high temperature and high pressure conditions.

Numerical simulation results of a field scale are used to design the scaled physical model, and the laboratory scale numerical simulation results will be compared with the experimental results.

1.4 Methodology of Research

To achieve the research objectives, the following methodologies will be used:

1) conduct numerical simulation studies for three oil sands areas in Alberta; Athabasca, Cold Lake, and Peace River areas. Reservoir parameters as well as operating conditions will be reviewed.

2) develop a simple economic indicator, STEP, to evaluate SAGD performance. STEP will be correlated with NPV and calculated based on production performance data from published studies in which SAGD related simulations were performed for validation.

3) design an automated process control system and conduct validation experiments for high temperature and high pressure conditions. Four key features of this new experimental facility – steam quality measurement, production cooling constraints,

3

oil-cut determination, and production pressure control – will be validated by using this advanced process control system in cylindrical core models.

4) Conduct scaled physical experiments for 2-dimensional SAGD and Fast-SAGD models. Experimental results will be analyzed, steam chamber shapes will be generated using thermocouple temperature data, and experimental results for SAGD and Fast-SAGD will be compared. Thereafter, experimental results will be compared with numerical simulation results.

4

2 LITERATURE REVIEW

2.1 Geological features in Alberta oil sands deposits

There are many reports on the Alberta oil sands geology (Mossop, 1980, Mossop et al., 1981, Wightman et al., 1989). The Alberta oil sands deposits are mainly contained in the Lower Cretaceous sands. These deposits are located in three geographic areas: Athabasca, Cold Lake, and Peace River (Figure 2.1). The bitumen was originally emplaced as a lighter hydrocarbon which has subsequently undergone significant in situ degradation following migration from some distant source area. The main features of the Alberta oil sands are their unconsolidated nature, high permeability, high oil viscosity and the fact that they are water-wet. Table 2.1 shows geological features in Canadian oil sands areas.
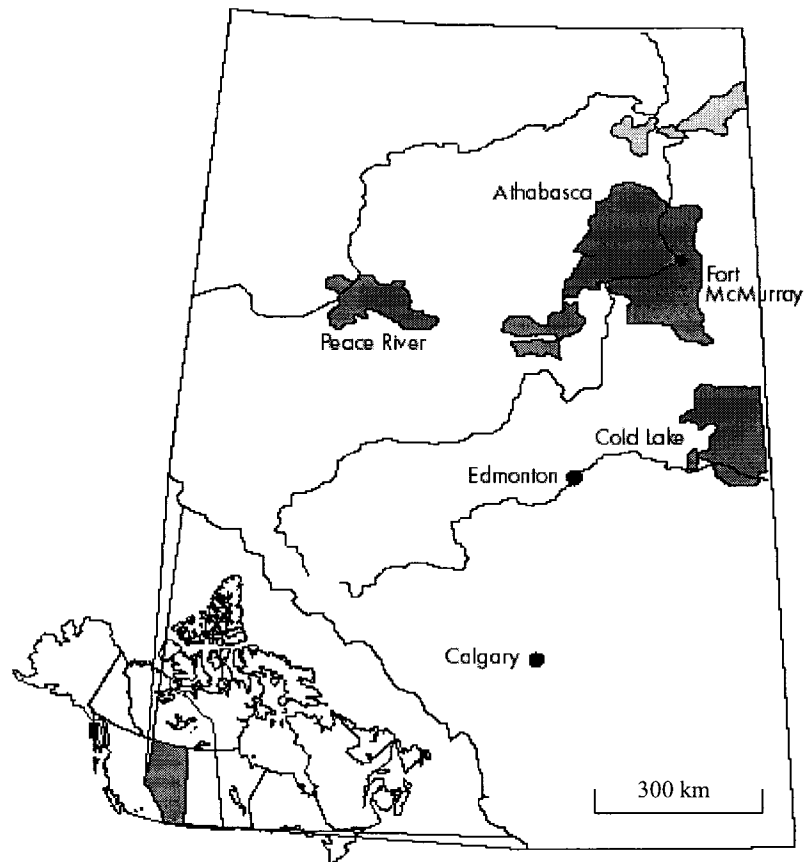
Figure 2.1: Alberta oil sands areas

5

Table 2.1: Geological features in Canadian oil sands areas (modified from Wightman et al., 1989)

Oil sands area	Formation		Depth (m)	Average thickness (m)	Density (°API)	Average porosity (%)	Depositional environment
Atha-basca	Grand Rapids	Upper	200~400	9	8	30	Shoreline and Shallow Marine
		Middle	230~430	5	8	30	
		Lower	270~470	6	8	30	
	Wabiskaw/ McMurray	Mine-able	0~120	38	8~10	29	Continental to Marine Shelf
		In-situ	80~750	19	8~10	28	
Cold Lake	Grand Rapids	Upper	275~500	6	11~15	30	Continental to Marine Shoreline
		Lower	325~525	12	9~12	31	
	Clearwater		375~500	12	10~11	30	Marine Shoreline
	Wabiskaw / McMurray		425~600	5	10~12	25	Marine Shelf / Continental
Peace River	Bluesky/ Gething		460~760	14	9	24	Estuarine to Shallow Marine

6

2.1.1 Athabasca area

Athabasca is the largest of the Cretaceous oil sands deposit in Alberta. It is the only deposit with surface mineable reserves. All of the reserves are contained within the McMurray formation which averages between 40 and 60 m in thickness. Porosity varies between 25 and 35 percent, and oil saturations of 10 to 18 weight percent are very common (Mossop et al., 1981).

The reservoir varies from surface to 750 m in depth. Overall, the vertical sedimentological succession represents an evolution from predominantly continental, fluvial, and floodplain environments to a shoreline estuarine complex as a result of rising sea level. The Grand Rapids formation was deposited in a high-energy, wave-dominated shoreline setting. Because of the original high-energy depositional environment, reservoirs tend to be clean and have good permeability and porosity. Bitumen pore-space saturation ranges from 40~70%, distributed through zones of net pay which vary from 5 to 25 m in thickness and lie at depths of 200 to 470 m (Wightman et al., 1989).

2.1.2 Cold Lake area

The Cold Lake oil sands deposit contains reserves in three formations starting from the bottom: McMurray, Clearwater, and Grand Rapids. Reservoir depths vary between 275 and 600 m. The McMurray formation consists of very fine to medium grained quartzose sands with associated shales. Individual reservoirs are of limited lateral extent. In this area, the McMurray formation is interpreted as being dominantly fluvial in origin. The Clearwater formation consists of nearshore marine sands and associated marine shales. Because the marine sands in the Clearwater interval tend to be laterally extensive and relatively free of internal heterogeneities, they constitute amongst the most attractive reservoirs for in situ recovery. The Grand Rapids formation at Cold Lake consists of interbedded sands and shales, deposited in mixed nearshore marine and continental environments. Despite the fact that the Grand Rapids formation contains the majority of the reserves at Cold Lake, the various reservoirs are not as continuous or homogenous as

7

those in the underlying Clearwater formation, and thus not as amendable to in situ recovery (Mossop et al., 1981)

2.1.3 Peace River area

Reserves in the Peace River oil sands are contained in the Gething-Bluesky interval, which is correlative with the McMurray-Wabiskaw zone in the Athabasca area. Bitumen within this area is trapped in an updip pinchout of the Cretaceous Gething-Bluesky formations against Mississippian carbonates. These sediments are interpreted to be dominantly continental in the southeastern area, becoming more marine towards the northwest. Within the Peace River oil sands deposit, the thickest and most continuous oil sands are found in tidal channel complexes, but high oil saturations are also found in widespread shoreline and shallow marine sands. The reservoir varies in depth from 300 to 750 m with zones of net pay up to 30 m thick. Within the oil leg of the reservoir, hydrocarbon emplacement appears to have halted or inhibited diagenesis relative to the underlying waterbearing sands in which authigenic clays are much more abundant (Wightman et al., 1989).

2.1.4 Geological characteristics in oil sands development

More than 90 percent of the Cretaceous oil sands reserves in Alberta are too deeply buried to be considered potentially recoverable by established surface mining techniques. Thus, there is a processing need to develop technologies capable of recovering bitumen in situ. Table 2.2 illustrates the primary bitumen-bearing horizons within the Cretaceous stratigraphic sequence.

The McMurray formation has had a history of shallow burial, and cementation and other diagenetic processes have had minimal impact on the sand texture. It is because the sediment is not consolidated, with no cementing agent to strengthen the material that the deposits are called oil sands, not sandstones. Another consequence of the sands'

8

unconsolidated character is that, in a flowing in situ well, special precautions must be taken to prevent production of the sand grains along with the oil (Mossop, 1980).

Perhaps the single most characteristic feature of the Alberta oil sands, and almost certainly the most fortunate, is that the grains are water-wet or hydrophilic (Mossop, 1980). The oil in the pores is not in direct contact with the mineral grains. Rather, each grain is surrounded by a thin film of water beyond which, in the center of the pore, is the oil. This hydrophilic tendency of the oil sands is fortunate because the hot water extraction process used in the mining operation would not work if the grains were other than water-wet. If the oil sands were oil wet, the interfacial forces between the bitumen and the quartz would be such that hot water extraction would not be possible (Takamura, 1985)

Table 2.2: Table of formations illustrating the primary oil sands and heavy oil horizons in Alberta (Wightman et al., 1989)

9
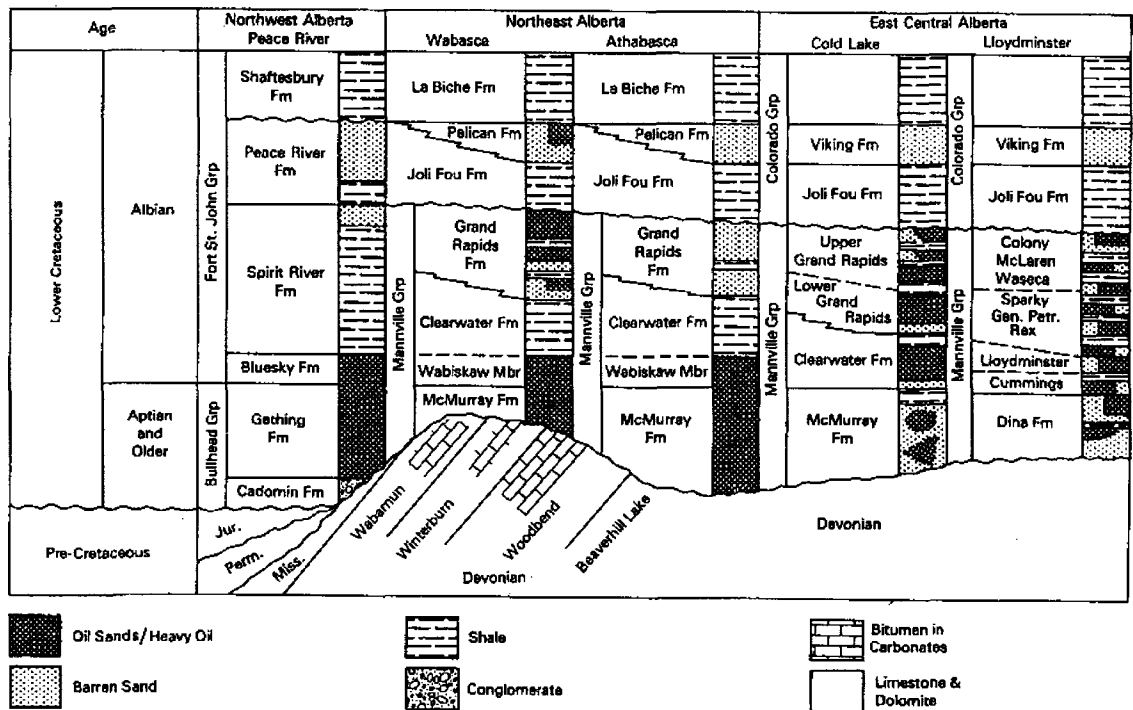
2.2 In-situ recovery methods for oil sands development

The Alberta oil sands have an average density of 10° API, average porosity of 30%, and favorable reservoir thickness (Table 2.1). The reservoirs in the Athabasca area may be mineable for shallow depths up to 85 m, but the reservoirs in the other areas must be recovered only by in-situ recovery methods. Even though there has been bitumen recovery from primary production (or cold production), it is very popular to inject steam for recovering high viscosity oil sands like the Canadian oil sands because the native viscosity of the bitumen at reservoir conditions is in excess of 100,000 cp. Once the temperature is increased to 200°C, the bitumen viscosity is reduced to several centipoises (Figure 2.2). At this temperature, the bitumen is mobilized and can flow easily to the production well. Cyclic Steam Stimulation (CSS) and Steam-Assisted Gravity Drainage (SAGD) have been used as the main in-situ recovery methods for the Canadian oil sands development.
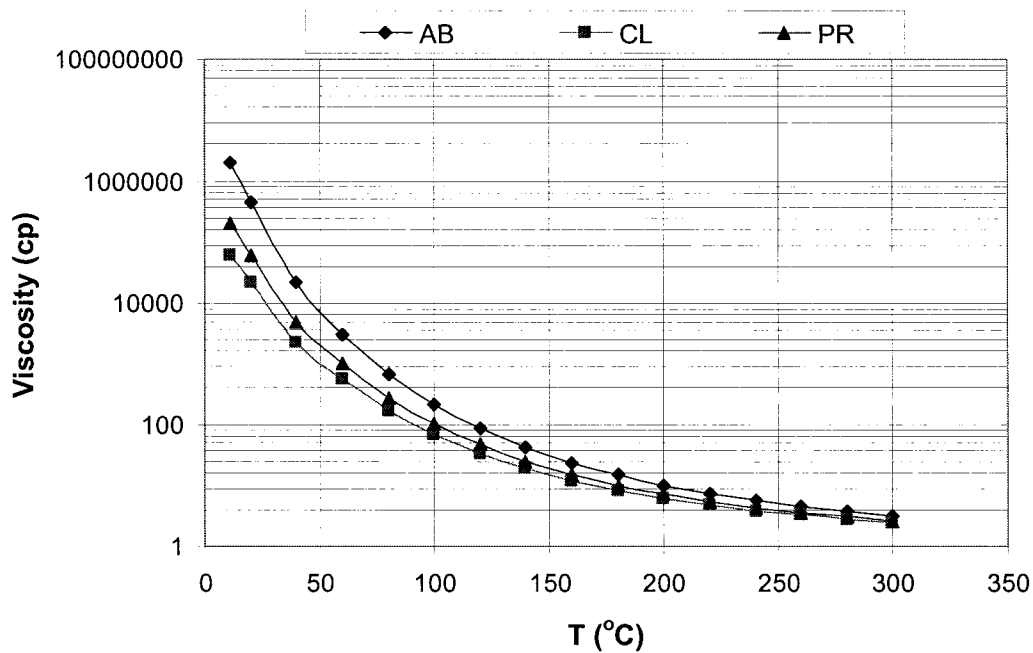
Figure 2.2: Typical viscosities of bitumen (sources: AB from Law et al., 2000; CL from Gong et al., 2002; PR generated from Glandt and Malcolm, 1991)

10

According to Batycky (1997), the choice of the in-situ recovery method depends on reservoir parameters (Table 2.3). CSS could be applied in reservoir qualities with as low as 1 Darcy permeability and in net sands as thin as 10 m. SAGD needs very clean sands of greater than 5 Darcy permeability and in reservoirs thicker than 20 m. Cold production, because of its non-thermal nature, can be applied in clean sands as thin as 2 m.

CSS and SAGD can be applied to recover bitumens with viscosities in excess of 100,000 cp. Cold production can be applied to produce heavy oil with viscosities of up to 10,000 cp. CSS and cold production, being strongly dependent on solution gas drive, favor higher gas-oil ratios (GOR).

Generally, deeper reservoirs favor CSS. SAGD can be operated in quite shallow depths. SAGD gives the highest production rate and ultimate recovery compared to CSS and cold production.

Table 2.3: Comparison of in-situ recovery processes (modified from Batycky, 1997)

	CSS	SAGD	Cold Production
Permeability (D)	> 1	> 5	> 2
Net pay (m)	10	20	3
Oil saturation (wt%)	9	12	9
Viscosity (cp)	Bitumen (>100,000)	Bitumen (>100,000)	Heavy oil (10,000)
Reservoir depth	moderate	shallow	moderate
GOR	High	Low	High
Thief zone tolerance	< 5m	little	little
Production rate (m³/d/well)	10	100	10
CSOR	4	3~4	-
Recovery factor	20~25%	40~50%	5~15%
Oil sands area to be applied	Cold Lake	Athabasca Peace River*	Cold Lake, Athabasca, Peace River

* Pressure Cycle Steam Drive is included in SAGD category

11

2.3 SAGD application for oil sands development

2.3.1 Mechanisms of the SAGD Process

The birth of SAGD was possible due to the development of horizontal drilling technology that enhanced productivity. The conventional SAGD, introduced by Butler et al. (1981) as shown in Figure 2.3, uses two horizontal wells, one injector and one producer. Usually the producer is placed as low in the reservoir as possible, and the injector is located several meters above the producer. The injected steam will reduce the bitumen viscosity, and then the heated bitumen and condensed steam will flow down into the producer by gravity force.

Figure 2.3: SAGD concept (after Butler et al., 1981)

There are two different kinds of drainage in the SAGD process, one is ceiling drainage and the other is slope drainage (Edmunds et al., 1988). The ceiling drainage can be seen during the steam chamber rise period. The injected steam rises to the top of the reservoir and reduces bitumen viscosity, and the mobile bitumen and condensed water flow down into the producer. During this process, there will be counter-current flow, which results in

12

emulsification of the condensed steam and bitumen, and the emulsification increases the viscosity of the flowing fluid inside the steam chamber, consequently reducing bitumen recovery efficiency (Chung and Butler, 1988). The ceiling drainage tends to happen largely when the steam is injected into the bottom of the reservoir. The slope drainage will happen during the steam chamber growth period, but mainly at the time when the steam chamber propagates sideways horizontally. During the slope drainage, the heated bitumen and condensed steam flow down into the producer along the steam chamber perimeter. The ceiling drainage plays an important role during the early stages of the SAGD process, while the slope drainage plays a more important role during the late stages of the SAGD process.

SAGD can be operated with relatively low pressure, about 400-900 kPa (Edmunds and Chhina, 2001). Recently Kisman (2003) investigated the lifting of bitumen to the surface during a low pressure SAGD operation. In his research, a two-stage lift system called ELift was designed to provide low subcool values at low pressures. The SAGD process, in which gravity is the main recovery mechanism, is not affected by pressure difference between injector and producer. A low pressure SAGD operation can reduce the steam-oil ratio (SOR) due to higher energy efficiency, however this results in lower productivity. Low pressure operation requires narrower well pattern, but less steam, therefore the proper operating pressure has to be decided after considering the number of wells and steam quantity needed in the operation.

2.3.2 Key features in the SAGD process

For successful SAGD performance, two important conditions should be satisfied. One is the preheating period, and the other is the steam trap control. The preheating period is needed to establish heat communication between injector and producer. The steam trap control is one way to enhance thermal efficiency by keeping steam inside of the reservoir instead of producing live steam along with the bitumen.

13

2.3.2.1 Preheating period

It is essential for an effective SAGD operation to reduce the viscosity of the bitumen between injector and producer. This procedure of establishing heat communication between two wells at the initial stage of SAGD is called the start-up period, and can be done by circulating steam into both injector and producer. The wells act as hot fingers in the reservoir, and heating is by conduction.

There have been other trials to establish communication between the wells, two of which are given below. The cyclic steam injection method was used to establish heat communication at the Senlac SAGD project in Saskatchewan (Boyle et al., 2003). Steam was injected with high pressure for three cycles. The other one is the solvent injection method used to establish communication between injection and production wells at the Hilda Lake SAGD project in Cold Lake (Donnelly, 1999). Because there is some initial injectivity, a solvent can be injected into the formation and followed with steam. It is therefore not necessary to rely entirely on thermal conduction to establish communication. The pre-heating period is affected by permeability and the spacing between injector and producer (I/P spacing). Usually, less than 6 months is reasonable for field SAGD projects. The I/P spacing of 5~10 m will help establish heat communication in 6 months or less (Shin and Polikar, 2004).

For a long horizontal well, the heat communication should be established along the entire length. If the initial heat communication is established partially instead of over the entire length of the well, it will have a negative effect on SAGD performance (Edmunds and Gittins, 1993)

2.3.2.2 Steam trap control

SAGD requires that the steam chamber be kept well drained, so that liquid does not accumulate over the producer, but neither is live steam produced (Edmunds, 2000). Steam trap control is the way to maintain the producing fluids' temperature just below the

14

saturation temperature of the steam (called sub-cool). It is implemented to prevent or reduce steam production from the reservoir. This steam trap control should result in keeping all the latent heat generated by the steam inside the reservoir and producing only bitumen and condensed hot water. Generally, values in the range of 5~40°C sub-cool are accepted for a SAGD operation (Edmunds, 2000, Ito and Suzuki, 1996). Ito and Suzuki (1996) investigated the required sub-cool to minimize steam-oil ratio (SOR), and suggested that 40°C of sub-cool is proper for a SAGD operation. If the sub-cool is increased, oil production is decreased but SOR is reduced. When sub-cool exceeds 50°C, the production is decreased and SOR is also increased.

2.3.3 Overview of SAGD operating facilities

SAGD operating facilities include four major parts: water treatment, steam generation, production separation, and production treatment (Figure 2.4). The treated water is fed to a steam generator to produce steam. The steam passes through a separator so that nearly 100 percent quality steam can be injected. The saturated blowdown water is exchanged for heat recovery and disposed of in a deep well. The produced fluids go to a separator to produce gas, bitumen, and water. The produced water is treated for recycling or disposal (Donnelly, 1997, O'Rourke et al., 1997). The following details of process facilities are for the typical SAGD projects (Gulf Canada, 2001).

2.3.3.1 Water treatment

There are two water sources for feeding the steam generator, one being raw water from an aquifer and the other recycling produced water from the production wells. During this treatment, water will be chlorinated, filtered, softened and chemically treated to increase the pH, remove free oxygen and prevent iron deposition. Such a water treatment system can provide approximately 90 percent of the water requirements by recycling produced water.

15

2.3.3.2 Steam generation

The steam generation equipment produces the 100 percent quality steam required for injection into the reservoir. This is achieved by producing 80 percent quality steam from a once-through steam generator, and removing the free water from the steam in a high-pressure steam separator to produce 100 percent quality steam. The boiler feed water is boosted and preheated by the produced water. The high-pressure, feed-water pumps supply boiler feed water to the steam generators at 13,000 kPa, producing an 80 percent quality steam at 11,000 kPa.

2.3.3.3 Separation of bitumen, water and gas

A high temperature separator is used in order to achieve the density differential necessary for a good separation of water and bitumen. Bitumen from the separator, which contains less than 5 percent water, flows into the desalter. A bitumen product with less than 0.5 % by weight basic sediment and water is obtained. Water from the inlet separator exchanges heat with boiler feed water in the produced water trim cooler. Produced gas from the well site separator is routed to the produced gas recovery system where the entrained steam is condensed and the gas is recovered for use as fuel gas.

2.3.3.4 Production treatment

The majority of the oil is separated from the water by gravity in the skim tank. The oil content in the produced water leaving the inlet separator is reduced from 2,000 to 200 ppm in the skim tank. The produced water flows to an induced gas flotation device to reduce the oil content to about 20 ppm. The oil coalescing filters reduce the remaining oil contents to approximately 1 ppm, which is suitable for boiler feed water.

16
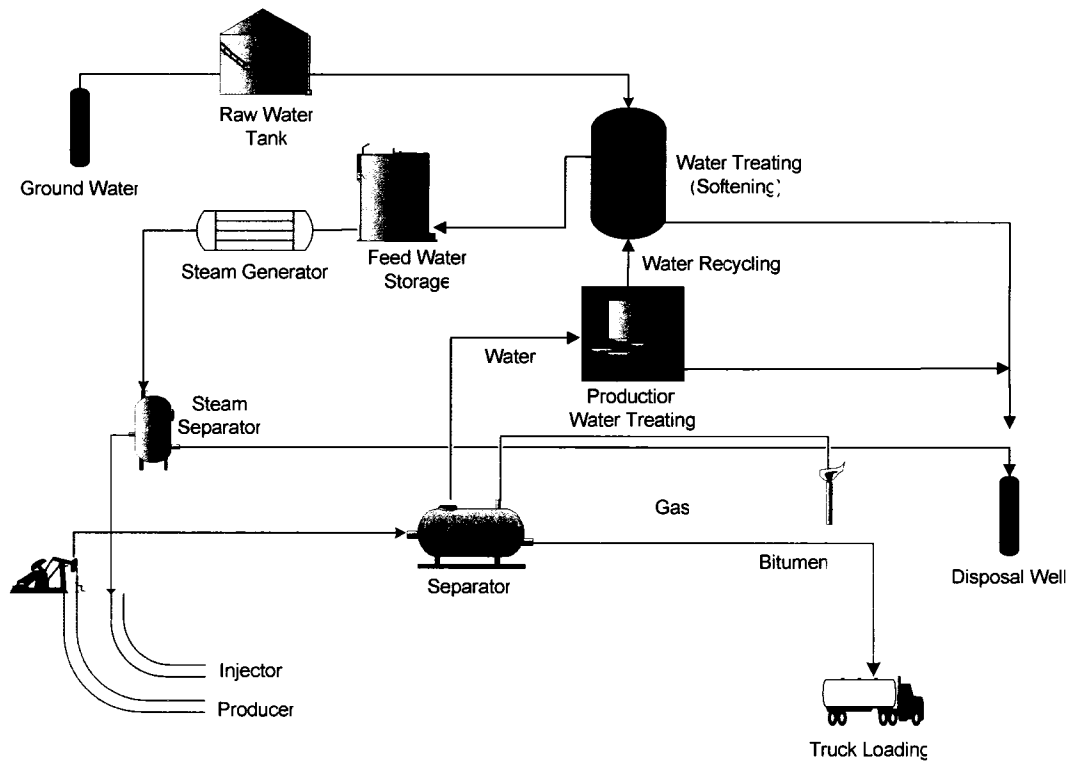
Figure 2.4: SAGD project facilities schematics (modified from Donnelly, 1997)

2.3.4 Sensitivity study of the SAGD process

The success of the SAGD process in the field depends on two main factors: reservoir parameters and operating conditions.

2.3.4.1 Reservoir parameters

Reservoir parameters, which can not be controlled, include reservoir thickness, reservoir permeability, bitumen viscosity, reservoir depth, shale barriers in the reservoir, gas zone in the overburden, and water zone in the overburden or underburden.

The thicker the reservoir, the better the thermal efficiency (less heat loss) and the larger the production in the SAGD process (Butler et al., 1981b, Ito et. al., 1998).

17

Higher permeability will result in higher ultimate recovery as well as lower CSOR, which are both favorable for SAGD performance. Sometimes, there may be permeability changes in the vertical direction depending on the depositional environment, and this may alter the recovery performance of the process (Venuto, 1989). A previous study showed that the fining upward depositional environment case gave better SAGD performance compared to the fining downward case (Shin and Polikar, 2004). During the SAGD process, the heated bitumen flows down into the producer as steam is injected, and at that time, more permeable flow paths are required. Therefore, a high permeability near the producer is better for SAGD performance. Also, the low permeability at the top of the reservoir can make the steam propagate into the horizontal direction rather than towards the overburden, therefore, enhancing thermal efficiency.

Water zones in the reservoir result in an inefficient SAGD performance (Singhal et al., 1996, Sugianto and Butler, 1990). However, the presence of a bottom water layer has less impact on oil recovery than when an overlying water layer is present (Doan et al., 1999). Gas cap, which may prevent heat loss to the overburden, is moderately beneficial for the SAGD performance (Good et al., 1997, Kisman et al., 1995). Also, small size shale barriers have a small effect on the SAGD process (Edmunds et al., 1988).

2.3.4.2 Operating conditions

The operating conditions, which can be controlled, include preheating period, the spacing between injector and producer (I/P spacing), steam injection pressure, maximum steam injection rate, and SAGD well pattern spacing.

The preheating period is affected by reservoir permeability and I/P spacing (Shin and Polikar, 2004). As the I/P spacing is related to both the preheating period and permeability, it is important to choose the I/P spacing in such a way that production is increased and the preheating period reduced. Too close an I/P spacing may cause difficulty in drilling, and also the injected steam may flow into the producer if the injected steam pressure is too high, therefore, reducing thermal efficiency.

18

Operating pressure (or steam injection pressure) is a very important parameter during the SAGD process because a higher operating pressure means higher steam temperature, therefore more energy is required. In a conventional SAGD operation, the maximum steam injection pressure is usually kept at or slightly above the reservoir pressure.

The SAGD process is operated as a pattern of several parallel horizontal well pairs in the field. A narrower pattern spacing gives lower SOR; however, it needs more wells (Butler, 1985). Therefore the well pattern spacing has to be chosen considering not only energy efficiency but also drilling costs.

2.4 Variations of SAGD Process Enhancements

The conventional SAGD process is a steam injection recovery method that uses two horizontal wells. In the Peace River area, a small pressure differential between adjacent pattern steam chambers was applied to enhance the SAGD process (Hamm and Ong, 1995). A steam drive process can be applied to the SAGD operation once sufficient bitumen mobility has been obtained between steam chambers. This is done by lowering the steam injection pressure in one steam chamber, while maintaining pressure in the adjacent steam chamber.

In contrast, other research has examined ways of reducing the operating costs by reducing the number of horizontal wells and the injected steam quantity or by enhancing the thermal efficiency in the reservoir.

2.4.1 Single Well SAGD

This technology uses a single horizontal well to produce oil instead of two horizontal wells. Steam is injected into insulated tubing and fluids are produced from the annulus (Oballa and Buchanan, 1996). This recovery method is effective where the primary production is high. Even though this method is less economical than conventional SAGD, single well SAGD can be applied in thin reservoirs less than 15 m thick where the dual

19

well SAGD is not effective due to the small thickness of the reservoir (McCormack et al., 1997, Singhal et al., 2000).

2.4.2 Steam and Gas Push (SAGP)

This recovery method was introduced to enhance SAGD efficiency by adding a small amount of non-condensable gases (NCG) such as natural gas or nitrogen (Butler et al., 2000). In laboratory scaled experiments (Butler et al., 2001), it was found that the saving of steam was less for higher oil viscosities.

2.4.3 Expanding Solvent SAGD (ES-SAGD)

This is one of the modifications of the SAGD process combining the benefits of steam and solvents in the recovery of heavy oil and bitumen. In this process, the solvent is injected with steam in a vapour phase, and then the condensed solvent around the interface of the steam chamber dilutes the oil in conjunction with heat, and reduces its viscosity. This method has been successfully field tested, and has resulted in improved oil production and SOR, and lower energy and water requirements as compared to conventional SAGD (Nasr et al., 2003).

2.4.4 Fast-SAGD

The Fast-SAGD recovery process invented by Polikar et al. (2000), combining the SAGD and CSS processes, helps propagate the steam chamber formed by SAGD sideways. As Fast-SAGD only requires an additional well beside the SAGD well pair, this method can partly solve the challenge of drilling the two horizontal wells one exactly above the other and reduce costs in a SAGD operation, and also enhance the thermal efficiency in the reservoir.

2.4.5 SAGD Wind-down

At a certain point during the SAGD process, it is no longer economic to operate SAGD

20

with steam injection due to high SOR. However, the reservoir is still hot and the energy in place can be utilized. The NCG or mixture of NCG and steam injection has been proposed as a wind-down process, which may maintain reservoir pressure and prolong oil production (Zhao et al., 2003).

2.5 Fast-SAGD Process

Fast-SAGD, combining the CSS and SAGD processes, uses offset wells, which are placed horizontally about 50 m away from the SAGD producer (Figure 2.5) and each offset well. These offset wells are operated alternatively as injector and producer. When the steam chamber reaches the top of the reservoir after the SAGD operation has begun, the CSS operation is started at the first offset well. The CSS operation at other offset wells will be started later with a certain schedule after the CSS operation at the first offset well. There are at least two cycles of CSS at the offset wells, and each cycle is composed of three phases: injection period of several months, soak period of a few weeks, and production period of several months. Steam is injected at higher pressure and rate than those used in the SAGD operation, but the pressure is below the fracturing pressure of the formation.

The Fast-SAGD process has the following features (Polikar et al., 2000): a) the CSS operation from the offset well propagates the SAGD steam chamber sideways and also speeds up the recovery of bitumen; b) the high pressure steam injection at the offset well results in enhanced bitumen recovery from the SAGD producer due to steam drive effect caused by pressure difference between the SAGD injector and the offset well; c) the additional steam injection into the SAGD injector after finishing the CSS operation is required to maintain the steam chamber, which has already been expanded by the CSS operation.

In the SAGD process, which generally is operated near the reservoir pressure, thermal expansion will affect petrophysical properties, but in the Fast-SAGD process, in which steam is injected at high pressure, shear dilation can be another important factor (Gong et

21

al., 2002). This type of geomechanical effect was previously observed in CSS process applications in the Cold Lake oil sands (Beattie et al., 1991, Ito and Singhal, 1999).
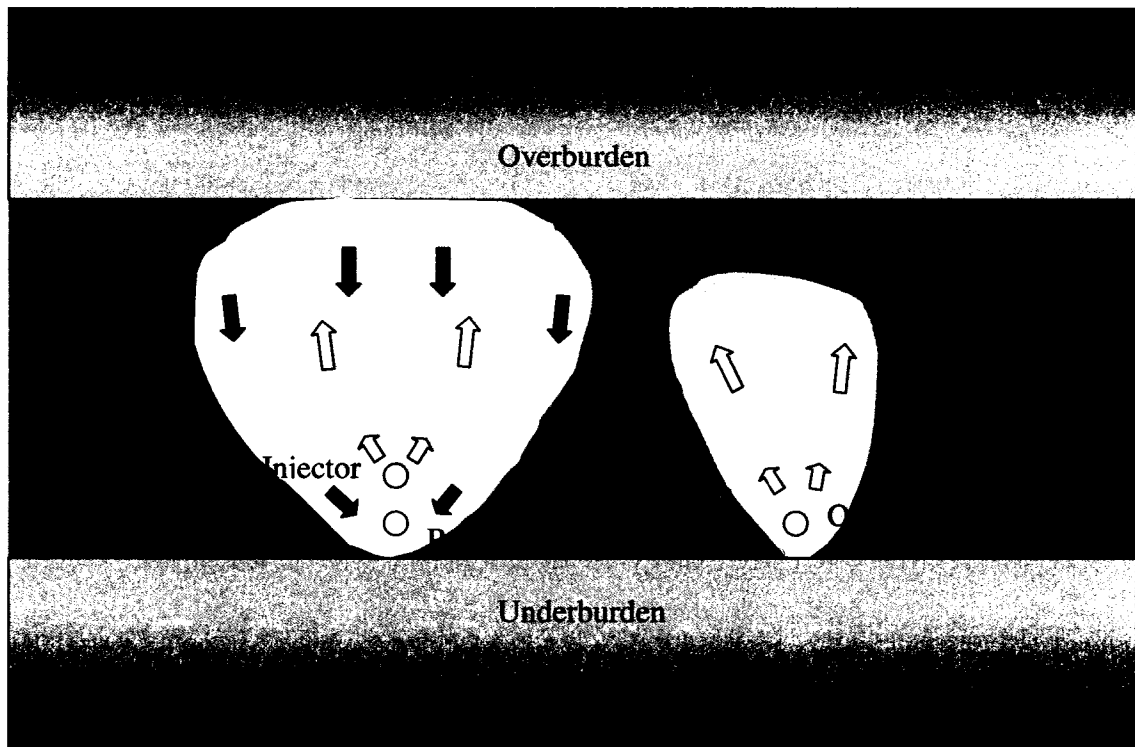
Figure 2.5: Fast-SAGD concept

2.6 Scaling of Physical Modelling

2.6.1 Scaled Model Studies for Steam Injection Processes

The most widely used scaling criteria were presented by Stegemeier et al. (1980) for low-pressure models and by Pujol and Boberg (1972) for high-pressure models. High pressure models use the same fluids as found in the field, so these models may scale the high temperature, high pressure phenomena such as rock-fluid interactions, fluids properties,

22

emulsification, steam distillation, gas solubility, and compressibility effects in a better manner than low pressure models. Low pressure models are easier to build and operate, and may give more accurate temperature and velocity distributions due to improved scaling of the pressure-temperature relationship for saturated steam. These models usually require a fluid with properties different from those of the fluid in the field to satisfy all the criteria considered important. In practice, it is difficult to find fluids that can satisfy these criteria, and compromises must be made as with high-pressure models.

Stegemeier et al. (1980) carried out vacuum model studies for their experiments at pressures well below atmospheric pressure. The results showed that the quantity of steam injected was the most important factor affecting the amount of oil recovered.

Pujol and Boberg (1972) examined the scaling accuracy of laboratory steam flooding models, especially with regard to the scaling of capillary pressure. They found that, for highly viscous oils, accurate scaling of capillary pressure was not crucial. This is because the ratio of capillary to viscous forces was so small that unscaled capillary pressures would have negligible effects on oil recovery.

Farouq Ali and Redford (1977) provided a thorough analysis of notable scaled laboratory thermal recovery studies. They examined the scaling groups derived for steam injection and in-situ combustion processes by various investigators.

Chung and Butler (1988) developed two-dimensional scaled reservoir models to test the SAGD theory. They found approximate agreement with numerical predictions for recovery from the Underground Test Facility.

Kimber et al. (1988) studied new scaling criteria for steam and steam-additive injection experiments. In these studies, five different approaches were adopted, with each approach scaling a selected mechanism of the recovery process while relaxing the remaining mechanisms. They proposed that Pujol and Boberg's procedure is effective for steam only processes where gravity dominates.

23

2.6.2 Scaling Procedure for the SAGD Process

For the scaling of SAGD physical modeling, the dimensional number and time were introduced to scale the model from the SAGD theory development (Butler et al. 1981) and they were able to achieve good agreement between the theoretical results and experimental ones. This scaling procedure gives the same result as Pujol and Boberg's (1972). The dimensional numbers B_3 and t^* should be the same for the model as for the field:

$$B_3 = \left(\sqrt{\frac{kgh}{\phi \Delta S_O \alpha m v_s}} \right)_{field} = \left(\sqrt{\frac{kgh}{\phi \Delta S_O \alpha m v_s}} \right)_{model} \qquad \text{(Equation 2.1)}$$

Since the temperature and pressure will be the same in the model and the field, the only variables that will differ will be "h_{field}" and "h_{model}". Assuming that porosity, saturation, and thermal diffusivity will be the same, then

$$(kh)_{field} = (kh)_{model} \qquad \text{(Equation 2.2)}$$

and the permeability of the sand to be used in the model will be

$$k_{model} = \left(\frac{h_{field}}{h_{model}} \right) k_{field} = R * k_{field} \qquad \text{(Equation 2.3)}$$

From the dimensionless time,

$$t^* = \left(\frac{t}{w} \sqrt{\frac{kg\alpha}{\phi \Delta S_O m v_s h}} \right)_{field} = \left(\frac{t}{w} \sqrt{\frac{kg\alpha}{\phi \Delta S_O m v_s h}} \right)_{model} \qquad \text{(Equation 2.4)}$$

Then, the time in the model will be

$$t_{model} = \left(\frac{h_{model}}{h_{field}} \right)^2 t_{field} = \left(\frac{1}{R^2} \right) * t_{field} \qquad \text{(Equation 2.5)}$$

24

3 NUMERICAL SIMULATIONS FOR THE SAGD PROCESS

3.1 Simulation model

Two-dimensional numerical simulations were performed with CMG's STARS using the petrophysical parameters of the three typical major reservoirs as described in the previous section. The numerical grid size is 1 m in the i and k directions, respectively, and 900 m along the horizontal well (j direction). The reservoir width (i direction) is assumed to be five times the size of the reservoir thickness. The total grid number of the base cases are 151 x 1 x 30 (i, j, k) for Athabasca, 101 x 1 x 20 (i, j, k) for Cold Lake, and 125 x 1 x 25 (i, j, k) for Peace River. The producer is located at the bottom of the reservoir and the injector is 5 to 15 m above the producer (Figure 3.1). No flow boundary but heat loss is assumed at the overburden. Steam injection pressure was set at 10 kPa higher than the production pressure, applying steam trap control.
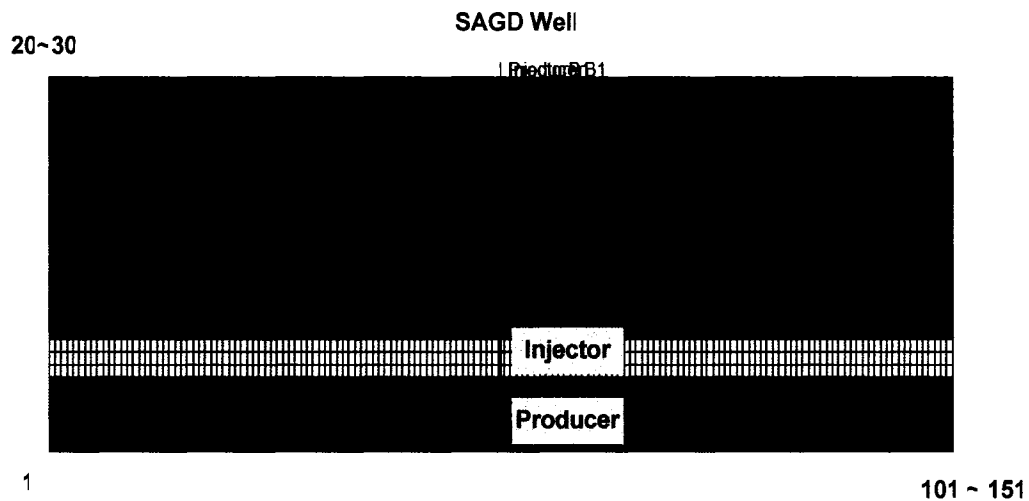
Figure 3.1: Grid system and well location for SAGD base cases

25

3.2 Simulation schemes for the SAGD process

Typical reservoir properties of the three oil sands areas have been set up for the proposed numerical simulations as the base cases (Table 3.1). Athabasca-type (AB) reservoir has the shallowest depth, the thickest reservoir and the highest permeability with highest bitumen viscosity. Cold Lake-type (CL) reservoir has the lowest bitumen viscosity and thinnest reservoir. Peace River-type (PR) reservoir represents the deepest, lowest permeability with middle range bitumen viscosity. Only Athabasca-type reservoir represents a dead oil case. The objective of the simulations is to define the best application of SAGD to each reservoir type.

Simulations were performed to conduct sensitivity analysis for SAGD operating conditions such as preheating period, I/P spacing, steam injection pressure, maximum steam injection rate, and well pattern spacing and also reservoir parameters such as reservoir thickness, reservoir permeability and rock thermal conductivity (Table 3.2). Steam injection pressure was increased starting at the initial reservoir pressure to ensure steam injectivity into the reservoir. The I/P spacing was increased from a minimum of 5 m as a lower value would make the drilling difficult and for avoiding the risk of steam production from the production well. Three cases of rock thermal conductivity were used within the range of sand thermal conductivities (Butler, 1997).

It is very important to find the proper operating conditions for SAGD application under various reservoir conditions. The simulation results have been evaluated to have the lowest cumulative steam-oil ratio (CSOR), highest recovery factor (RF) and highest calendar day oil rate (CDOR). A case which has low CSOR with high CDOR will give a favourable economic case; however if a case has high CSOR with high CDOR or low CSOR with low CDOR, an economic analysis will be required to evaluate the most favourable operating condition.

26

Table 3.1: Reservoir properties for numerical simulation as the base cases

Parameter		Athabasca-type (AB) [1]	Cold Lake-type (CL) [2]	Peace River-type (PR) [3]
Reservoir pressure, kPa		1,500	3,100	4,500
Depth to top of reservoir, m		200	400	600
Reservoir thickness, m		30	20	25
Reservoir width, m		151	101	125
I/P spacing, m		5	10	10
Vertical permeability (K_v), Darcy		2.5	1.25	0.65
Permeability ratio (K_h/K_v)		2	2	3
Porosity		0.35	0.32	0.28
Oil saturation		0.8	0.7	0.8
Oil viscosity, cp	at 12 °C	2,000,000	60,000	200,000
	at steam temp	10	4	4
Methane gas mole fraction		-	0.11	0.15
Capillary pressure		0 kPa		
Rock compressibility [2]		9.6×10^{-6} kPa^{-1}		
Formation heat capacity [2]		2,350 kJ/m^3-K		
Rock thermal conductivity [2]		6.6×10^5 J/m-d- °C		
Oil thermal conductivity [2]		1.15×10^4 J/m-d- °C		
Water thermal conductivity [2]		5.35×10^4 J/m-d- °C		
Gas thermal conductivity [2]		1.4×10^2 J/m-d- °C		

[1] : Law et al. (2000)   [2] : Gong et al. (2002)
[3] : Glandt and Malcolm (1991), Hamm and Ong (1995)

Finally, in order to obtain the most favourable operation conditions, net present value (NPV) calculations were performed for each simulation case to take the time factor into account. The economic calculations assume that a project is cost-effective as long as the instantaneous SOR is below a value of 4, therefore, the CSOR, CDOR and RF in the simulation results are the values corresponding to the instantaneous SOR. As the main purpose of this study is to find the most favourable operation condition, a simple

27

economic evaluation was introduced instead of full scale economic evaluation. Capital costs have not been taken into account, assuming that these are similar for all the cases studied in each reservoir type. However, only drilling costs (assuming three million dollars for a SAGD well pair and one million dollars for a single well) have been considered in the comparison of the SAGD and Fast-SAGD cases because they have different well patterns which will affect the project economics. NPV calculations only considered the cost of steam ($5/bbl) and the price of bitumen ($20/bbl) at a 10% discount rate per year.

Table 3.2: Numerical simulation conditions for sensitivity studies of the SAGD process

Parameters		Athabasca-type (AB)	Cold Lake-type (CL)	Peace River-type (PR)
1) Operating conditions				
Steam injection pressure, kPa (Steam temperature, $^{\circ}$C)		1,500 (199) 3,000 (234) 4,500 (258)	3,100 (236) 4,500 (258) 6,000 (276)	4,500 (258) 6,000 (276) 7,500 (292)
Max. steam injection rate, m^3/d		400 ~ 1,400	200 ~ 700	300 ~ 1,000
I/P spacing, m		5 ~ 15	5 ~ 15	5 ~ 15
Well pattern spacing, m		60 ~ 210	60 ~ 150	60 ~ 150
2) Reservoir parameters				
Reservoir thickness, m		15, 20, 25, 30		
Reservoir permeability (K$_v$), Darcy		0.625, 1.25, 2.5		
Rock thermal conductivity, J/m-d-$^{\circ}$C	Low	1.4×10^5		
	Middle	3.5×10^5		
	High	6.6×10^5		

28

3.3 Simulation results for Athabasca-type reservoirs

The base case simulation conditions for the Athabasca-type reservoirs are: preheating period of 75 days, I/P spacing of 5 m, operating pressure of 1,500 kPa, maximum steam injection rate of 700 m^3/d, well pattern spacing of 150 m, horizontal well length of 900 m, reservoir thickness of 30 m, reservoir permeability (K_v) of 2.5 Darcy. Table 3.3 shows the simulation results for the Athabasca-type reservoir cases related to eight operating conditions and reservoir parameters. Individual results are given below.

3.3.1 Preheating period

The simulation conditions are: operating pressure of 1,500 kPa, maximum steam injection rate of 700 m^3/d, well pattern spacing of 150 m. Simulation results showed that the proper preheating period is 75 days for an I/P spacing of 5 m, 213 days for an I/P spacing of 10 m, and 458 days is for an I/P spacing of 15 m (Figure 3.2). There is not much enhancement in NPV even if the preheating periods are longer than these periods for each I/P spacing case. The preheating period is related to the oil viscosity and the I/P spacing. The more viscous the oil and the larger the I/P spacing are, the longer the preheating period is. A preheating period of 75 days for an I/P spacing of 5 m is economically adequate for successful SAGD performance.
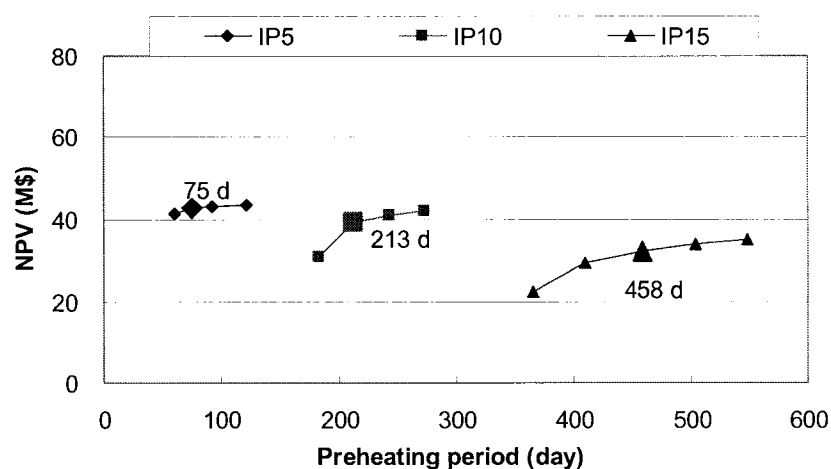
Figure 3.2a: Effect of preheating period on NPV

29
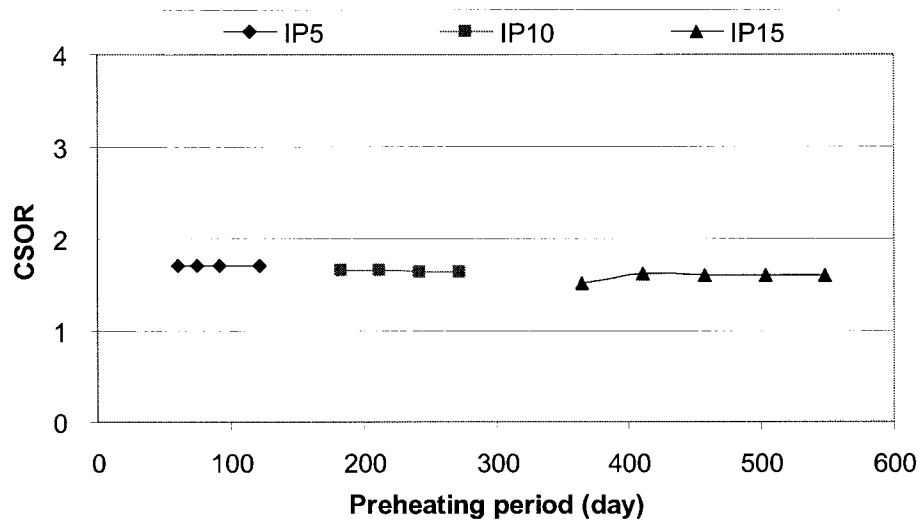
Figure 3.2b: Effect of preheating period on CSOR
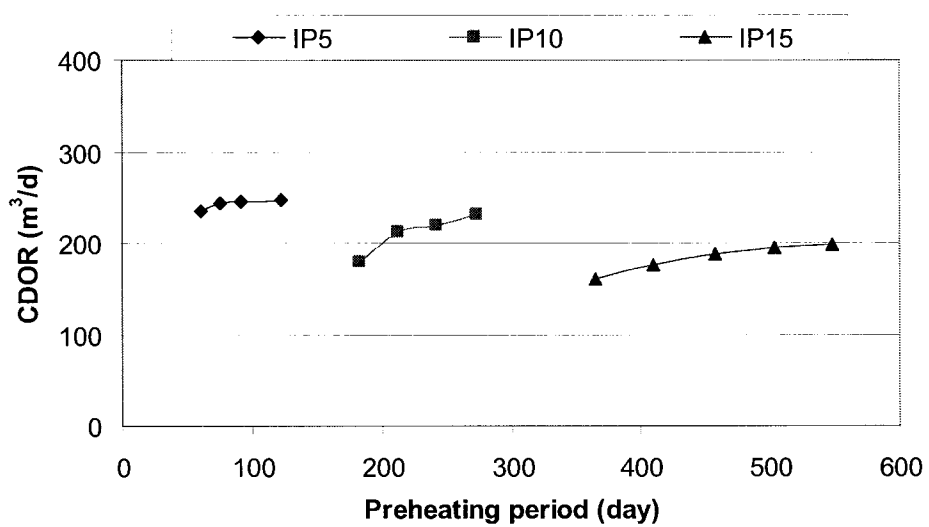
Figure 3.2c: Effect of preheating period on CDOR

30

Table 3.3: SAGD simulation results for Athabasca-type reservoirs

Case	Cum. Production (m^3)	CSOR	CDOR (m^3/d)	RF	NPV (M$)
Preheating period					
60 d	958,334	1.71	236	0.84	41.1
75 d	961,188	1.71	243	0.84	42.8
90 d	957,989	1.71	245	0.84	43.0
120 d	960,818	1.70	247	0.84	43.5
Injector to Producer (I/P) spacing					
5 m	961,188	1.71	243	0.84	42.8
10 m	959,971	1.64	213	0.84	39.0
15 m	960,603	1.61	187	0.84	32.3
Operating pressure					
1,500 kPa	961,188	1.71	243	0.84	42.8
3,000 kPa	949,378	1.99	359	0.83	43.0
4,500 kPa	931,850	2.18	430	0.82	39.5
Max. steam injection rate					
400 m^3	962,856	1.75	196	0.84	31.7
500 m^3	962,974	1.72	223	0.84	38.1
600 m^3	959,957	1.71	239	0.84	41.7
700 m^3	961,188	1.71	243	0.84	42.8
Well pattern spacing					
60 m	383,088	1.38	234	0.83	24.9
90 m	577,074	1.51	235	0.84	32.9
120 m	770,144	1.62	240	0.84	39.0
150 m	953,556	1.70	246	0.84	43.4
180 m	1,135,750	1.79	251	0.83	46.5
210 m	1,314,704	1.87	252	0.82	48.7
Reservoir thickness (well pattern spacing 100 m)					
15 m	282,996	2.17	171	0.74	13.3
20 m	399,762	1.82	210	0.79	21.5
25 m	520,446	1.66	226	0.82	28.6
30 m	638,640	1.54	242	0.84	35.1
Reservoir permeability (K_v)					
0.625 D	356,857	3.24	65	0.31	5.3
1.25 D	907,805	2.06	141	0.80	23.3
2.5 D	961,188	1.71	243	0.84	42.8
Rock thermal conductivity					
Low	973,795	1.68	156	0.85	35.6
Middle	970,017	1.69	208	0.85	41.9
High	961,188	1.71	243	0.84	42.8

31

3.3.2 Injector to Producer spacing

The simulation conditions are: preheating period of 75 days, operating pressure of 1,500 kPa, maximum steam injection rate of 700 m^3/d, well pattern spacing of 150 m. The simulations showed that, as the I/P spacing was increased from 5 m to 15 m, the NPV decreased (Figure 3.3). The CDOR also decreased from 243 m^3/d to 187 m^3/d, and the CSOR decrease was very small, from 1.71 to 1.61. The I/P spacing does not affect the ultimate recovery too much because the recovery factors are 0.84 for all cases. An I/P spacing of the 5 m gave the best SAGD performance: the highest NPV, highest CDOR, and lowest CSOR. High viscosity and permeability of the Athabasca-type reservoir will give more effective SAGD performance with smaller I/P spacing. The narrower the I/P spacing is, the higher the NPV is. However, it is not only difficult to drill the well pairs with a small I/P spacing, but also there is the risk that steam will directly flow into the production well.
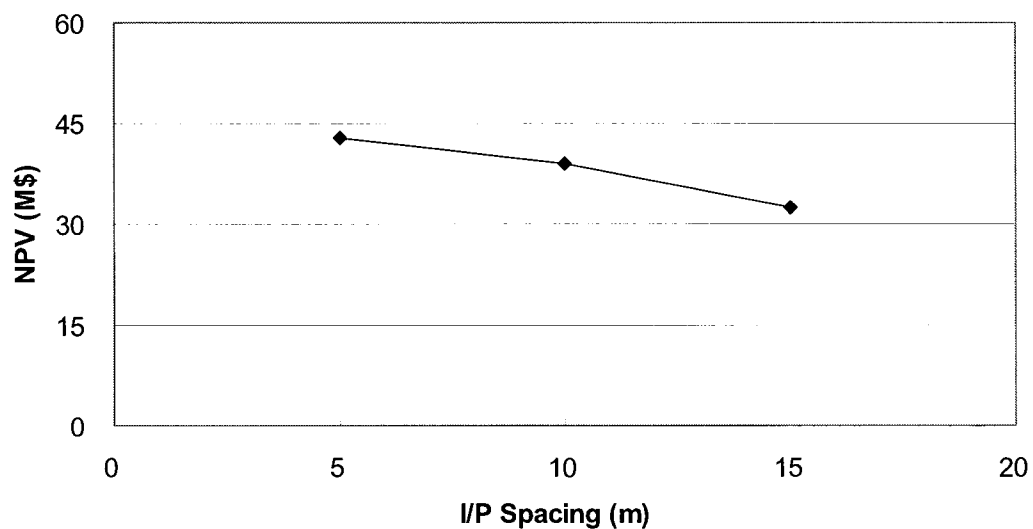
Figure 3.3a: Effect of I/P spacing on NPV
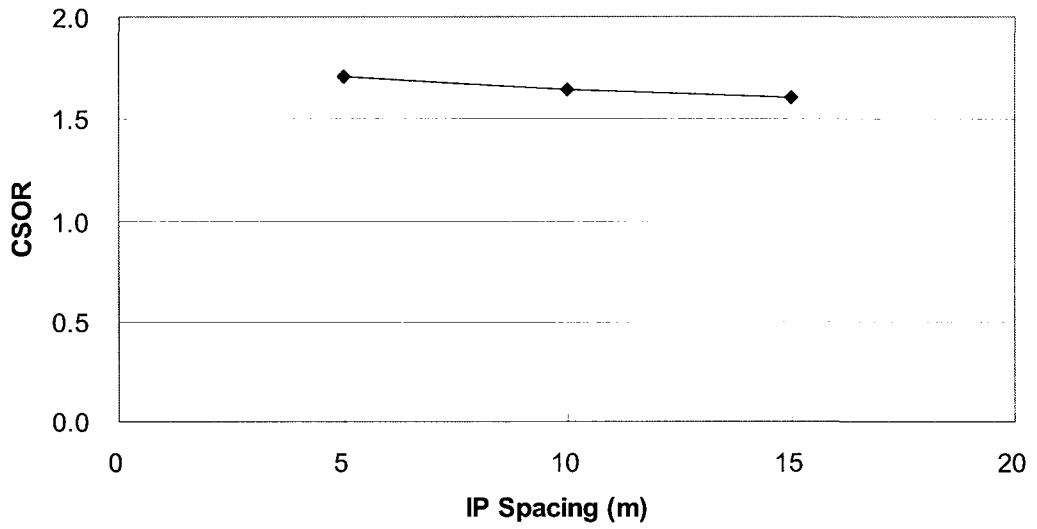
Figure 3.3b: Effect of I/P spacing on CSOR
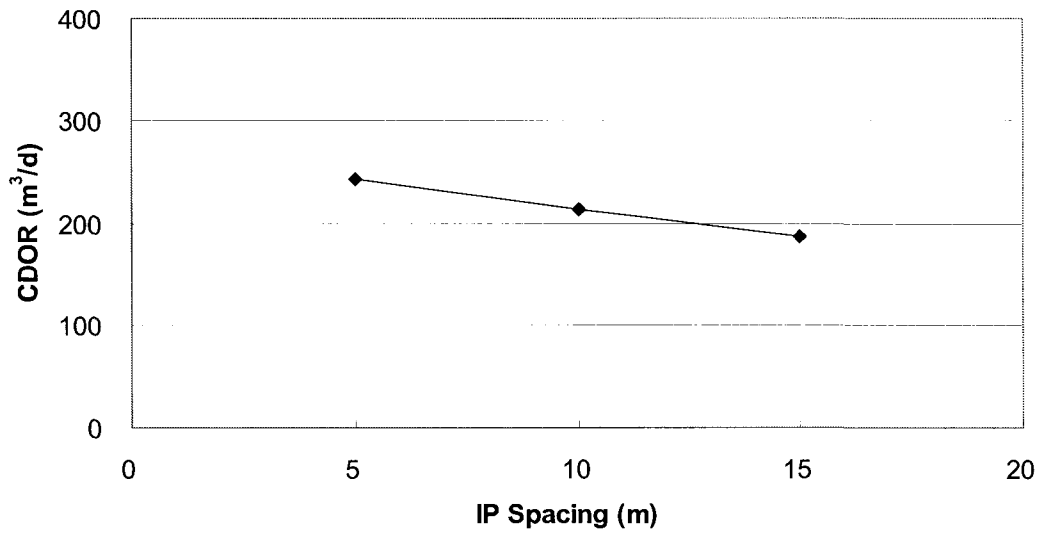
Figure 3.3c: Effect of I/P spacing on CDOR

33

3.3.3 Steam injection pressure

The simulation conditions are: preheating period of 75 days, I/P spacing of 5 m, maximum steam injection rate of 700 m³/d, well pattern spacing of 150 m. The simulation results showed that, as the steam injection pressure was increased from 1,500 to 4,500 kPa, CSOR and CDOR increased (Figure 3.4), but the recovery factor decreased (Table 3.3). A steam injection pressure of 1,500 and 3,000 kPa gave almost the same NPV value, however, the 1,500 kPa case had lower CSOR and higher RF (0.84 over 0.83). Therefore, a pressure higher than 3,000 kPa is not good as the steam injection pressure for Athabasca-type reservoir. The shallow depth of Athabasca-type reservoirs studied (200 m) would make a low pressure SAGD operation feasible.
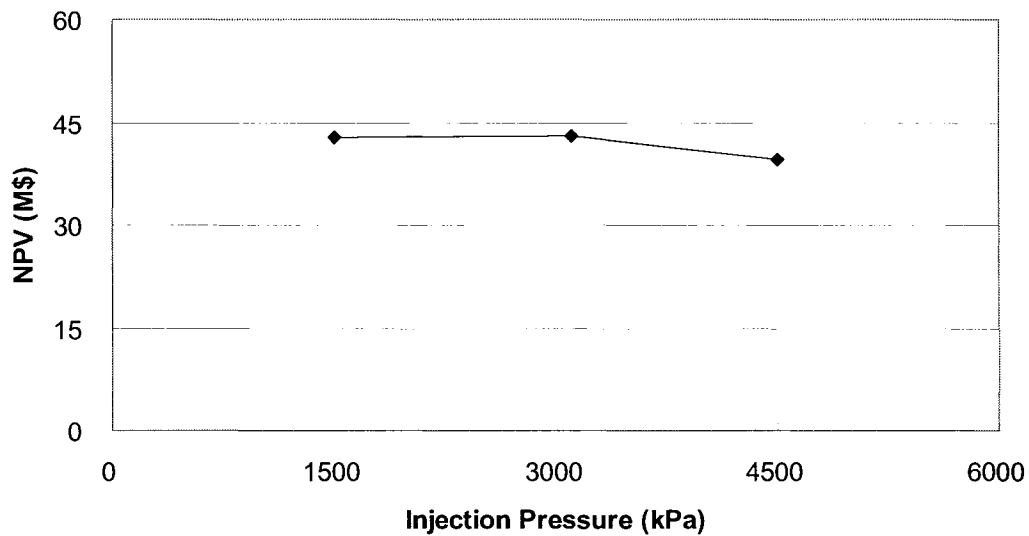
Figure 3.4a: Effect of injection pressure on NPV

34
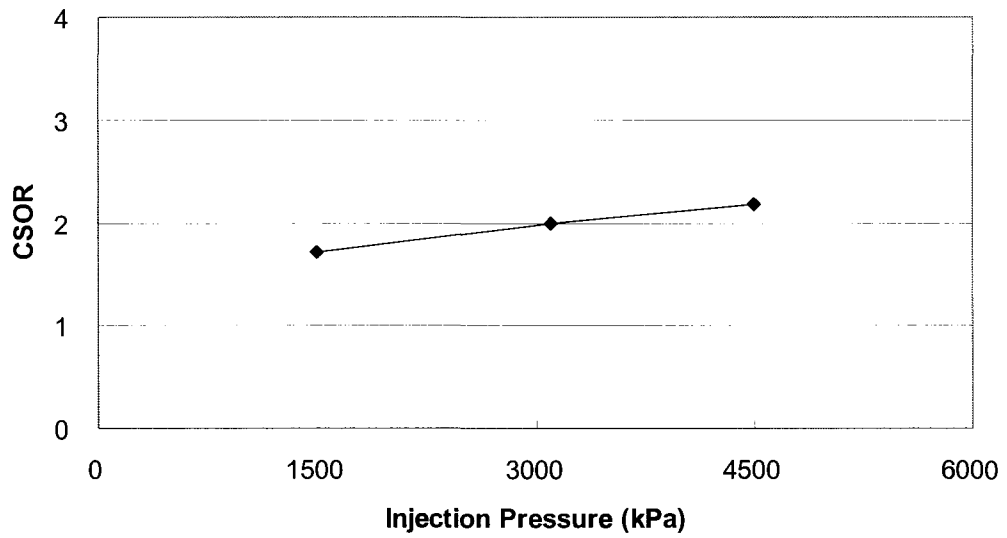
Figure 3.4b: Effect of injection pressure on CSOR
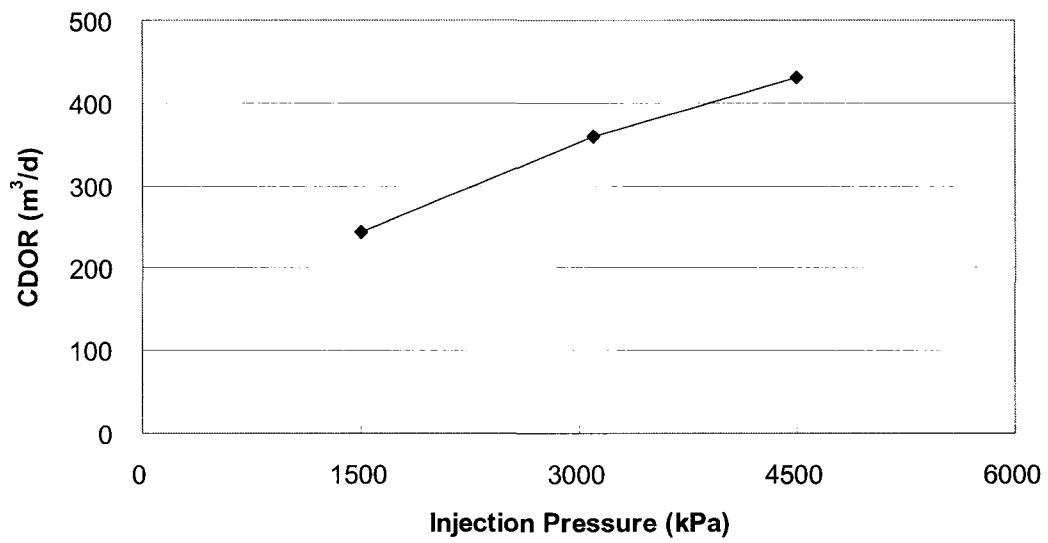
Figure 3.4c: Effect of injection pressure on CDOR

35

3.3.4 Maximum steam injection rate

The simulation conditions are: preheating period of 75 days, I/P spacing of 5 m, operating pressure of 1,500 kPa, well pattern spacing of 150 m. As the steam injection rate was increased, CSOR decreased and CDOR increased slightly. The recovery factor was constant at 0.84. The NPV was the highest for an injection rate of 700 m^3/d (Figure 3.5).
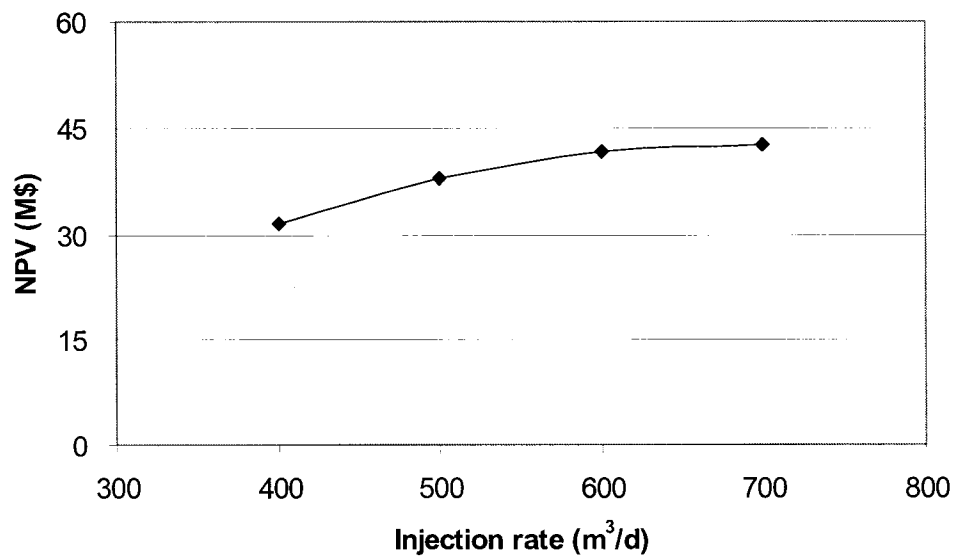
Figure 3.5a: Effect of steam injection rate on NPV

36
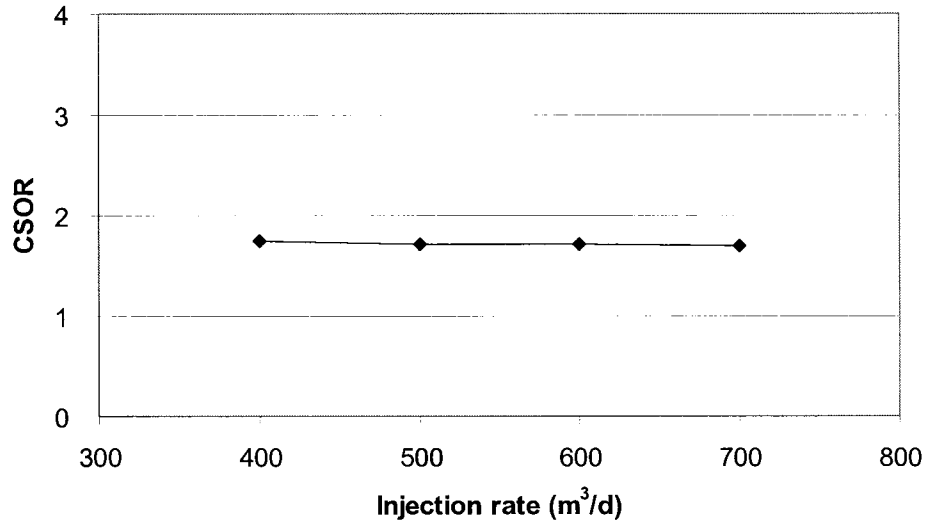
Figure 3.5b: Effect of steam injection rate on CSOR
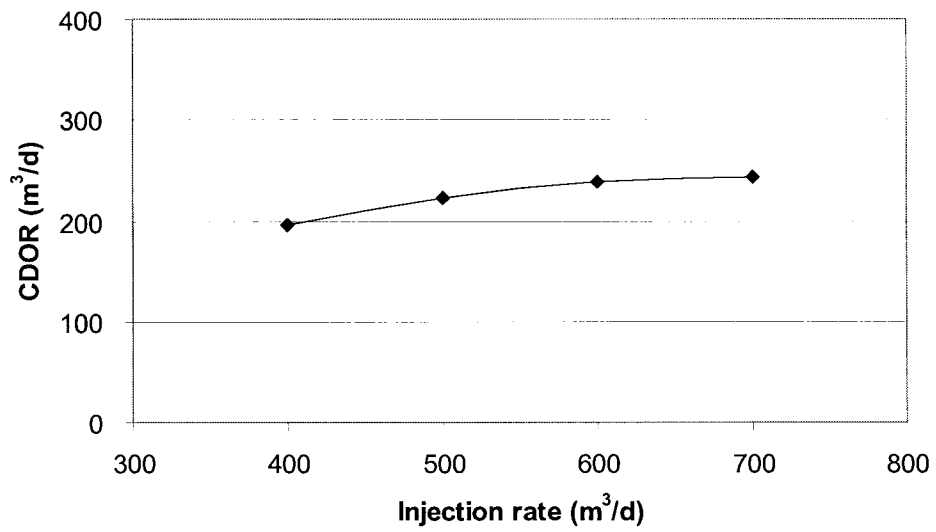
Figure 3.5c: Effect of steam injection rate on CDOR

37

3.3.5 SAGD well pattern spacing

The simulation conditions are: preheating period of 75 days, I/P spacing of 5 m, operating pressure of 1,500 kPa, maximum steam injection rate of 700 m^3/d. Simulation results for an Athabasca-type reservoir, as the well pattern spacing is increased, indicates that the NPV, CSOR, and CDOR all increase (Figure 3.6), but the ultimate recovery is almost constant with a value of 0.84 (Table 3.3). The recovery factor is considered a key parameter in determining the proper well pattern spacing, however, for a thick reservoir with high permeability like the Athabasca-type, recovery factor does not change as the well pattern spacing is increased. As a result, a larger than 150 m well pattern spacing can be applied for the Athabasca-type reservoir.
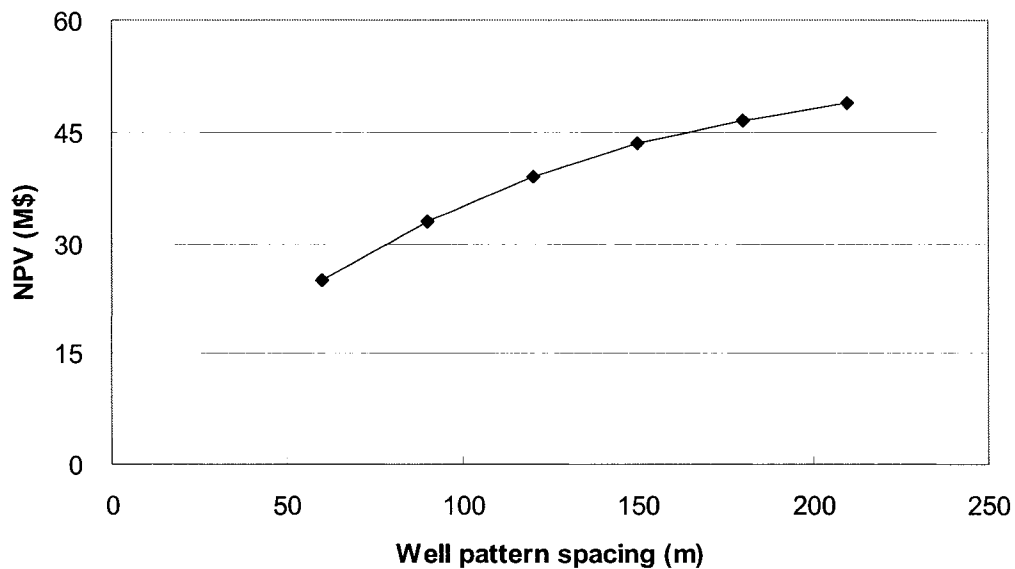
Figure 3.6a: Effect of well pattern spacing on NPV

38
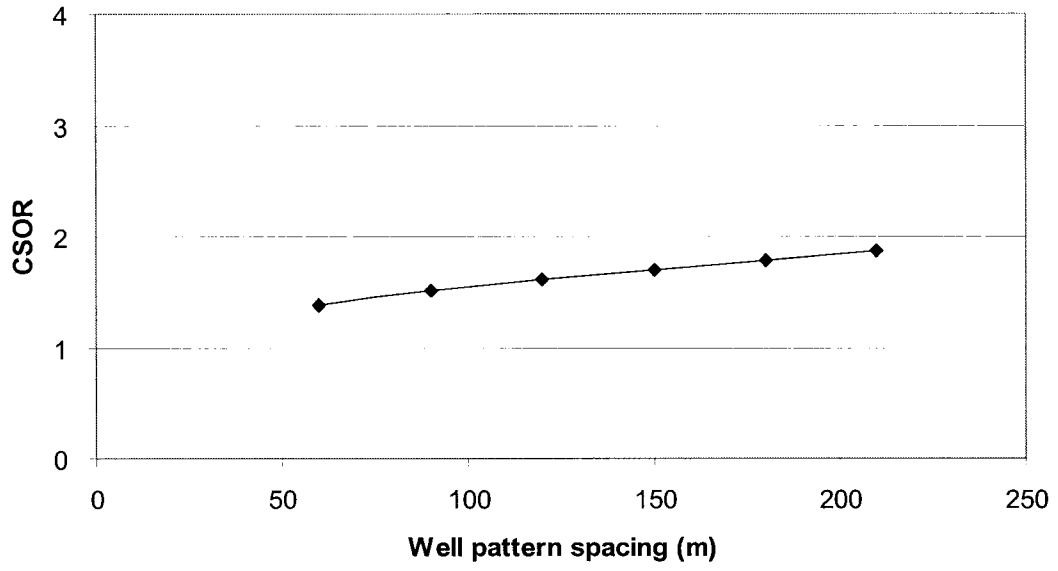
Figure 3.6b: Effect of well pattern spacing on CSOR
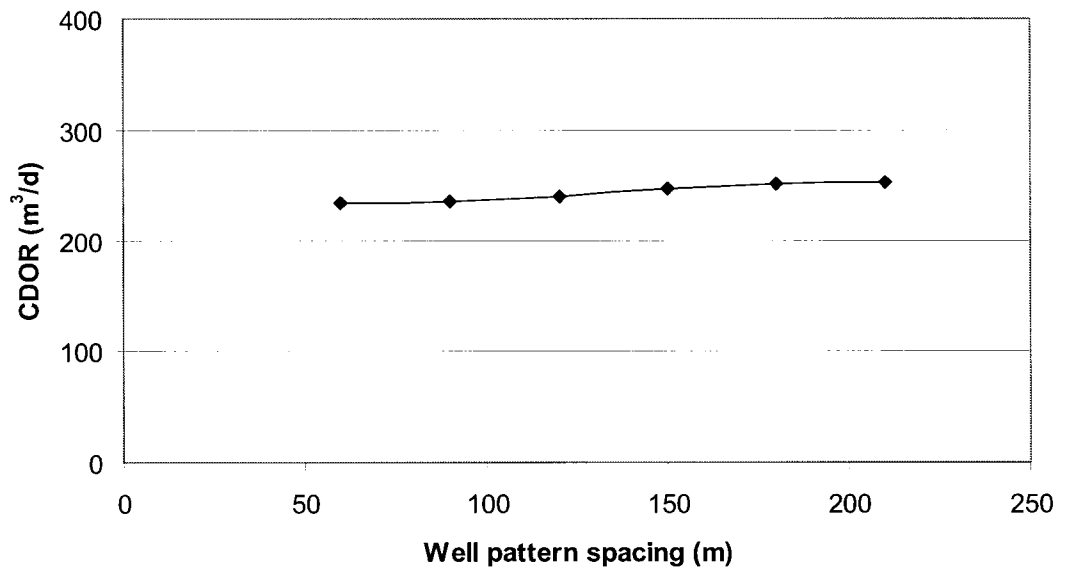
Figure 3.6c: Effect of well pattern spacing on CDOR

39

3.3.6 Reservoir thickness

These simulations were conducted to evaluate the effect of reservoir thickness on SAGD performance under the following conditions: I/P spacing of 5 m, maximum steam injection rate of 700 m^3/d, operating pressure of 1,500 kPa, well pattern spacing of 150 m, and permeability (K_v) of 2.5 Darcy (K_h/K_v = 2). As the thickness is increased, the NPV and CDOR increase and CSOR decreases (Figure 3.7). If the reservoir thickness is less than 15 m, the thermal efficiency of the SAGD process becomes lower, as CSOR is higher and CDOR lower.
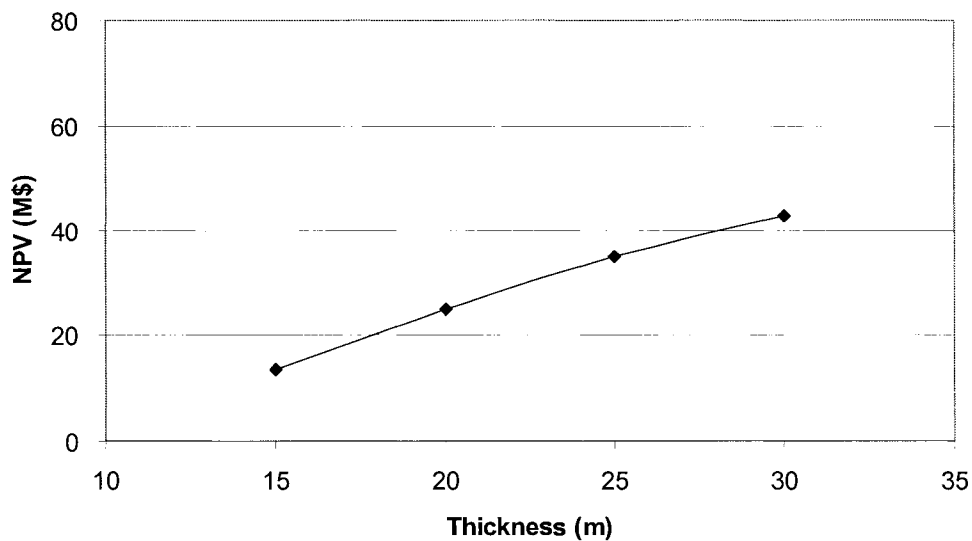
Figure 3.7a: Effect of reservoir thickness on NPV

40
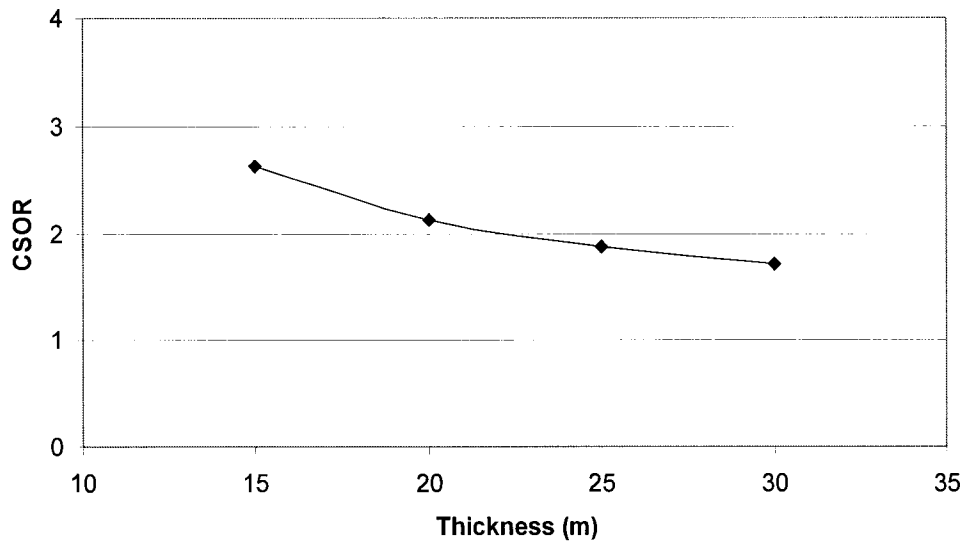
Figure 3.7b: Effect of reservoir thickness on CSOR
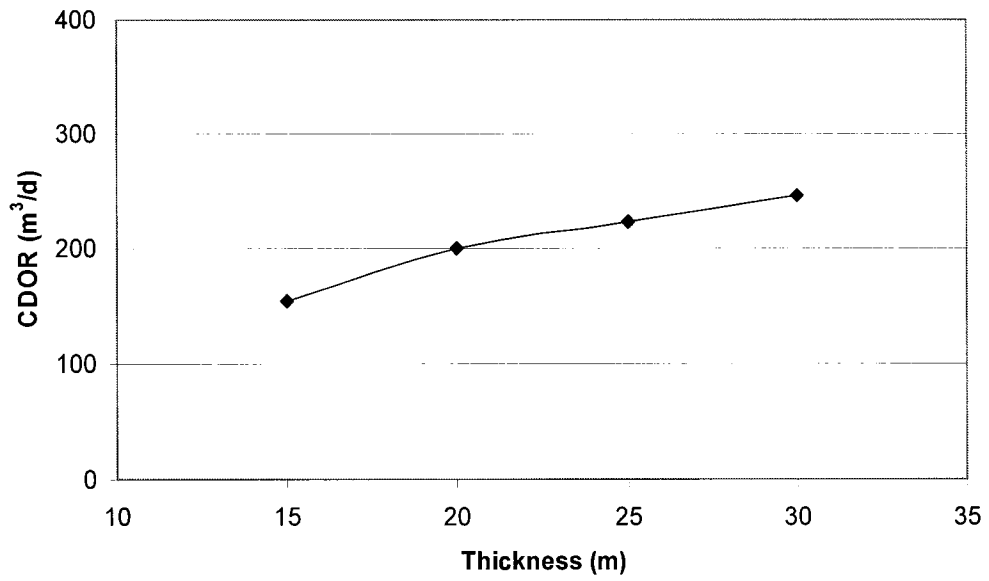
Figure 3.7c: Effect of reservoir thickness on CDOR

41

3.3.7 Reservoir permeability

The simulation conditions are: preheating period of 75 days, I/P spacing of 5 m, operating pressure of 1,500 kPa, maximum steam injection rate of 700 m^3/d, well pattern spacing of 150 m, reservoir thickness of 30 m.

The simulation results indicated that SAGD performance improved as the permeability (K_v) increased; giving lower CSOR, higher CDOR and recovery factor (Figure 3.8). A vertical permeability of 0.625 Darcy seems too low for an efficient SAGD process as the ultimate recovery is less than 0.4. If the vertical permeability is higher than 1.25 Darcy, all SAGD performance parameters are enhanced enough for a project to be economical.
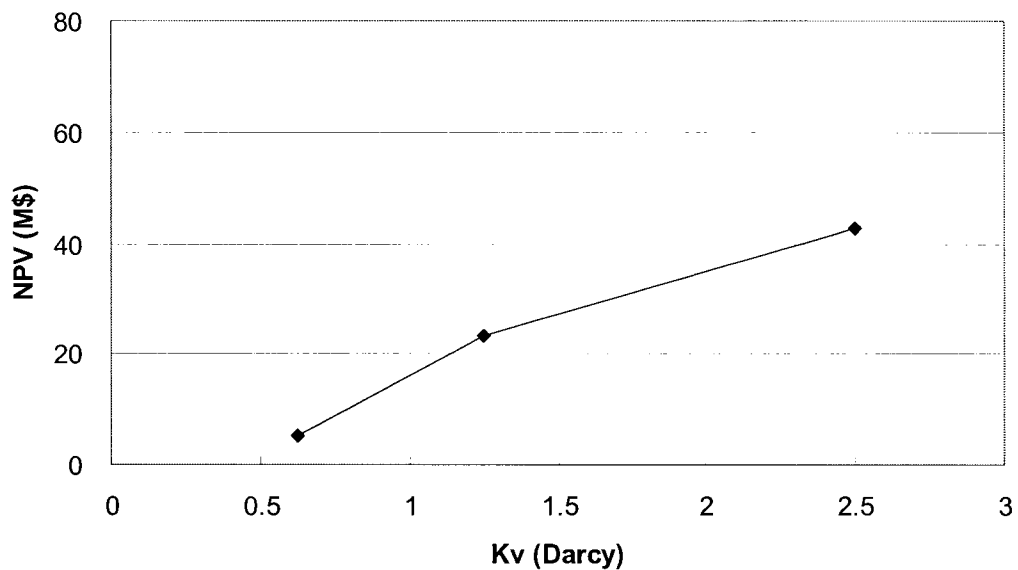
Figure 3.8a: Effect of reservoir permeability on NPV

42
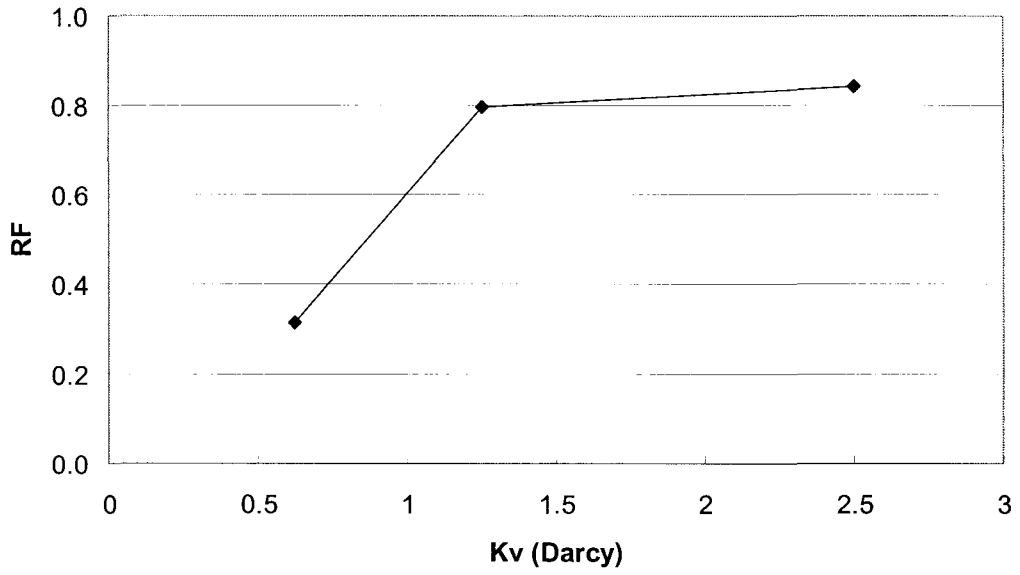
Figure 3.8b: Effect of reservoir permeability on RF
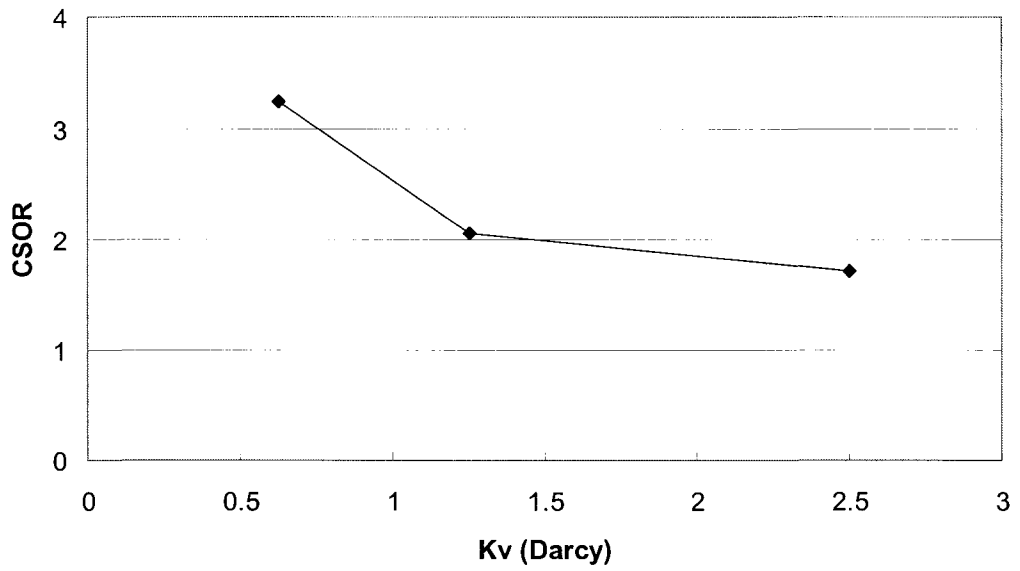
Figure 3.8c: Effect of reservoir permeability on CSOR

43
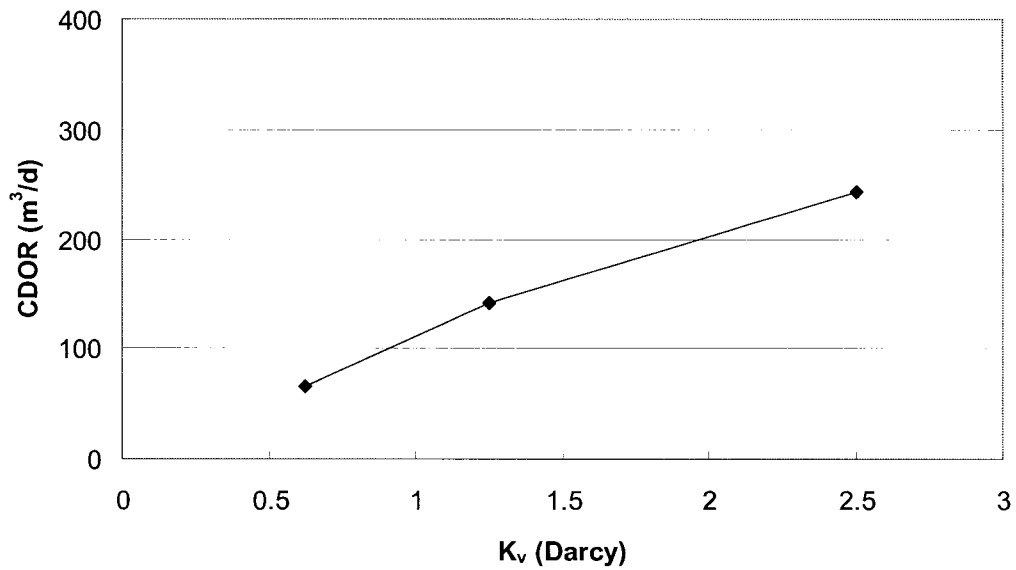
Figure 3.8d: Effect of reservoir permeability on CDOR

3.3.8 Rock thermal conductivity

The simulation conditions are: preheating period of 75 days, I/P spacing of 5 m, operating pressure of 1,500 kPa, maximum steam injection rate of 700 m^3/d, well pattern spacing of 150 m, reservoir thickness of 30 m.

Three different cases were simulated to evaluate the effect of rock thermal conductivity within the range of sand thermal conductivities. The simulation results showed that, as the rock thermal conductivity is increased, the NPV increases because of the higher CDOR which resulted from a shorter operation time (Figure 3.9). However, the rock thermal conductivity does not enhance CSOR. The higher rock thermal conductivity for the Athabasca-type reservoirs helps the steam chamber to expand faster vertically and horizontally, therefore reducing the operating time.

44
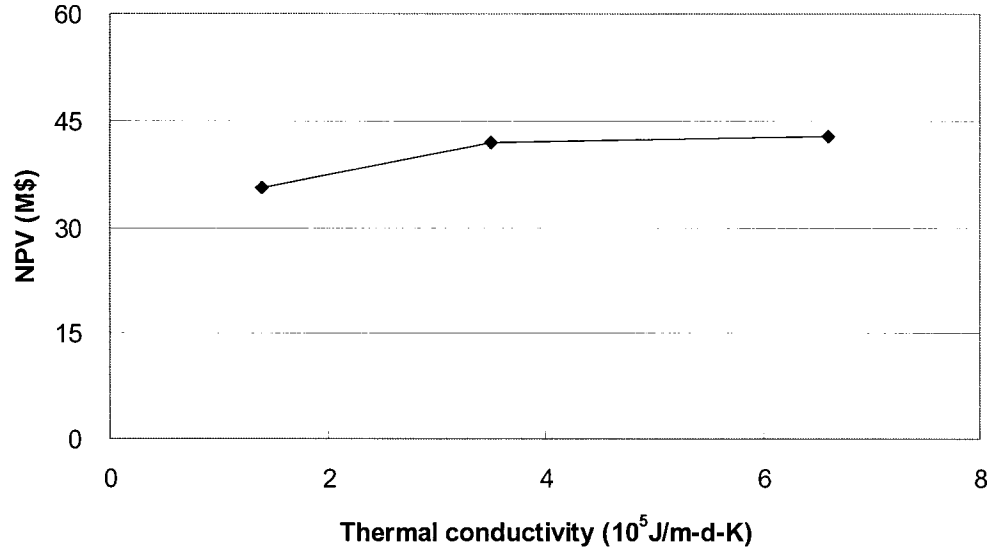
Figure 3.9a: Effect of rock thermal conductivity on NPV
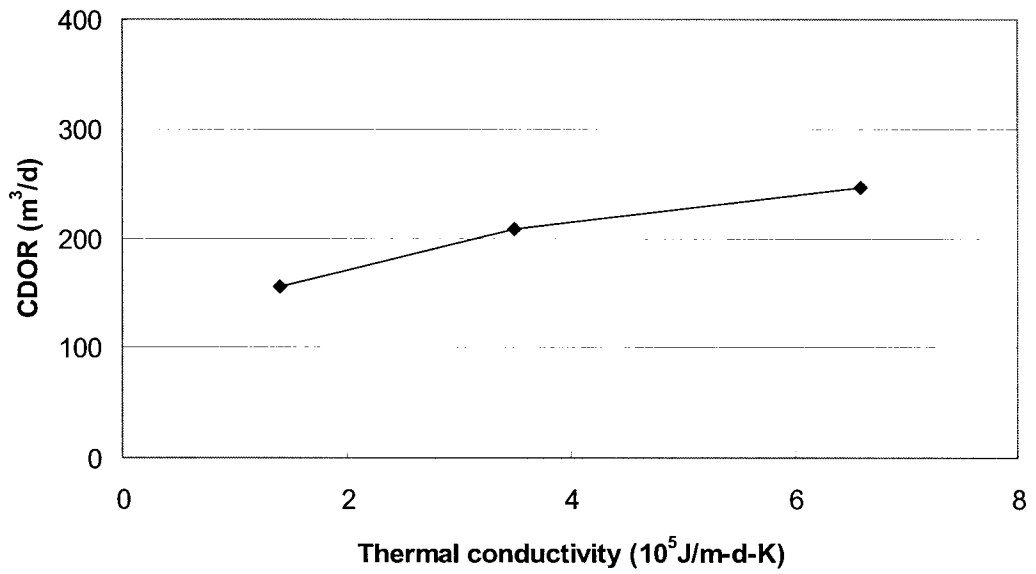
Figure 3.9b: Effect of rock thermal conductivity on CDOR

45
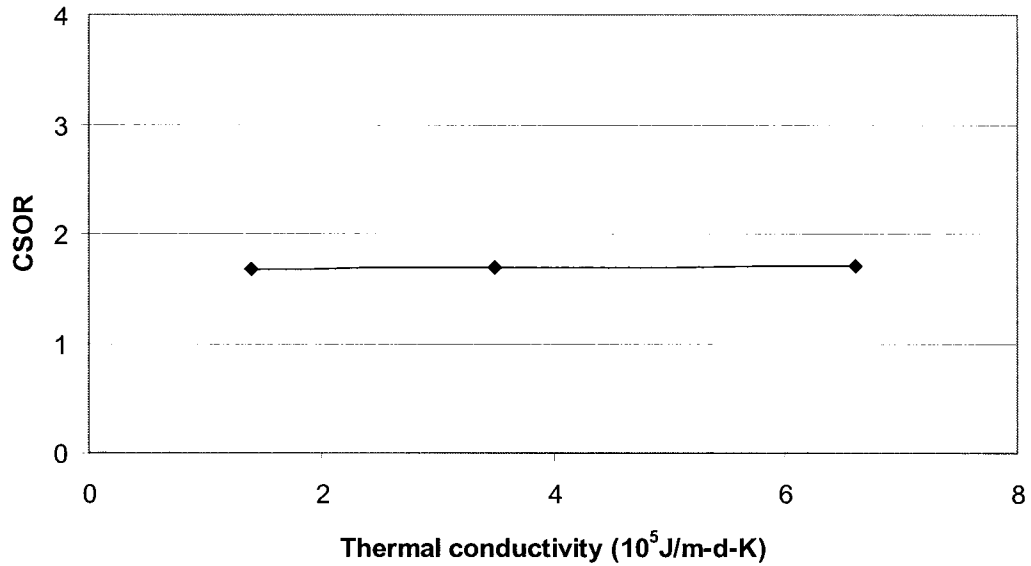
Figure 3.9c: Effect of rock thermal conductivity on CSOR

3.3.9 Best SAGD operating conditions

The most favourable SAGD operating conditions for Athabasca-type reservoirs were derived from the numerical simulations. With the following reservoir parameters: permeability (K_v) of 2.5 Darcy, reservoir thickness of 30 m, reservoir pressure of 1500 kPa, and bitumen viscosity of 1,000,000 cp, the most favourable operating conditions are: I/P spacing of 5 m, maximum steam injection rate of 700 m^3/d at a maximum injection pressure of 1,500 kPa, and well pattern spacing of 180 m. The simulations conducted with these best operating conditions gave the following results: CSOR of 1.79, CDOR of 251 m^3/d, and RF of 0.83.

46

3.4 Simulation results for Cold Lake-type reservoirs

The base case simulation conditions for the Cold Lake-type reservoirs are: preheating period of 180 days, I/P spacing of 10 m, operating pressure of 3,100 kPa, maximum steam injection rate of 400 m^3/d, well pattern spacing of 100 m, reservoir thickness of 20 m, reservoir permeability (K_v) of 1.25 Darcy. Table 3.4 shows the simulation results for the Cold Lake-type reservoir cases related to eight operating conditions and reservoir parameters. Individual results are given below.

3.4.1 Preheating period

The simulation conditions are: operating pressure of 3,100 kPa, maximum steam injection rate of 400 m^3/d, well pattern spacing of 100 m. Simulation results showed that the proper preheating period is 50 days for an I/P spacing of 5 m, 180 days for an I/P spacing of 10 m, and 315 days is for an I/P spacing of 15 m (Figure 3.10). There is not much enhancement in NPV even if the preheating periods are longer than these periods for each I/P spacing case. A preheating period of 50 days for an I/P spacing of 5 m is economically adequate for successful SAGD performance. The preheating periods for Cold Lake-type is shorter than that for Athabasca-type because the lower viscosity and porosity of the Cold Lake-type would give an overall higher thermal conductivity due to the higher thermal conductivity of the rock matrix compared to that of the fluids.

47
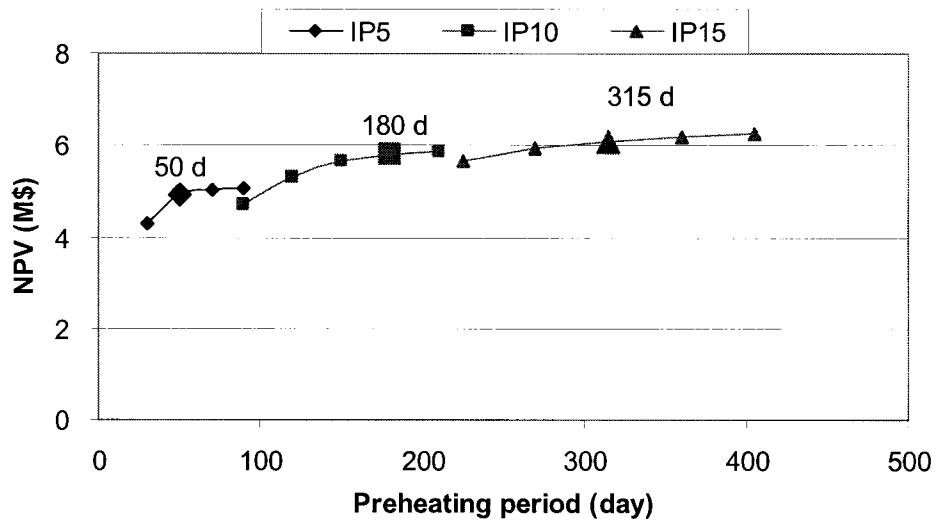
Figure 3.10a: Effect of preheating period on NPV
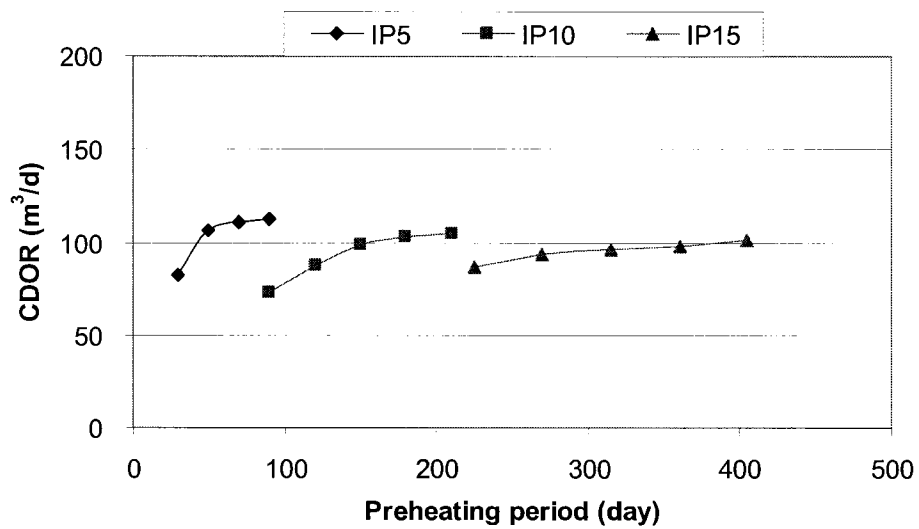
Figure 3.10b: Effect of preheating period on CDOR

48
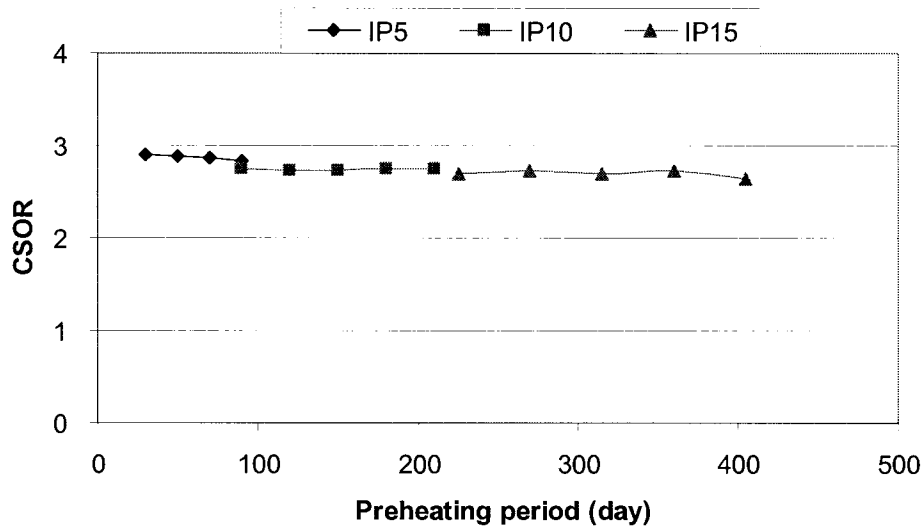
Figure 3.10c: Effect of preheating period on CSOR

3.4.2 Injector to Producer spacing

The simulation conditions are: preheating period of 180 days, operating pressure of 3,100 kPa, maximum steam injection rate of 400 m^3/d, well pattern spacing of 100 m. The simulations showed that, as the I/P spacing was increased from 5 m to 15 m, the NPV and ultimate recovery increased. The CSOR decreased from 2.89 to 2.69, and the CDOR decreased from 106 m^3/d to 96 m^3/d (Figure 3.11). An I/P spacing of 15 m resulted in the best SAGD performance: highest NPV and lowest CSOR. The low permeability of the Cold Lake-type reservoir will give more effective SAGD performance with larger I/P spacing. There is not much enhancement in NPV even if the I/P spacing is greater than 10 m. Also, the larger I/P spacing may cause slow thermal communication in the field which is most likely not homogenous. Therefore, an I/P spacing of 10 m might be feasible for Cold Lake-type reservoir.

49

Table 3.4: SAGD simulation results for Cold Lake-type reservoir

Case	Cum. Production (m^3)	CSOR	CDOR (m^3/d)	RF	NPV (M$)
Preheating period					
90 d	189,077	2.75	73	0.46	4.7
120 d	183,509	2.73	88	0.45	5.3
150 d	185,523	2.73	98	0.46	5.7
180 d	187,808	2.74	103	0.46	5.8
210 d	187,340	2.74	105	0.46	5.9
Injector to Producer (I/P) spacing					
5 m	172,424	2.89	106	0.42	4.9
10 m	187,808	2.74	103	0.46	5.8
15 m	200,751	2.69	96	0.49	6.1
Operating pressure (I/P spacing 5 m)					
3,100 kPa	172,424	2.89	106	0.42	4.9
4,500 kPa	157,060	3.24	141	0.39	3.2
6,000 kPa	150,708	3.73	159	0.37	1.0
Max. steam injection rate					
200 m^3	287,357	3.63	52	0.71	1.3
300 m^3	274,478	3.11	85	0.67	5.2
400 m^3	189,302	2.75	103	0.47	5.8
500 m^3	187,808	2.74	103	0.46	5.8
Well pattern spacing					
60 m	170,231	2.40	102	0.69	6.6
80 m	219,076	2.80	96	0.67	6.3
100 m	170,433	2.61	100	0.42	5.9
120 m	172,196	2.61	101	0.35	5.9
150 m	171,489	2.62	100	0.28	5.8
Reservoir thickness (well pattern spacing 100 m)					
15 m	76,738	2.76	103	0.25	2.7
20 m	170,433	2.61	100	0.42	5.9
25 m	349,142	2.72	104	0.69	9.9
30 m	448,466	2.49	128	0.73	14.0
Reservoir permeability (K_v)					
0.625 D	155,435	3.45	60	0.38	1.9
1.25 D	187,808	2.74	103	0.46	5.8
2.5 D	291,757	2.91	132	0.72	8.3
Rock thermal conductivity (I/P spacing 5 m)					
Low	127,184	2.39	80	0.31	5.4
Middle	144,541	2.65	98	0.36	5.2
High	172,424	2.89	106	0.42	4.9

50
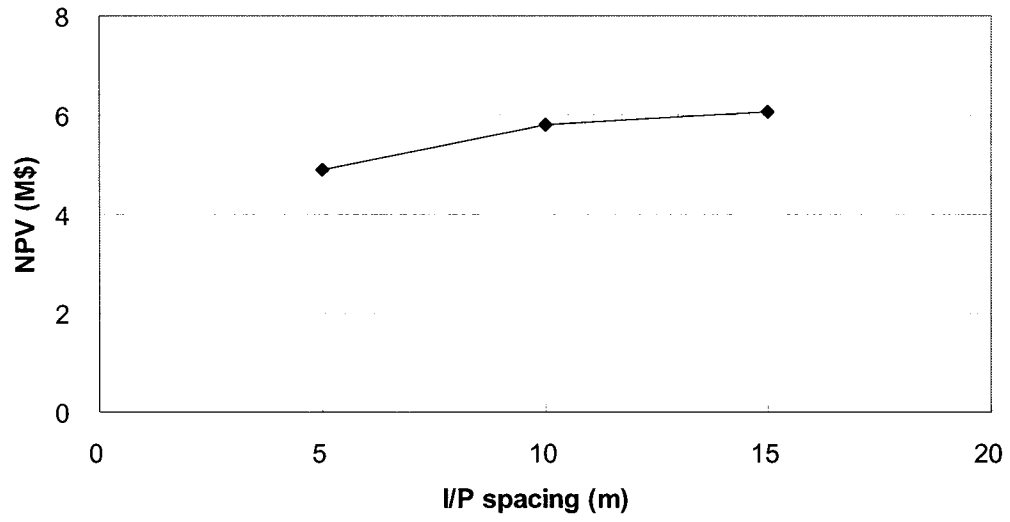
Figure 3.11a: Effect of I/P spacing on NPV
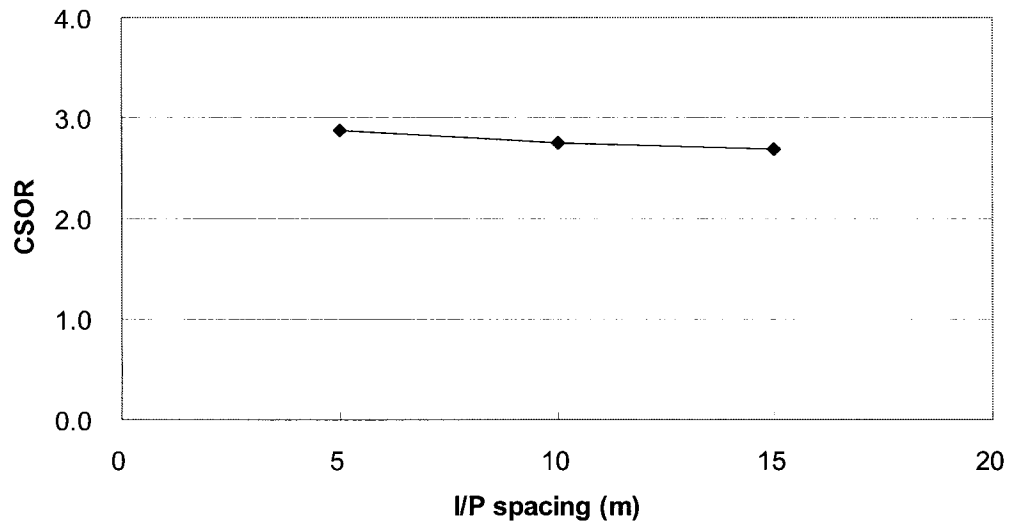
Figure 3.11b: Effect of I/P spacing on CSOR

51
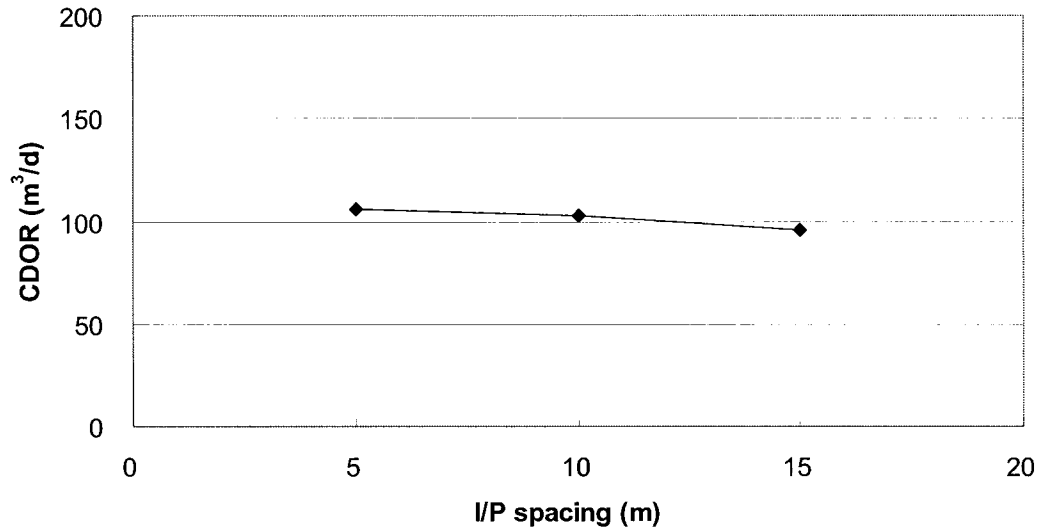
Figure 3.11c: Effect of I/P spacing on CDOR

3.4.3 Steam injection pressure

The simulation conditions are: preheating period of 180 days, I/P spacing of 5 m, maximum steam injection rate of 400 m^3/d, well pattern spacing of 100 m. The simulation results showed that, as the steam injection pressure was increased from 3,100 to 6,000 kPa, CSOR and CDOR increased (Figure 3.12). A steam injection pressure of 3,100 kPa gave the highest NPV with the lowest CSOR. Therefore, a steam injection pressure of 3,100 kPa is the proper SAGD operating pressure for Cold Lake-type reservoirs. For this type of thin reservoirs, the higher the injection pressure, the higher the heat loss to the overburden. An operating pressure of 3,100 kPa is the lowest operating pressure required at the reservoir depth of Cold Lake-type reservoirs (400 m).

52
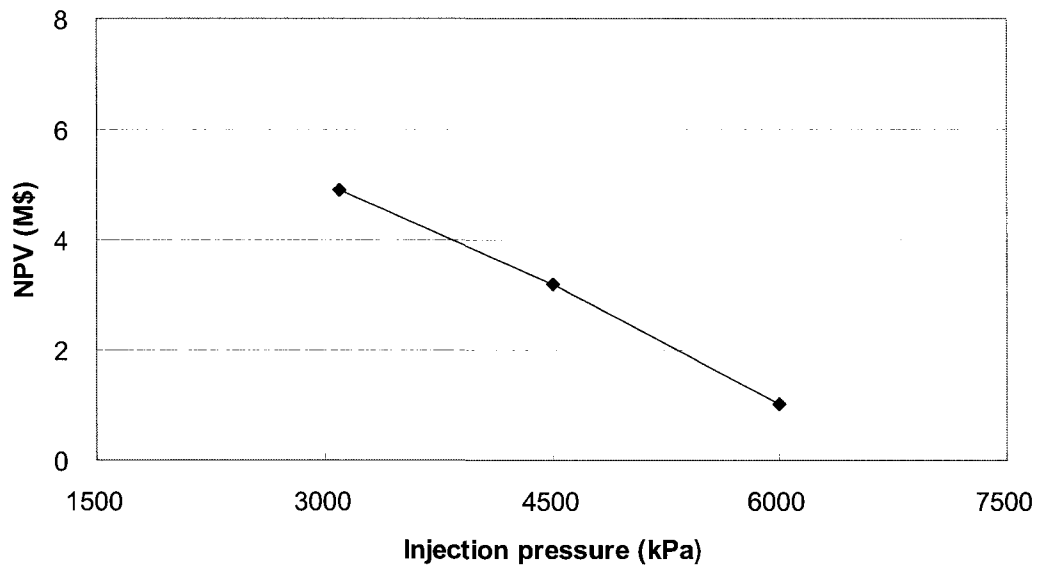
Figure 3.12a: Effect of injection pressure on NPV
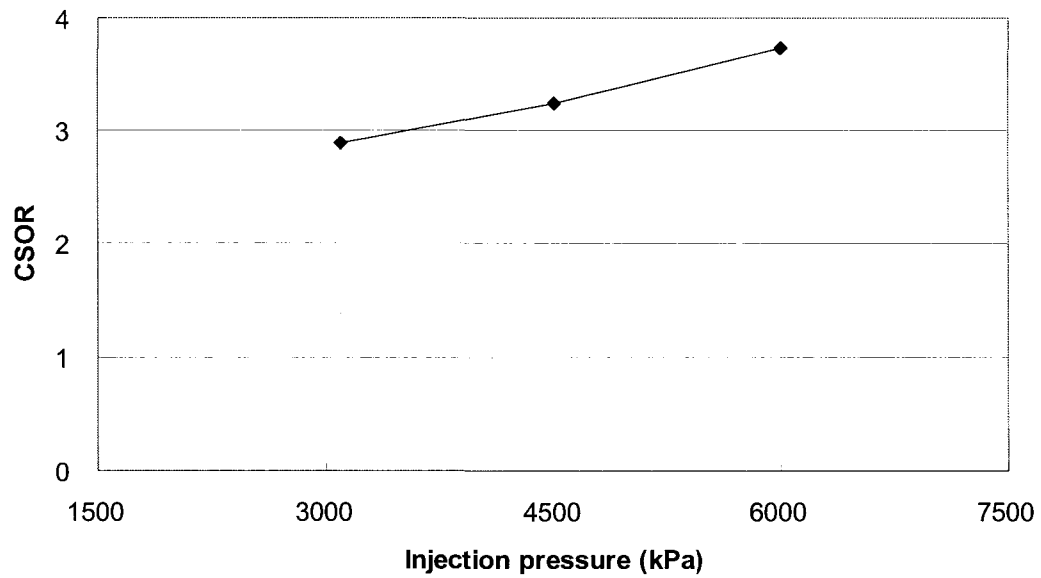
Figure 3.12b: Effect of injection pressure on CSOR

53
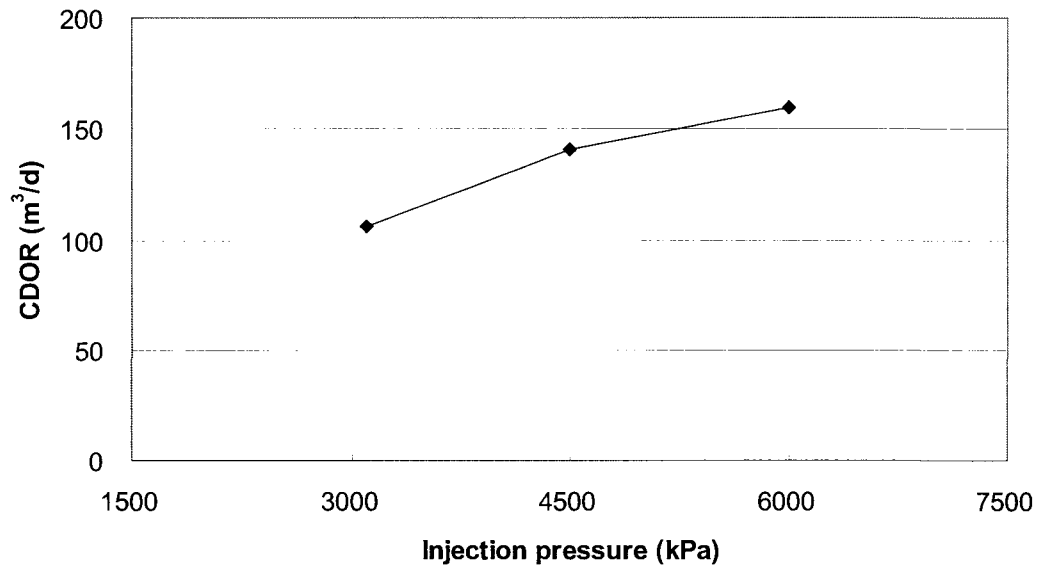
Figure 3.12c: Effect of injection pressure on CDOR

3.4.4 Maximum steam injection rate

The simulation conditions are: preheating period of 180 days, I/P spacing of 10 m, maximum operating pressure of 3,100 kPa, well pattern spacing of 100 m. As the steam injection rate was increased, CSOR decreased and CDOR increased. A steam injection rate of less than 300 m^3/d gives high ultimate recovery (Table 3.4), but the CSOR is too high due to poor thermal efficiency. Also, the CDOR is low because of long project life. The NPV was the highest for the case of 400 m^3/d (Figure 3.13).

54
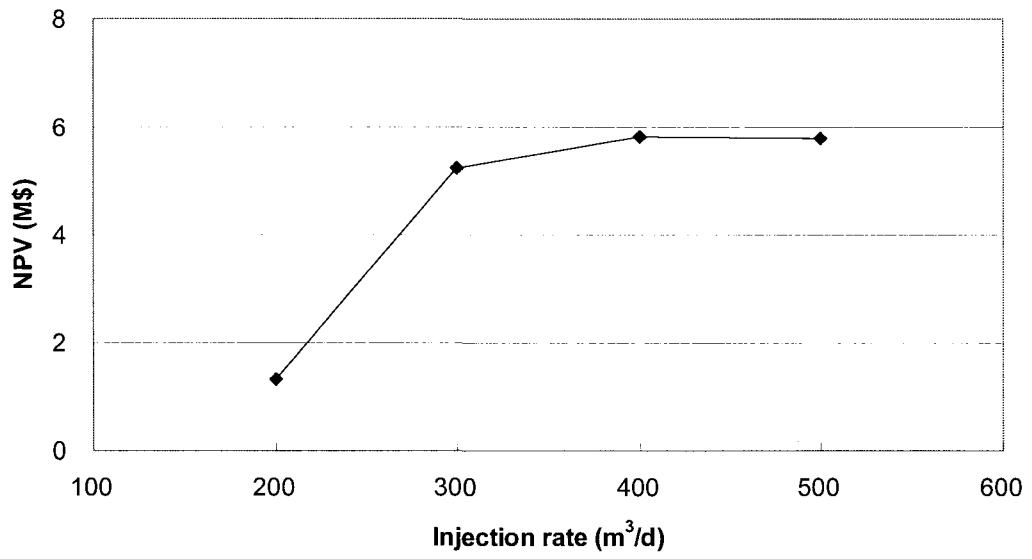
Figure 3.13a: Effect of steam injection rate on NPV
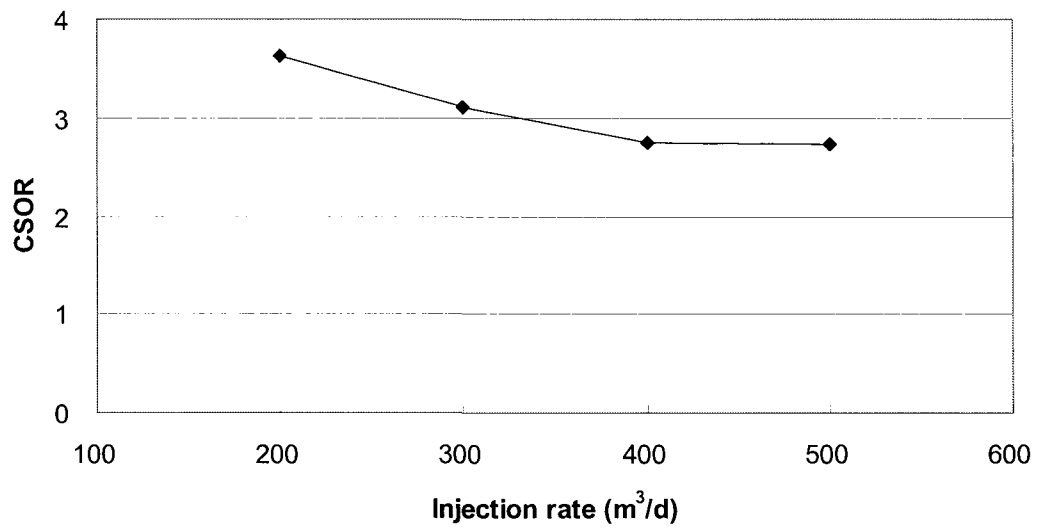
Figure 3.13b: Effect of steam injection rate on CSOR

55
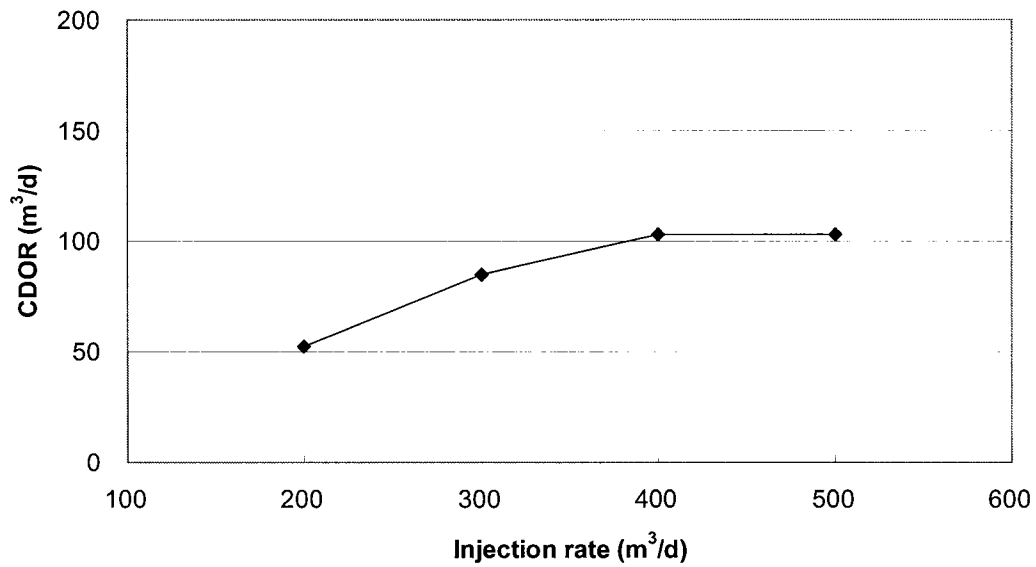
Figure 3.13c: Effect of steam injection rate on CDOR

3.4.5 SAGD well pattern spacing

The simulation conditions are: preheating period of 180 days, I/P spacing of 10 m, operating pressure of 3,100 kPa, maximum steam injection rate of 400 m^3/d. Simulation results for a Cold Lake-type reservoir, as the well pattern spacing is increased, indicate that the NPV and ultimate recovery decrease (Figure 3.14). The CDOR is almost constant at a value of 100 m^3/d (Table 3.4). The recovery factor is considered a key parameter in determining the proper well pattern spacing. If the well spacing is larger than 100 m, the recovery factor drops to 0.4. A narrower well pattern spacing will give a more economical SAGD operation. A well pattern spacing of about 80 m can be applied for the thinner Cold Lake-type reservoirs.

56
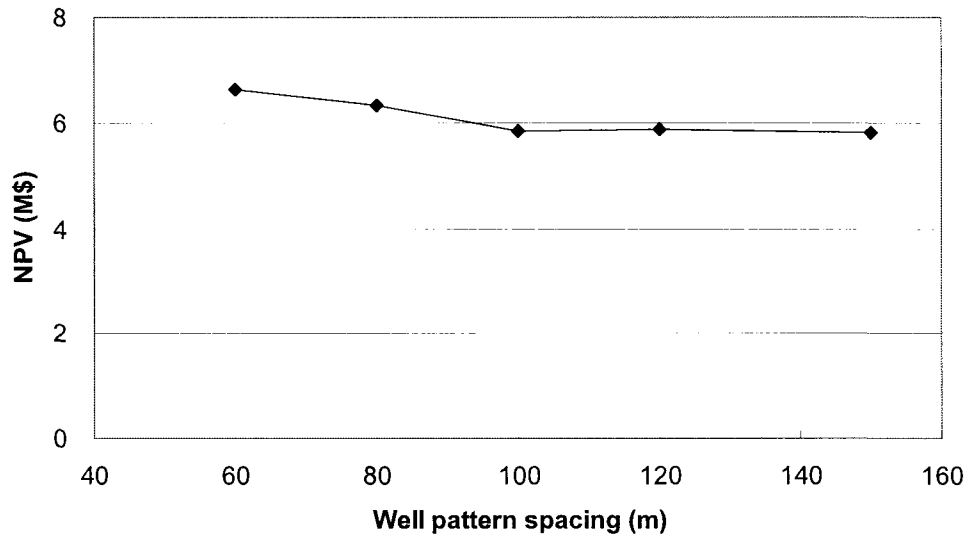
Figure 3.14a: Effect of well pattern spacing on NPV
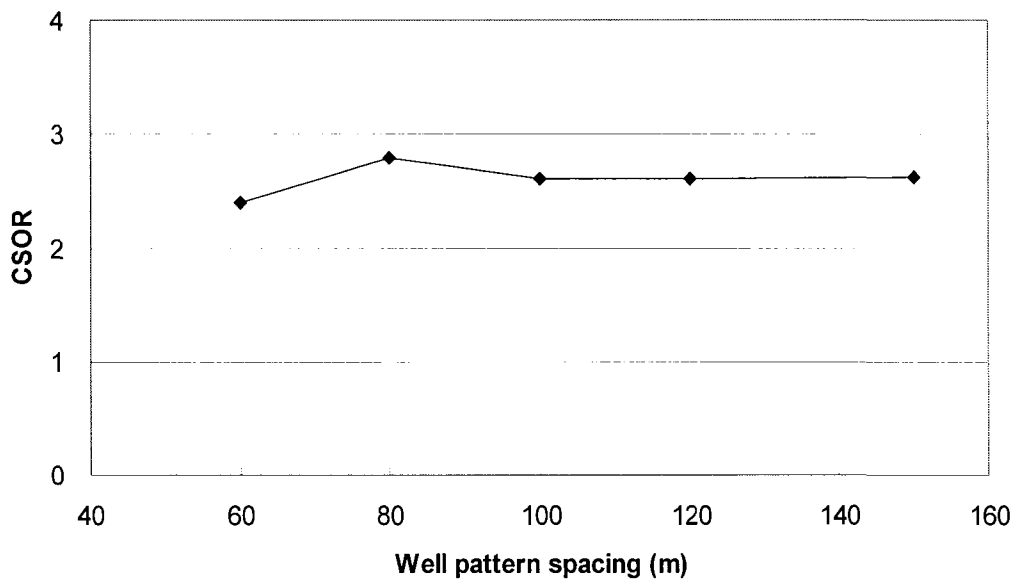
Figure 3.14b: Effect of well pattern spacing on CSOR

57
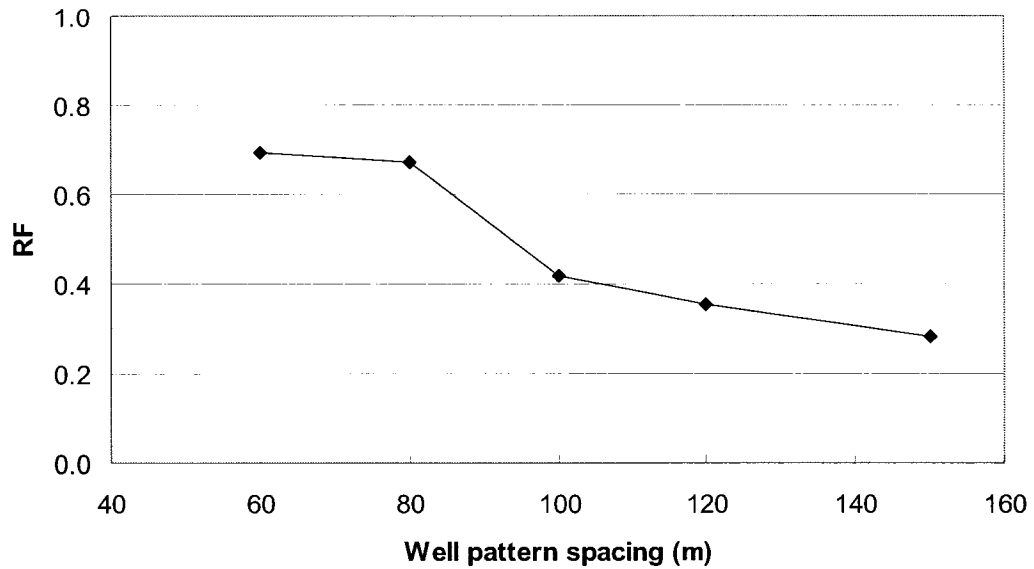
Figure 3.14c: Effect of well pattern spacing on RF

3.4.6 Reservoir thickness

These simulations were conducted to evaluate the effect of reservoir thickness on SAGD performance under the following conditions: I/P spacing of 5 m, operating pressure of 3,100 kPa, maximum steam injection rate of 400 m^3/d, well pattern spacing of 100 m, and permeability (K_v) of 1.25 Darcy ($K_h/K_v = 2$). As the thickness is increased, the NPV and CDOR increase and CSOR goes through a maximum and decreases (Figure 3.15). If the reservoir thickness is greater than 20 m, CDOR is larger than 100 m^3/d and RF is larger than 0.4 (Table 3.4). Therefore, a reservoir thickness of 20 m can be considered as the lower economic limit for the SAGD operation of Cold Lake-type reservoirs.
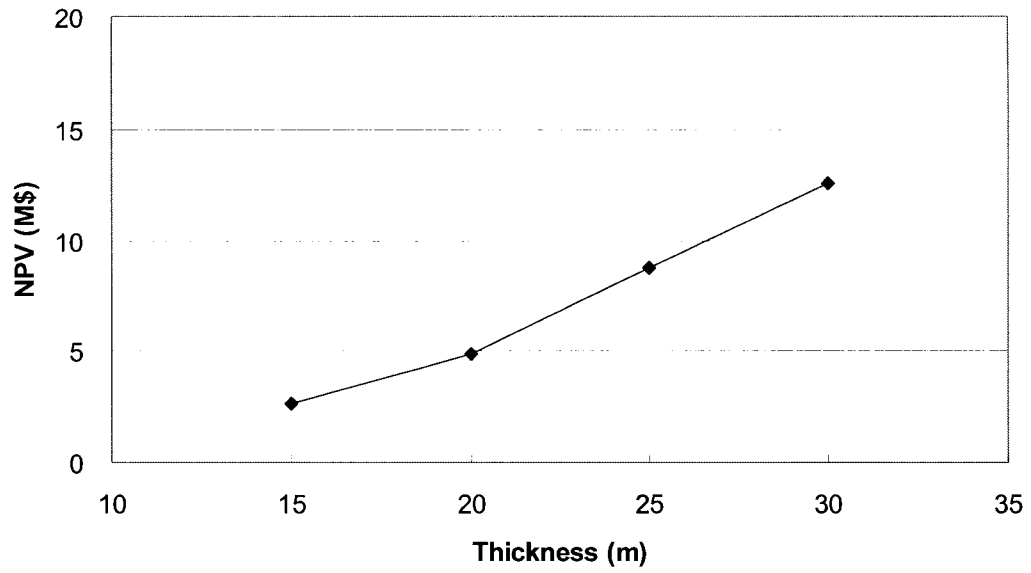
Figure 3.15a: Effect of reservoir thickness on NPV
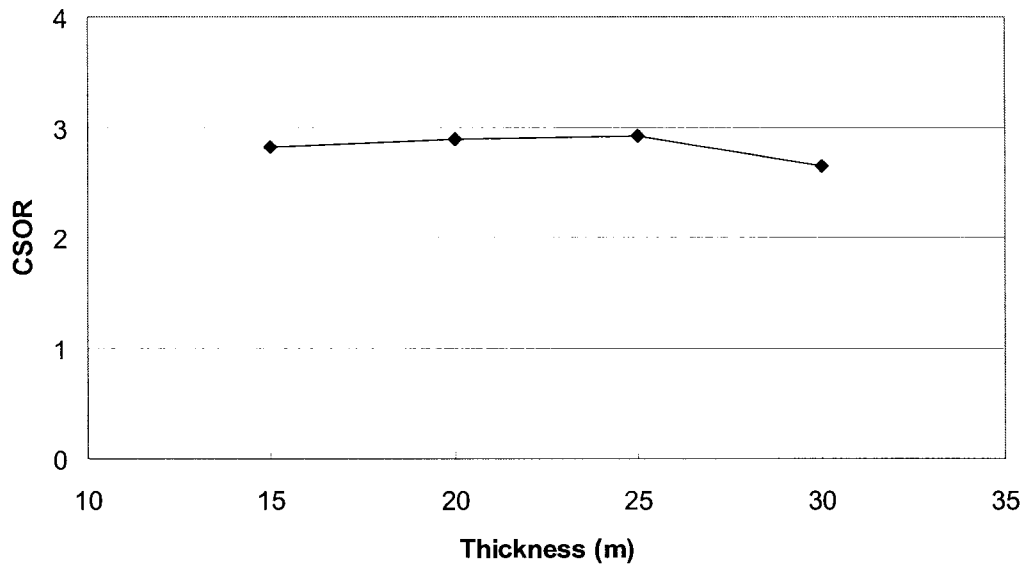
Figure 3.15b: Effect of reservoir thickness on CSOR

59
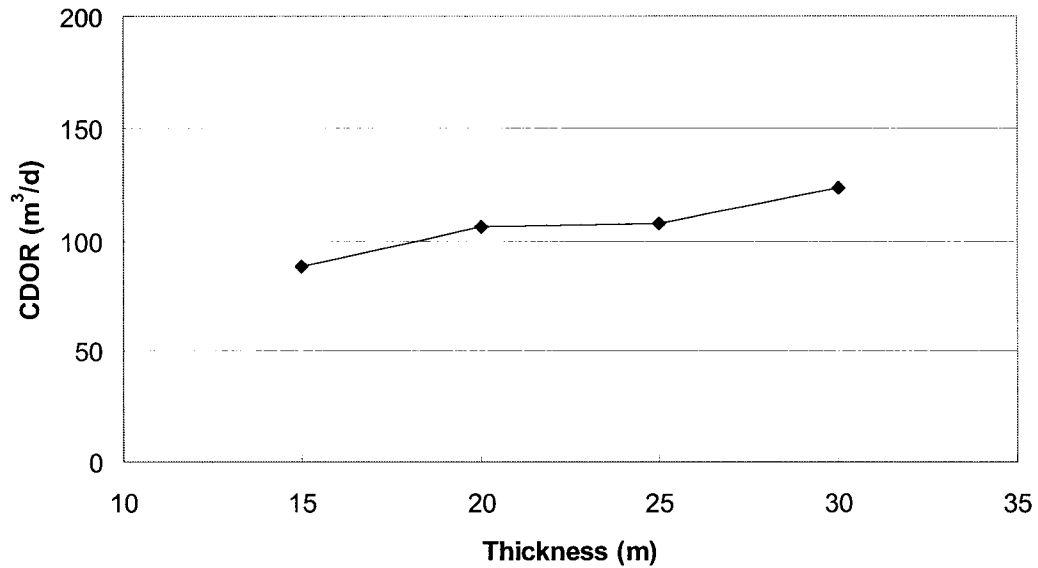
Figure 3.15c: Effect of reservoir thickness on CDOR

3.4.7 Reservoir permeability

The simulation conditions are: preheating period of 180 days, I/P spacing of 10 m, operating pressure of 3,100 kPa, maximum steam injection rate of 400 m^3/d, well pattern spacing of 100 m, reservoir thickness of 20 m.

The simulation results indicated that SAGD performance improved as the permeability (K_v) increased; giving lower CSOR, higher CDOR and recovery factor (Figure 3.16). A vertical permeability of 0.625 Darcy seems too low for an efficient SAGD process as the ultimate recovery is less than 0.4. If the vertical permeability is higher than 1.25 Darcy, all the SAGD performance parameters become good economic indicators. As a reservoir thickness of 20 m is the lower economic limit for an efficient SAGD performance, CSOR increases slightly even if the permeability is as high as 2.5 Darcy. The CSOR is lower in the 1.25 Darcy case compared to the 2.5 Darcy case because the 2.5 Darcy case produced more oil for a longer project life until an instantaneous SOR of 4 was reached.

60
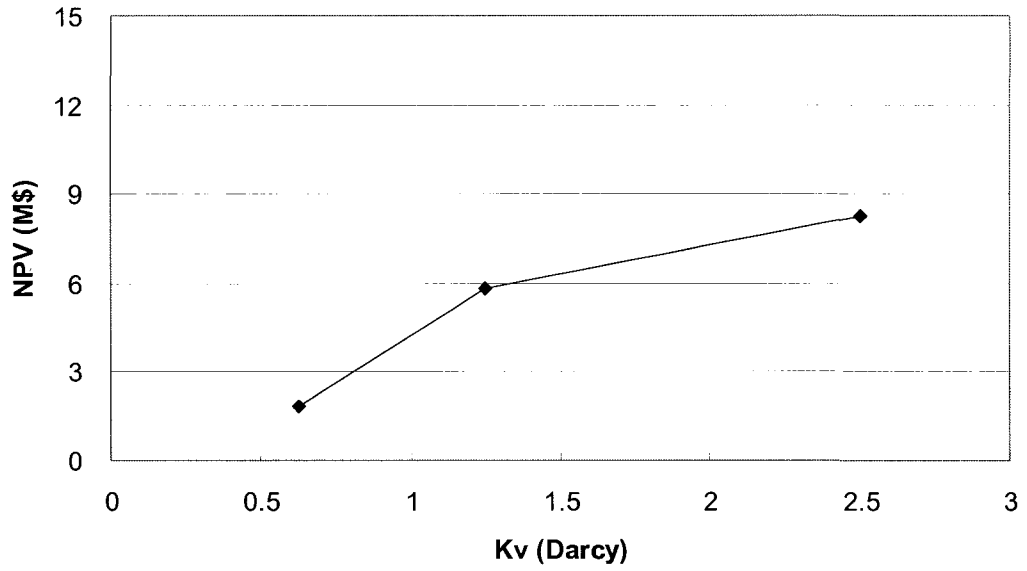
Figure 3.16a: Effect of reservoir permeability on NPV
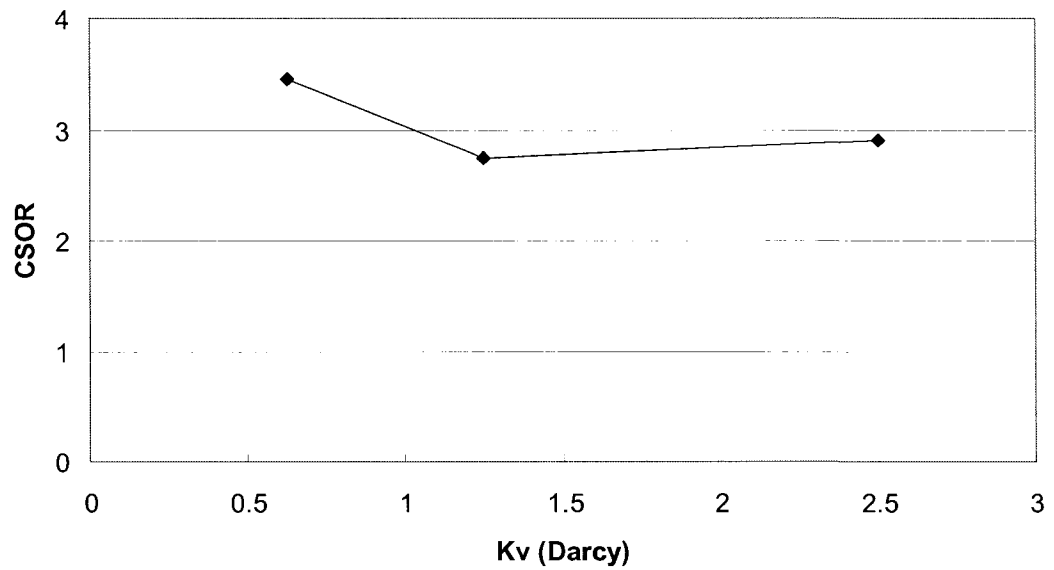
Figure 3.16b: Effect of reservoir permeability on CSOR

61
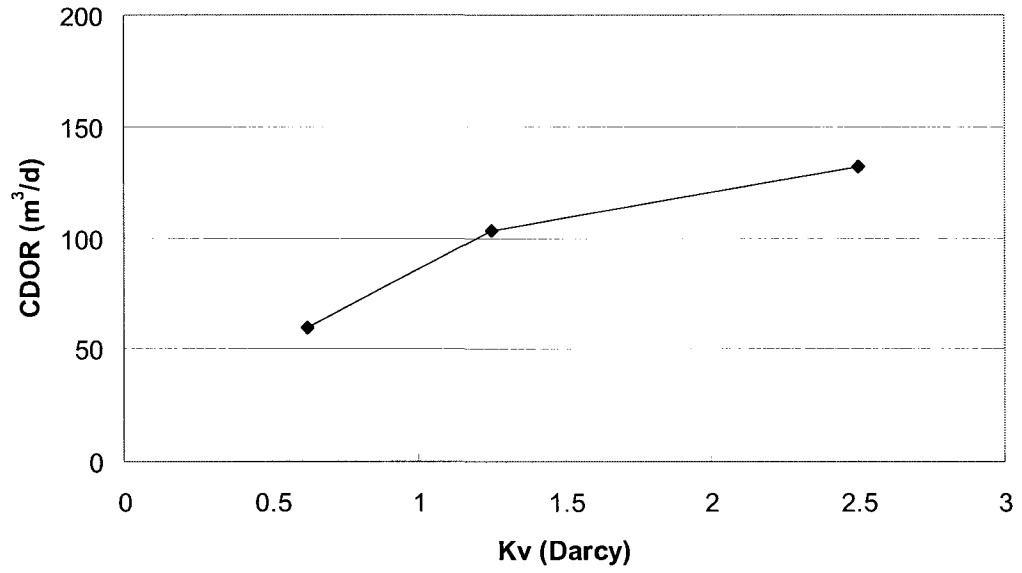
Figure 3.16c: Effect of reservoir permeability on CDOR
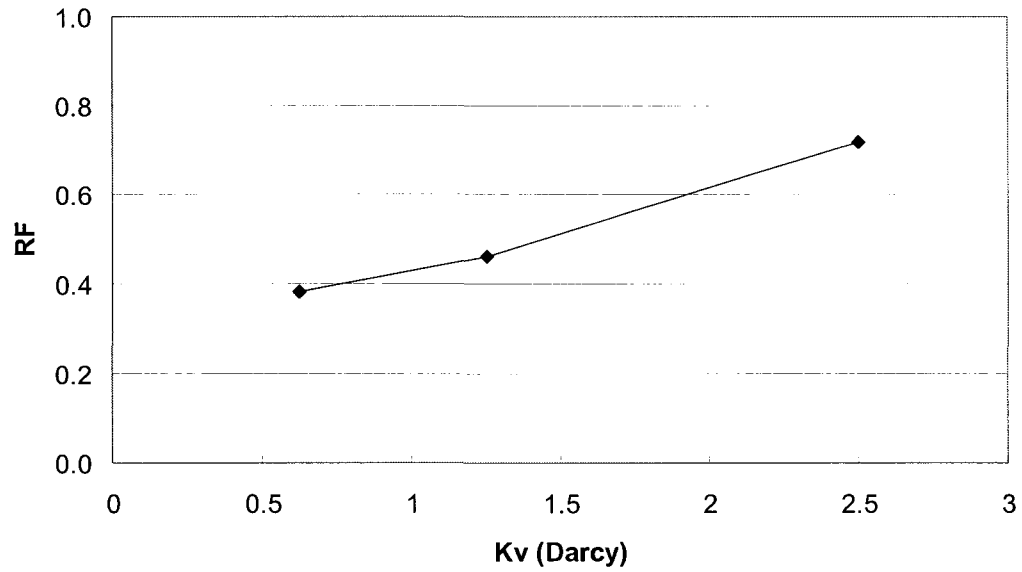
Figure 3.16d: Effect of reservoir permeability on RF

62

3.4.8 Rock thermal conductivity

The simulation conditions are: preheating period of 180 days, I/P spacing of 10 m, operating pressure of 3,100 kPa, maximum steam injection rate of 400 m³/d, well pattern spacing of 100 m, reservoir thickness of 25 m, permeability (K_v) of 1.25 Darcy.

The simulation results showed that, as the rock thermal conductivity increased, the NPV decreased slightly due to higher CSOR, which means poor thermal efficiency (Figure 3.17). Ultimate recovery increased, as well as CDOR. Thinner reservoirs like this Cold Lake-type give inefficient SAGD performance if the rock thermal conductivity is high because of the rapid heat loss to the overburden.
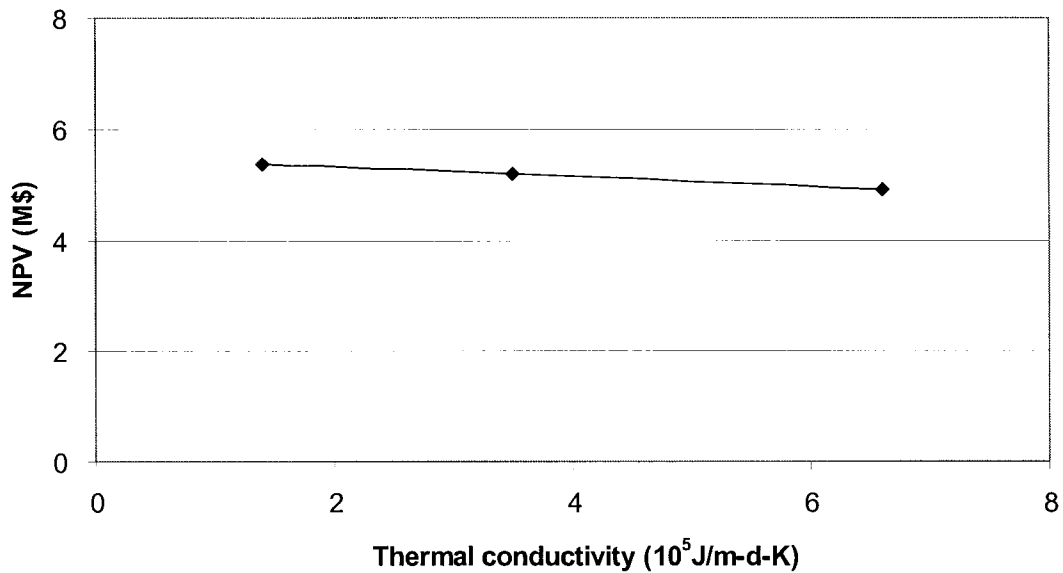
Figure 3.17a: Effect of rock thermal conductivity on NPV
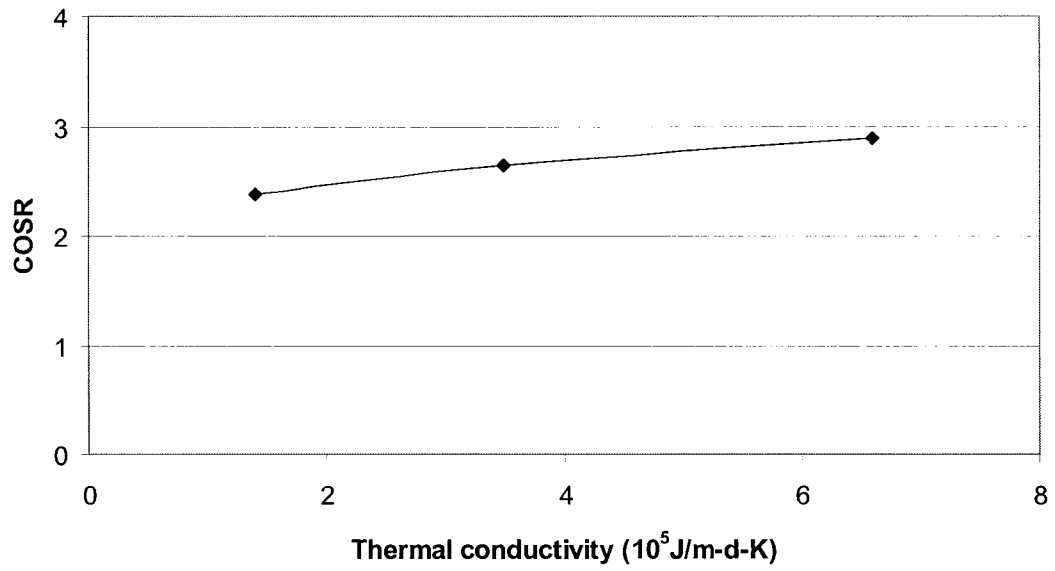
Figure 3.17b: Effect of rock thermal conductivity on CSOR
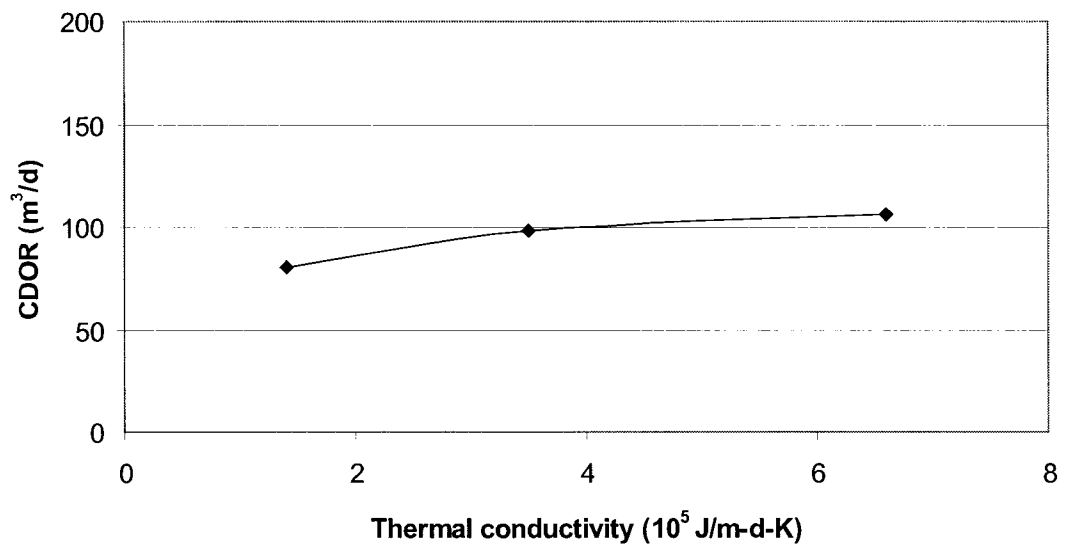
Figure 3.17c: Effect of rock thermal conductivity on CDOR

64

3.4.9 Best SAGD operating conditions

The most favourable SAGD operating conditions for Cold Lake-type reservoirs were derived from the numerical simulations. With the following reservoir parameters; permeability (K_v) of 1.25 Darcy, reservoir thickness of 20 m, and bitumen viscosity of 60,000 cp, the most favourable operating conditions are: I/P spacing of 10 m, maximum steam injection rate of 400 m^3/d at a maximum injection pressure of 3,100 kPa, and well pattern spacing of 80 m.

The simulations conducted with these best conditions gave the following results: CSOR of 2.80, CDOR of 96 m^3/d, and RF of 0.67. At least 20 m of reservoir thickness is required for an economical SAGD process in Cold Lake-type reservoirs.

3.5 Simulation results for Peace River-type reservoirs

The base case simulation conditions for the Peace River-type reservoirs are: preheating period of 150 days, I/P spacing of 10 m, operating pressure of 4,500 kPa, maximum steam injection rate of 600 m^3/d, well pattern spacing of 125 m, reservoir thickness of 25 m, reservoir permeability (K_v) of 0.65 Darcy. Table 3.5 shows the simulation results for the Peace River-type reservoir cases related to eight operating conditions and reservoir parameters. Individual results are given below.

3.5.1 Preheating period

The simulation conditions are: operating pressure of 4,500 kPa, maximum steam injection rate of 600 m^3/d, well pattern spacing of 125 m. Simulation results showed that the proper preheating period for an I/P spacing of 5 m is 50 days, 150 days is for an I/P spacing of 10 m, and 285 days for an I/P spacing of 15 m (Figure 3.18). There is not much enhancement in NPV even if the preheating periods are longer than these periods for each I/P spacing case. A preheating period of 50 days for an I/P spacing of 5 m is economically adequate for successful SAGD performance. The porosity of Peace River,

65

the lowest of the typical three oil sands areas (0.28), may result in the shortest preheating period, even though the overall economics is lowest in this type reservoir.
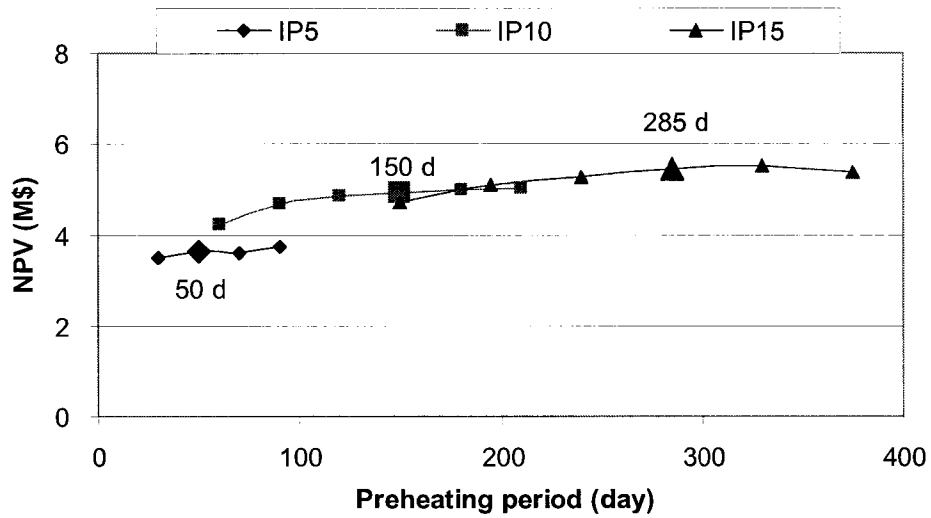
Figure 3.18a: Effect of preheating period on NPV
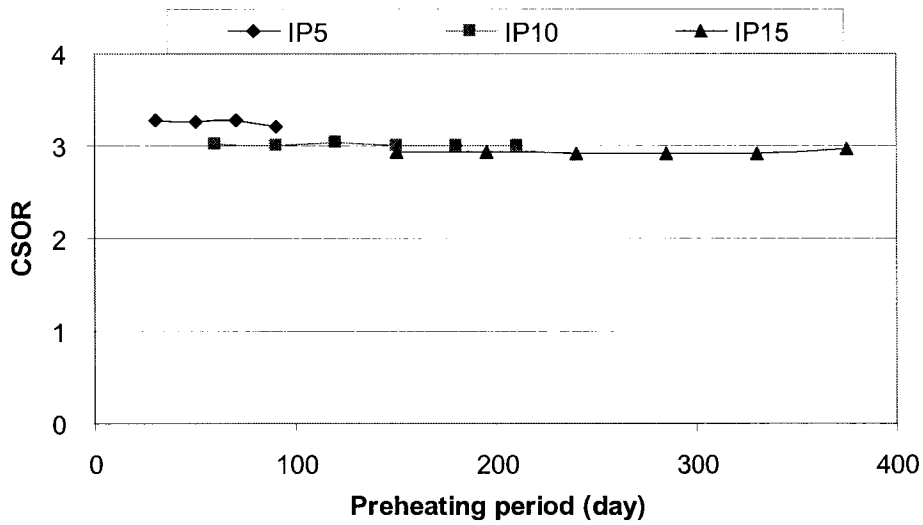
Figure 3.18b: Effect of preheating period on CSOR

66
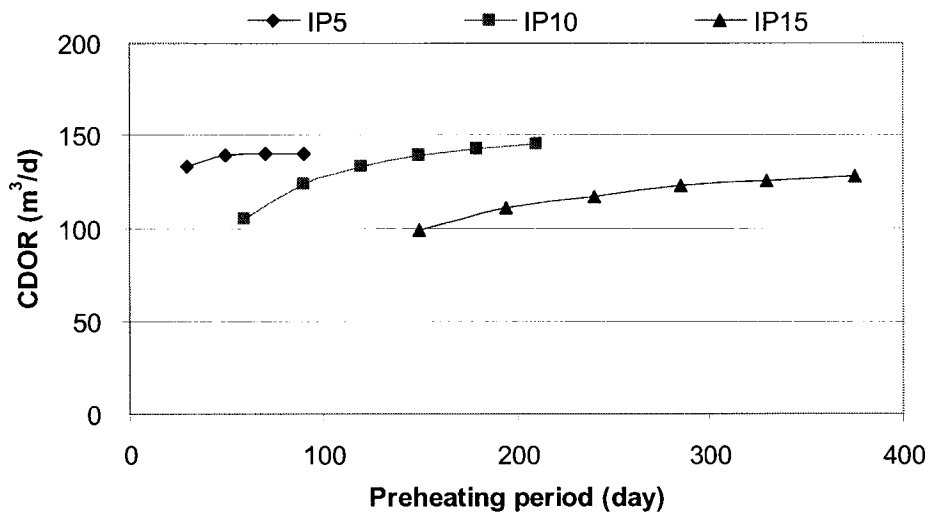
Figure 3.18c: Effect of preheating period on CDOR

3.5.2 Injector to Producer spacing

The simulation conditions for are: operating pressure of 4,500 kPa, maximum steam injection rate of 600 m³/d, well pattern spacing of 125 m. The simulations showed that, as the I/P spacing was increased from 5 m to 15 m, the NPV and ultimate recovery increased (Table 3.5). The CSOR decreased slightly from 3.00 to 2.91, and the CDOR decreased from 139 m³/d to 123 m³/d (Figure 3.19). An I/P spacing of 15 m gave the best SAGD performance: highest NPV and lowest CSOR. The low permeability of the Peace River reservoirs will give more effective SAGD performance with larger I/P spacing. There is not much enhancement in NPV even if the I/P spacing is greater than 10 m. Also, the larger I/P spacing may cause slow thermal communication in the field which is most likely not homogenous. Therefore, an I/P spacing of 10 m is recommended for Peace River-type reservoir.

67

Table 3.5: SAGD simulation results for Peace River- type reservoir

Case	Cum. Production (m³)	CSOR	CDOR (m³/d)	RF	NPV (M$)
Preheating period					
90 d	196,955	3.01	124	0.31	4.7
120 d	204,757	3.04	133	0.33	4.9
150 d	195,942	3.00	139	0.31	4.9
180 d	196,269	3.00	142	0.31	5.0
210 d	196,792	3.00	145	0.31	5.0
Injector to Producer (I/P) spacing					
5 m	193,170	3.26	139	0.31	3.6
10 m	195,942	3.00	139	0.31	4.9
15 m	217,816	2.91	123	0.35	5.5
Operating pressure (I/P spacing 5 m)					
4,500 kPa	193,170	3.26	139	0.31	3.6
6,000 kPa	171,008	3.77	165	0.27	1.0
7,500 kPa	65,967	4.44	149	0.11	-0.9
Max. steam injection rate					
300 m³	436,324	3.87	75	0.69	0.5
400 m³	380,231	3.59	105	0.60	3.8
500 m³	227,220	3.13	136	0.36	4.9
600 m³	196,269	3.00	142	0.31	5.0
Well pattern spacing					
60 m	206,708	2.66	146	0.67	6.9
80 m	266,922	3.00	131	0.65	6.5
100 m	208,820	3.05	145	0.41	5.4
120 m	205,662	3.04	146	0.34	5.1
150 m	196,489	2.99	147	0.26	5.1
Reservoir thickness (well pattern spacing 100 m)					
15 m	59,701	3.34	109	0.20	1.1
20 m	119,382	2.98	125	0.29	3.3
25 m	324,742	3.33	130	0.64	5.1
30 m	410,784	3.03	153	0.67	9.1
Reservoir permeability (Kv)					
0.65 D	196,269	3.00	142	0.31	5.0
1.25 D	234,071	2.81	213	0.37	7.6
2.5 D	449,116	3.12	221	0.71	10.6
Rock thermal conductivity (I/P spacing 5 m)					
Low	181,529	2.62	104	0.29	6.2
Middle	188,698	3.02	124	0.30	4.7
High	193,170	3.26	139	0.31	3.6
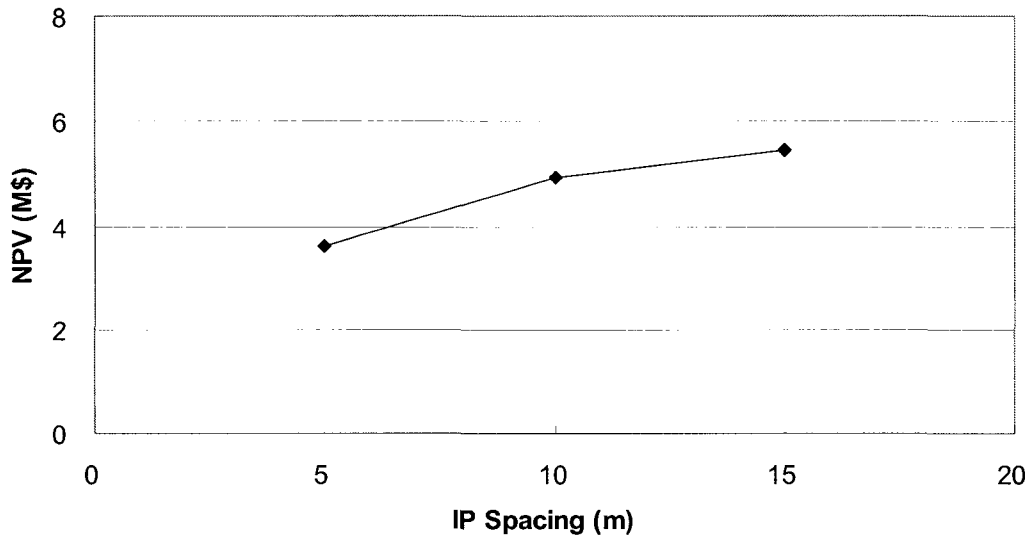
Figure 3.19a: Effect of I/P spacing on NPV
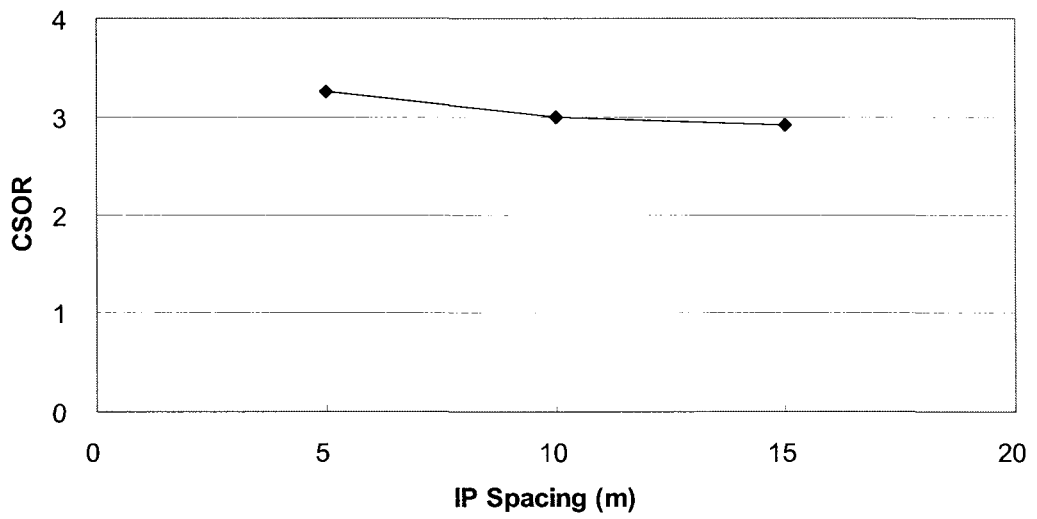
Figure 3.19b: Effect of I/P spacing on CSOR

69
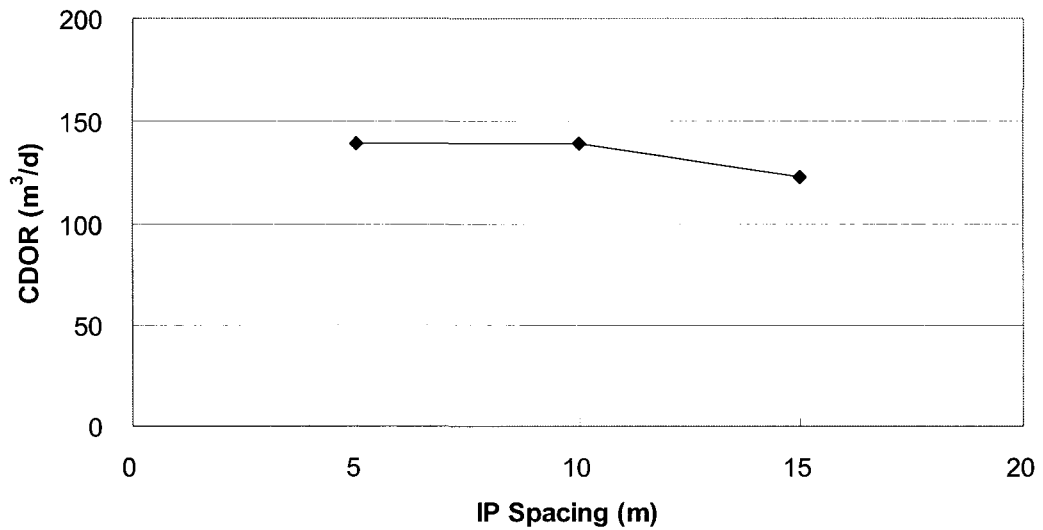
Figure 3.19c: Effect of I/P spacing on CDOR

3.5.3 Steam injection pressure

The simulation conditions are: preheating period of 150 days, I/P spacing of 10 m, maximum steam injection rate of 600 m³/d, well pattern spacing of 125 m. The simulation results showed that, as the steam injection pressure was increased from 4,500 to 7,500 kPa, CSOR and CDOR increased (Figure 3.20), and the recovery factor decreased (Table 3.5). A steam injection pressure of 4,500 kPa gave the highest NPV with lowest CSOR. Therefore, a steam injection pressure of 4,500 kPa is the proper SAGD operating pressure for Peace River-type reservoirs. For this type of low permeability reservoirs, the higher the injection pressure, the higher the heat loss to the overburden. An operating pressure of 4,500 kPa is the lowest operating pressure required at the reservoir depth of Peace River reservoirs (600 m).

70
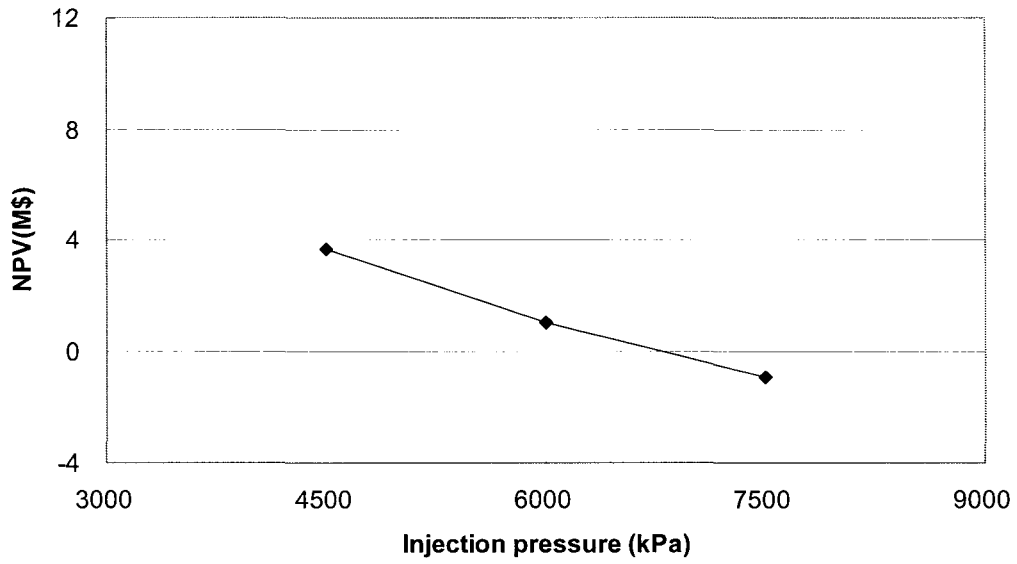
Figure 3.20a: Effect of steam injection pressure on NPV
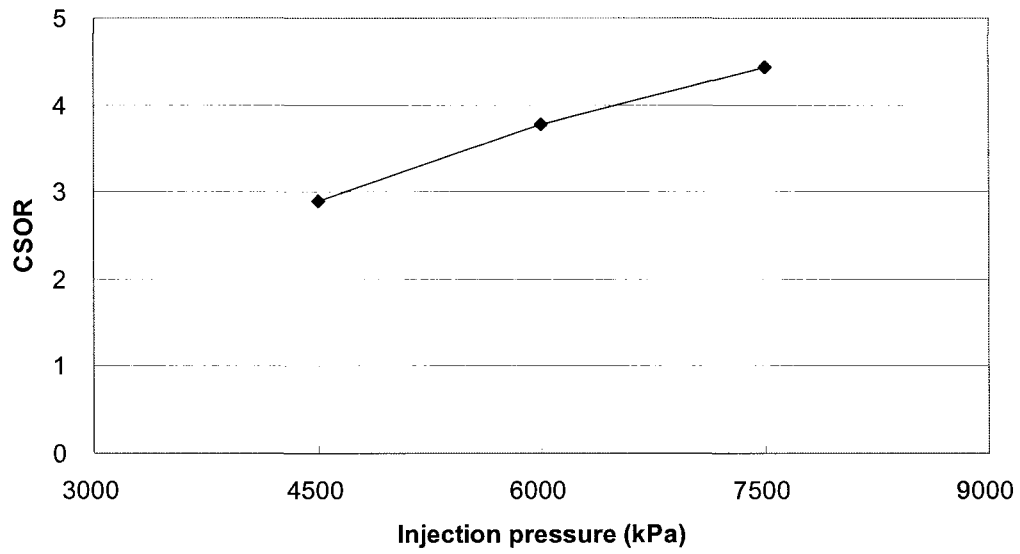
Figure 3.20b: Effect of steam injection pressure on CSOR

71
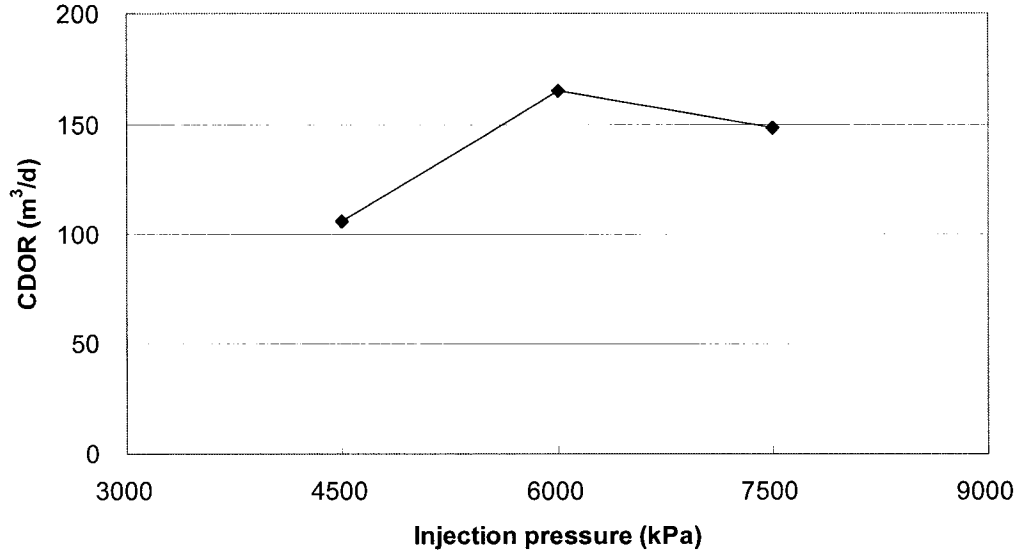
Figure 3.20c: Effect of steam injection pressure on CDOR

3.5.4 Maximum steam injection rate

The simulation conditions are: preheating period of 150 days, I/P spacing of 10 m, operating pressure of 4,500 kPa, well pattern spacing of 125 m. As the steam injection rate was increased, CSOR and ultimate recovery decreased, and CDOR increased (Table 3.5). A steam injection rate of less than 400 m^3/d gives high ultimate recovery, but the CSOR is too high due to poor thermal efficiency. Also, the CDOR is low because of long project life. The NPV was the highest in the case of 600 m^3/d (Figure 3.21).

72
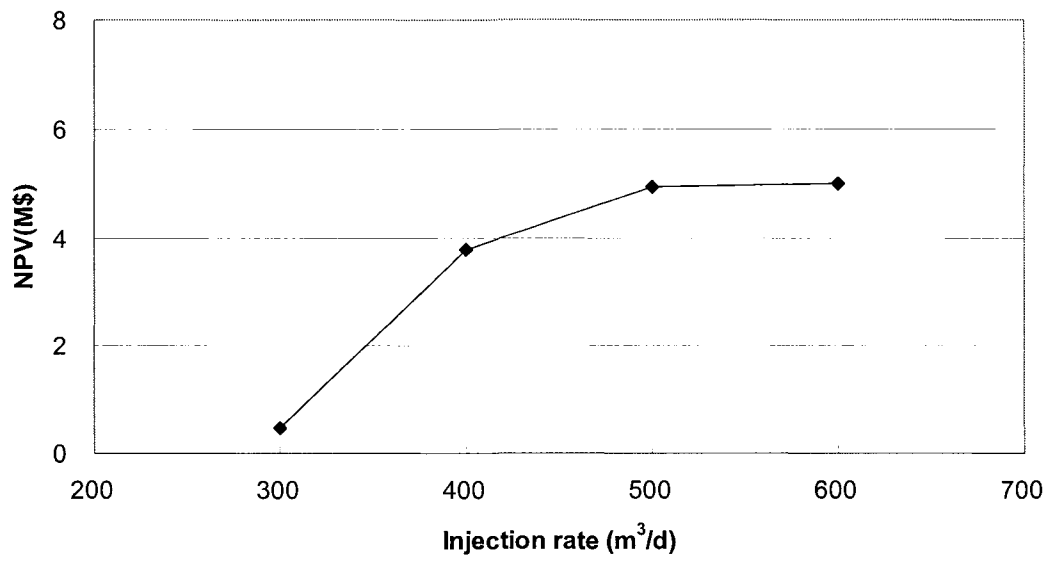
Figure 3.21a: Effect of steam injection rate on NPV
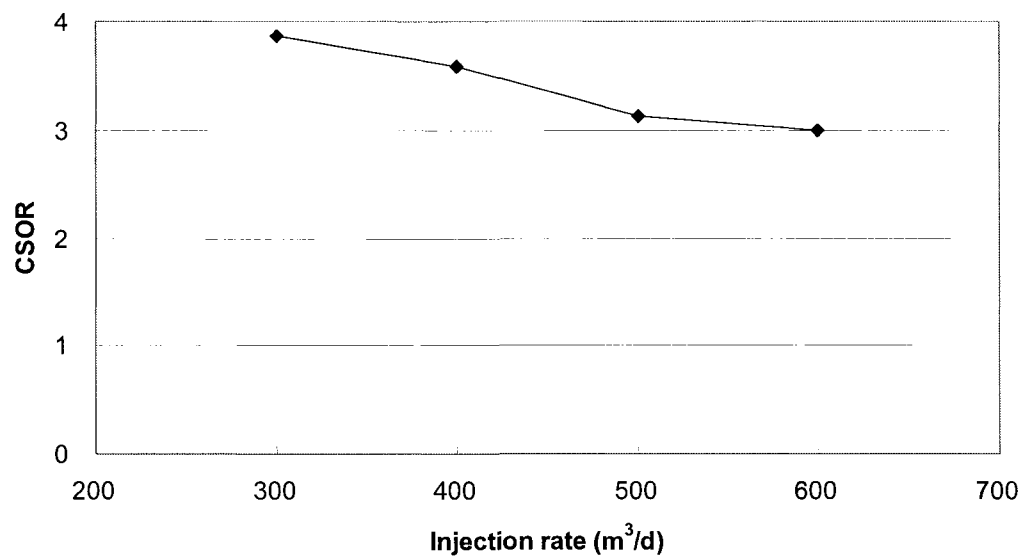
Figure 3.21b: Effect of steam injection rate on CSOR

73
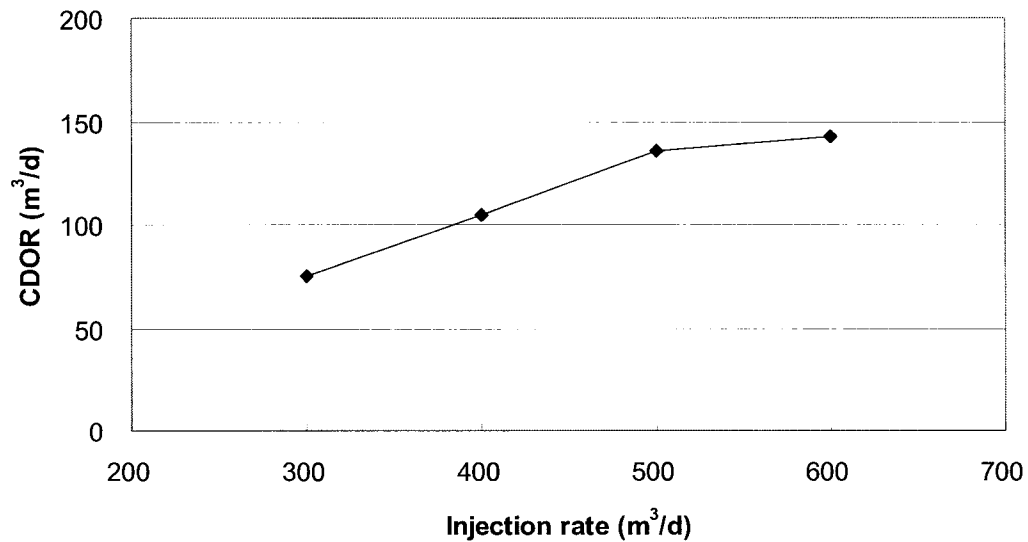
Figure 3.21c: Effect of steam injection rate on CDOR

3.5.5 SAGD well pattern spacing

The simulation conditions are: preheating period of 150 days, I/P spacing of 10 m, operating pressure of 4,500 kPa, maximum steam injection rate of 600 m^3/d. Simulation results for a Peace River-type reservoir, as the well pattern spacing is increased, indicate that the NPV decreases. The CDOR is almost constant at a value of 145 m^3/d except for the 80 m case (Figure 3.22). The recovery factor is considered a key parameter in determining the proper well pattern spacing. If the well spacing is larger than 100 m, the recovery factor drops below 0.4. A narrower well pattern spacing will give a more economical SAGD operation. A well pattern spacing of about 80 m can be applied for Peace River-type reservoirs.

74
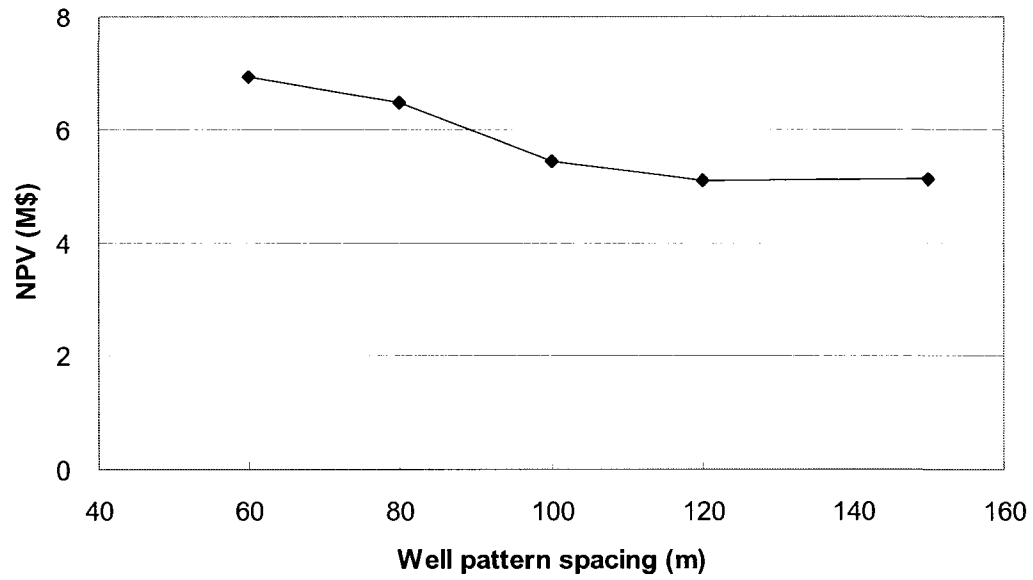
Figure 3.22a: Effect of well pattern spacing on NPV
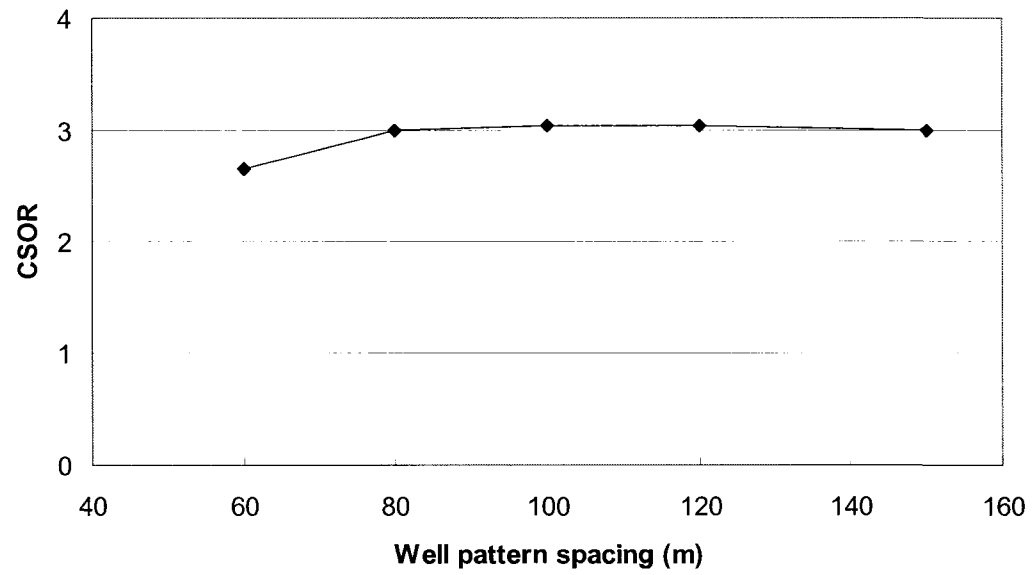
Figure 3.22b: Effect of well pattern spacing on CSOR

75
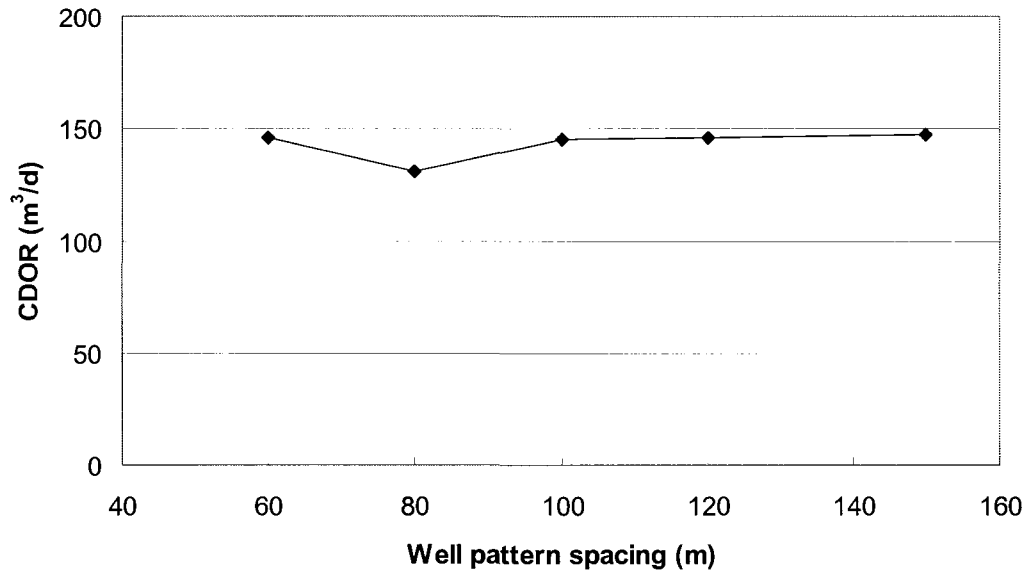
Figure 3.22c: Effect of well pattern spacing on CDOR
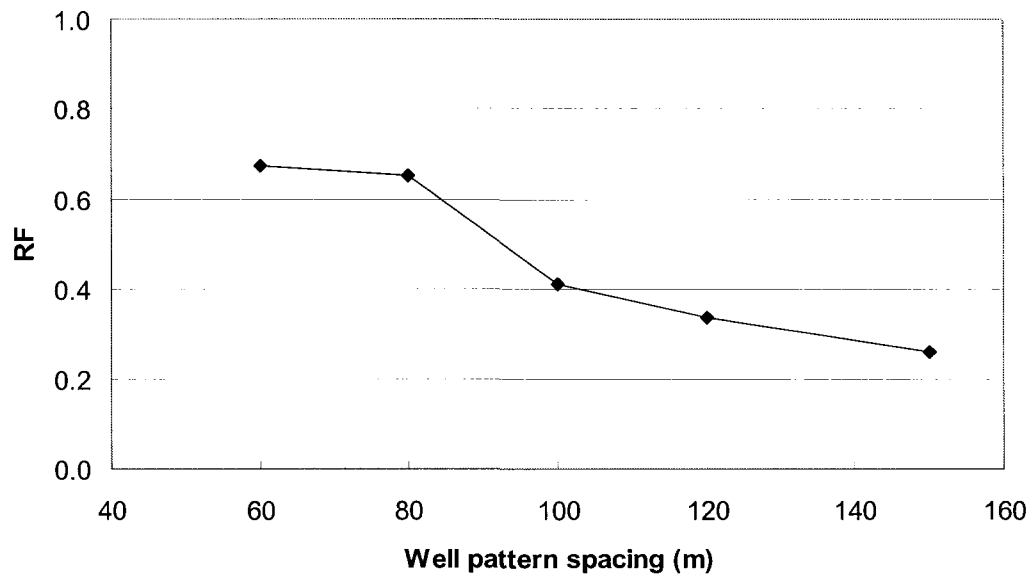
Figure 3.22d: Effect of well pattern spacing on RF

76

3.5.6 Reservoir thickness

These simulations were conducted to evaluate the effect of reservoir thickness on SAGD performance under the following conditions: I/P spacing of 5 m, operating pressure of 4,500 kPa, maximum steam injection rate of 600 m^3/d, well pattern spacing of 100 m, permeability (K_v) of 0.65 Darcy ($K_h/K_v = 3$). As the thickness is increased, the CDOR and recovery factor increase and CSOR decreases slightly (Figure 3.23). Even if the reservoir thickness is greater than 25 m, there is not enough enhancement for a SAGD project to be economical: low recovery factor and high CSOR. Considering the capital costs, it is assumed that the NPV value has to be higher than 5 million dollars for an economic SAGD project. Therefore, it is believed that a low permeability of 0.65 Darcy is inefficient for the SAGD application.
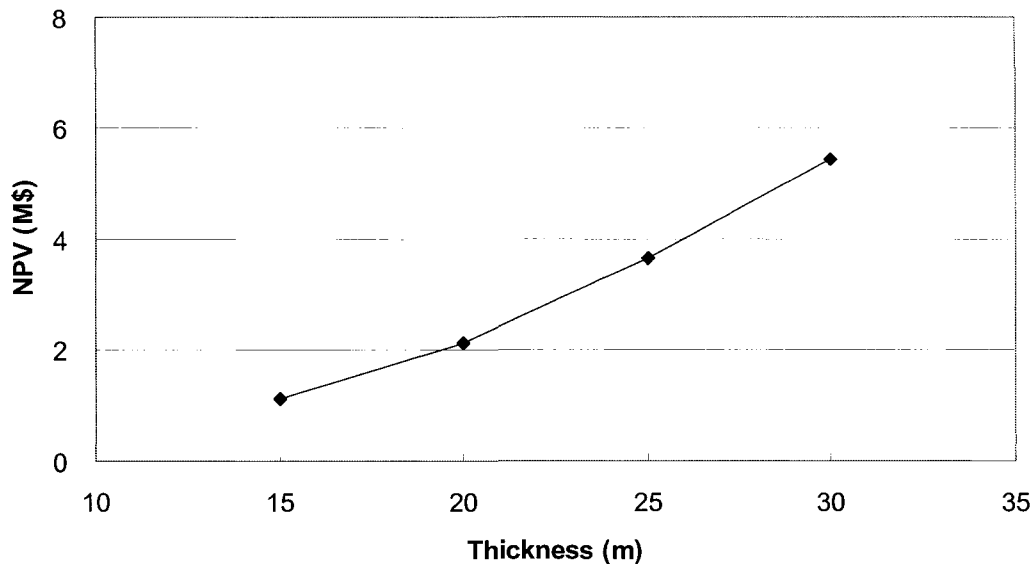
Figure 3.23a: Effect of reservoir thickness on NPV

77
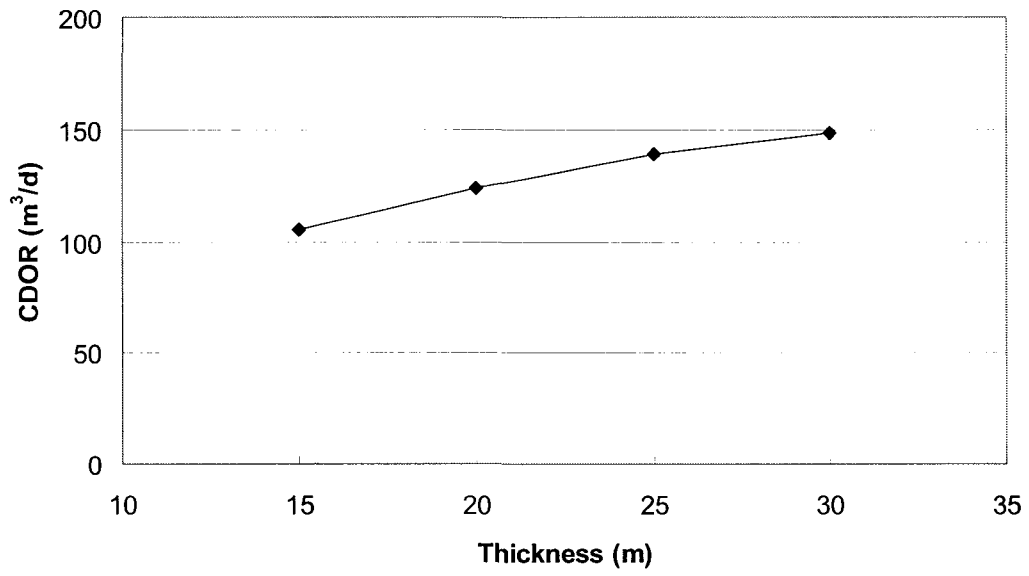
Figure 3.23b: Effect of reservoir thickness on CDOR
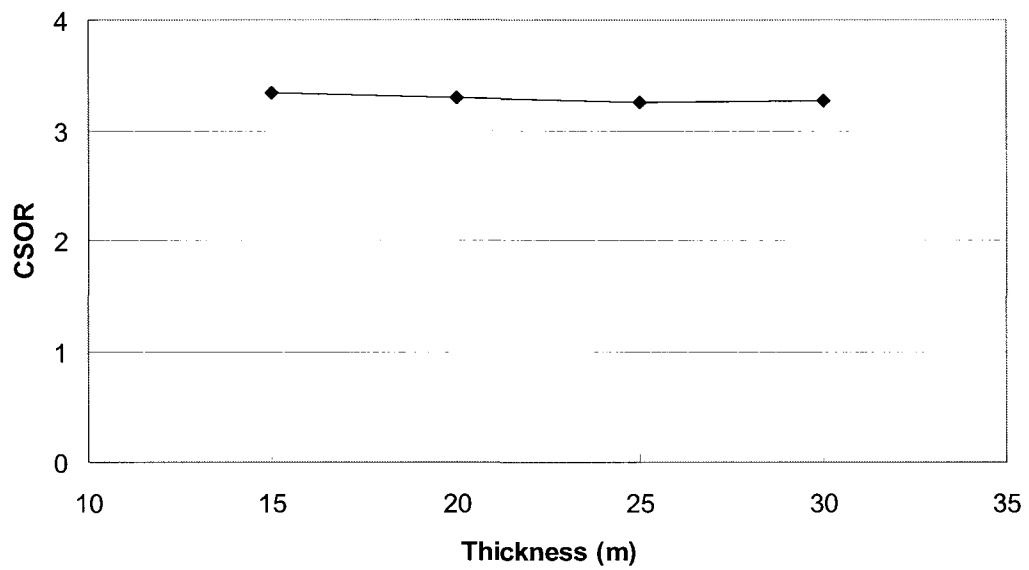
Figure 3.23c: Effect of reservoir thickness on CSOR

78

3.5.7 Reservoir permeability

The simulation conditions are: preheating period of 150 days, I/P spacing of 10 m, operating pressure of 4,500 kPa, maximum steam injection rate of 600 m^3/d, reservoir thickness of 25 m.

The simulation results indicated that SAGD performance improved as the permeability (K_v) increased; giving lower CSOR, higher CDOR and recovery factor (Figure 3.24). A vertical permeability of 0.65 Darcy seems too low for an efficient SAGD process as the ultimate recovery is less than 0.4. If the vertical permeability is higher than 1.25 Darcy, all the SAGD performance parameters become good economic indicators. The CSOR is lower in the 1.25 Darcy case compared to the 2.5 Darcy case because the 2.5 Darcy case produced more oil for a longer project life until an instantaneous SOR of 4 was reached.
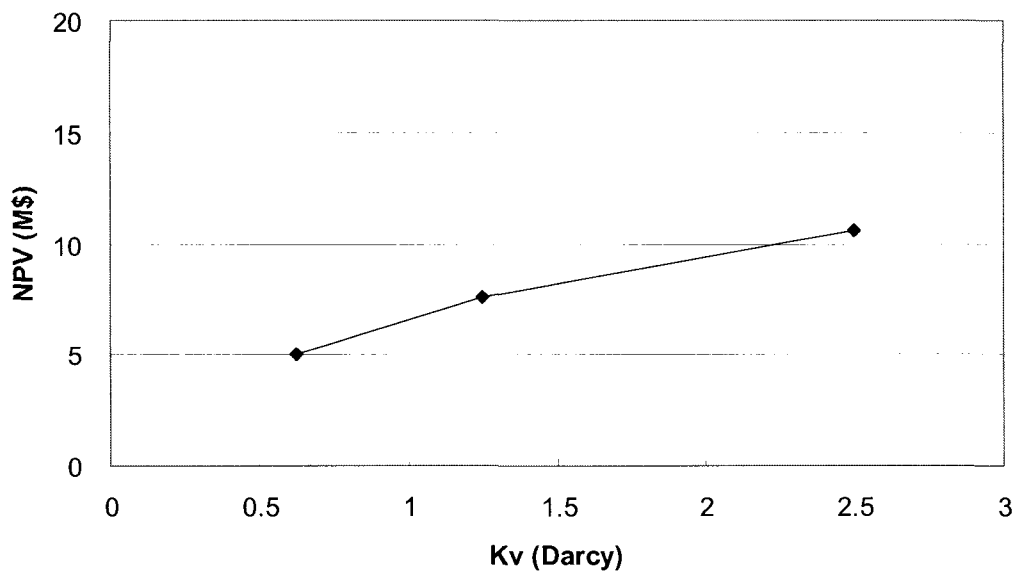
Figure 3.24a: Effect of reservoir permeability on NPV

79
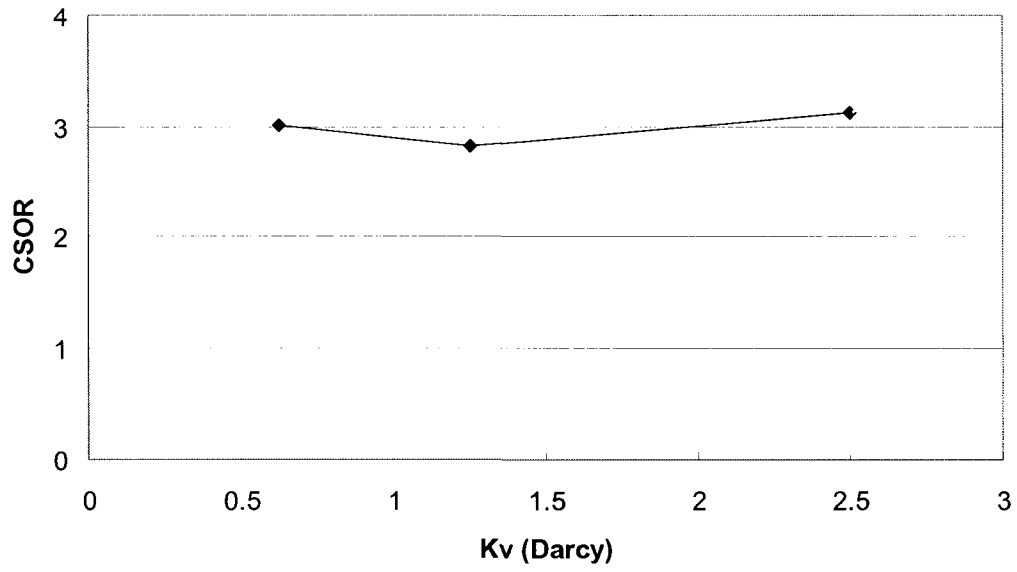
Figure 3.24b: Effect of reservoir permeability on CSOR
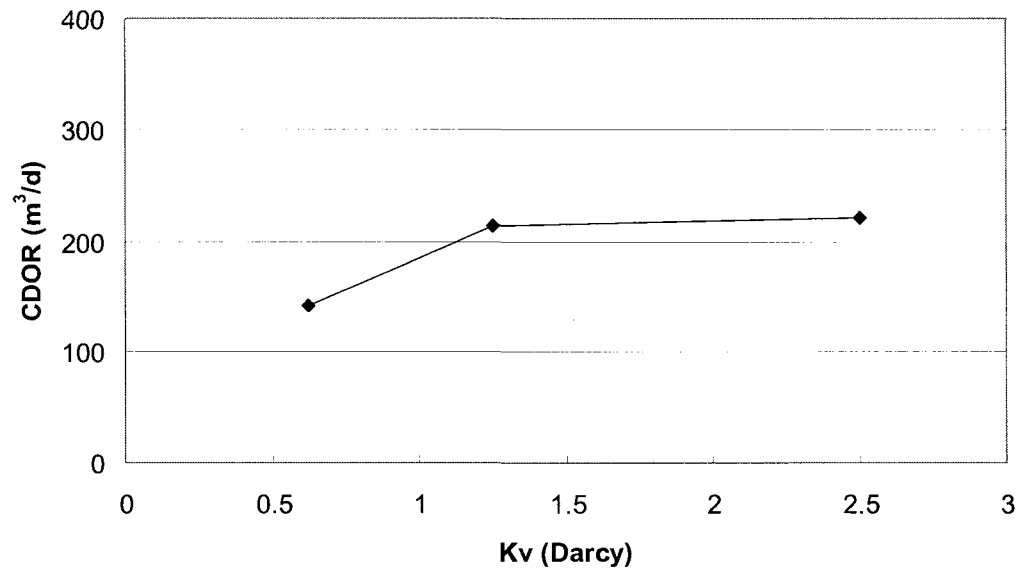
Figure 3.24c: Effect of reservoir permeability on CDOR

80
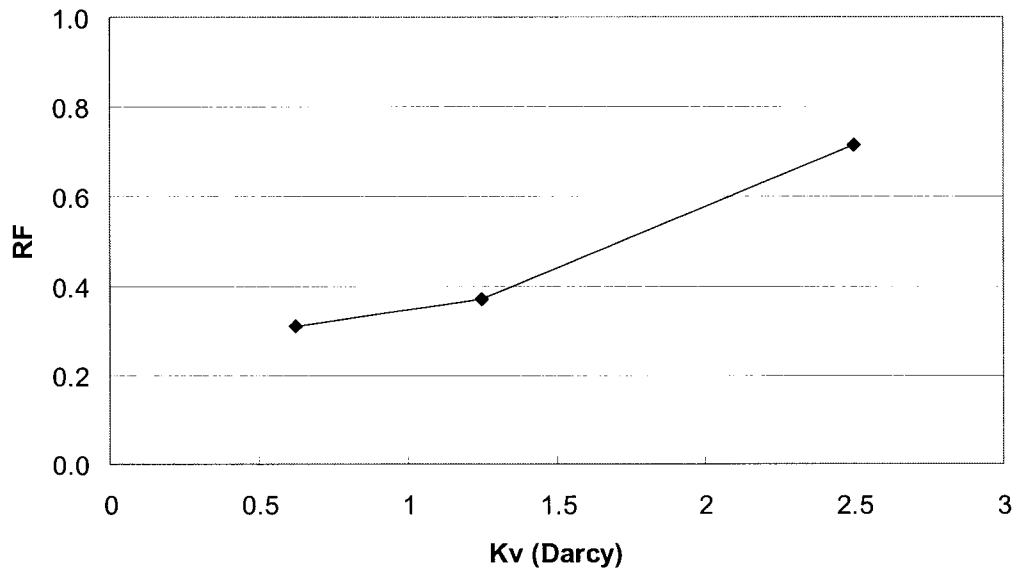
Figure 3.24d: Effect of reservoir permeability on RF

3.5.8 Rock thermal conductivity

The simulation conditions are: preheating period of 150 days, I/P spacing of 10 m, operating pressure of 4,500 kPa, maximum steam injection rate of 600 m^3/d, reservoir thickness of 25 m.

The simulation results showed that, as the rock thermal conductivity increased, the NPV decreased because of the higher CSOR which means poor thermal efficiency. Ultimate recovery increased, as well as CDOR (Figure 3.25). Low rock thermal conductivity gives better SAGD performance in Peace River-type reservoirs.

81
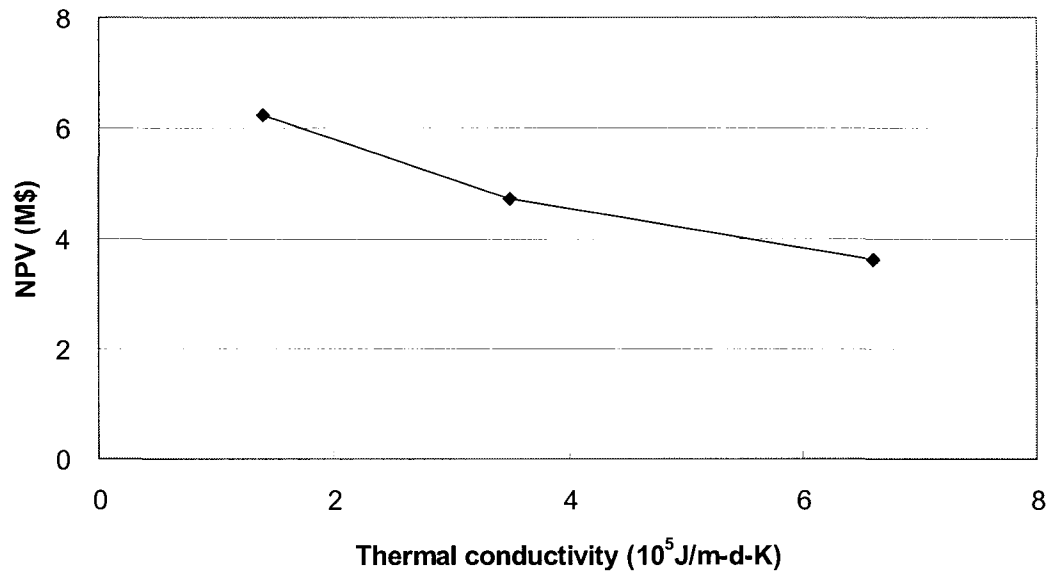
Figure 3.25a: Effect of rock thermal conductivity on NPV
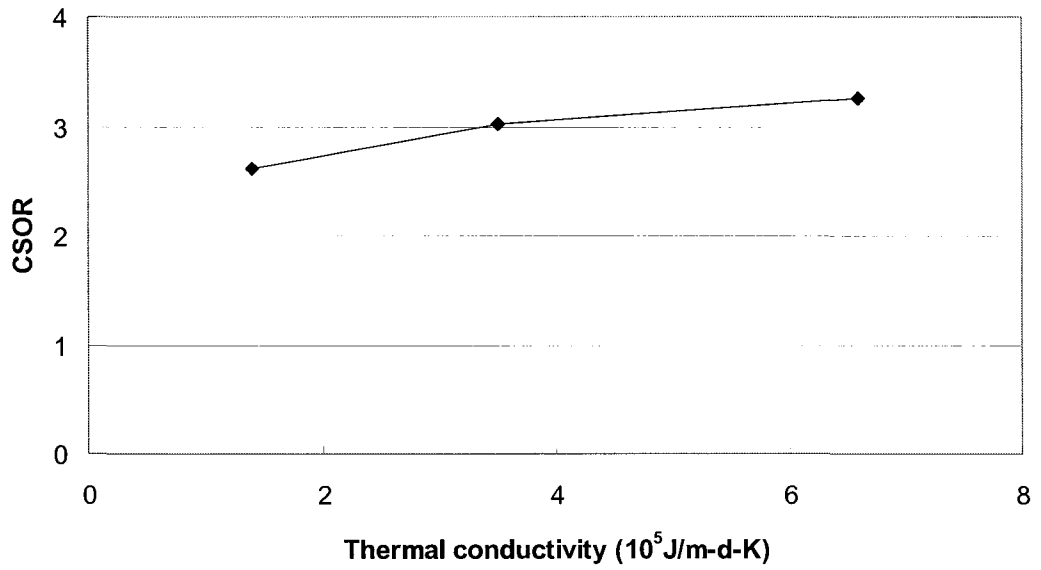
Figure 3.25b: Effect of rock thermal conductivity on CSOR

82
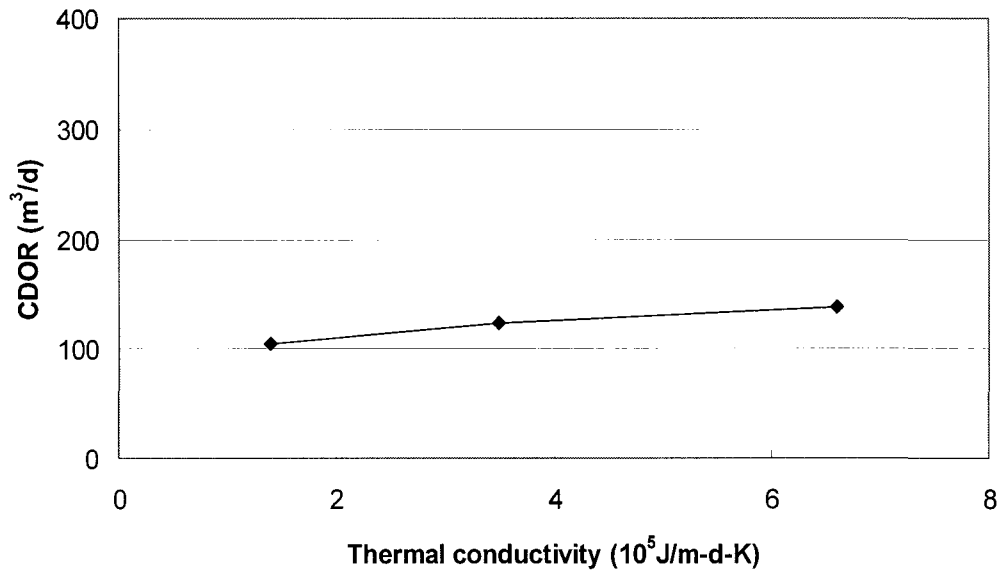
Figure 3.25c: Effect of rock thermal conductivity on CDOR

3.5.9 Best SAGD operating conditions

The most favourable SAGD operating conditions for Peace River-type reservoirs were derived from the numerical simulations. With the following reservoir parameters; permeability (K_v) of 0.65 Darcy, reservoir thickness of 25 m, and bitumen viscosity of 200,000 cp, the most favourable operating conditions are: I/P spacing of 10 m, maximum steam injection rate of 600 m^3/d at a maximum injection pressure of 4,500 kPa, and well pattern spacing of 80 m.

The simulations conducted with these best operating conditions gave the following results: CSOR of 3.00, CDOR of 130 m^3/d, and RF of 0.65. It is believed that permeability should be greater than 0.65 Darcy for a successful SAGD process.

83

4 NUMERICAL SIMULATIONS FOR THE FAST-SAGD PROCESS

The Fast-SAGD process was introduced by Polikar et al. (2000), combining the SAGD and CSS processes. The CSS helps the steam chamber formed by SAGD to propagate sideways, and will also enhance the thermal efficiency in the reservoir. The CSS process from the offset well results in the enhancement of the Fast-SAGD process due to the higher steam injection pressure which results in geomechanical and steam drive effects (Gong et al., 2002). Shin and Polikar (2004) investigated the best operating conditions of Fast-SAGD for a typical reservoir.

In this study, base case simulations of the Fast-SAGD process for the three reservoir types were conducted, and compared with the SAGD process.

4.1. Simulation model and schemes

The two-dimensional simulation model was designed as a symmetrical grid system, assuming that an offset well is located on both sides of the SAGD well pair. The total grid number is 101 x 1 x 20~30 (i, j, k) for the SAGD model and 151 x 1 x 20~30 (i, j, k) for the Fast-SAGD model (Figures 4.1a, 4.1b). Offset wells were placed 50 m away from the SAGD producer. The following procedure was used for the Fast-SAGD operation:

1) start the SAGD well pairs in SAGD mode
2) start CSS at the offset well after 1.5 years
3) keep injecting steam into the SAGD well after start of CSS

The CSS at each offset well was operated for two cycles, with the conditions indicated in Table 4.1. The first cycle was operated with three phases: nine months of injection, two weeks of soak, and two and half months of production.

SAGD   SAGD

20~30

Injector   Injector

Producer   Producer

1   101

Figure 4.1a: Grid system and well locations for SAGD

SAGD   Offset   Offset   SAGD

20~30

Injector   Injector

Producer   Producer

1   51   101   151
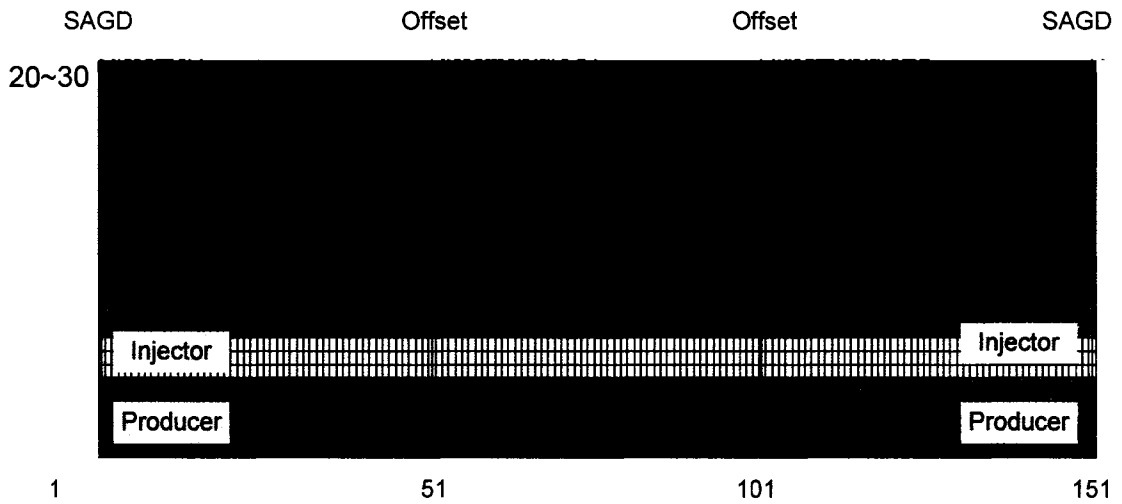
Figure 4.1b: Grid system and well locations for Fast-SAGD

85

For the second cycle, the operation consisted of six months of injection, two weeks of soak, and then the production period. In the offset well, steam is injected into the reservoir at pressures as high as 4,500 to 8,000 kPa, which is lower than reservoir fracturing pressure, depending on reservoir type (Table 4.1).

It is important to select the proper time to begin the CSS operation at the first offset well. The startup time of the CSS operation for the base case was selected based on previous research results of the Fast-SAGD process (Polikar et al., 2000, Gong et al., 2002). In this study, the initiation time of the CSS at the first offset well was 1.5 years after the beginning of the SAGD operation. This is the time at which the steam chamber reached the top of the reservoir and began to propagate sideways.

The CSS operation at the offset well results in the steam chamber expanding sideways (Figure 4.2). For an effective Fast-SAGD performance, the expanded steam chamber at the SAGD injector must be maintained after the cyclic steam injection at the offset well by injecting additional steam.

Table 4.1: Simulation conditions for the Fast-SAGD base cases

Condition	Athabasca-type		Cold Lake-type		Peace River-type	
	SAGD well pair	Offset well	SAGD well pair	Offset well	SAGD well pair	Offset well
Max. injection pressure (kPa)	1,510	4,500	3,110	8,000	4,510	8,000
Max. injection rate (CWE m^3/d)	600	1,600	400	800	400	800
Production pressure (kPa)	1,500	1,500	3,100	3,100	4,500	4,500
Extra steam after CSS (CWE m^3/d)	600	-	400	-	400	-
CSS start-up time	-	1.5 yr	-	1.5 yr	-	1.5 yr

SAGD   SAGD

Figure 4.2a: SAGD steam chamber temperature profile after 5 years

SAGD   Offset   Offset   SAGD
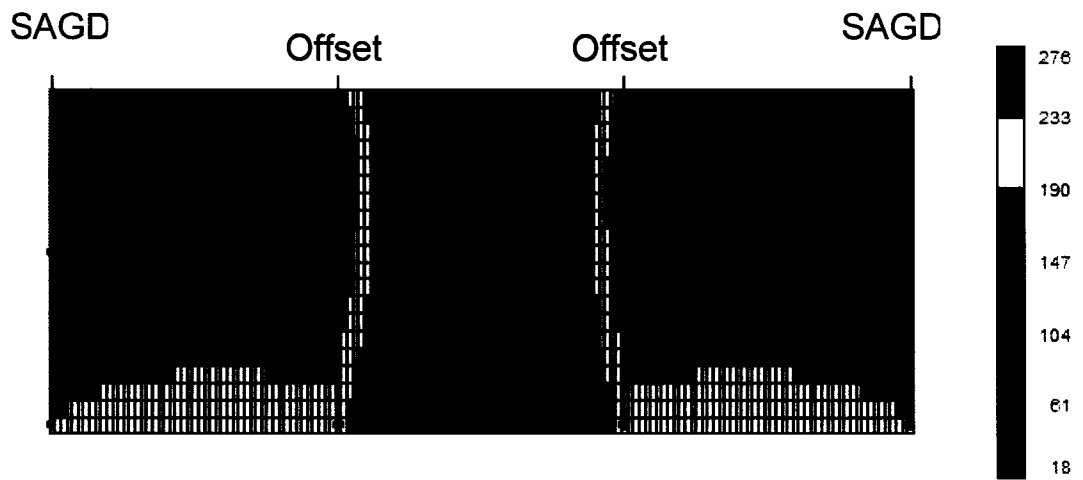
Figure 4.2b: Fast-SAGD steam chamber temperature profile after 5 years

87

4.2 Simulation results for Athabasca-type reservoirs

This reservoir type has the shallowest depth, the thickest pay and the highest permeability with highest bitumen viscosity. The simulations were conducted under the following conditions: I/P spacing of 5 m, reservoir permeability (Kv) of 2.5 Darcy, and reservoir thickness of 30 m. Table 4.2 shows simulation results for the shallow Athabasca-type reservoir cases related to three operating conditions and reservoir thickness.

Table 4.2: Fast-SAGD simulation results for Athabsca-type reservoirs

Case	Cum. Production (m^3)	CSOR	CDOR (m^3/d)	RF	NPV (M$)
1) Offset well location					
40 m	755,486	1.49	247	0.83	44.4
50 m	969,052	1.41	234	0.85	55.7
60 m	1,170,032	1.44	227	0.86	61.0
70 m	1,368,452	1.54	237	0.86	66.6
2) CSS startup time at the offset well					
1 yr	982,530	1.41	187	0.86	51.2
1.5 yrs	969,052	1.41	234	0.85	55.7
2 yrs	953,820	1.51	240	0.84	52.7
2.5 yrs	970,064	1.54	249	0.85	53.0
3) Steam injection pressure at the offset well					
3,000 kPa	989,804	1.44	173	0.87	49.8
4,500 kPa	969,052	1.41	234	0.85	55.7
6,000 kPa	961,134	1.46	247	0.84	55.1
4) Reservoir thickness					
15 m	218,968	2.51	145	0.38	15.6
20 m	619,499	2.03	201	0.81	29.7
25 m	773,204	1.69	240	0.81	41.6
30 m	949,412	1.52	258	0.83	53.9

4.2.1 Offset Well Location

To choose the most favourable distance between the offset well and the SAGD well pair, the simulations were conducted with a maximum offset well pressure of 4,500 kPa, a maximum steam injection rate of 1,600 m^3/d at the offset well, and additional steam injection of 600 m^3/d into the SAGD injector.

NPV increased with distance because of larger well configuration. The CSOR has the lowest value at 50 m offset well distance, and the CDOR the highest value at 40 m offset well distance (Figure 4.3). The larger offset well distance can be applied in thicker and high permeable reservoirs, but this distance has to be chosen considering drilling costs. In this type of reservoir, larger than 50 m of offset well spacing will be economic.
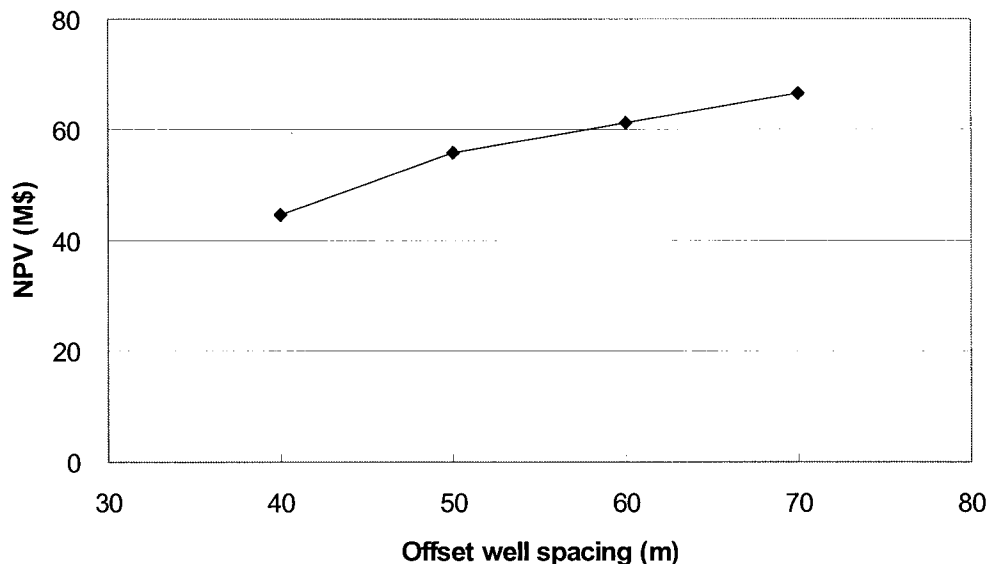
Figure 4.3a: Effect of offset well spacing on NPV

89
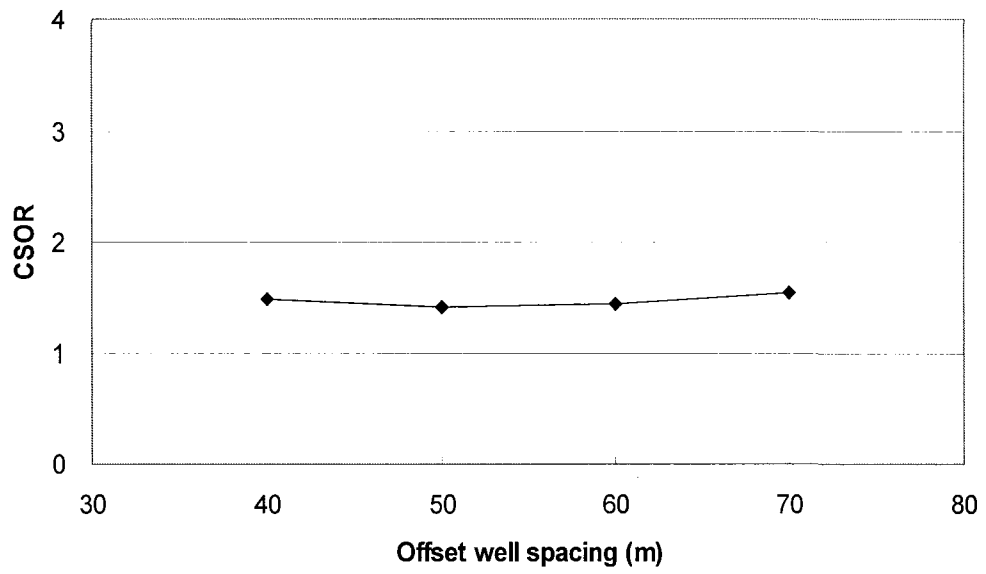
Figure 4.3b: Effect of offset well spacing on CSOR
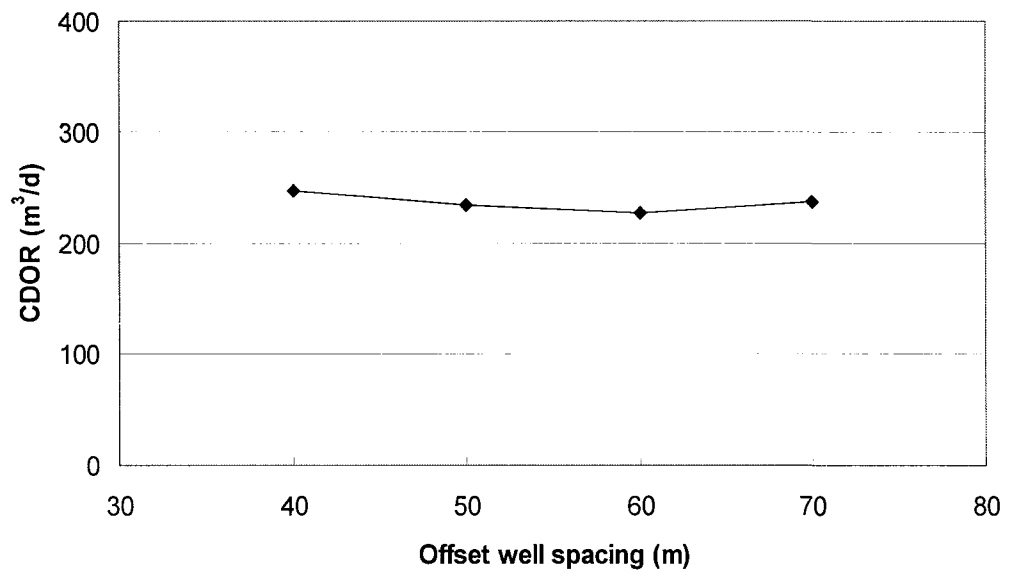
Figure 4.3c: Effect of offset well spacing on CDOR

90

4.2.2 CSS startup time at the Offset Well

The proper CSS startup time at the offset well is important during the Fast-SAGD process. This startup time will change depending on the offset well distance. Simulations were conducted with an offset well spacing of 50 m and a steam injection pressure of 4,500 kPa.

The results showed that NPV was highest in the case of 1.5 years with lowest CSOR (Figure 4.4). The CDOR increased, as the startup time was increased, however there was no big increase after 1.5 years. The CSS startup time of 1.5 years is the proper one for this reservoir type.
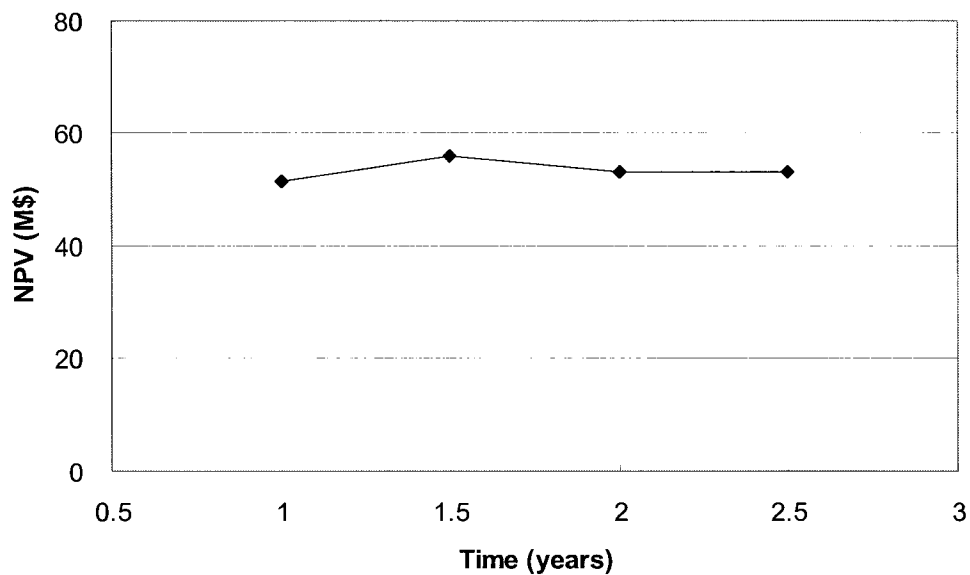
Figure 4.4a: Effect of CSS startup time at the offset well on NPV

91
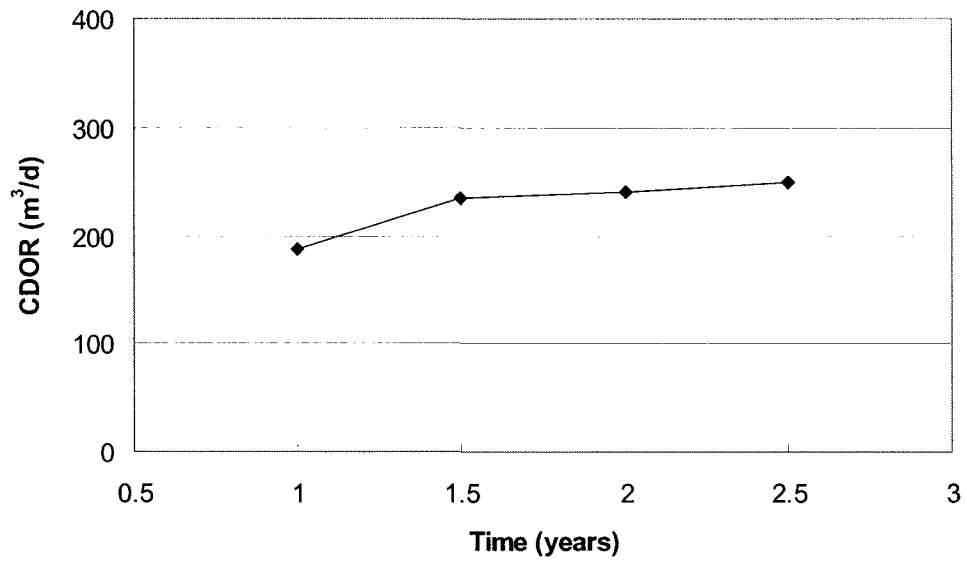
Figure 4.4b: Effect of CSS startup time at the offset well on CDOR
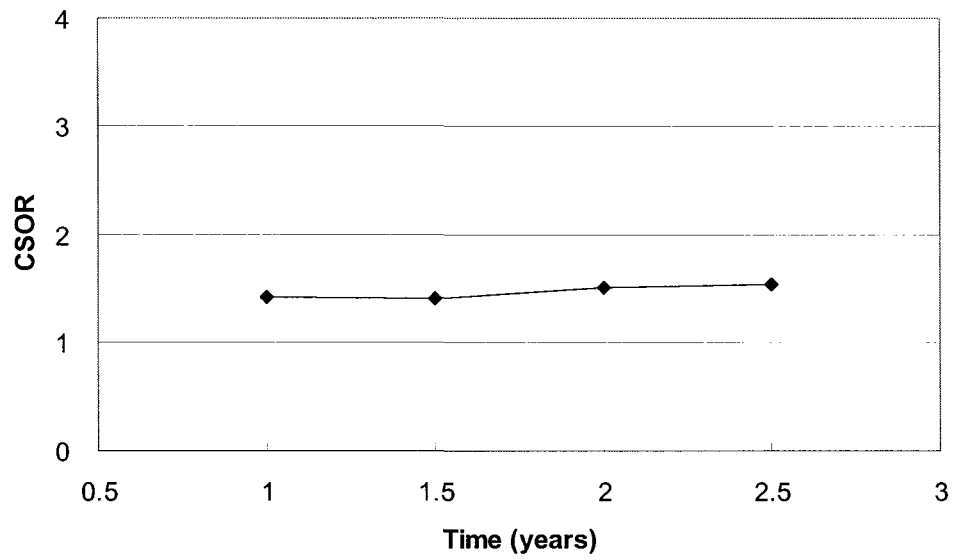
Figure 4.4c: Effect of CSS startup time at the offset well on CSOR

92

4.2.3 Steam Injection Pressure at the Offset Well

Simulations were conducted to determine the proper steam injection pressure at the offset well. With the offset well spacing of 50 m, the simulation results showed that NPV value was highest at 4,500 kPa due to the higher CDOR and lower CSOR (Figure 4.5). Even though the CDOR was highest at the injection pressure of 6,000 kPa, NPV value was not highest because of higher CSOR. An injection pressure of 4,500 kPa at the offset well is adequate in this type reservoir.
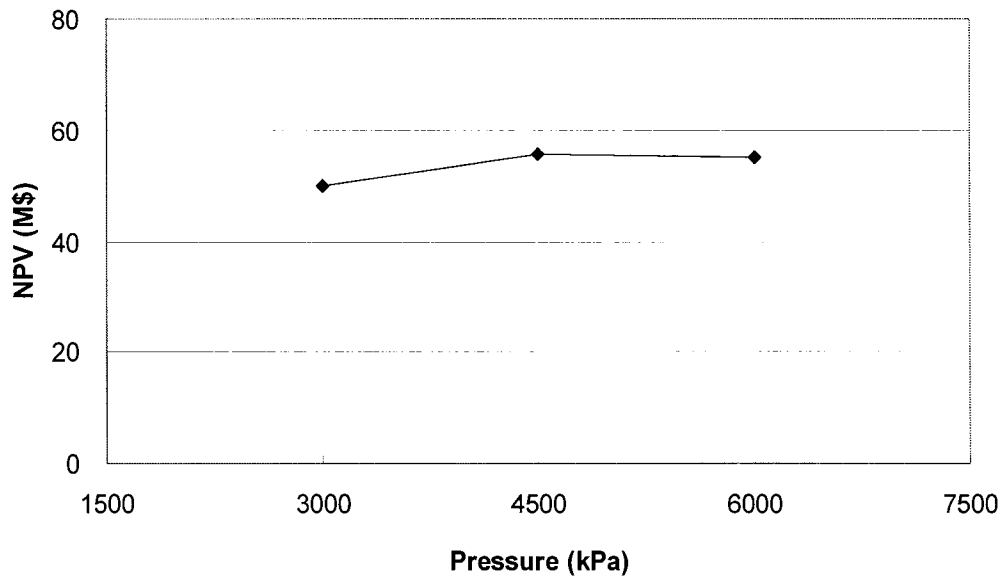
Figure 4.5a: Effect of steam injection pressure at the offset well on NPV

93
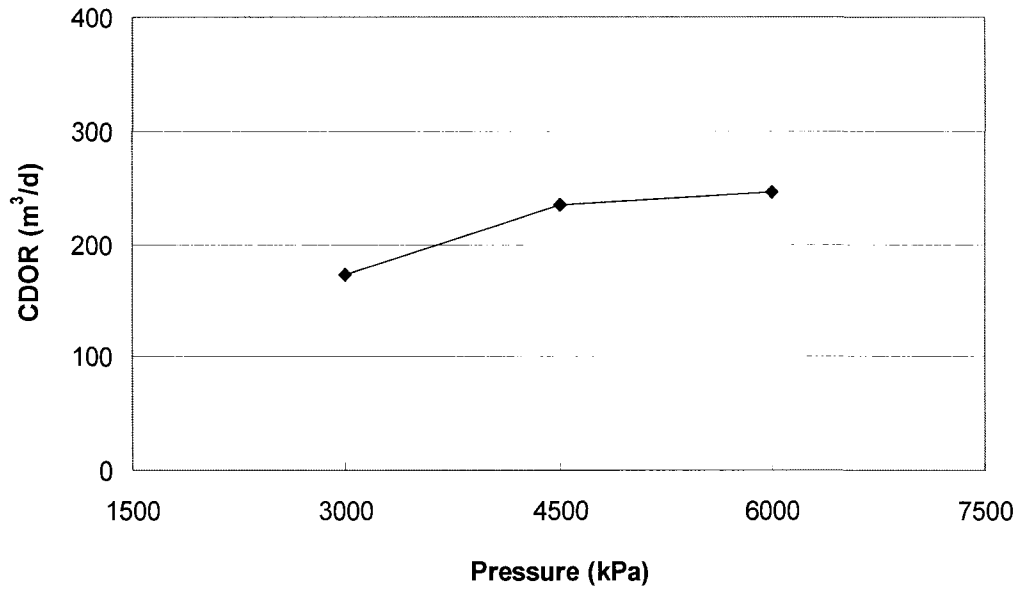
Figure 4.5b: Effect of steam injection pressure at the offset well on CDOR
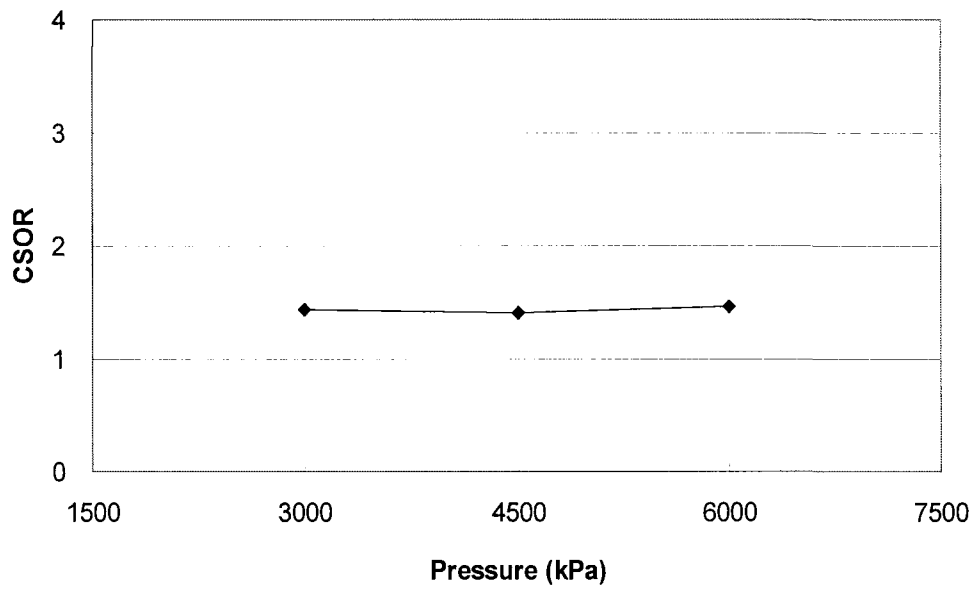
Figure 4.5c: Effect of steam injection pressure at the offset well on CSOR

94

4.2.4 Reservoir Thickness

The simulations were conducted to evaluate the effect of reservoir thickness on the Fast-SAGD performance. As the thickness is increased, CSOR decreases and both CDOR and RF increase (Figure 4.6). RF is higher than 0.8 for a reservoir thicker than 20 m. Even if the pay thickness is as thin as 15 m for the high permeable Athabasca-type reservoir, the Fast-SAGD seems to be an economical operation: NPV is higher than 15 M$ (Table 4.2).

4.2.5 Best operating conditions

Simulation results for a shallow Athabasca-type reservoir, which is a thick and highly permeable reservoir, give the following best operating conditions: offset well spacing of 50 m, CSS startup time of 1.5 years, and steam injection pressure of 4,500 kPa at the offset well.
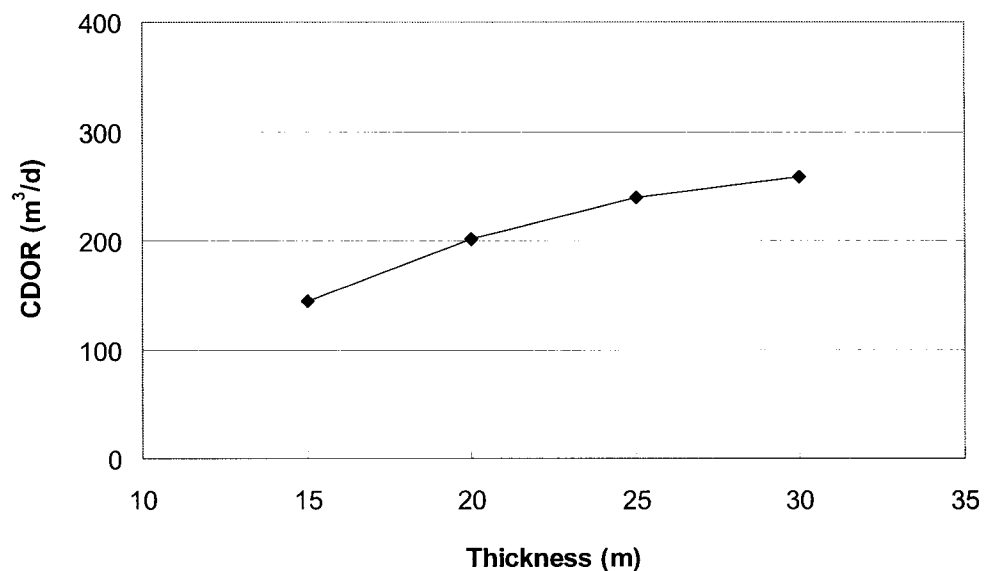
Figure 4.6a: Effect of reservoir thickness on CDOR

95
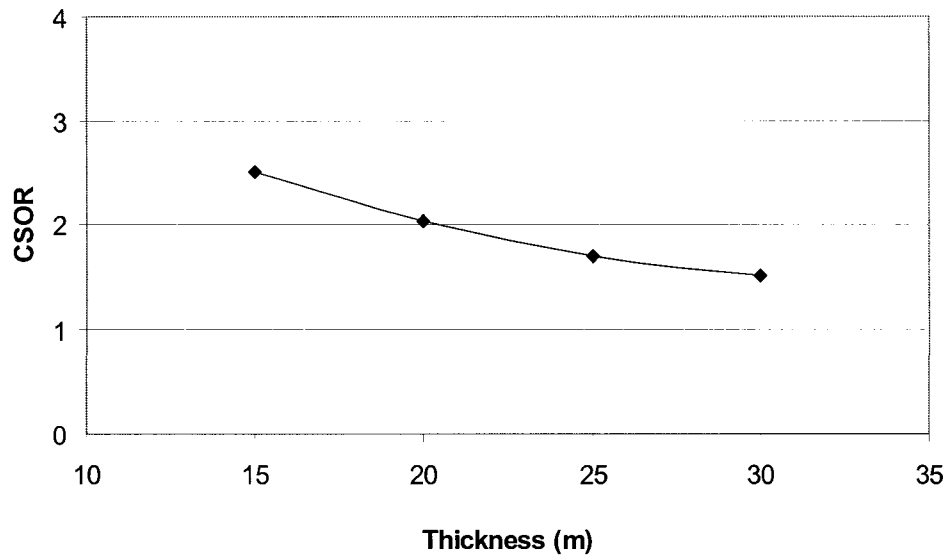
Figure 4.6b: Effect of reservoir thickness on CSOR
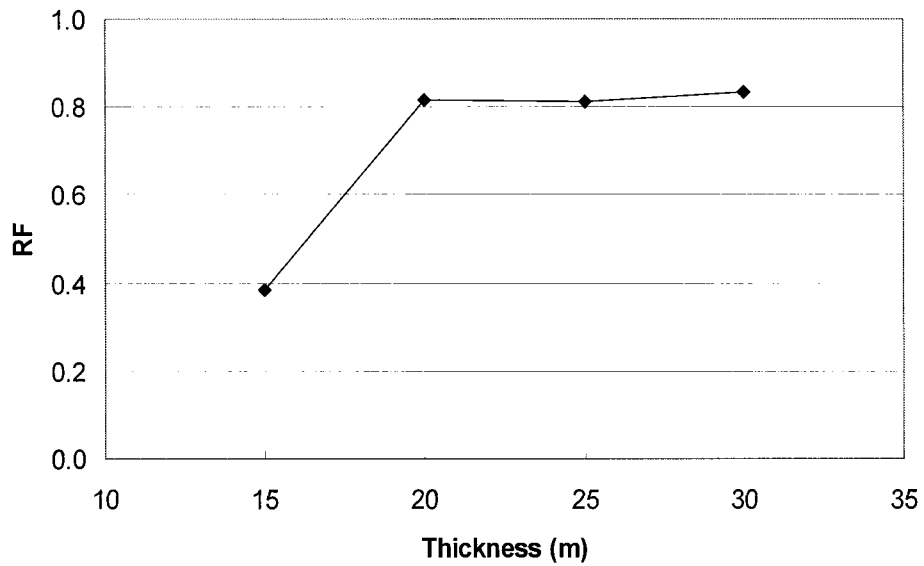
Figure 4.6c: Effect of reservoir thickness on RF

96

4.3 Simulation results for Cold Lake-type reservoirs

This reservoir type has the thinnest pay and lowest bitumen viscosity. The simulations were conducted under the following conditions: I/P spacing of 10 m, reservoir permeability (Kv) of 1.25 Darcy, and reservoir thickness of 20 m. Table 4.3 shows simulation results for the Cold Lake-type reservoir cases related to three operating conditions and reservoir thickness.

Table 4.3: Fast-SAGD simulation results for Cold Lake-type reservoirs

Case	Cum. Production (m^3)	CSOR	CDOR (m^3/d)	RF	NPV (M$)
1) Offset well location					
40 m	359,424	2.40	121	0.74	13.7
50 m	407,633	2.31	109	0.67	15.3
60 m	465,272	2.65	96	0.64	12.9
70 m	517,044	2.82	91	0.61	11.8
2) CSS startup time at the offset well					
1 yr	418,730	2.52	76	0.69	11.6
1.5 yrs	407,633	2.31	109	0.67	15.3
2 yrs	434,422	2.52	111	0.71	14.6
2.5 yrs	443,707	2.69	106	0.73	12.8
3) Steam injection pressure at the offset well					
4,500 kPa	394,263	3.07	54	0.65	7.7
6,000 kPa	397,324	2.45	91	0.65	13.2
8,000 kPa	407,633	2.31	109	0.67	15.3
4) Reservoir thickness					
15 m	276,954	3.03	105	0.61	6.6
20 m	407,633	2.31	109	0.67	15.3
25 m	554,606	2.22	117	0.73	20.8
30 m	685,302	2.09	124	0.75	26.2

4.3.1 Offset Well Location

To choose the best distance between the offset well and the SAGD well pair, the simulations were conducted with a maximum offset well pressure of 8,000 kPa, a maximum steam injection rate of 800 m³/d at the offset well, and additional steam injection of 400 m³/d into the SAGD injector.

NPV was highest at the offset well spacing of 50 m with lowest CSOR (Figures 4.7a, 4.7b), and CDOR was highest at 40 m offset well distance (Figure 4.7c). It might be said that less than 50 m of offset well spacing is adequate for the thin reservoirs.
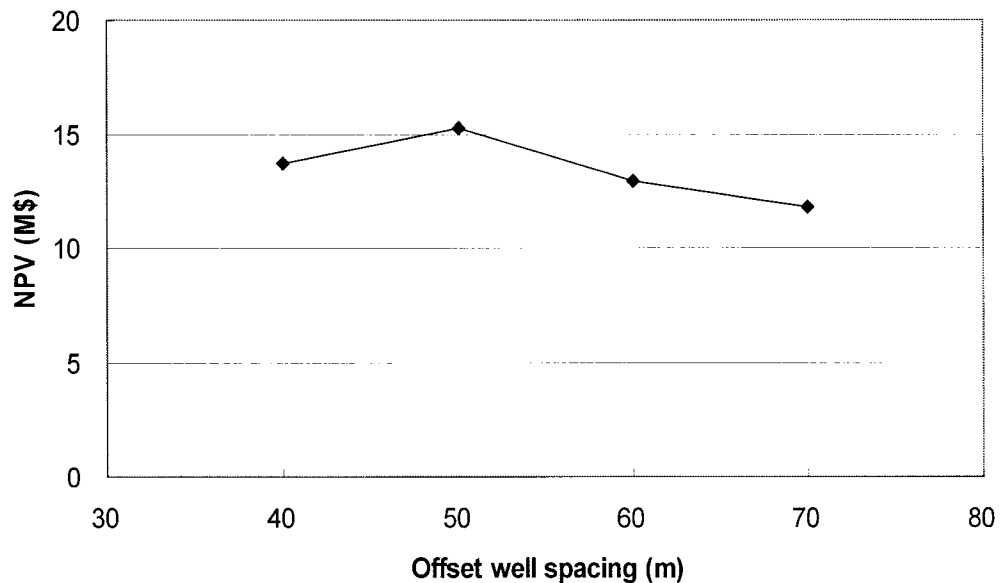
Figure 4.7a: Effect of offset well spacing on NPV

98
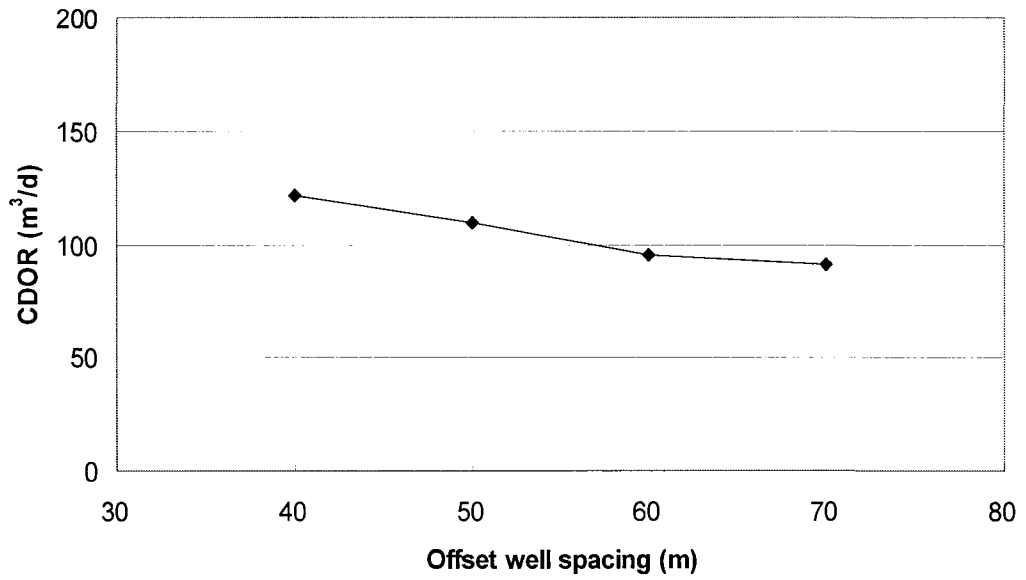
Figure 4.7b: Effect of offset well spacing on CDOR
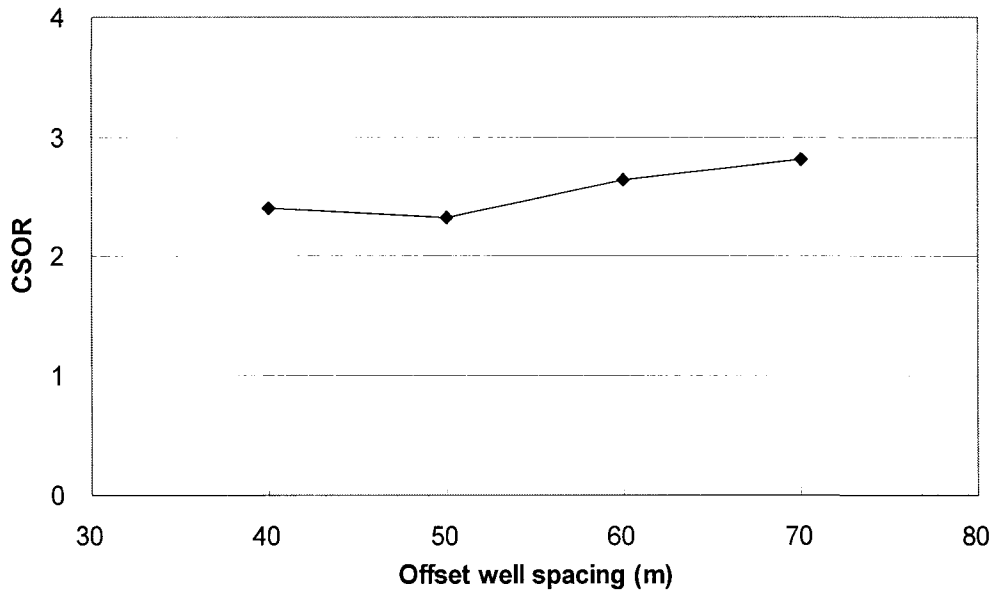
Figure 4.7c: Effect of offset well spacing on CSOR

99

4.3.2 CSS startup time at the Offset Well

Simulations were conducted with an offset well spacing of 50 m and a steam injection pressure of 8,000 kPa. The results showed that NPV was highest in the case of 1.5 years with the lowest CSOR and high CDOR (Figure 4.8).

The startup time of 1 year seems to be too early for the CSS startup time during the Fast-SAGD process due to the lower CDOR. The CSS startup time of 1.5 years is the proper one for this reservoir type.
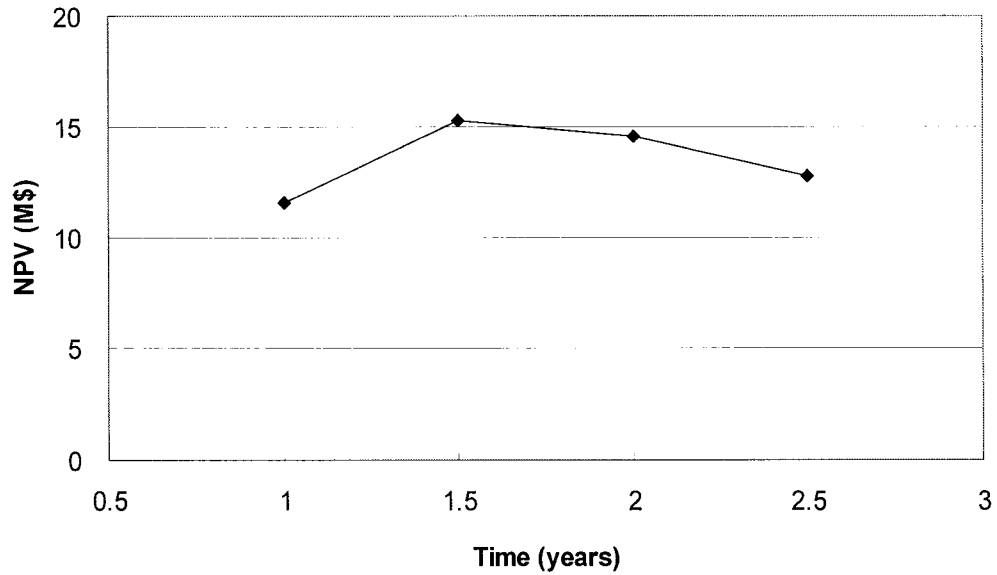
Figure 4.8a: Effect of CSS startup time at the offset well on NPV

100
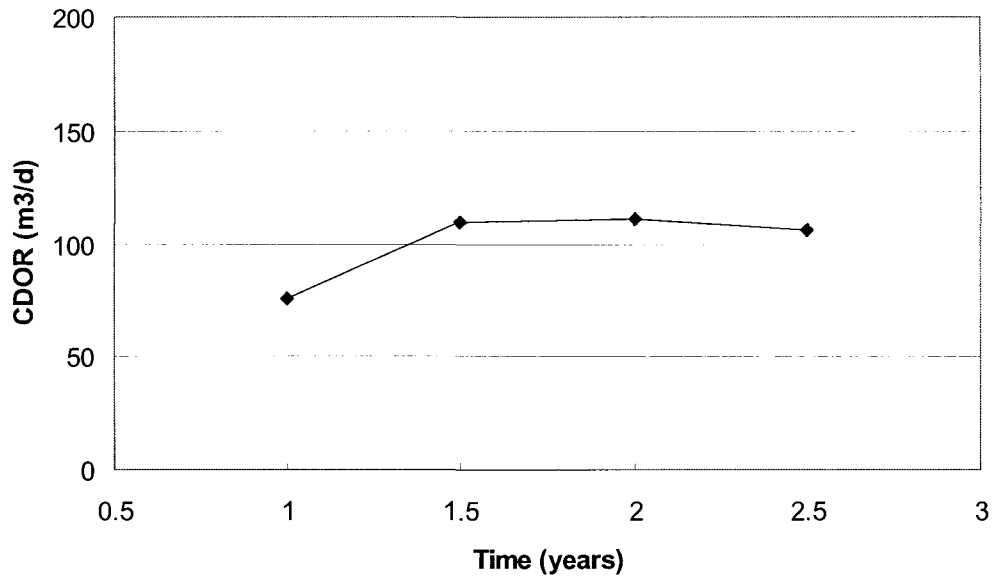
Figure 4.8b: Effect of CSS startup time at the offset well on CDOR
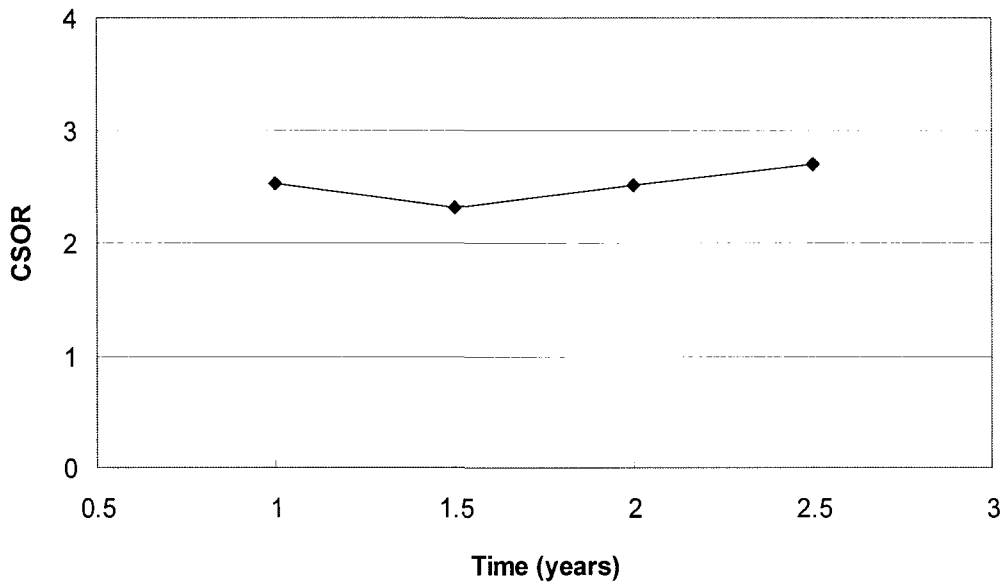
Figure 4.8c: Effect of CSS startup time at the offset well on CSOR

101

4.3.3 Steam Injection Pressure at the Offset Well

With the offset well spacing of 50 m, the simulation results showed that the NPV value was highest at 8,000 kPa due to the highest CDOR and lowest CSOR (Figures 4.9a).

As the steam injection pressure is increased, CDOR increases and CSOR decreases (Figure 4.9b, 4.9c). An injection pressure of 8,000 kPa at the offset well is adequate in this reservoir type.
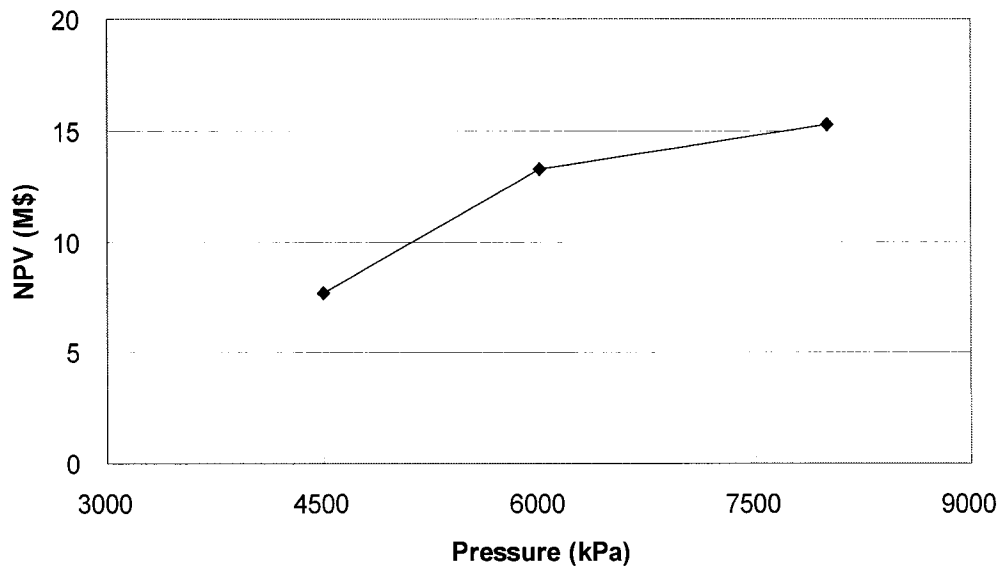
Figure 4.9a: Effect of steam injection pressure at the offset well on NPV

102
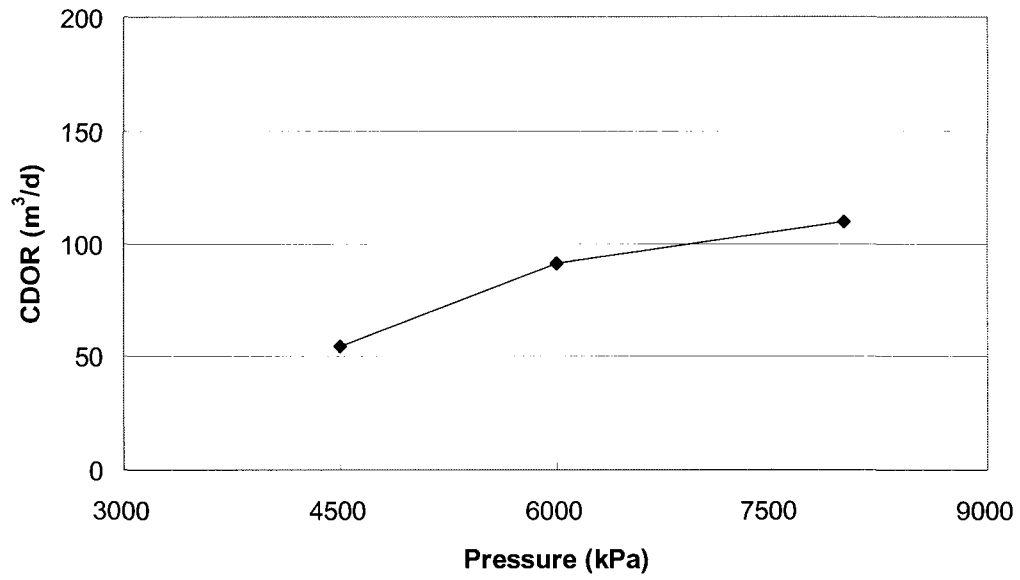
Figure 4.9b: Effect of steam injection pressure at the offset well on CDOR
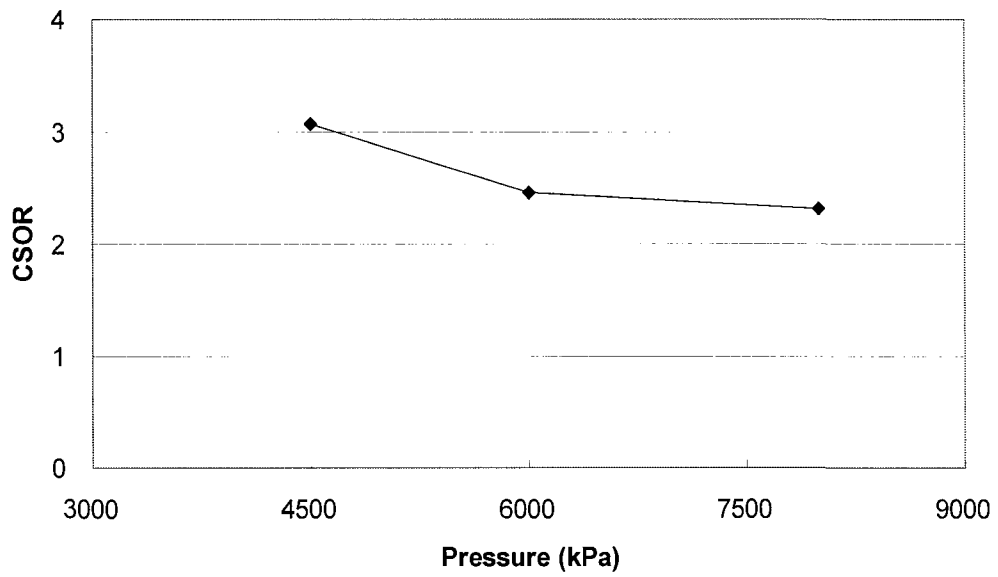
Figure 4.9c: Effect of steam injection pressure at the offset well on CSOR

103

4.3.4 Reservoir Thickness

The simulations were conducted to evaluate the effect of reservoir thickness on the Fast-SAGD performance. As the thickness is increased, CSOR decreases and both CDOR and RF increase (Figures 4.10a, 4.10b, 4.10c). At least the pay thickness should be thicker than 20 m for an economical Fast-SAGD operation: NPV is higher than 15.3 M$ (Figure 4.10d).

4.3.5 Best operating conditions

Simulation results for a Cold Lake-type reservoir, which is thin and moderately permeable, give the following most favourable operating conditions: offset well spacing of 40 m, CSS startup time of 1.5 years, and steam injection pressure of 8,000 kPa at the offset well.
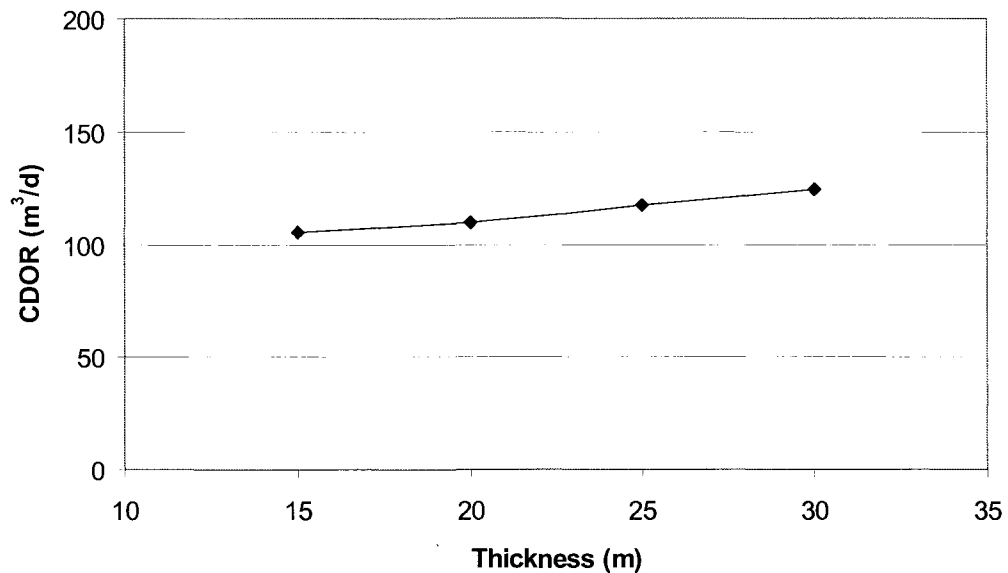
Figure 4.10a: Effect of reservoir thickness on CDOR

104
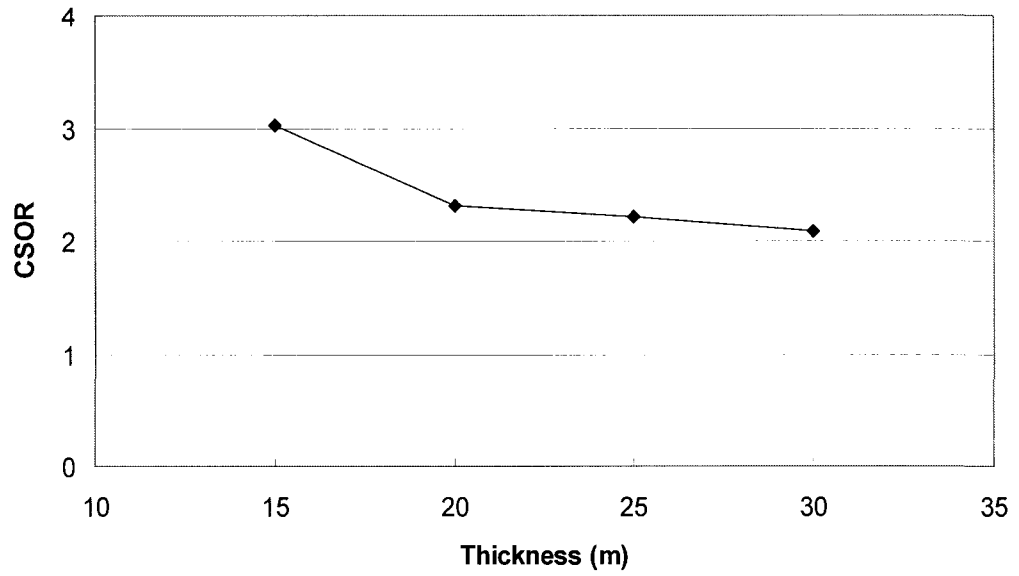
Figure 4.10b: Effect of reservoir thickness on CSOR
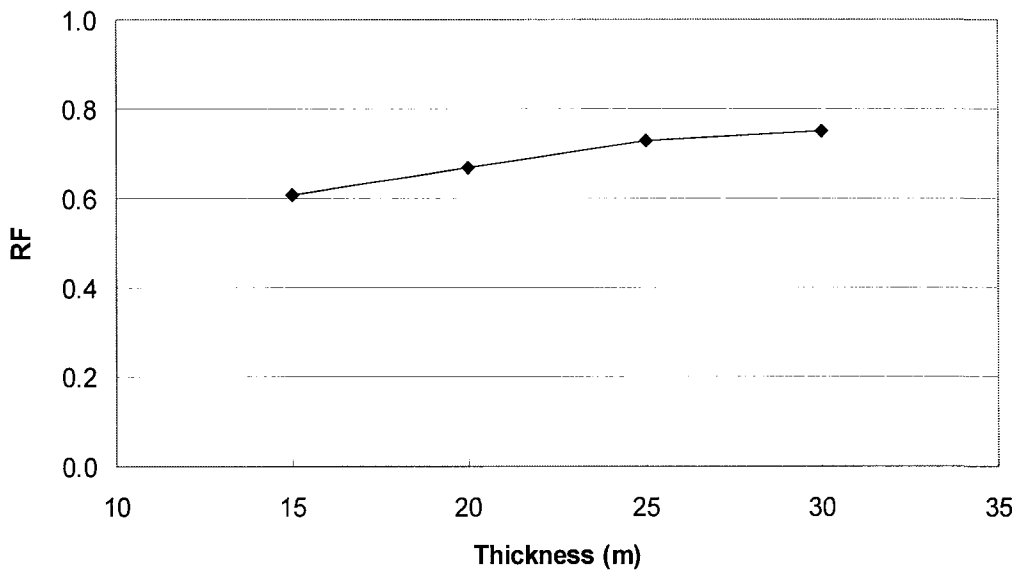
Figure 4.10c: Effect of reservoir thickness on RF

105
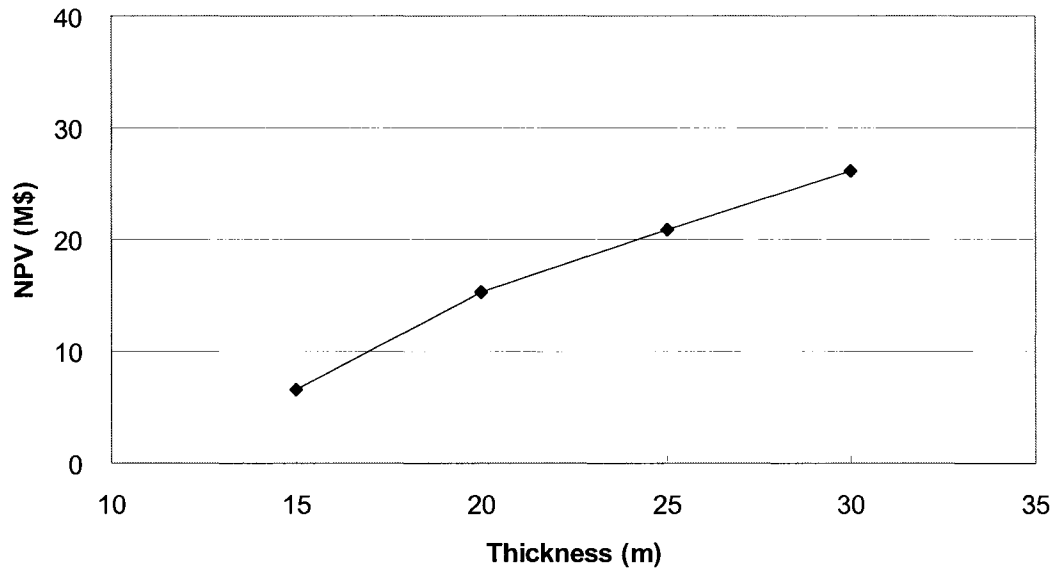
Figure 4.10d: Effect of reservoir thickness on NPV

4.4 Simulation results for Peace River-type reservoirs

This reservoir type represents the deepest, lowest permeability reservoir with middle range bitumen viscosity in the Alberta oil sands. The simulations were conducted under the following conditions: I/P spacing of 10 m, reservoir permeability (Kv) of 0.65 Darcy, and reservoir thickness of 25 m. Table 4.4 shows simulation results for the Peace River-type reservoir cases related to three operating conditions and reservoir thickness.

4.4.1 Offset Well Location

Simulations were conducted with a maximum offset well pressure of 8,000 kPa, a maximum steam injection rate of 800 m^3/d at the offset well, and additional steam injection of 400 m^3/d into the SAGD injector. NPV was highest at the offset well spacing of 50 m due to the highest CDOR and lowest CSOR (Figure 4.11). It might be said that around 50 m of offset well spacing is adequate for this reservoir type.

106

Table 4.4: Fast-SAGD simulation results for Peace River-type reservoirs

Case	Cum. Production (m³)	CSOR	CDOR (m³/d)	RF	NPV (M$)
1) Offset well location					
40 m	408,065	3.00	118	0.67	9.7
50 m	430,507	2.90	124	0.57	10.8
60 m	496,002	3.01	121	0.54	10.6
70 m	571,329	3.25	106	0.54	8.6
2) CSS startup time at the offset well					
1 yr	474,750	3.02	111	0.62	10.3
1.5 yrs	430,507	2.90	124	0.57	10.8
2 yrs	488,048	3.20	115	0.64	8.9
2.5 yrs	418,814	3.02	124	0.55	9.3
3) Steam injection pressure at the offset well					
6,000 kPa	415,521	3.04	107	0.55	9.9
7,000 kPa	428,950	2.97	115	0.56	10.0
8,000 kPa	430,507	2.90	124	0.57	10.8
4) Reservoir thickness					
15 m	196,083	3.85	95	0.43	-0.3
20 m	299,978	3.27	115	0.49	5.3
25 m	430,507	2.90	124	0.57	10.8
30 m	601,432	2.88	119	0.66	14.3
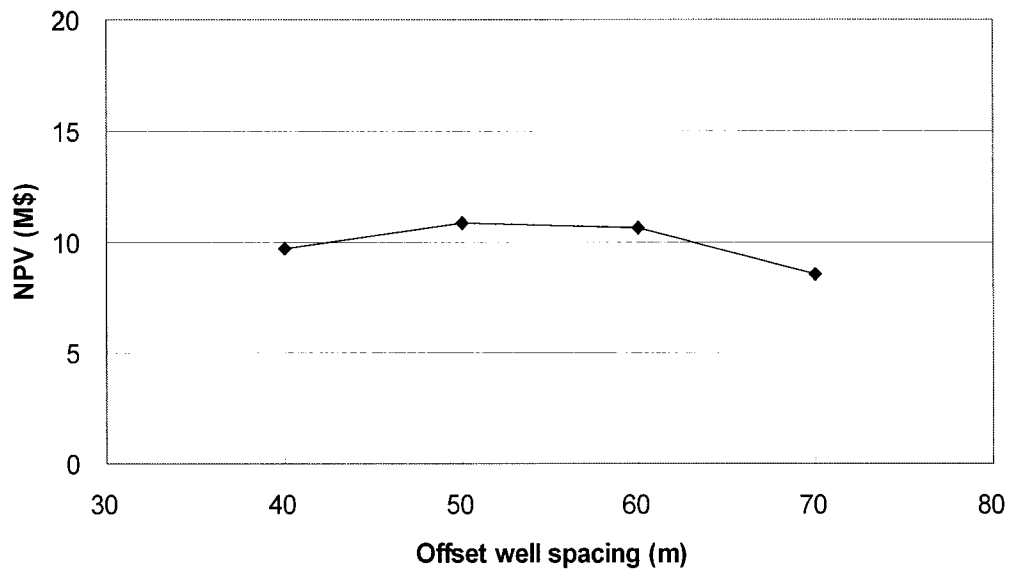
Figure 4.11a: Effect of offset well spacing on NPV

107
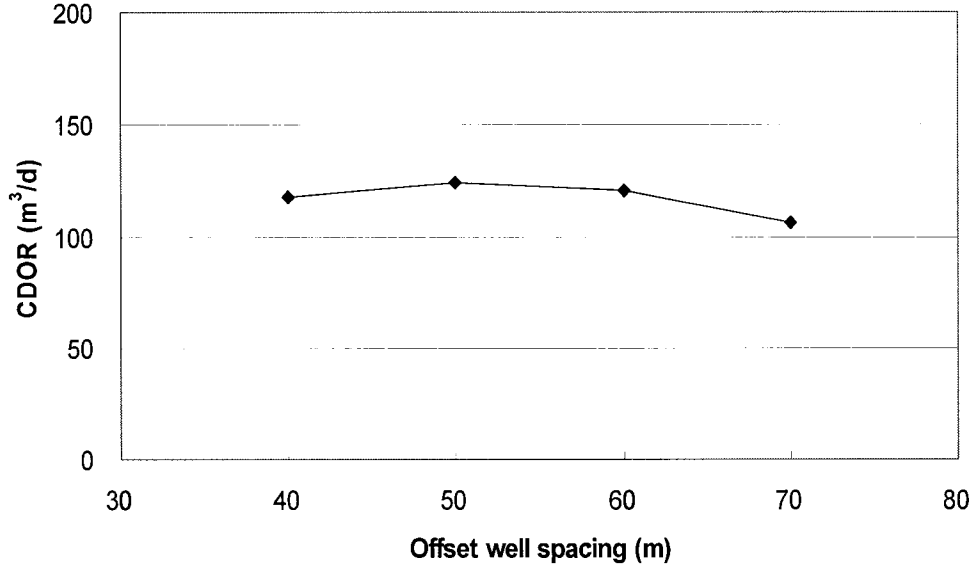
Figure 4.11b: Effect of offset well spacing on CDOR
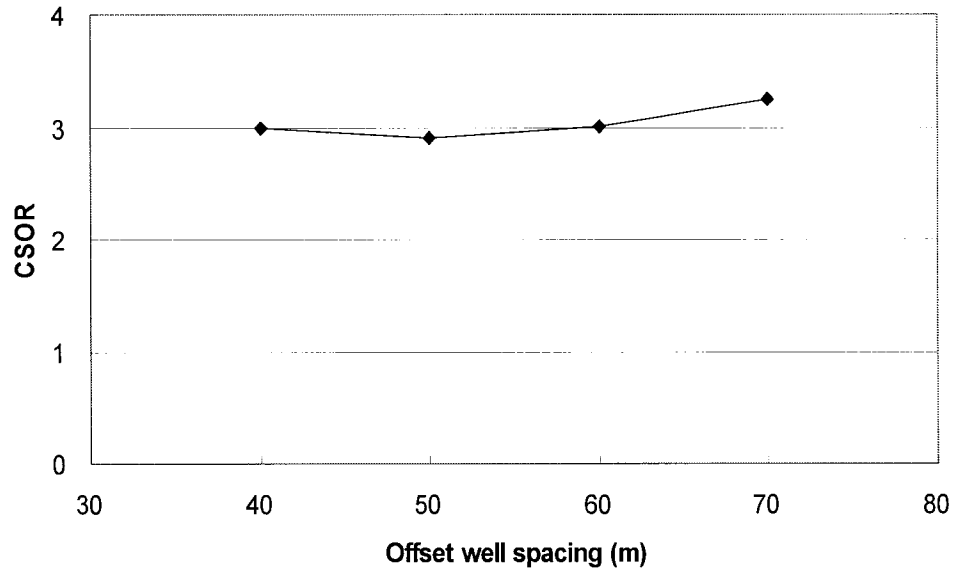
Figure 4.11c: Effect of offset well spacing on CSOR

108

4.4.2 CSS startup time at the Offset Well

Simulations were conducted with an offset well spacing of 50 m and a steam injection pressure of 8,000 kPa. The results showed that NPV was highest in the case of 1.5 years with the lowest CSOR (Figure 4.12). CDOR was highest and CSOR was lowest in the case of 1.5 years CSS startup time.
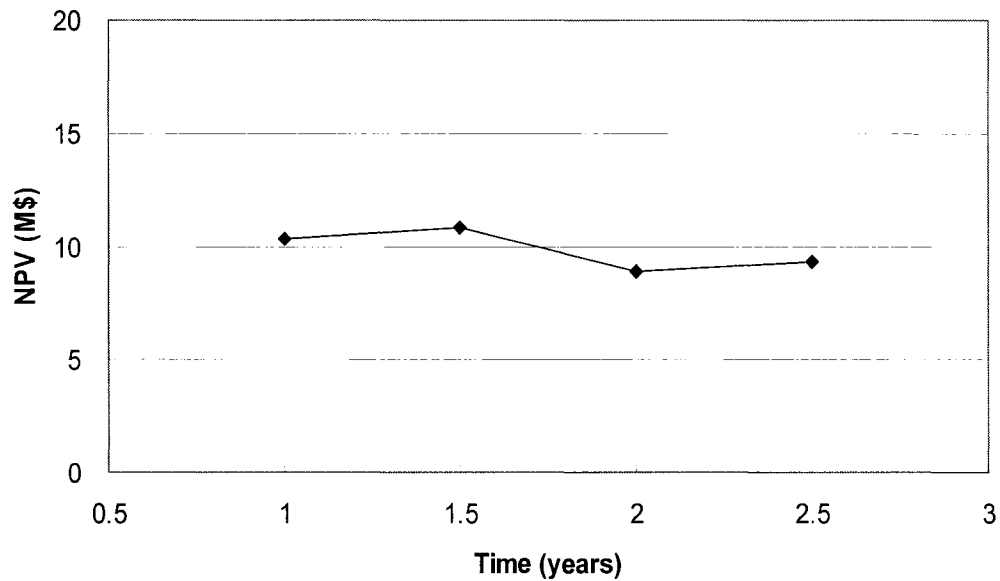
Figure 4.12a: Effect of CSS startup time at the offset well on NPV

109
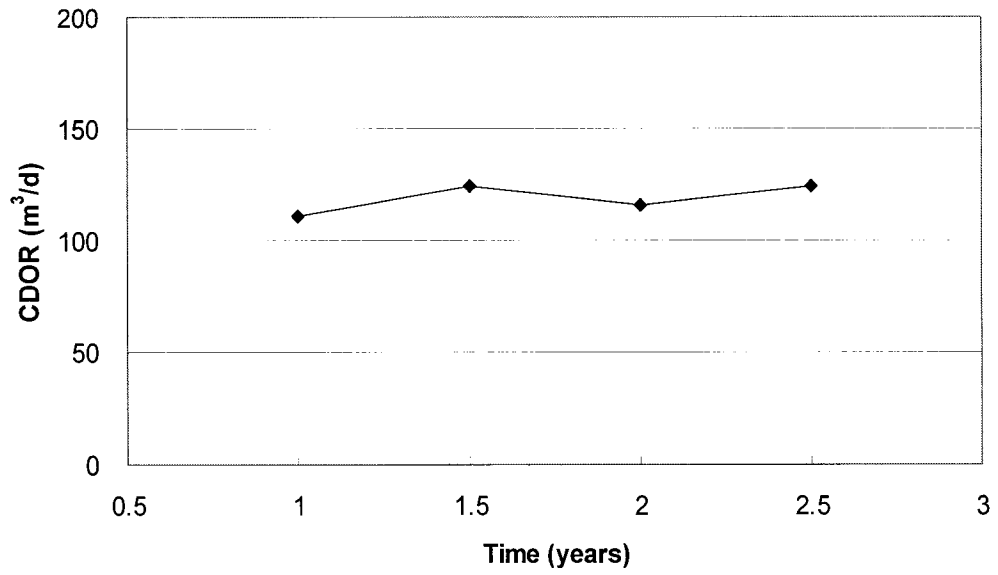
Figure 4.12b: Effect of CSS startup time at the offset well on CDOR
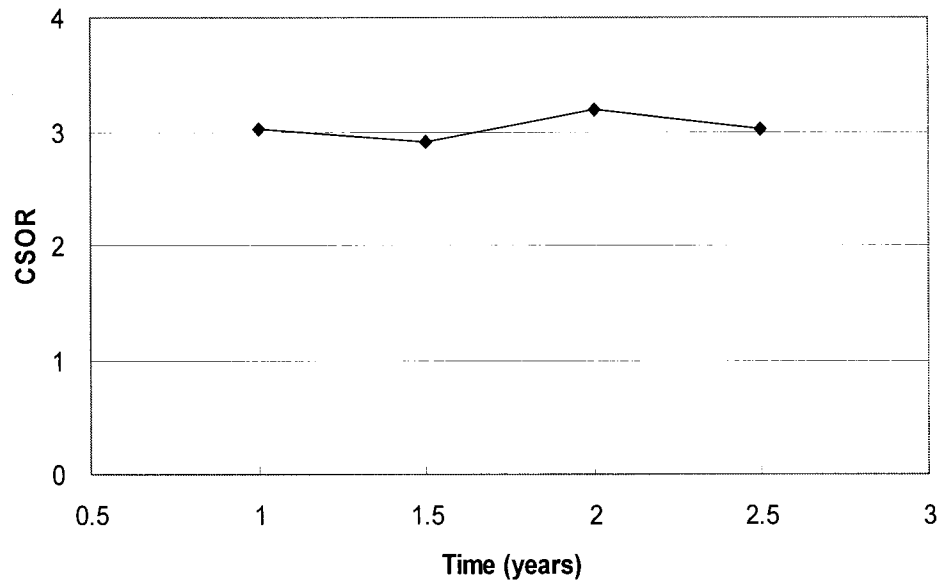
Figure 4.12c: Effect of CSS startup time at the offset well on CSOR

110

4.4.3 Steam Injection Pressure at the Offset Well

With the offset well spacing of 50 m, the simulation results showed that the NPV value was highest at 8,000 kPa due to the highest CDOR and lowest CSOR (Figure 4.13).

As the steam injection pressure is increased, CDOR increases and CSOR decreases. An injection pressure of 8,000 kPa at the offset well is adequate in this reservoir type.
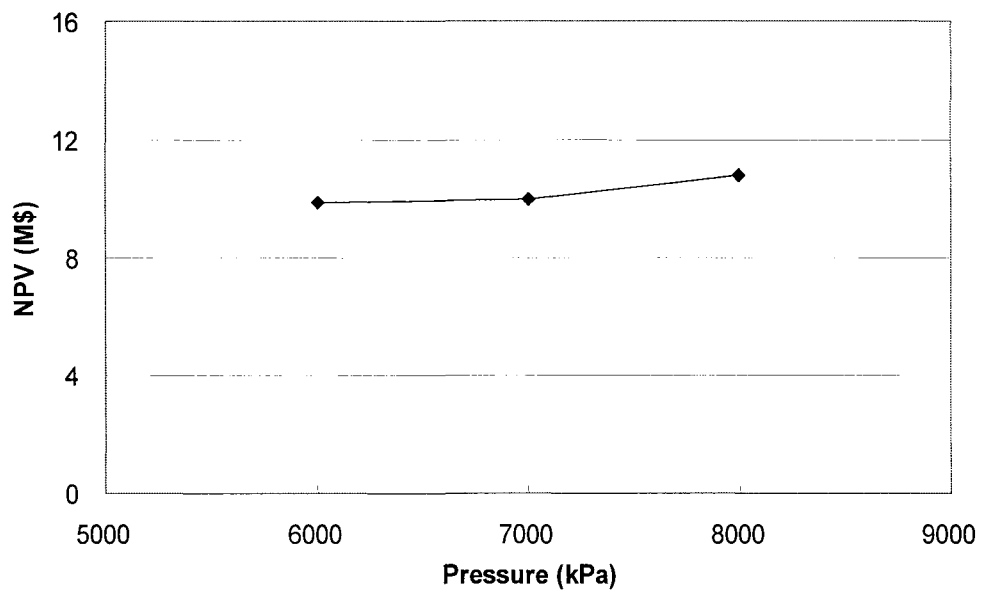
Figure 4.13a: Effect of steam injection pressure at the offset well on NPV
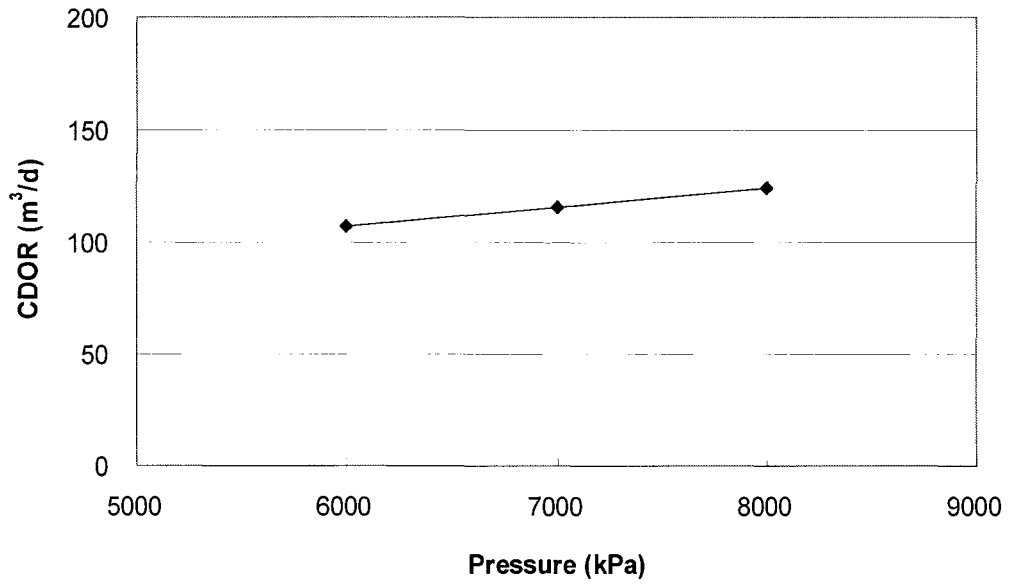
Figure 4.13b: Effect of steam injection pressure at the offset well on CDOR
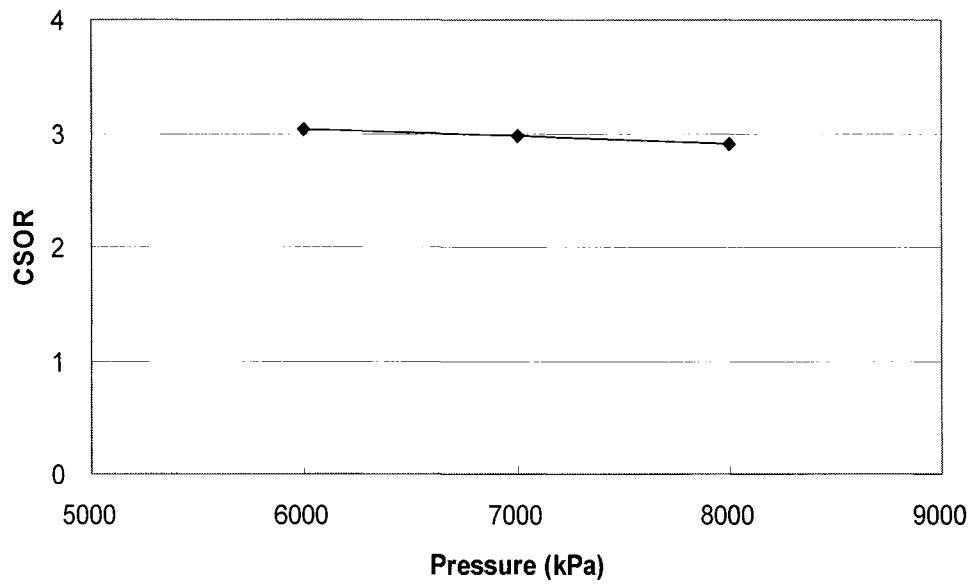
Figure 4.13c: Effect of steam injection pressure at the offset well on CSOR

112

4.4.4 Reservoir Thickness

The simulations were conducted to evaluate the effect of reservoir thickness on the Fast-SAGD performance. As the thickness is increased, CSOR decreases and both CDOR and RF increase (Figures 4.14a, 4.14b, 4.14c). At least the pay thickness should be thicker than 25 m for an economical Fast-SAGD operation: NPV is higher than 10.8 M$ (Figure 4.14d)

4.4.5 Best operating conditions

Simulation results for a Peace River-type reservoir, which is moderately thick with low permeability, give the following most favourable operating conditions: offset well spacing of 40 m, CSS startup time of 1.5 years, and steam injection pressure of 8,000 kPa at the offset well.
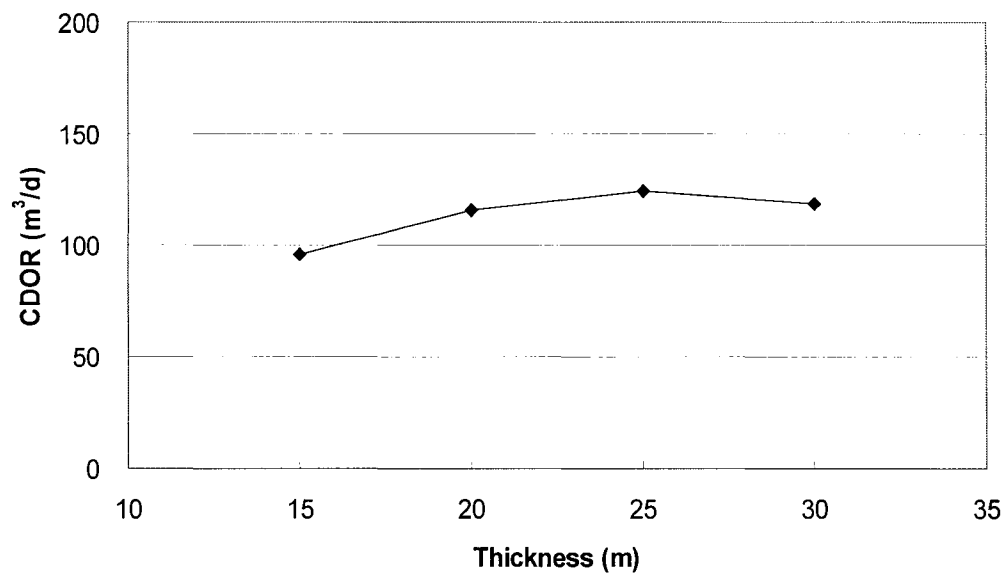
Figure 4.14a: Effect of reservoir thickness on CDOR

113
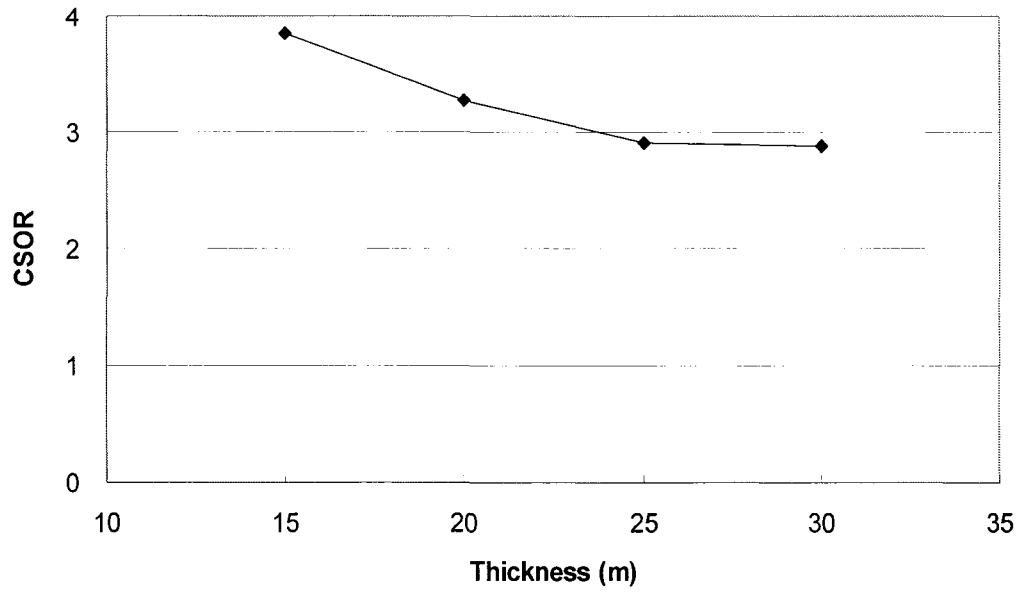
Figure 4.14b: Effect of reservoir thickness on CSOR
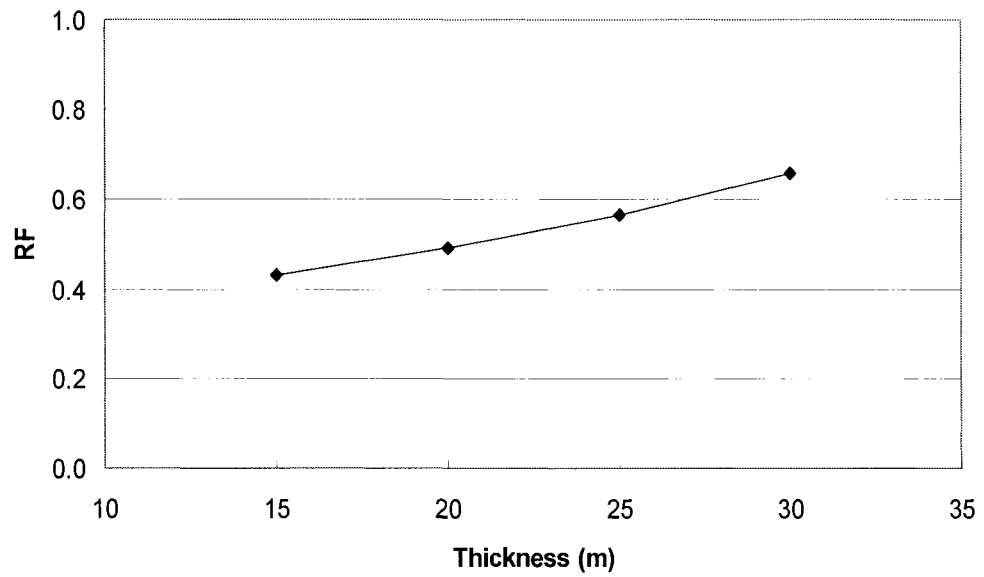
Figure 4.14c: Effect of reservoir thickness on RF

114
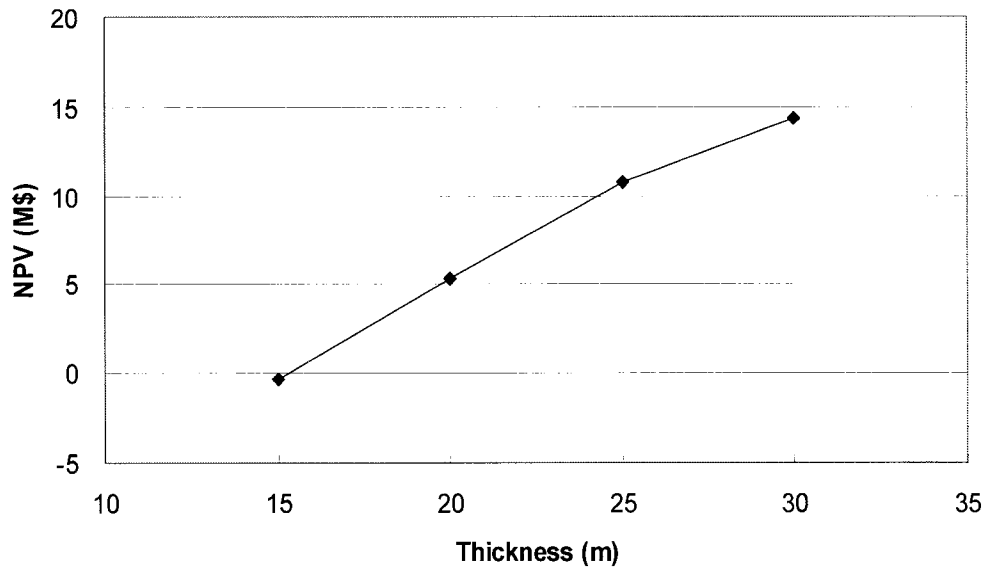
Figure 4.14d: Effect of reservoir thickness on NPV

4.5 Comparison of SAGD and Fast-SAGD processes

Table 4.5 shows simulation results for both the SAGD and Fast-SAGD cases. As a comparison, CDOR was calculated per producer; one producer for SAGD and two producers for Fast-SAGD. Drilling costs were considered for the NPV calculations, assuming three million dollars for a SAGD well pair and one million dollars for a single offset well.

Because of the difference in the well configuration, 101 m well pattern spacing for SAGD and 151 m well pattern spacing for Fast-SAGD, the economics of the Fast-SAGD process may be better than the SAGD process. C-NPV, an NPV adjusted for the case of having the same development area (multiply the SAGD case by 1.5), is introduced to compensate for this well pattern problem.

4.5.1 Athabasca-type reservoir

The simulation was conducted under the following conditions: I/P spacing of 5 m, reservoir permeability (K_v) of 2.5 Darcy, and reservoir thickness of 30 m. Simulation

115

results showed that CSOR decreased slightly from 1.54 to 1.52. CDOR increased and the ultimate recovery also decreased slightly (Table 4.5). Fast-SAGD reached the economic production limit (SOR =4) in 5 years, but SAGD in 7 years (Figure 4.15).

Even though the cumulative production of the Fast-SAGD case is higher than SAGD, applying the Fast-SAGD process seems to have no benefit in this type of reservoir with well configuration considered assuming the same development area.

Table 4.5: Fast-SAGD simulation results

Case		Cum. Production (m^3)		CSOR	Operating time (day)	CDOR (m^3/d)	RF	NPV* (M$)
		SAGD well	Offset well					
Atha-basca	F-SAGD	949,412		1.52	1,838	258	0.83	48.9
		579,152	370,260					
	SAGD	638,640		1.54	2,636	242	0.84	32.1
Cold Lake	F-SAGD	407,633		2.31	1,865	109	0.67	10.3
		257,628	150,005					
	SAGD	170,433		2.61	1,711	100	0.42	2.9
Peace River	F-SAGD	430,507		2.90	1,730	124	0.57	5.8
		307,508	122,999					
	SAGD	324,742		3.33	2,493	130	0.64	2.1

NPV* : drilling costs included

116
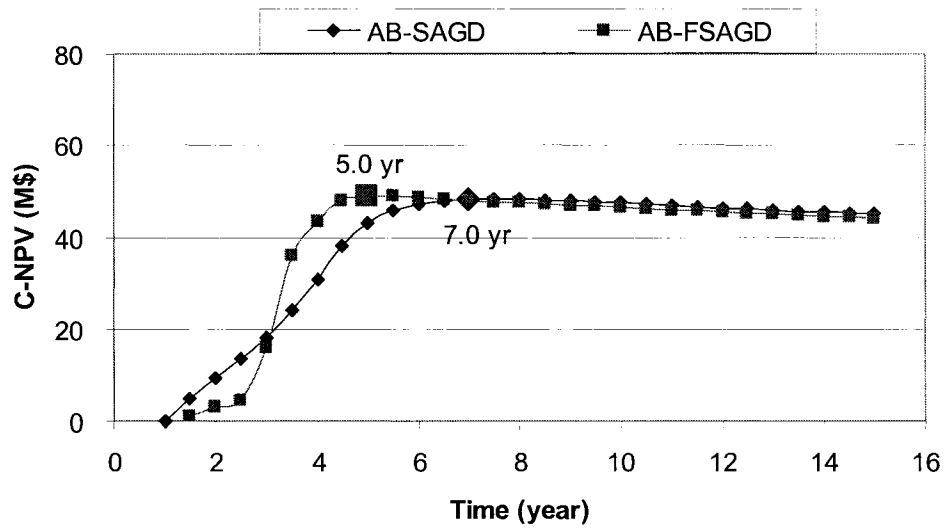
Figure 4.15a: C-NPV curves for SAGD and Fast-SAGD
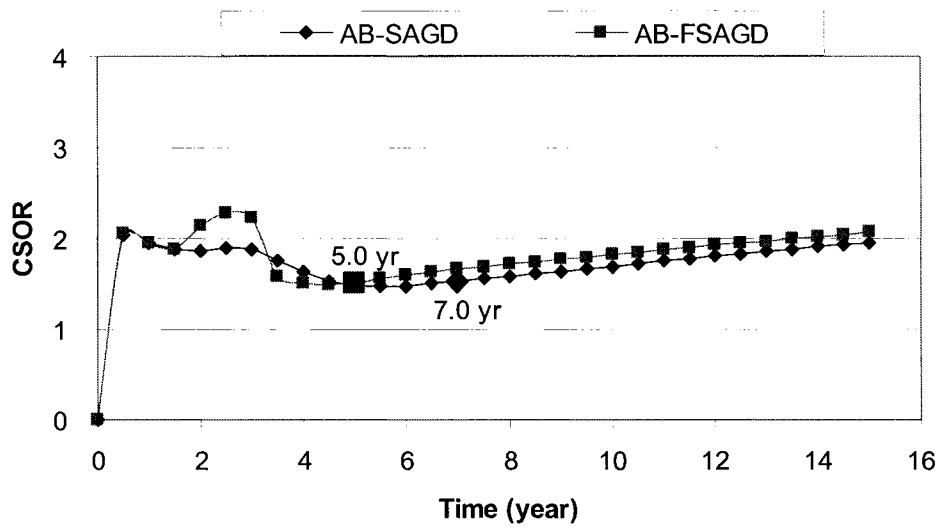
Figure 4.15b: CSOR curves for SAGD and Fast-SAGD

117
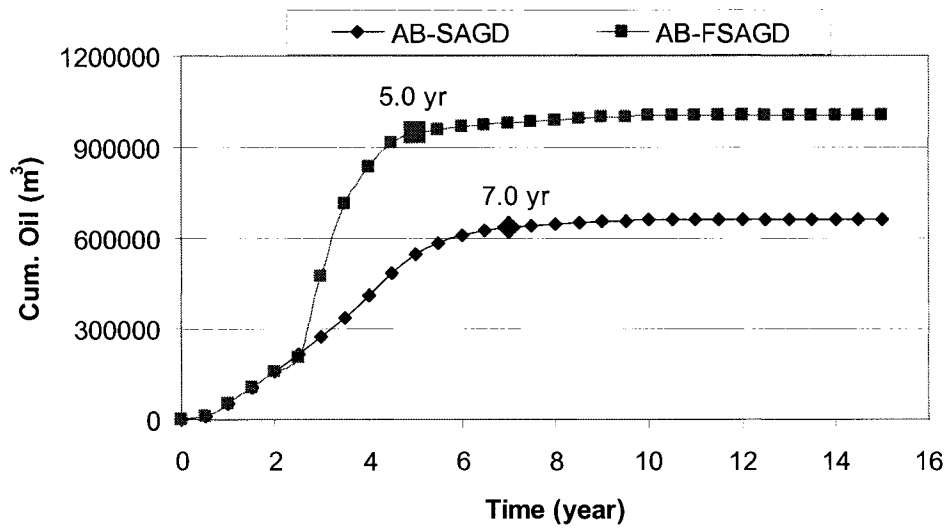
Figure 4.15c: Cumulative oil production curves for SAGD and Fast-SAGD

4.5.2 Cold Lake-type reservoir

The simulation was conducted under the following conditions: I/P spacing of 10 m, reservoir permeability (K_v) of 1.25 Darcy, and reservoir thickness of 20 m. Simulation results showed that CSOR decreased from 2.61 to 2.31. CDOR and ultimate recovery both increased (Table 4.5). Fast-SAGD and SAGD both reached the economic production limit in about 5 years (Figure 4.16). Cold Lake-type reservoirs are too thin (20 m) to apply the SAGD process due to its low thermal efficiency. The Fast-SAGD case had lower CSOR due to higher thermal efficiency and higher CDOR, which means higher productivity. The overall performance of the Fast-SAGD process was enhanced by 2.4 times based on the C-NPV calculations.

118
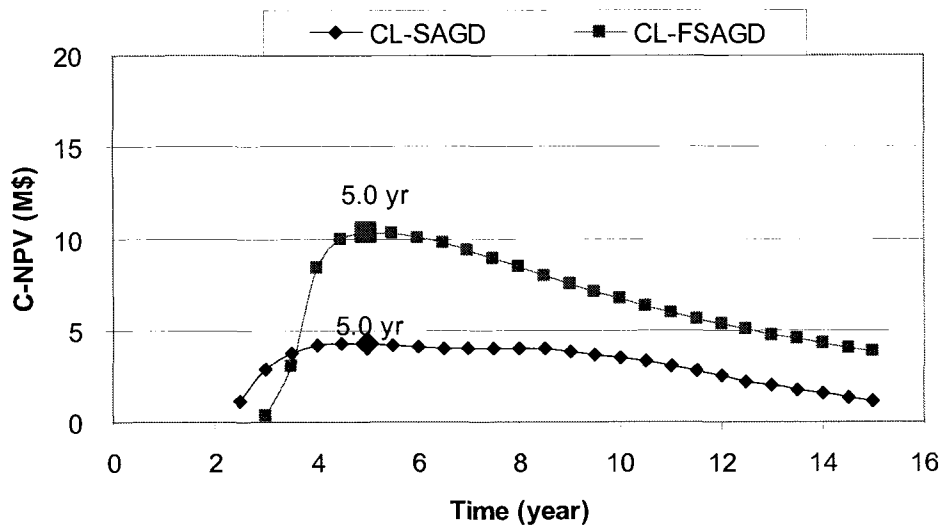
Figure 4.16a: C-NPV curves for SAGD and Fast-SAGD
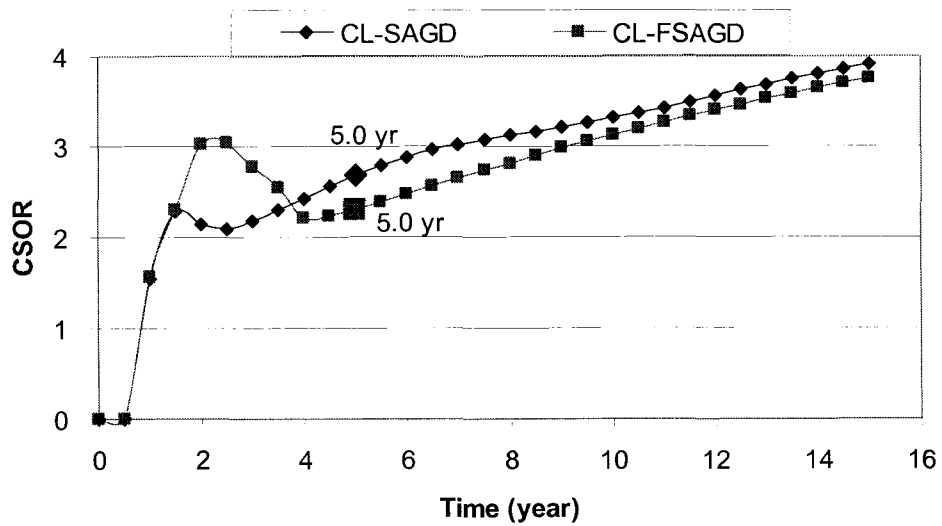
Figure 4.16b: CSOR curves for SAGD and Fast-SAGD

119
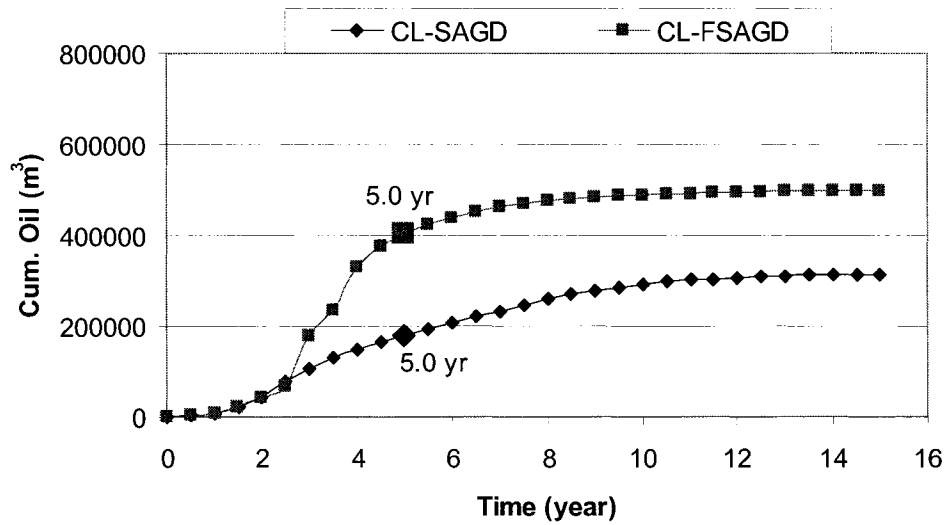
Figure 4.16c: Cumulative oil production curves for SAGD and Fast-SAGD

4.5.3 Peace River-type reservoir

The simulation was conducted under the following conditions: I/P spacing of 10 m, reservoir permeability (K_v) of 0.65 Darcy, and reservoir thickness of 25 m. Simulation results showed that CSOR decreased from 3.33 to 2.90. CDOR and ultimate recovery also decreased (Table 4.5). Fast-SAGD reached the economic production limit in 5 years, but SAGD in 7 years (Figure 4.17). The Fast-SAGD process resulted in enhanced thermal efficiency (lower CSOR), but lower ultimate recovery. Finally, the overall performance of the Fast-SAGD process was enhanced by 1.6 times based on the NPV calculations.

120
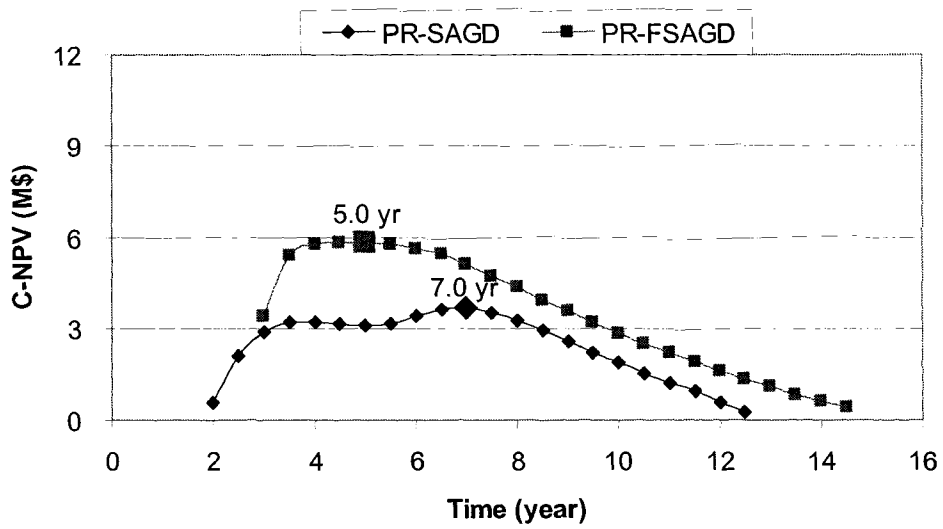
Figure 4.17a: C-NPV curves for SAGD and Fast-SAGD
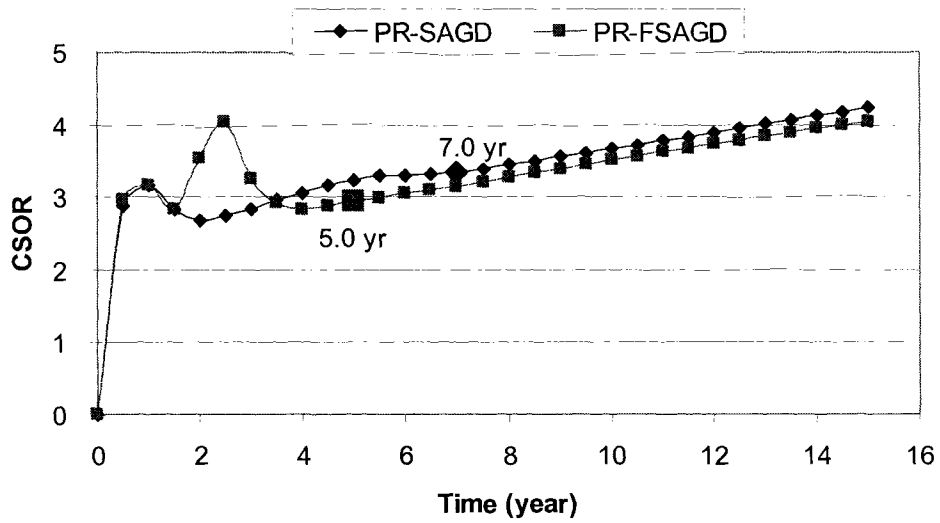
Figure 4.17b: CSOR curves for SAGD and Fast-SAGD

121
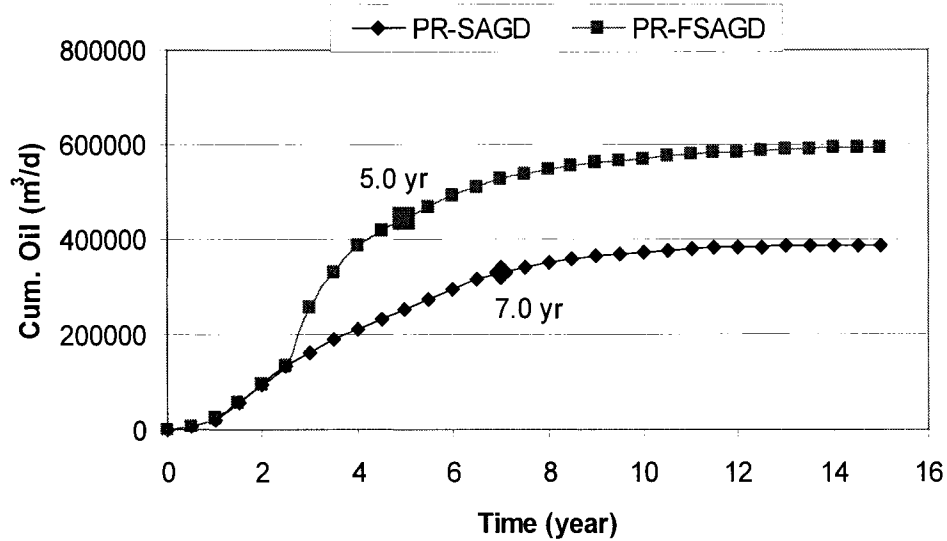
Figure 4.17c: Cumulative oil production curves for SAGD and Fast-SAGD

4.5.4 SAGD and Fast-SAGD performances for Alberta oil sands areas

Simulation results (Table 4.5) showed that the Fast-SAGD cases had lower CSOR due to higher thermal efficiency in all three areas, and higher CDOR per producer, which means higher productivity, except for the Peace River case (Figures 4.18a and 4.18b). The ultimate recovery of Fast-SAGD was enhanced in the Cold Lake case, but reduced in the Peace River case (Figure 4.18c).

The Fast-SAGD process in Cold Lake-type which has the same project life, gave an additional bitumen production over the SAGD process on the basis of the SAGD producer only. This is due to the steam drive effect caused by the pressure differential between the SAGD well pair and the offset well operated in CSS mode.

The NPV was always higher in the Fast-SAGD cases because of the Fast-SAGD process efficiency and the difference in the well configuration (Figure 4.18d). Finally, the overall

122

economics of Fast-SAGD, measured by C-NPV, increased in all three areas (Figure 4.18e). Cold Lake-type reservoirs showed the largest improvement with the Fast-SAGD process compared to the SAGD process. Peace River-type reservoirs had the second largest improvement. However, there was not much improvement in Athabasca-type reservoirs.
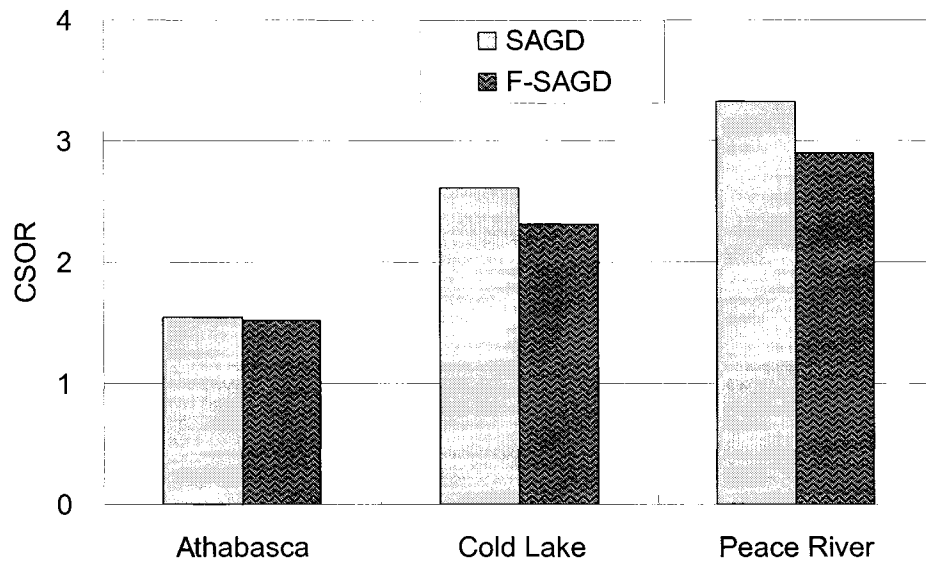
Figure 4.18a: Comparison of CSOR at three areas
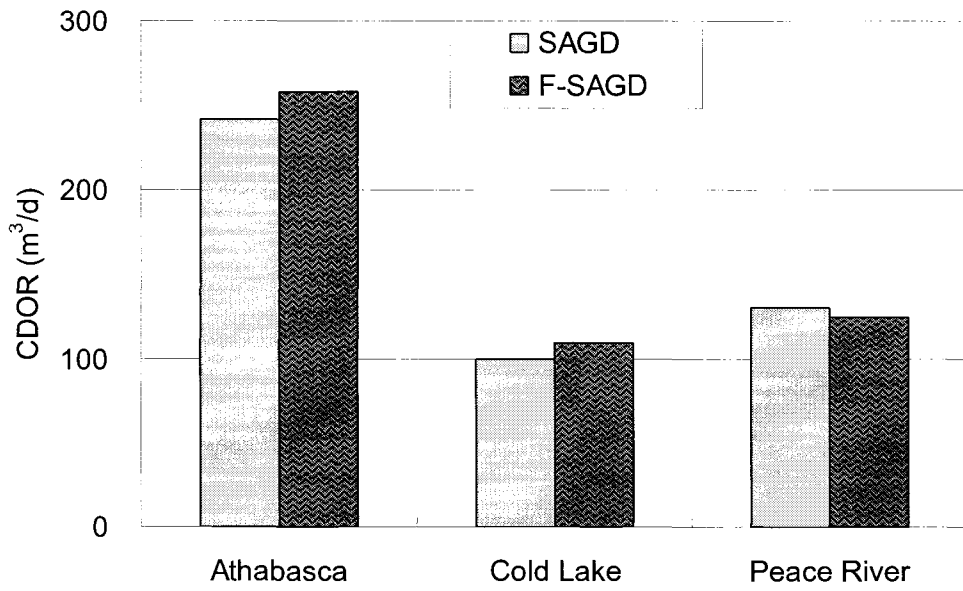
Figure 4.18b: Comparison of CDOR at three areas
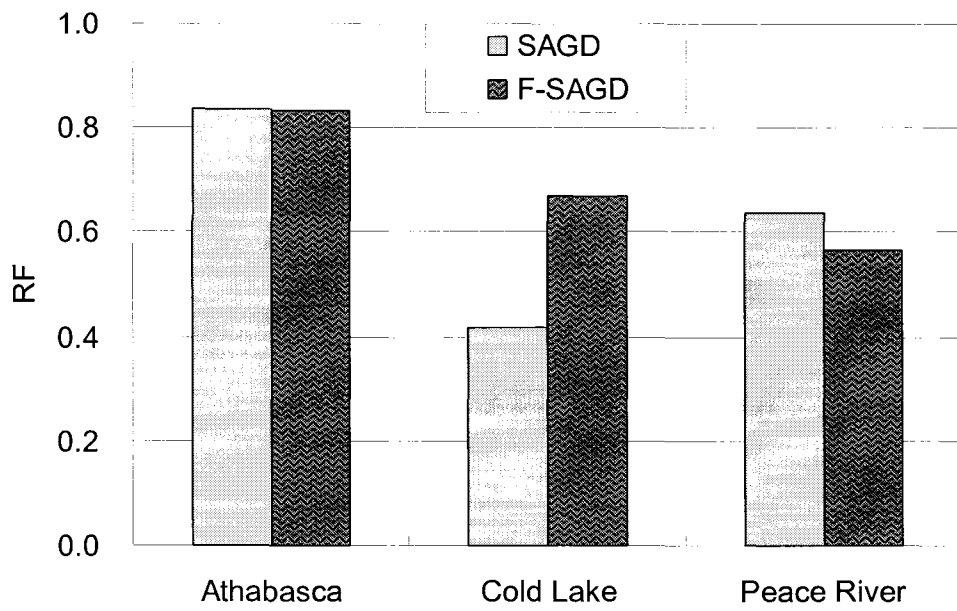
Figure 4.18c: Comparison of Recovery factor at three areas

124
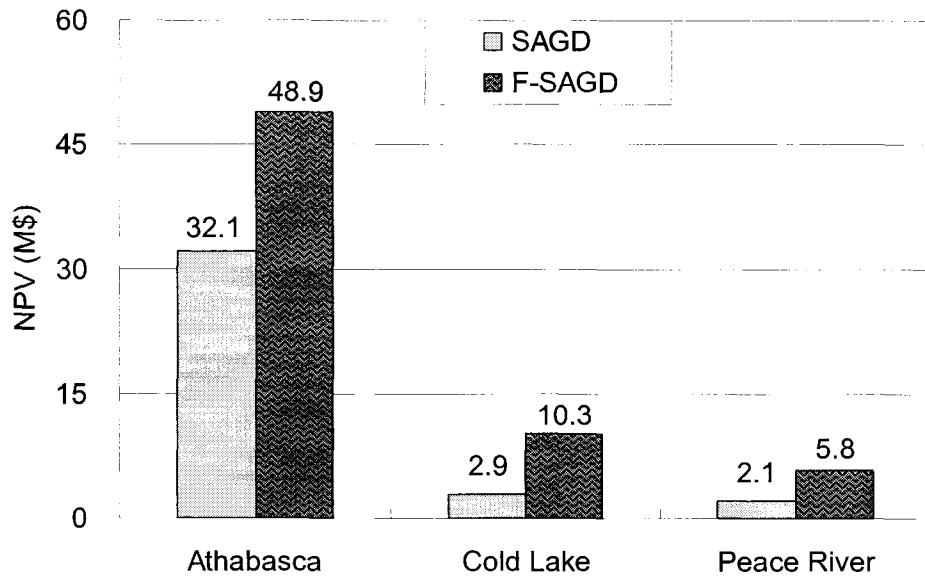
Figure 4.18d: Comparison of NPV at three areas
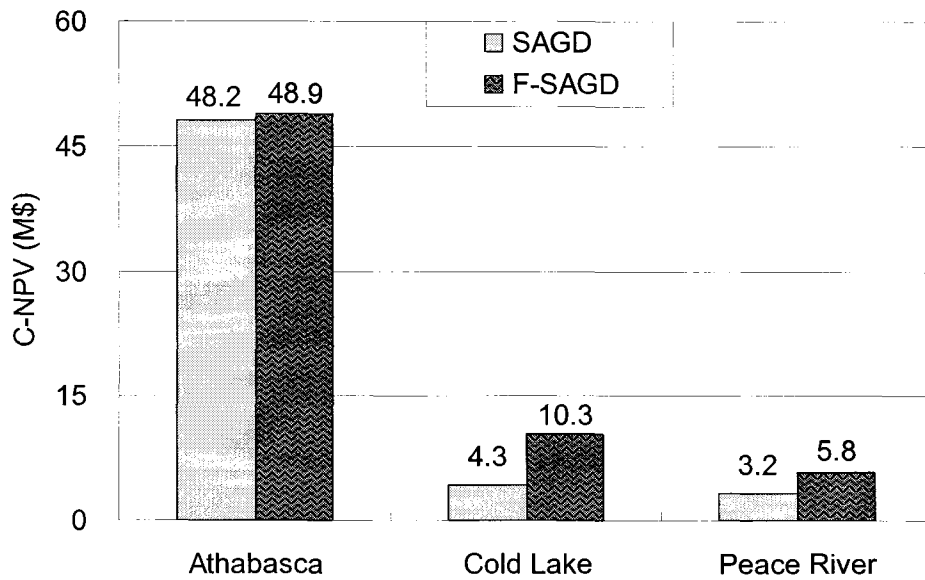
Figure 4.18e: Comparison of C-NPV at three areas

125

4.6 Multi-offset wells operation for the Fast-SAGD process

In the previous section, Cold Lake type reservoirs showed the largest improvement with the Fast-SAGD process compared to the SAGD process. Therefore, the multi-offset wells operation for the Fast-SAGD process was investigated with the Cold Lake-type reservoirs.

The grid system and the position of the wells are shown in Figure 4.19. The offset wells are located on one side of the SAGD well pair, and each offset well was placed 50 m away from the SAGD well pair or each offset well.
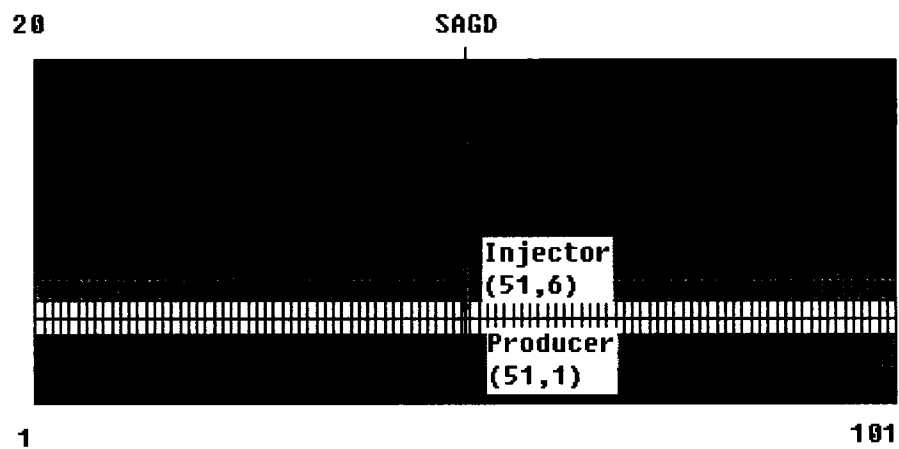
Figure 4.19a: Grid system and well position for SAGD

126
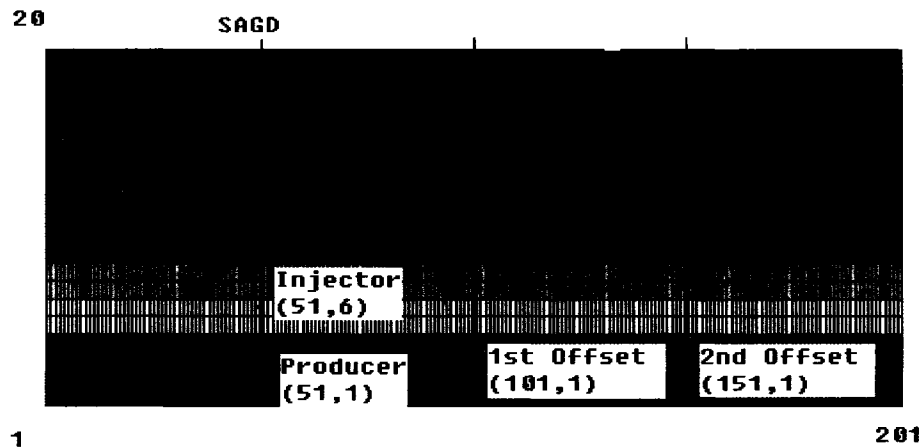
Figure 4.19b: Grid system and well position for Fast-SAGD

4.6.1 CSS startup times at the offset wells

It is important to select the proper time to begin the CSS operation at the first offset well. The startup time of the CSS operation was decided based on previous research regarding the Fast-SAGD process (Polikar et al., 2000, Gong et al., 2002). In this study, the initiation time of the CSS at the first offset well was 547 days after the beginning of the SAGD operation. This is the time at which the steam chamber reached the top of the reservoir and began to propagate sideways.

The startup time for the CSS operation at the second offset well was decided with the steam-oil ratio (SOR) indicating the economic limit of steam injection recovery. In this case, it was 1,460 days when SOR is four and at this time most of the bitumen (about 3/4) between the SAGD well pairs and the first offset well was already recovered (Figure 4.20).

In the case of two offset wells, most of the bitumen between the SAGD well pairs and the second offset well had been produced around 2,550 days (Figure 4.21). This will be the startup time for CSS operation at the third offset well. The offset wells are propagating and expanding the steam chamber laterally after it is formed by the SAGD process.

127
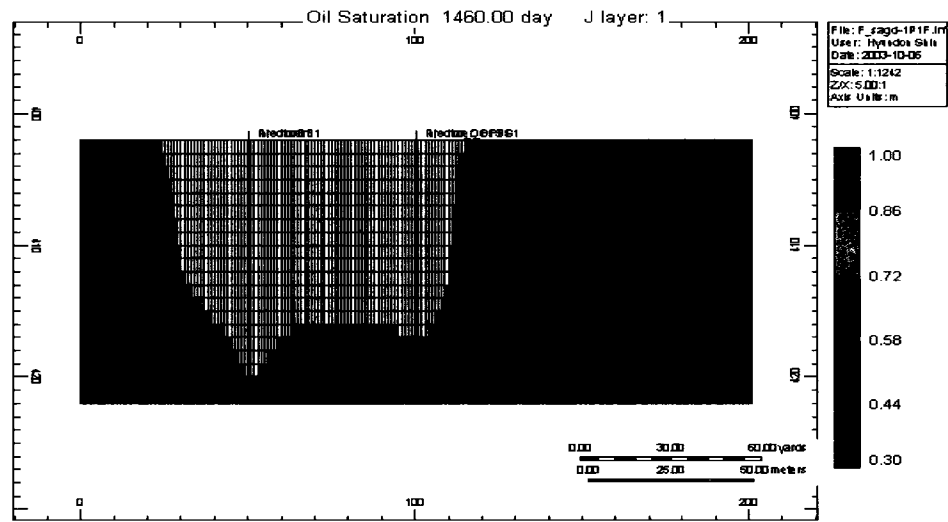
Figure 4.20: Oil saturation profile after 1,460 days
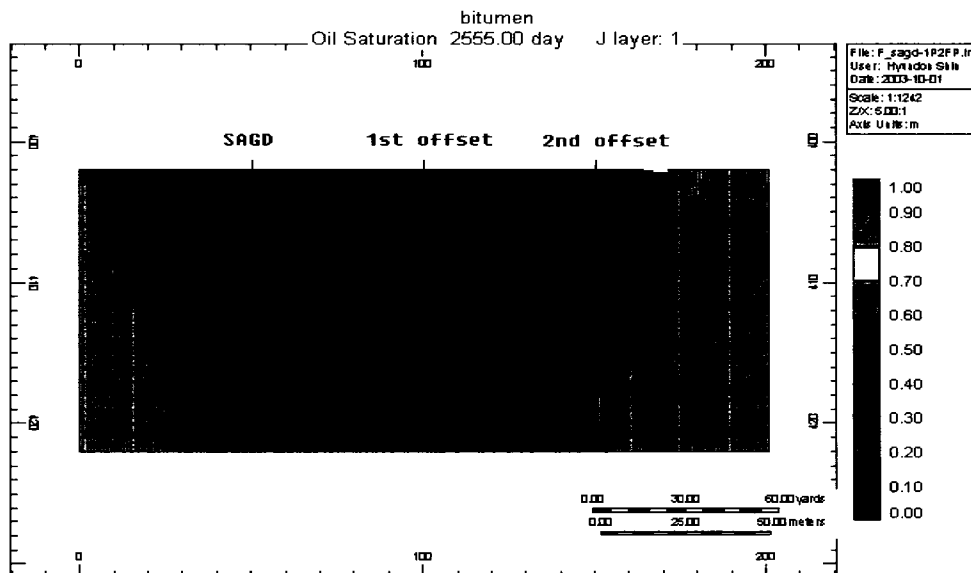
Figure 4.21: Oil saturation profile after 2,550 days

128

4.6.2 Number of offset wells

To know how many offset wells can be located and operated effectively beside a SAGD well pair for the Fast-SAGD operation, simulations were conducted with increasing the number of offset wells along one side only. Simulation results (Table 4.6) showed that the Fast-SAGD cases had lower CSOR due to higher thermal efficiency and higher CDOR which means higher productivity compared to the SAGD case (Figures 4.22 and 4.23). Fast-SAGD cases always have smaller operating time.

As the number of offset well was increased, CSOR increased and CDOR per well decreased (Figure 4.24), and NPV increased mainly due to the higher production rate from larger well configurations. C-NPV, considering the same development area, is highest in the case of two offset wells' operation (Figure 4.25).

When three parallel offset wells along one side were operated in the Fast-SAGD mode (F-SAGD-1P3FP), the results showed similar productivity (CDOR) but higher thermal efficiency and CSOR reduced by 11%, compared to the SAGD case (SAGD-1P). Finally, C-NPV of the case of three offset wells is still higher than the SAGD case: 10.0 over 8.5 (M$3.4 multiply by 2.5). Considering that the offset wells can be operated along both sides of the SAGD well pair in the field, we can expect better results than those in this study, and the operation of three offset wells might be economical for Fast-SAGD.

129

Table 4.6: Fast-SAGD Simulation results for multi-offset well operation

Case	Cum. Production (m³)	CSOR	Operating time (day)	CDOR (m³/d)		NPV (M$)
				/area	/well	
SAGD-1P	293,323	3.13	3,272	90	44.8	3.4
F-SAGD-1P1FP	309,372	2.45	1,840	168	56.0	7.2
F-SAGD-1P2FP	507,166	2.60	2,638	192	48.1	10.1
F-SAGD-1P3FP	626,884	2.78	2,812	223	44.6	10.0

(Well configurations)

SAGD
o Injector
O Producer
SAGD-1P

SAGD
o offset
O   O
F-SAGD-1P1FP

SAGD
O   offset   offset
O   O   O
F-SAGD-1P2FP

SAGD
O   offset   offset   offset
O   O   O   O
F-SAGD-1P3FP
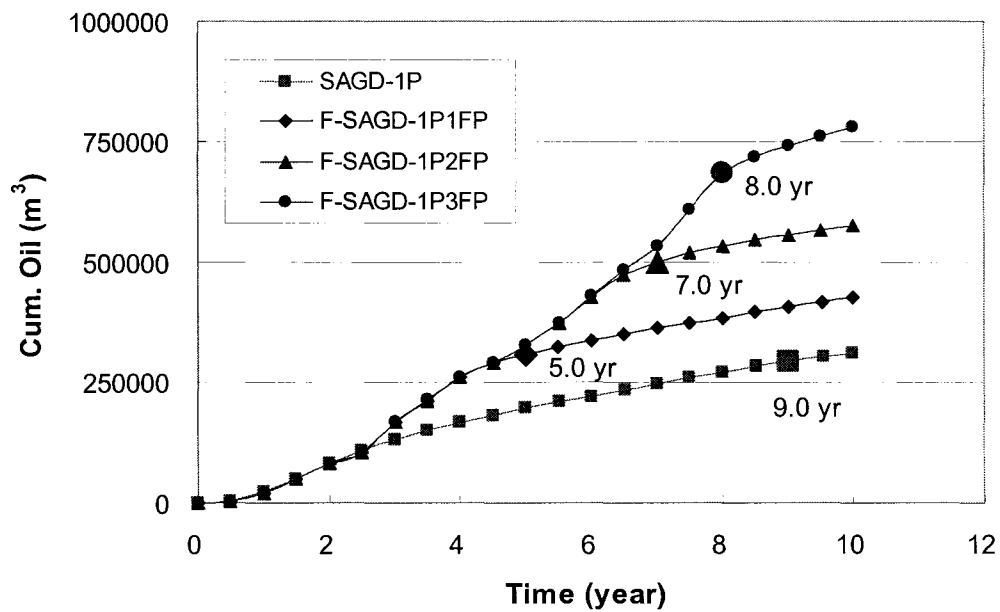
Figure 4.22: Oil production curves for Fast-SAGD

130
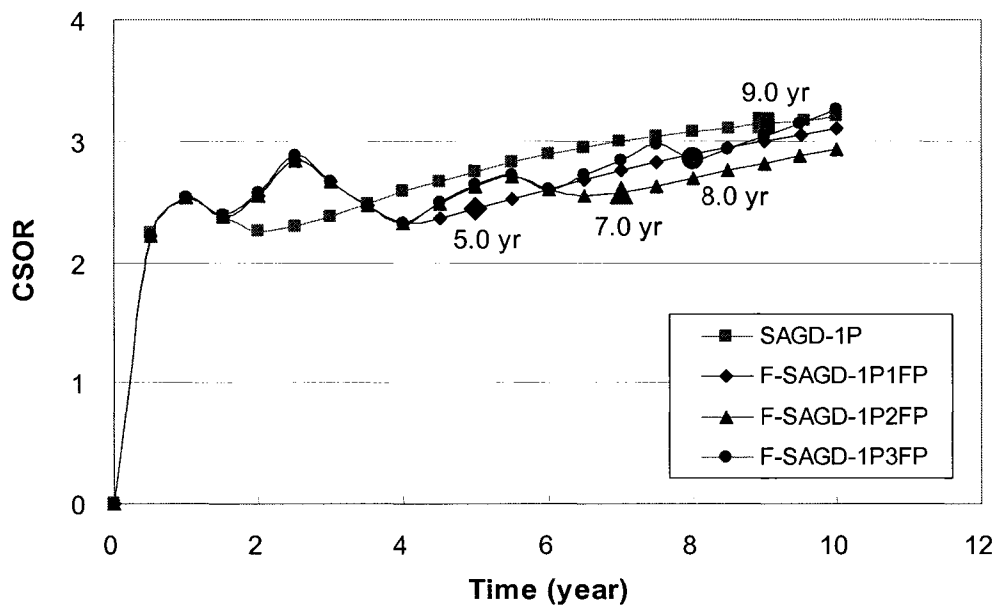
Figure 4.23: CSOR curves for Fast-SAGD
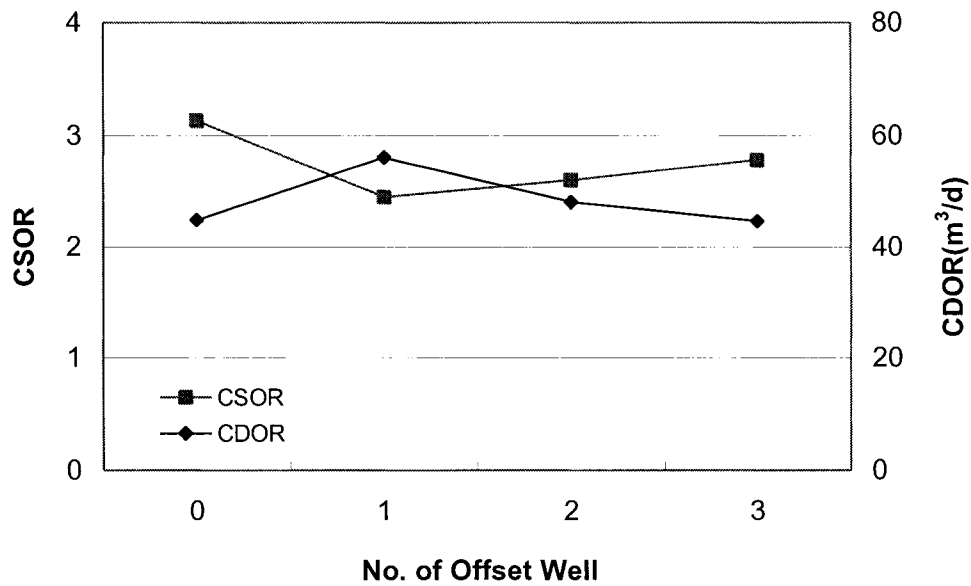
Figure 4.24: Effect of offset well number on CSOR and CDOR for Fast-SAGD

131
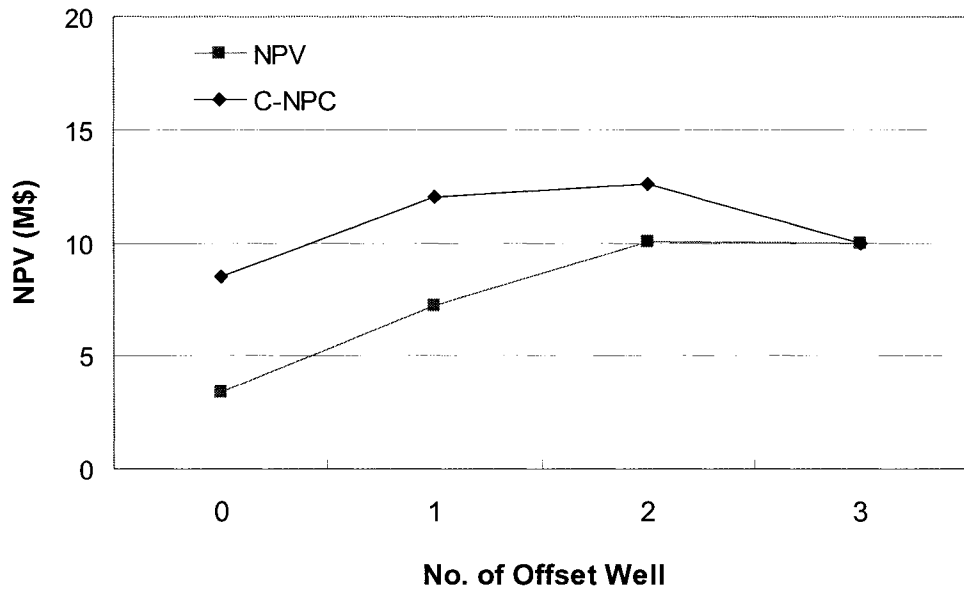
Figure 4.25: Effect of offset well number on NPV for Fast-SAGD

132

5 ECONOMIC INDICATOR FOR SAGD PERFORMANCE

The steam-assisted gravity drainage (SAGD) process has been tested in the field and has proven to be an effective recovery method with more than 50% recovery efficiency in the Alberta oil sands (Athabasca, Cold Lake and Peace River deposits).

Before a SAGD project is implemented in the field, a sensitivity analysis is usually required for defining the SAGD operating conditions: pre-heating period, steam injection pressure, steam injection rate and injector to producer spacing (I/P spacing). The economics of a SAGD project are related to several production performance parameters. The most significant of those are steam-oil ratio (SOR), ultimate recovery (recovery factor RF), calendar day oil rate (CDOR), and project life. Our main goal is to maximize oil production with the least amount of steam and in the shortest time.

There is very little research regarding an economic indicator for thermal recovery. Kisman and Ruitenbeek (1986) introduced a performance indicator for thermal recovery. They developed a model for the economic and performance evaluation of thermal recovery projects including steam stimulation, steam drive and combustion processes.

In this chapter, a new simple economic parameter, named STEP (simple thermal efficiency parameter, Equation 5-1), was introduced to define SAGD operating conditions for Athabasca-, Cold Lake-, and Peace River-type reservoirs.

$$STEP = \frac{RF \times CDOR}{CSOR^{2.4}}$$

(Equation 5.1)

Four operating conditions were analyzed for the SAGD process. They are: preheating period, I/P spacing, steam injection pressure, and steam injection rate.

The net present value (NPV) of each case is first calculated to evaluate SAGD performance. Then, STEP is calculated from three performance parameters: CSOR, CDOR, and RF. Finally, STEP is correlated with NPV for each best-case scenario. If the

133

correlation between STEP and NPV is good, STEP can be used as a simple economic indicator instead of NPV.

5.1 Development of new economic indicator (STEP)

A sensitivity study was performed for the SAGD simulations described in this study to define the lowest cumulative steam-oil ratio (CSOR), highest RF and highest CDOR in order to obtain the most favourable operating conditions. If a case has the lowest CSOR and the highest CDOR and RF, this gives the best operating conditions. However, there are cases which have low CSOR and low RF or CDOR. In this case, it is difficult to define the most favourable operating conditions without an economic parameter such as NPV or rate of return.

5.1.1 STEP as a qualitative indicator

In this study, the economic calculations assume that a project is cost-effective as long as the instantaneous SOR is below a value of 4. Capital costs have not been taken into account, assuming that these are similar for all the cases studied because the same well configurations and development plan are considered. NPV calculations only considered the cost of steam ($5/bbl) and price of bitumen ($20/bbl), at a 10% discount rate.

STEP, based on CSOR, CDOR and RF for the time corresponding to SOR = 4, was developed for each simulation case. The economics of a SAGD project are expected to improve as RF and CDOR increase, and CSOR decreases.

Simulation results showed that NPV has a linear relationship with RF and CDOR, but a decreasing exponential relationship with CSOR (Figures 5.1a and 5.1b). The magnitudes of the exponents in the STEP formula have been adjusted to give the highest correlation coefficient between NPV and STEP. A higher STEP value can be expected for the case of high RF, high CDOR and low CSOR. CSOR is included to account for thermal efficiency, and CDOR is for productivity and project life. RF is included to account for

134

recovery efficiency because the case of high CDOR with low RF indicates short project life.
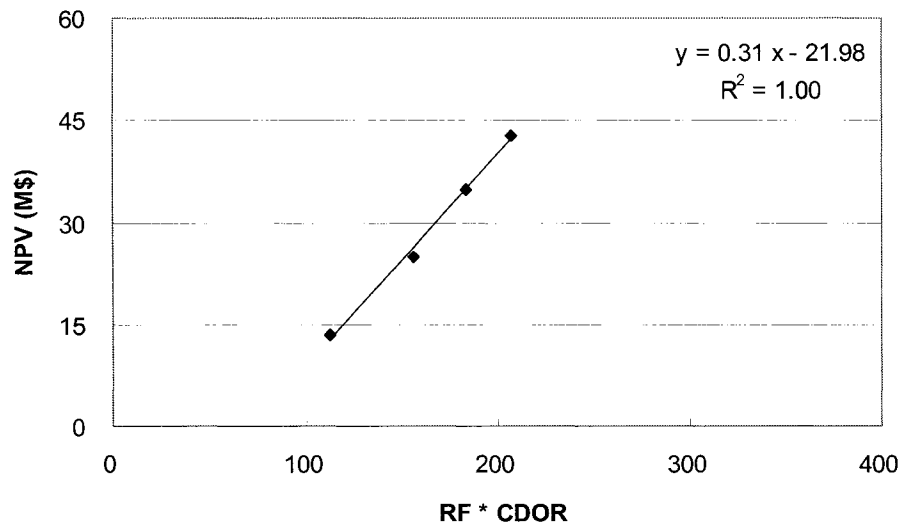
Figure 5.1a: Example of relationship between NPV and RF*CDOR
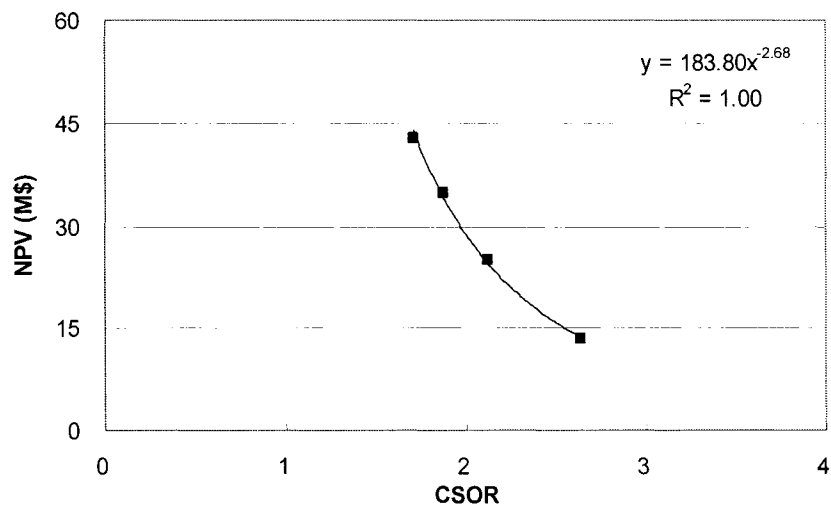
Figure 5.1b: Example of relationship between NPV and CSOR

135

5.1.2 STEP as a quantitative indicator

STEP was initially introduced to evaluate the performance of a SAGD project under the sensitivity study. It was proposed as a simple economic indicator during the SAGD evaluation procedure instead of NPV.

In order to have a quantitative economic criterion, STEP has been modified using the following equation:

$$STEP = \frac{(RF/0.5) \times (CDOR/0.111)}{(CSOR/3)^{2.4}}$$

(Equation 5.2)

The economic limit for each SAGD performance parameter is assumed to be 3 for CSOR, 0.111 m^3/d/m of horizontal well length for CDOR, and 0.5 for RF. It may be said that STEP is greater than 1 in the case of an economic SAGD project. This modified STEP can be used as a quantitative as well as a qualitative economic indicator.

5.2 Validation of STEP as an economic indicator

For validating this new economic indicator, STEP calculations have been performed using data from two published studies in which SAGD related simulations were performed. The first study will show a STEP application as a qualitative economic indicator, and the second one as a quantitative economic indicator.

5.2.1 STEP validation as a qualitative indicator

The first validation study used the data from Gao et al. (2002) in which five different cases have been investigated through numerical simulations for the extra heavy oil Liaohe field in China.

This case study, which provides no economic parameters but points out the best case, shows that most of the cases have the highest STEP values for the best case. The first

136

four cases (Figures 5.2, 5.3, 5.4, 5.5) are related to the SAGD operating conditions, and indicate that STEP always has the highest value when the case is best. Only one case (Figure 5.6), comparing various operating methods, does not give the highest STEP value for the best case. The STEP value of the best case has almost the same value as the highest STEP value (2.2 versus 2.4). The basis for the thermal methods of that study (Gao et al., 2002) is steam stimulation, either with different well configurations or as a precursor to other steam flooding processes. As the different operating methods will give different production profiles, the performance parameters like CSOR, CDOR, and RF vary broadly (Table 5.1).

Even if STEP has been developed for evaluating SAGD performance, the above shows that it may be applied to the evaluation of other thermal recovery methods.
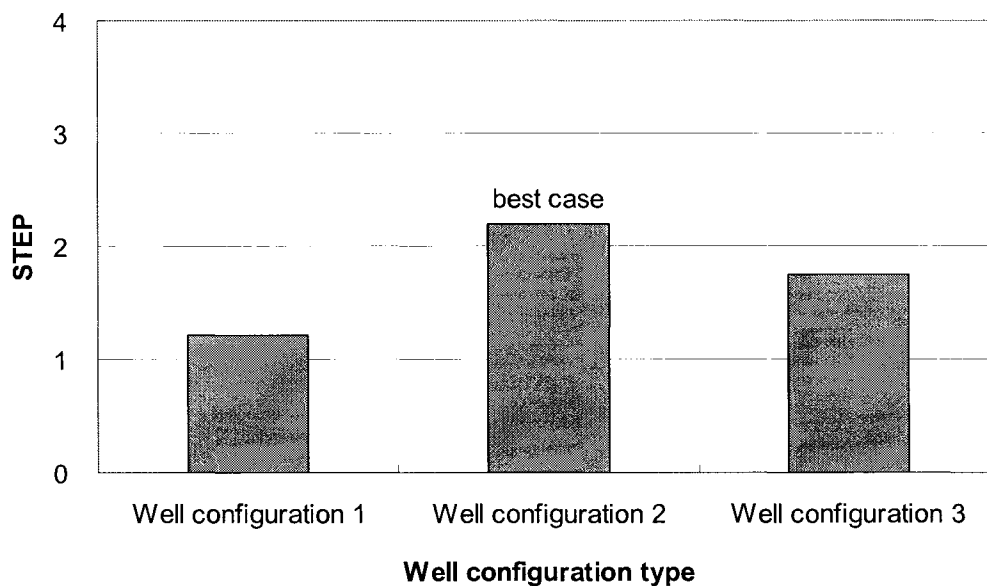
Figure 5.2: Effect of well configuration type on STEP

137
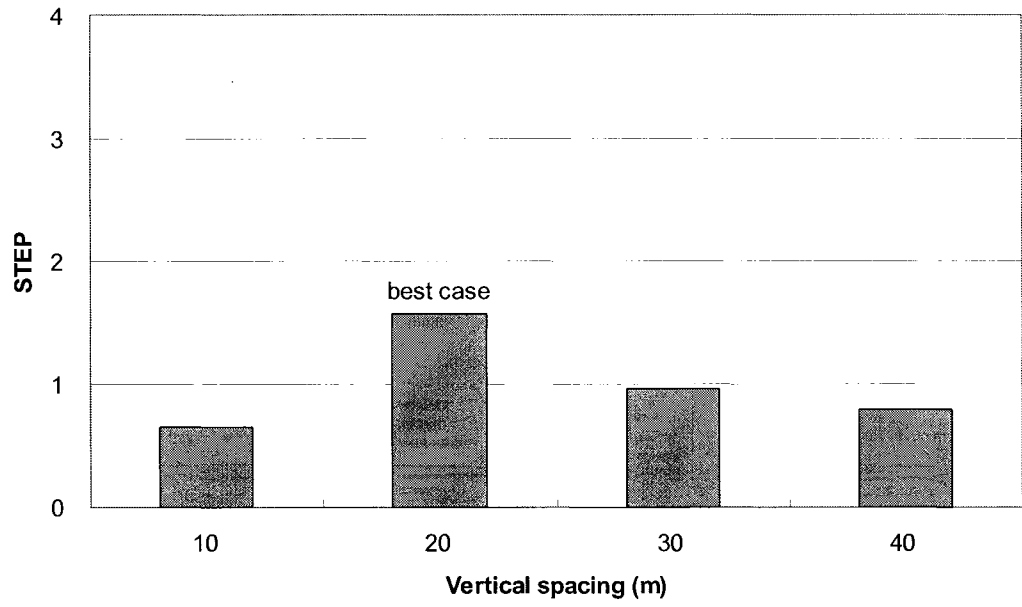
Figure 5.3: Effect of vertical spacing on STEP
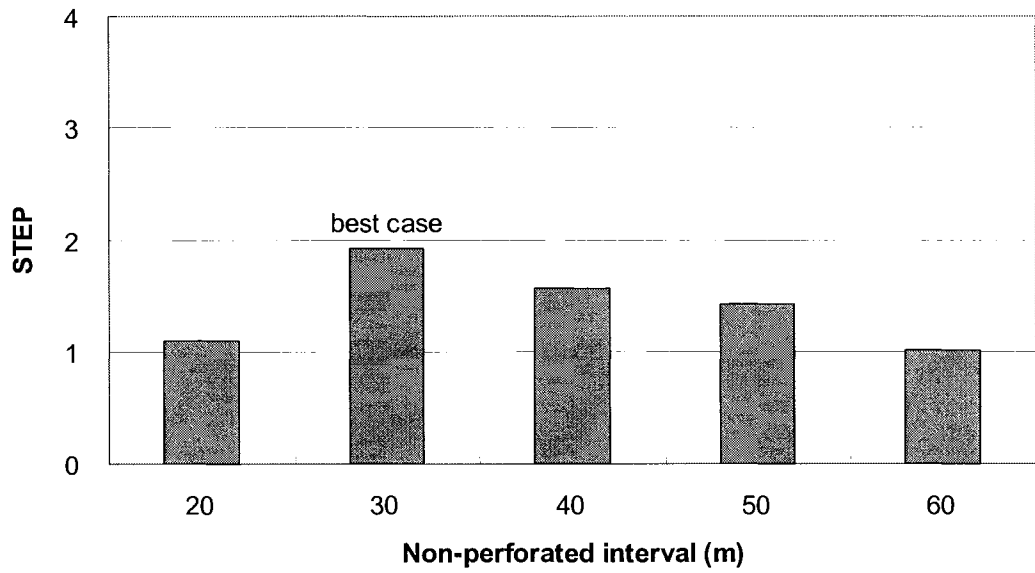
Figure 5.4: Effect of non-perforated interval on STEP

138
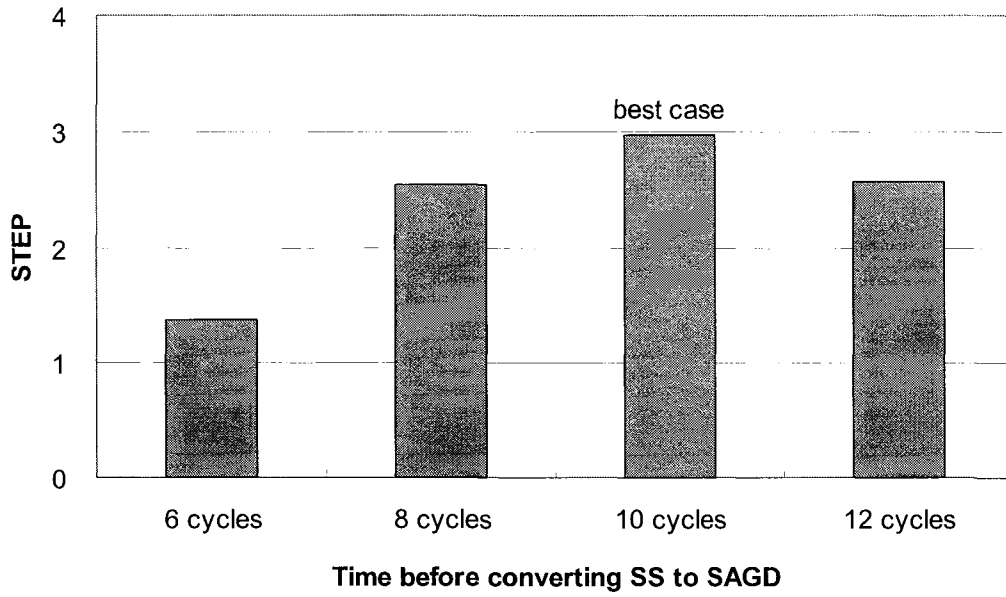
Figure 5.5: Effect of cyclic steam cycles before converting to SAGD on STEP
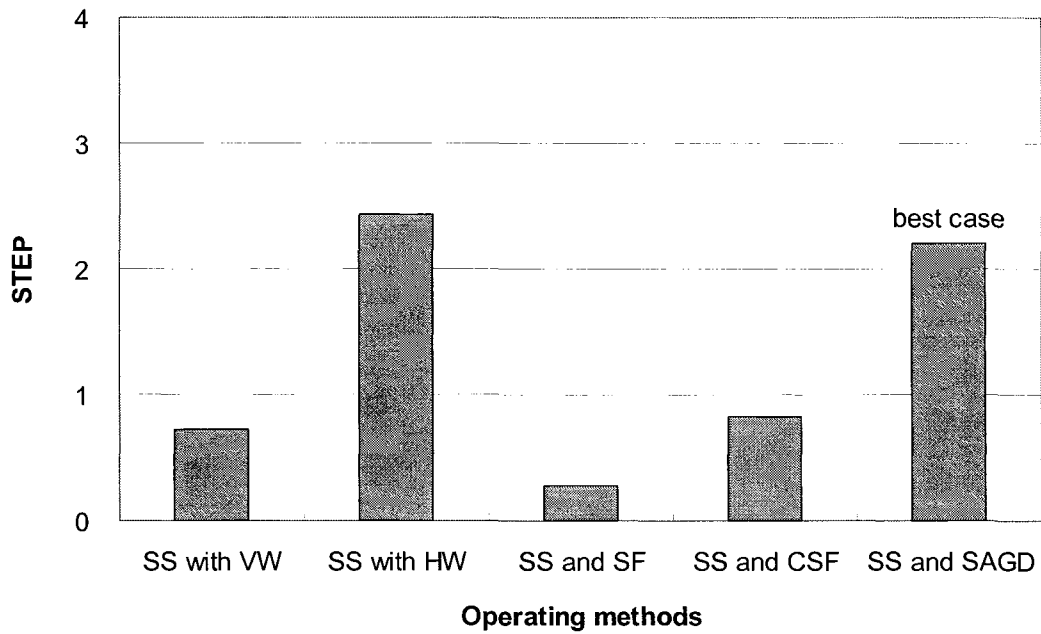
Figure 5.6: Effect of the operating methods on STEP

139

Table 5.1: Summary of simulation results (data from Gao et al. (2002))

Case	CSOR	CDOR $(m^3/d/m)$	RF	STEP
1) Well configurations for SAGD				
Type 1	4.07	0.384	0.37	1.2
Type 2	3.70	0.435	0.47	2.2
Type 3	3.85	0.414	0.43	1.8
2) Vertical spacing between the wells				
10 m	4.78	0.416	0.27	0.7
20 m	4.13	0.483	0.39	1.6
30 m	4.82	0.412	0.40	1.0
40 m	5.44	0.366	0.51	0.8
3) Non-perforated thickness				
20 m	4.65	0.427	0.41	1.1
30 m	4.07	0.488	0.45	1.9
40 m	4.13	0.483	0.39	1.6
50 m	4.20	0.474	0.38	1.4
60 m	4.48	0.443	0.33	1.0
4) Time converting SAGD				
6 cycles	4.31	0.399	0.46	1.4
8 cycles	3.70	0.444	0.53	2.6
10 cycles	3.57	0.444	0.57	3.0
12 cycles	3.65	0.419	0.55	2.6
5) Recovery methods				
SS with VW	1.83	0.066	0.18	0.7
SS with HW	1.53	0.133	0.20	2.4
SS and SF	4.67	0.184	0.24	0.3
SS and CSF	2.82	0.172	0.23	0.8
SS and SAGD	3.70	0.435	0.47	2.2

5.2.2 STEP validation as a quantitative indicator

The second validation study used the data from Edmunds and Chhina (2001) in which SAGD operating pressures have been investigated through numerical simulations for reservoir thicknesses of 10 and 25 m and permeabilities (K_v) of 2.8 and 5.6 Darcies,

140

which are representative of high-grade McMurray reservoirs in the Athabasca oil sands (Table 5.2). In their study, simulations were stopped when RF reached 0.55. Capital costs were considered for ROR and NPV calculations.

Table 5.2: Summary of simulation results (data from Edmunds and Chhina (2001))

Case	CSOR	CDOR $(m^3/d/m)$	RF	ROR (%)	STEP
1) 25 m and 5.6 Darcy					
300 kPa	1.52	0.171	0.55	30.7	8.7
400 kPa	1.61	0.207	0.55	32.4	9.1
500 kPa	1.68	0.241	0.55	33.0	9.6
750 kPa	1.83	0.313	0.55	33.5	10.2
1,000 kPa	1.97	0.373	0.55	34.2	10.1
1,500 kPa	2.22	0.472	0.55	29.0	9.4
3,000 kPa	2.85	0.650	0.55	26.9	7.3
2) 25 m and 2.8 Darcy					
500 kPa	1.90	0.150	0.55	26.1	4.4
750 kPa	2.04	0.194	0.55	27.1	4.9
1,000 kPa	2.17	0.230	0.55	28.2	5.0
1,500 kPa	2.40	0.288	0.55	27.0	4.9
3,000 kPa	3.02	0.408	0.55	24.7	4.0
3) 10 m and 5.6 Darcy					
500 kPa	2.67	0.105	0.55	6.8	1.4
750 kPa	2.82	0.133	0.55	9.4	1.5
1,000 kPa	2.96	0.155	0.55	9.9	1.6
1,500 kPa	3.22	0.188	0.55	10.0	1.6
3,000 kPa	3.99	0.245	0.55	8.5	1.2
4) 10 m and 2.8 Darcy					
500 kPa	3.25	0.065	0.55	12.9	0.5
750 kPa	3.36	0.084	0.55	14.0	0.6
1,000 kPa	3.50	0.099	0.55	15.2	0.7
1,500 kPa	3.76	0.122	0.55	14.6	0.7
3,000 kPa	4.57	0.161	0.55	11.3	0.6

This case study, which provides economic parameters (ROR and NPV), shows a good linear relationship between ROR and STEP. In all cases except one (10 m and 5.6 Darcy), the 1000 kPa simulation has the higest ROR and STEP (Table 5.2). The overall

141

correlation coefficient for all cases is 0.85 (Figure 5.7). If these cases are categorized based on permeability, the correlation coefficient is higher than 0.98 for both the 5.6 Darcy and 2.8 Darcy cases (Figures 5.8a and 5.8b); however if these are categorized based on thickness, the correlation coefficient is 0.80 for the 25 m case (Figures 5.9a) and 0.59 for the 10 m case (Figure 5.9b). Specifically, for the non-economic cases (10 m cases), the correlation shows a negative linear relationship with a low coefficient. This implies that reservoir thickness will affect the economics of the project much more than reservoir permeability even for similar recovery cases during the SAGD process investigated by Edmunds and Chhina (2001).
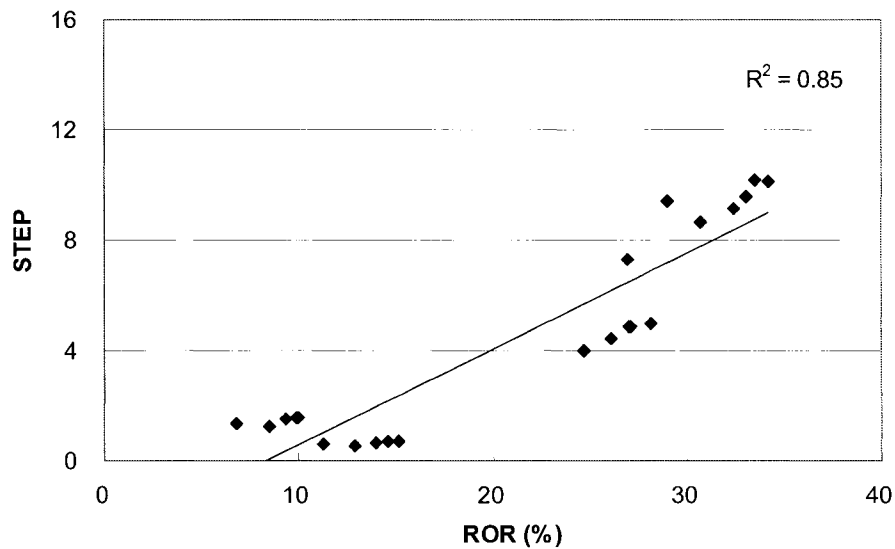
Figure 5.7: Correlation between ROR and STEP for all cases

142
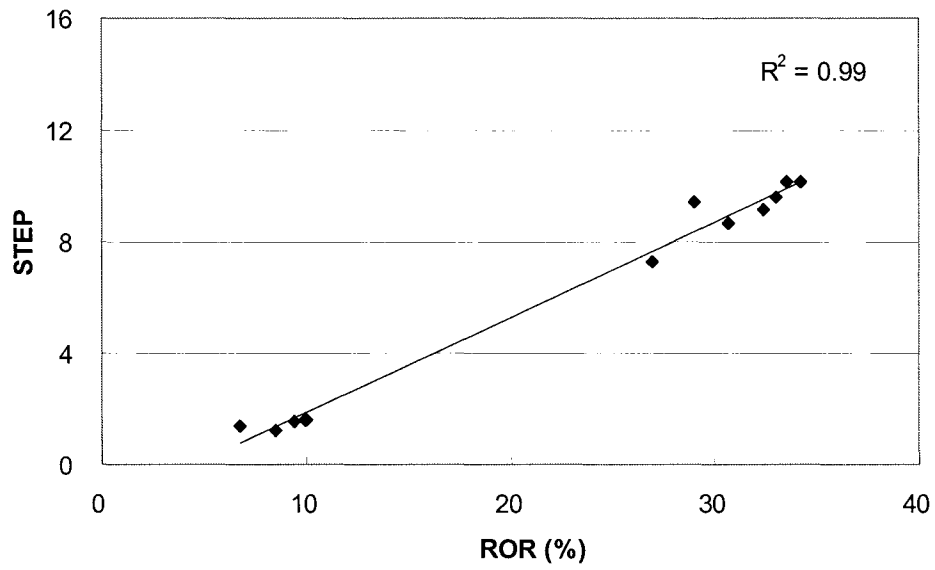
Figure 5.8a: Correlation between ROR and STEP for 5.6 Darcy case
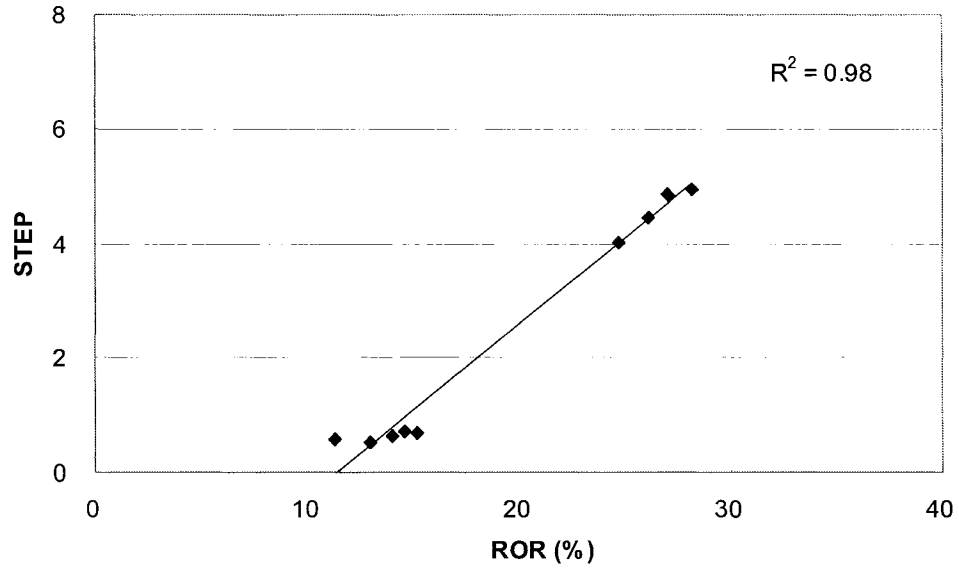
Figure 5.8b: Correlation between ROR and STEP for 2.8 Darcy case

143
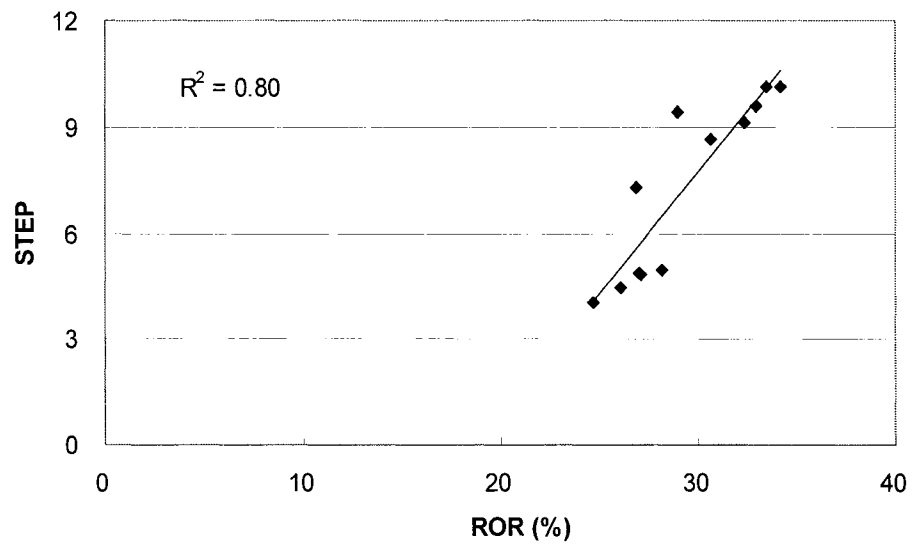
Figure 5.9a: Correlation between ROR and STEP for 25 m case
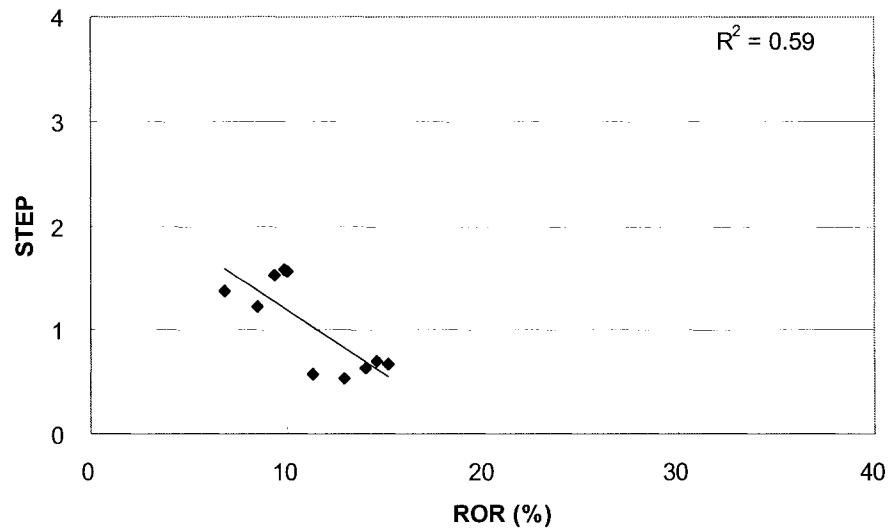
Figure 5.9b: Correlation between ROR and STEP for 10 m case

144

STEP is greater than 4 in the case of ROR values higher than 24 %. On the other hand, STEP is smaller than 2 in the case of ROR values lower than 15 %, which might be considered as an economic limit for SAGD performance. As these simulations were stopped at RF of 0.55, no matter what the project economics were, calculated STEP values should be different from the actual STEP values which should be used as a quantitative economic indicator in our research where the simulations were stopped at SOR = 4. Based on full scale economic analysis of these cases, if the STEP value is higher than 2, it will be an economic SAGD operation.

5.3 Evaluating SAGD operating conditions using STEP

As the same procedure is used for evaluating SAGD performance using STEP for the three cases, only the Athabasca case will be demonstrated. For the Cold Lake and Peace River cases, the best SAGD operating conditions will be determined, and a correlation between NPV and STEP calculated.

5.3.1 Athabasca-type reservoirs

Table 5.3 shows simulation results for the Athabasca-type reservoir cases related to four operating conditions. Individual results are given below.

5.3.1.1 Preheating period

Simulation results showed that, as the preheating period was increased, CDOR increased slightly but there was no change in CSOR (Figure 5.10a). A preheating period of 75 days for an I/P spacing of 5 m is economically adequate for a successful SAGD performance because there is not much enhancement in NPV even if the preheating period is longer (Figure 5.10b). Even though both NPV and STEP values varied within a small range, a linear relationship was found to exist between STEP and NPV, with a correlation coefficient of 1.00 (Figure 5.10c).

145

Table 5.3: SAGD simulation results for Athabasca-type reservoir

Case	CSOR	CDOR (m^3/d)	RF	NPV (M$)	STEP
1) Preheating period					
60 d	1.71	236	0.84	41.1	54.7
75 d	1.71	243	0.84	42.8	56.7
90 d	1.71	245	0.84	43.0	57.1
120 d	1.70	247	0.84	43.5	57.8
2) Injector to Producer (I/P) spacing					
5 m	1.71	243	0.84	42.8	56.7
10 m	1.64	213	0.84	39.0	54.3
15 m	1.61	187	0.84	32.3	50.4
3) Operating pressure					
1,500 kPa	1.71	243	0.84	42.8	56.7
3,000 kPa	1.99	359	0.83	43.0	57.7
4,500 kPa	2.18	430	0.82	39.5	54.2
4) Max. steam injection rate					
400 m^3	1.75	196	0.84	31.7	43.3
500 m^3	1.72	223	0.84	38.1	51.3
600 m^3	1.71	239	0.84	41.7	55.6
700 m^3	1.71	243	0.84	42.8	56.7
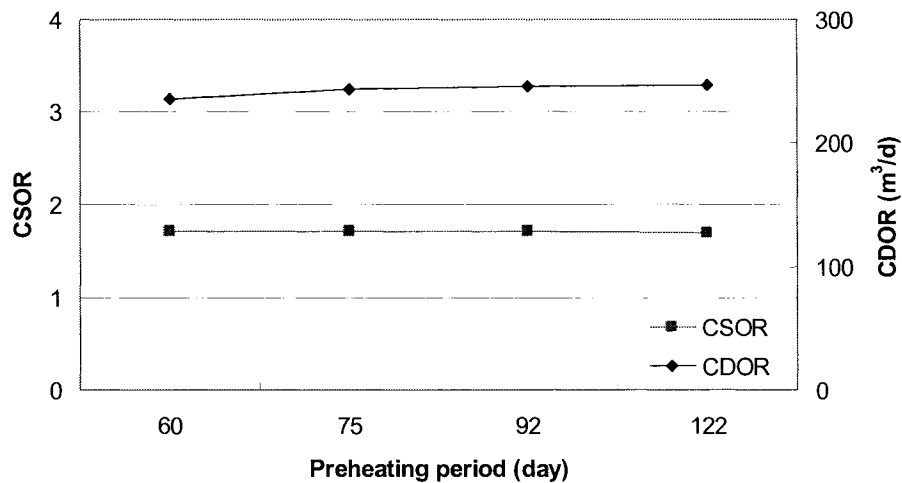
Figure 5.10a: Effect of preheating period on CSOR and CDOR

146
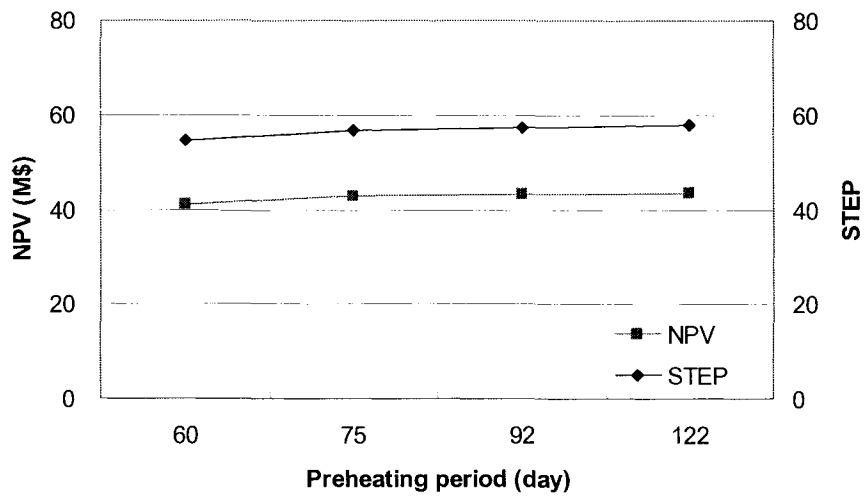
Figure 5.10b: Effect of preheating period on NPV and STEP
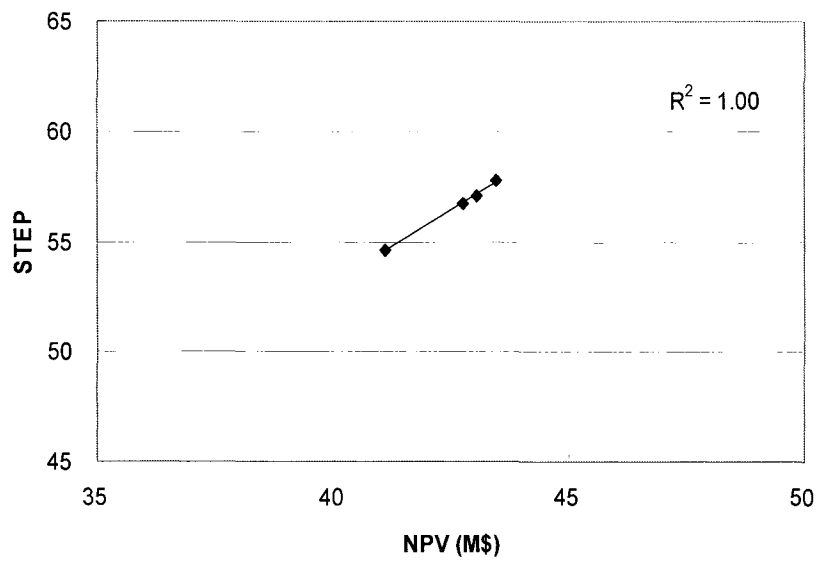
Figure 5.10c: Correlation of NPV and STEP

147

5.3.1.2 Injector to Producer spacing

The simulation results showed that, as the I/P spacing was increased from 5 m to 15 m, CDOR, CSOR and NPV decreased (Figures 5.11a and 5.11b). In other words, the productivity decreases but thermal efficiency increases. The I/P spacing of 5 m case gave the best SAGD performance: the highest NPV and CDOR. There was a linear relationship between STEP and NPV, with a correlation coefficient of 1.00 (Figure 5.11c)
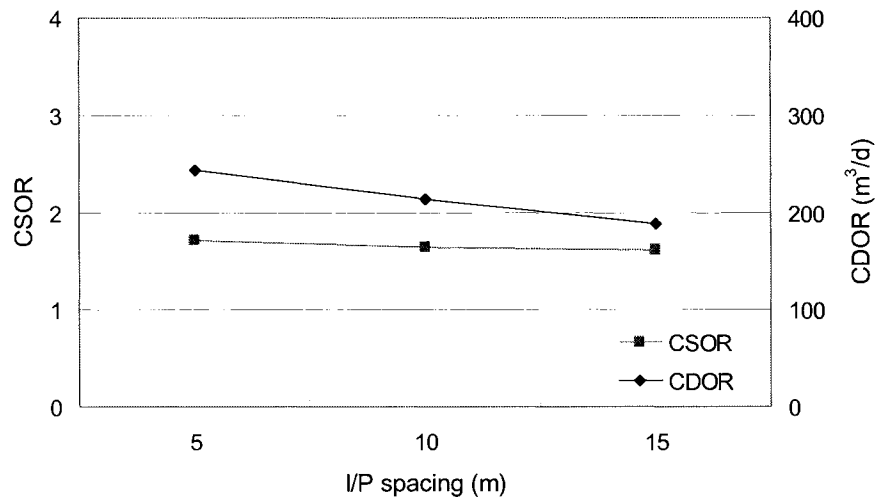
Figure 5.11a: Effect of I/P spacing on CSOR and CDOR
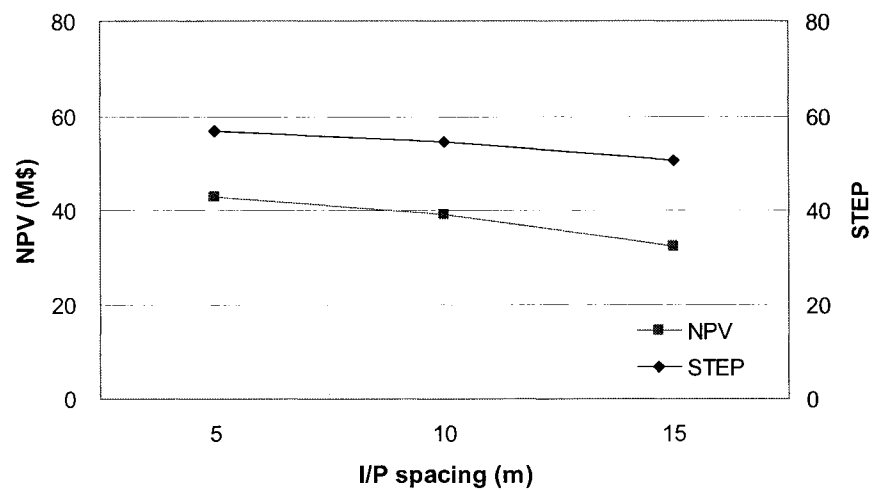
Figure 5.11b: Effect of I/P spacing on NPV and STEP

148
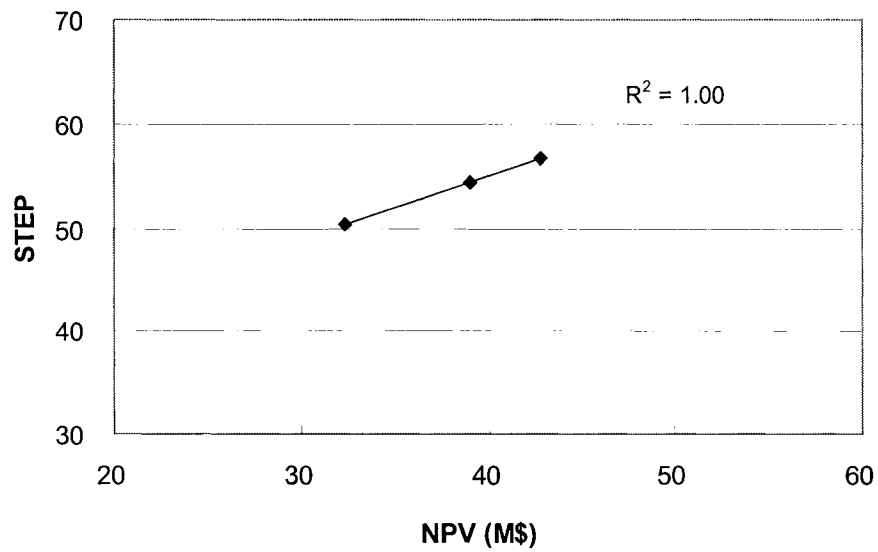
Figure 5.11c: Correlation of NPV and STEP

5.3.1.3 Steam injection pressure

The simulation results showed that, as the steam injection pressure was increased from 1,500 to 4,500 kPa, CSOR and CDOR increased (Figure 5.12a); the productivity increased but thermal efficiency decreased. A steam injection pressure of 3,000 kPa gave the highest NPV (Figure 5.12b), however, the 1,500 kPa case had the same NPV with lower CSOR and higher RF (0.84 over 0.83). Therefore, a pressure higher than 3,000 kPa is not good as the SAGD operating pressure for shallow Athabasca-type reservoirs. The correlation coefficient between STEP and NPV, was 0.96 (Figure 5.12c).

149
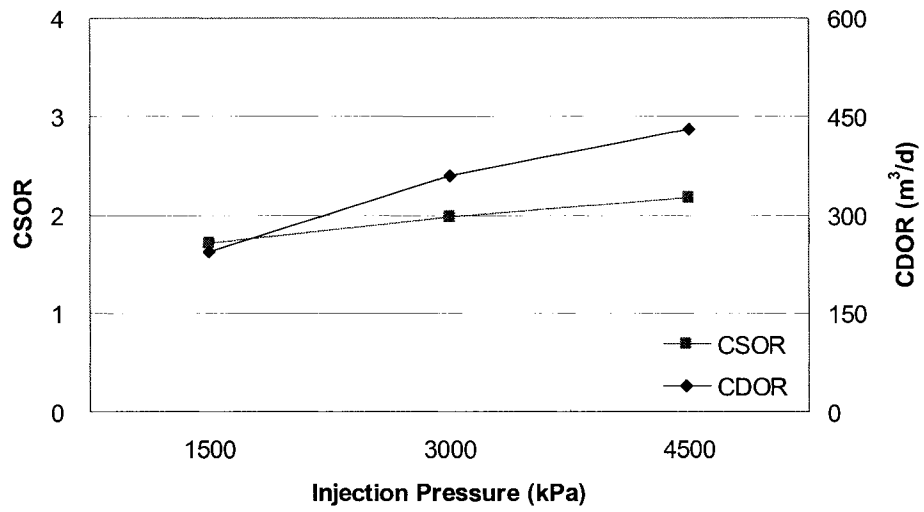
Figure 5.12a: Effect of injection pressure on CSOR and CDOR
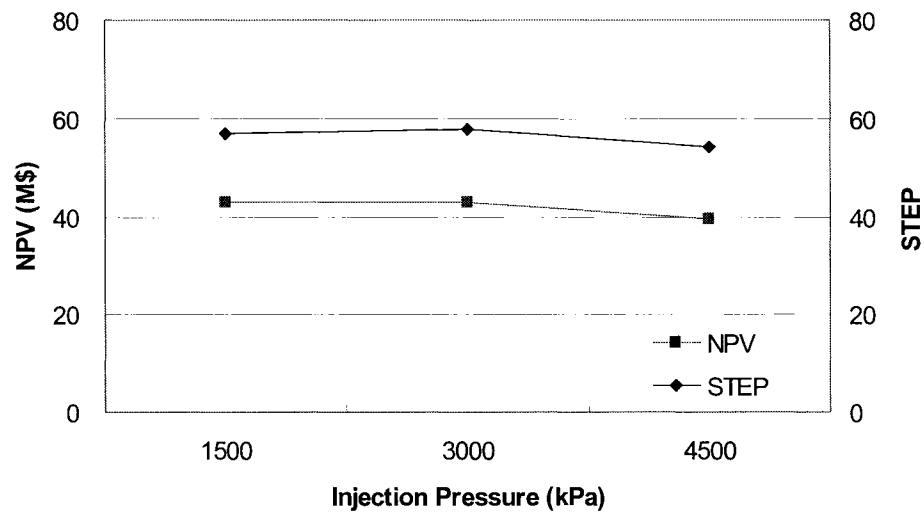
Figure 5.12b: Effect of injection pressure on NPV and STEP

150
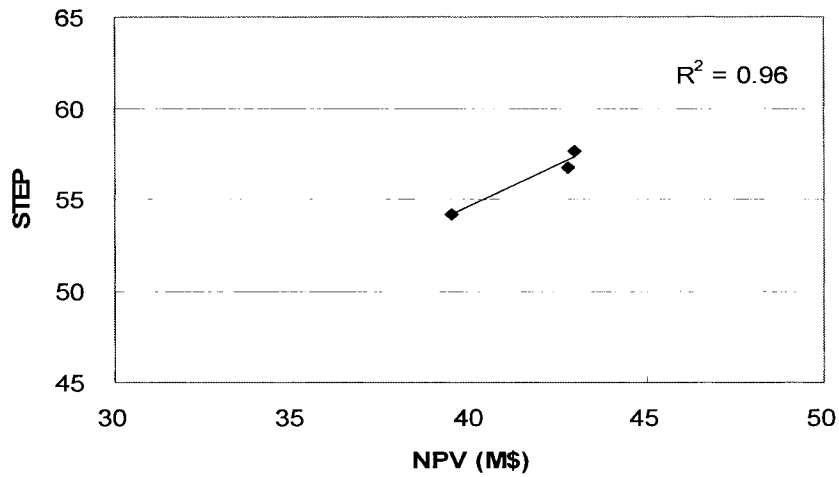
Figure 5.12c: Correlation of NPV and STEP

5.3.1.4 Maximum steam injection rate

The simulations were conducted with a maximum steam injection pressure of 1,500 kPa. As the steam injection rate was increased, CSOR decreased slightly and CDOR increased (Figure 5.13a). The NPV and STEP were the highest for an injection rate of 700 m^3/d (Figure 5.13b). There was a linear relationship between STEP and NPV, with a correlation coefficient of 1.00 (Figure 5.13c)
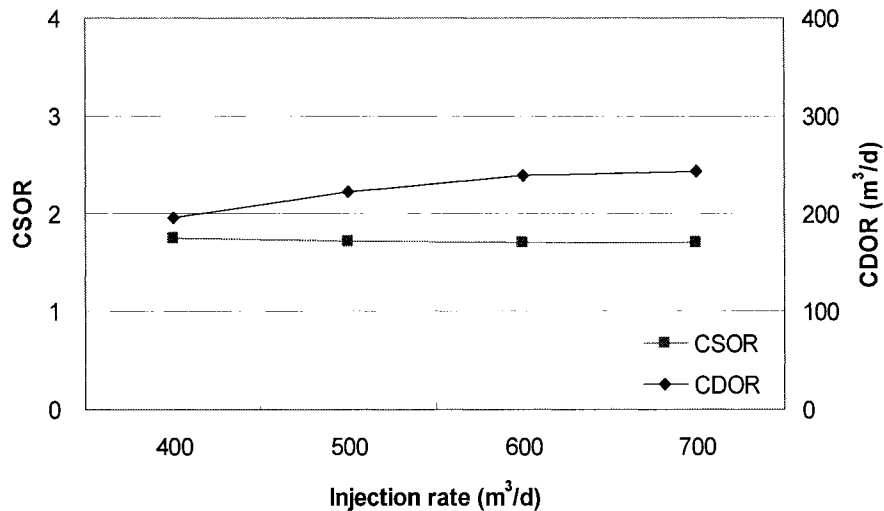
Figure 5.13a: Effect of injection rate on CSOR and CDOR

151
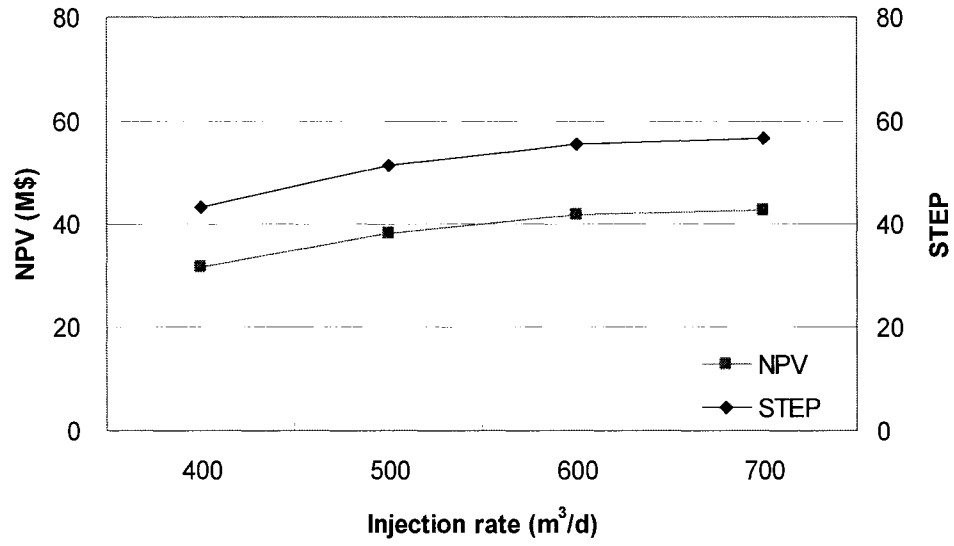
Figure 5.13b: Effect of injection rate on NPV and STEP
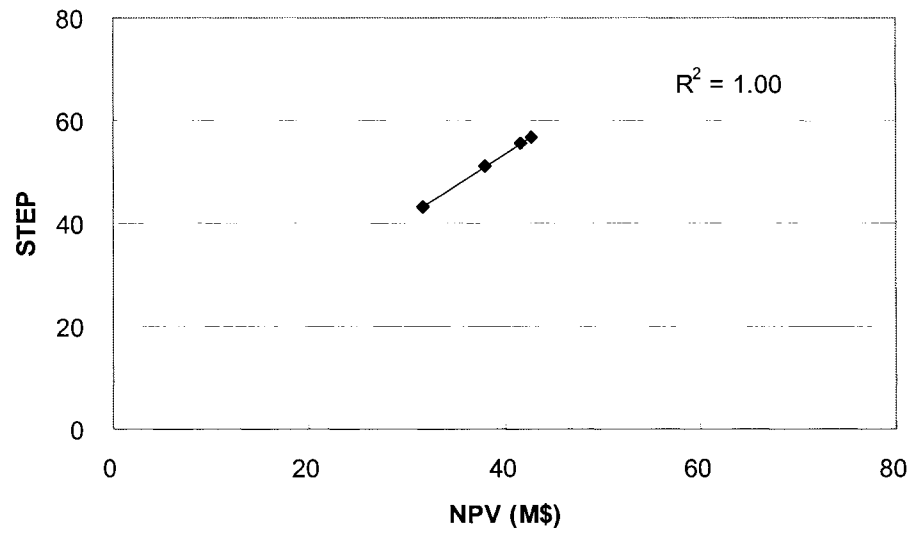
Figure 5.13c: Correlation of NPV and STEP

152

5.3.1.5 Best SAGD operating conditions

The most favourable SAGD operating conditions for the Athabasca-type reservoirs were determined from the numerical simulations in order to have the highest NPV and STEP. With reservoir parameters of: permeability (K_v) of 2.5 Darcy, reservoir thickness of 30 m, and bitumen viscosity of 1,000,000 cp, the most favourable operating conditions were found to be: I/P spacing of 5 m, maximum steam injection rate of 700 m^3/d at a maximum injection pressure of 1,500 kPa.

A linear relationship was found to exist between STEP and NPV with a correlation coefficient in excess of 0.96 for most of the cases (Table 5.4), and 0.88 overall for the cases of Athabasca-type reservoirs (Figure 5.14).

Table 5.4: Correlation coefficients between NPV and STEP

Best case	Correlation coefficient (R^2)		
	AB	CL	PR
Preheating period	1.00	0.99	1.00
I/P spacing	1.00	1.00	1.00
Operating pressure	0.96	0.97	0.91
Max. steam injection rate	1.00	1.00	0.99
Overall case	0.88	0.85	0.87

153
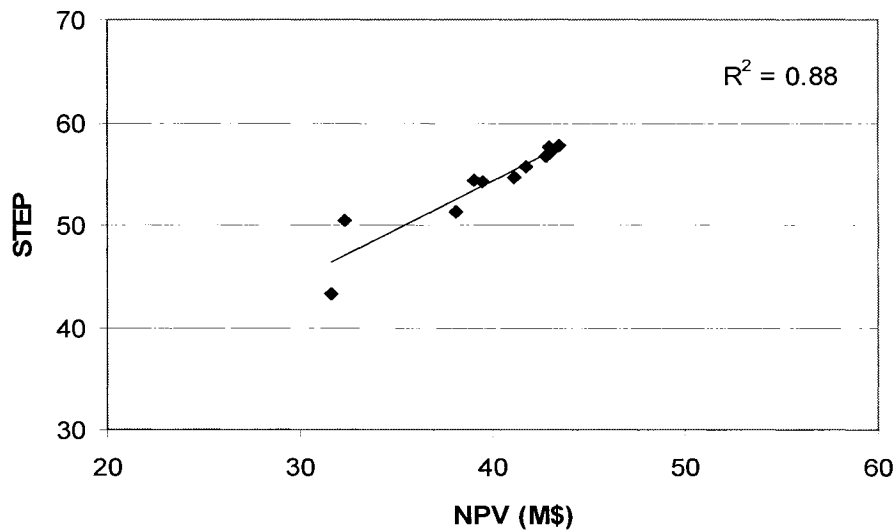
Figure 5.14: Correlation of NPV and STEP for Athabasca-type

5.3.2 Cold Lake-type reservoirs

Table 5.5 shows the simulation results for the Cold Lake-type reservoir cases related to the four operating conditions discussed earlier. Detailed individual results are given below.

The most favourable SAGD operating conditions for Cold Lake-type reservoirs were determined from the numerical simulation results to have the highest NPV and STEP. With reservoir parameters of: permeability (K_v) of 1.25 Darcy, reservoir thickness of 20 m, and bitumen viscosity of 60,000 cp, the most favourable operating conditions were found to be: I/P spacing of 15 m and maximum steam injection rate of 400 m^3/d at a maximum injection pressure of 3,100 kPa.

A linear relationship was found to exist between STEP and NPV, with a correlation coefficient in excess of 0.97 for most of the cases (Table 5.4), and 0.85 overall for the cases of Cold Lake-type reservoirs (Figure 5.15).

154

Table 5.5: SAGD simulation results for Cold Lake-type reservoir

Case	CSOR	CDOR (m³/d)	RF	NPV (M$)	STEP
1) Preheating period					
90 d	2.75	73	0.46	4.7	3.0
120 d	2.73	88	0.45	5.3	3.6
150 d	2.73	98	0.46	5.7	4.0
180 d	2.74	103	0.46	5.8	4.2
210 d	2.74	105	0.46	5.9	4.3
2) Injector to Producer (I/P) spacing					
5 m	2.89	106	0.42	4.9	3.5
10 m	2.74	103	0.46	5.8	4.2
15 m	2.69	96	0.49	6.1	4.4
3) Operating pressure (I/P spacing 5 m)					
3,100 kPa	2.89	106	0.42	4.9	3.5
4,500 kPa	3.24	141	0.39	3.2	3.2
6,000 kPa	3.73	159	0.37	1.0	2.5
4) Max. steam injection rate					
200 m³	3.63	52	0.71	1.3	1.7
300 m³	3.11	85	0.67	5.2	3.8
400 m³	2.75	103	0.47	5.8	4.2
500 m³	2.74	103	0.46	5.8	4.2
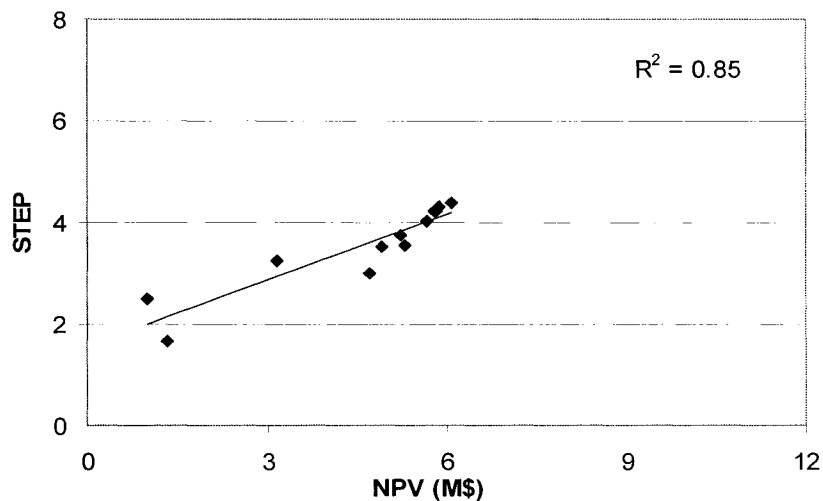
Figure 5.15: Correlation of NPV and STEP for Cold Lake-type

155

5.3.3 Peace River-type reservoirs

Table 5.6 shows the simulation results for the Peace River-type reservoir cases related to the four operating conditions. Detailed individual results are given below.

The most favourable SAGD operating conditions for Peace River-type reservoirs were determined from the numerical simulations. With reservoir parameters of: permeability (K_v) of 0.65 Darcy, reservoir thickness of 25 m, and bitumen viscosity of 200,000 cp, the most favourable operating conditions were found to be: I/P spacing of 15 m and maximum steam injection rate of 600 m^3/d at a maximum injection pressure of 4,500 kPa.

A linear relationship was found to exist between STEP and NPV, with a correlation coefficient in excess of 0.91 for most of cases (Table 5.4), and 0.87 overall for the cases of Peace River type reservoirs (Figure 5.16).
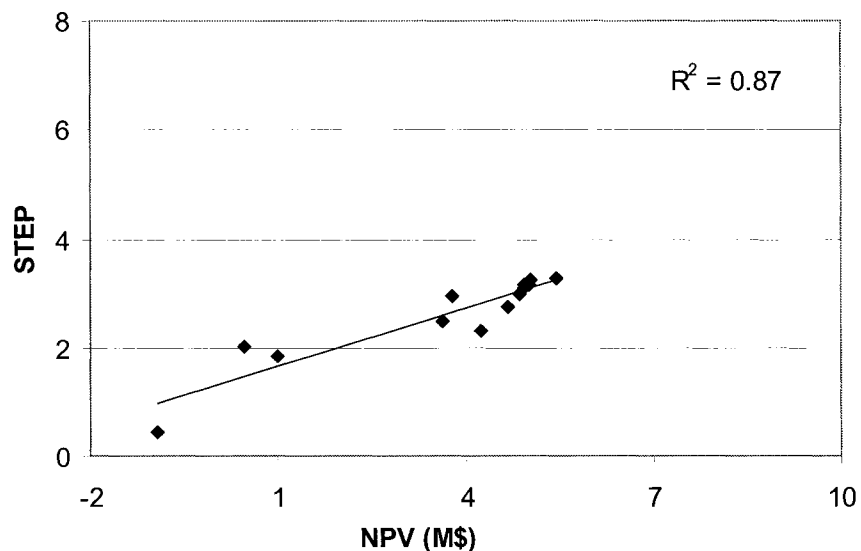
Figure 5.16: Correlation of NPV and STEP for Peace River type

156

Table 5.6: SAGD simulation results for Peace River type-reservoir

Case	CSOR	CDOR (m^3/d)	RF	NPV (M$)	STEP
1) Preheating period					
90 d	3.01	124	0.31	4.7	2.8
120 d	3.04	133	0.33	4.9	3.0
150 d	3.00	139	0.31	4.9	3.1
180 d	3.00	142	0.31	5.0	3.2
210 d	3.00	145	0.31	5.0	3.2
2) Injector to Producer (I/P) spacing					
5 m	3.26	139	0.31	3.6	2.5
10 m	3.00	139	0.31	4.9	3.1
15 m	2.91	123	0.35	5.5	3.3
3) Operating pressure (I/P spacing 5 m)					
4,500 kPa	2.89	106	0.31	3.6	2.5
6,000 kPa	3.77	165	0.27	1.0	1.9
7,500 kPa	4.44	149	0.11	-0.9	0.4
4) Max. steam injection rate					
300 m^3	3.87	75	0.69	0.5	2.0
400 m^3	3.59	105	0.60	3.8	3.0
500 m^3	3.13	136	0.36	4.9	3.2
600 m^3	3.00	142	0.31	5.0	3.2

5.3.4 Correlation of NPV and STEP for all three reservoir types

The relationship between NPV and STEP for all three areas has been analyzed. Athabasca-type reservoirs gives the highest NPV and STEP value, and Peace River-type gives the lowest NPV and STEP.

There is a linear relationship between NPV and STEP with a correlation coefficient 0.99 (Figure 5.17) for all the cases of three Alberta oil sands areas. Comparing the best cases for three typical reservoirs, there is a good linear relationship between STEP and NPV with a correlation coefficient of 1.00 (Figure 5.18).

157
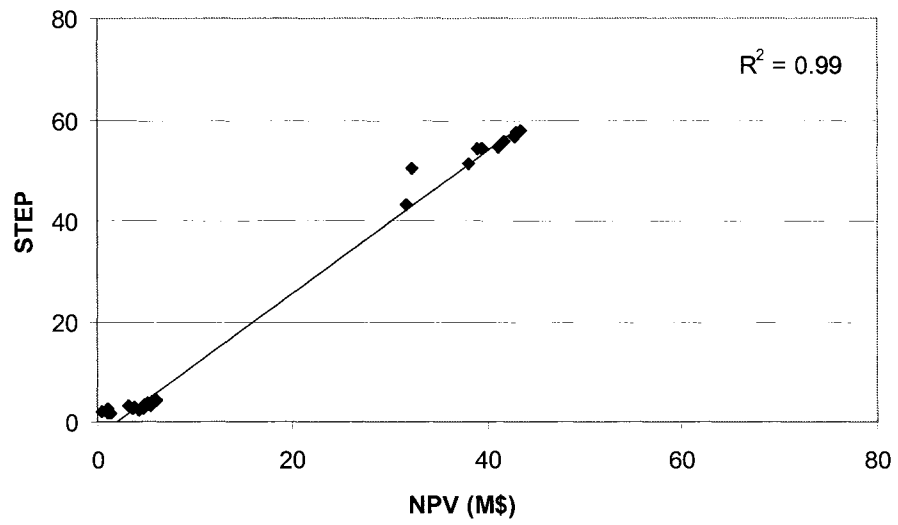
Figure 5.17: Correlation of NPV and STEP for all cases
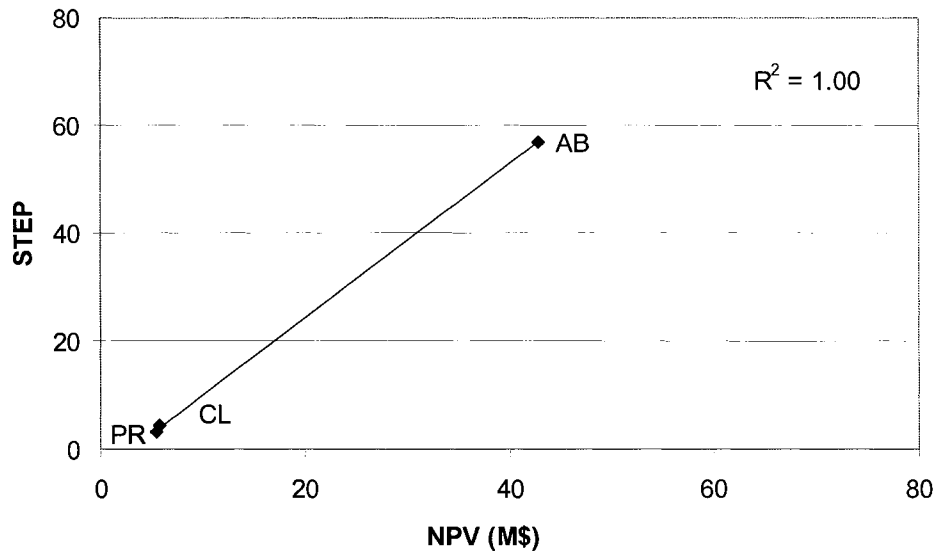
Figure 5.18: Correlation of NPV and STEP for the best cases

158

5.4 Screening reservoir parameters for SAGD using STEP

STEP was used as a qualitative indicator for evaluating SAGD operating conditions in a previous section. In this section, STEP has been used for screening two important reservoir parameters, thickness and permeability, in three typical Alberta oil sands reservoirs: Athabasca, Cold Lake, and Peace River.

5.4.1 Athabasca-type reservoirs

The reservoir parameters for the base case simulation are: permeability (K_v) of 2.5 Darcy, reservoir thickness of 30 m, and bitumen viscosity of 1,000,000 cp. The operating conditions are an injector to producer (I/P) spacing of 5 m and a maximum injection pressure of 1,500 kPa. Table 5.7 shows the sensitivity of the simulation results for Athabasca-type reservoir cases where two reservoir parameters, thickness and permeability, are modified.

Table 5.7: SAGD simulation results for Athabasca-type reservoir

Case	CSOR	CDOR (m³/d/m)	RF	NPV (M$)	STEP
1) Reservoir thickness (well pattern spacing 100 m)					
15 m	2.63	0.172	0.72	13.5	3.1
20 m	2.12	0.222	0.78	25.0	7.1
25 m	1.87	0.248	0.82	34.9	11.4
30 m	1.71	0.273	0.84	42.8	16.1
2) Reservoir permeability (K_v)					
0.625 D	3.24	0.072	0.31	5.3	0.3
1.25 D	2.06	0.157	0.80	23.3	5.6
2.5 D	1.71	0.270	0.84	42.8	15.9

5.4.1.1 Reservoir thickness

A linear relationship was found to exist between STEP and NPV with a correlation coefficient of 0.99 (Figure 5.19a). As the reservoir thickness is increased, NPV and

159

STEP increase (Figure 5.19b). A 15 m thickness is still economic for this type of reservoir: the calculated STEP value of 3.1 is higher than 1.
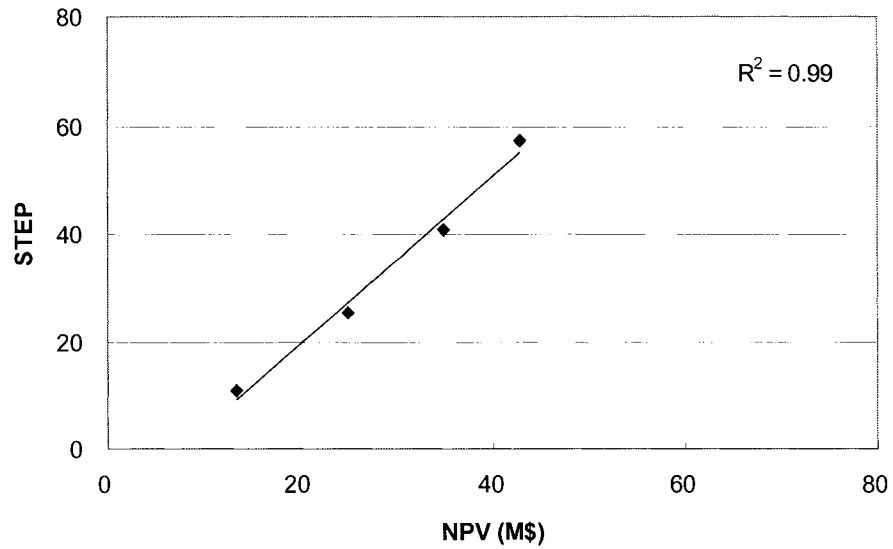
Figure 5.19a: Correlation of NPV and STEP
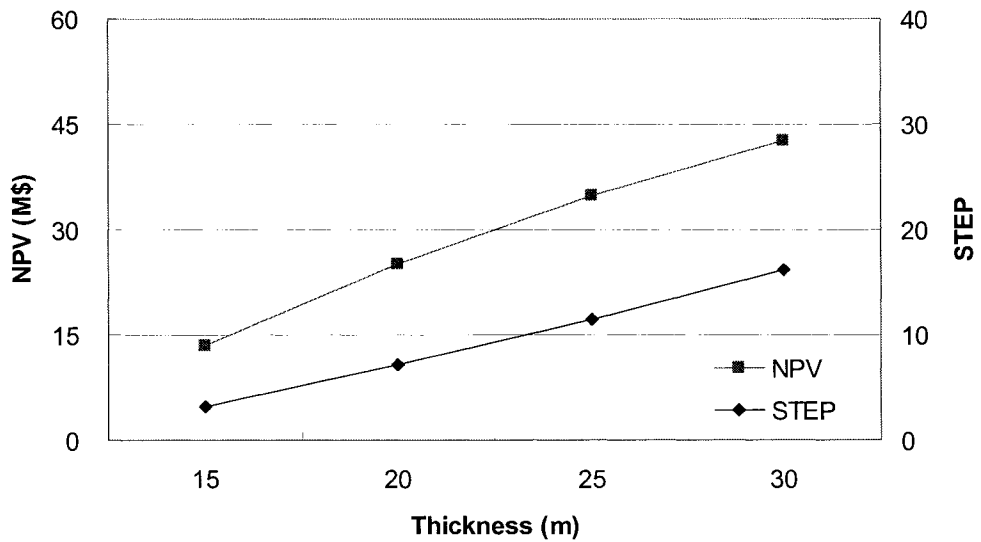
Figure 5.19b: Effect of reservoir thickness on NPV and STEP

160

5.4.1.2 Reservoir permeability

A linear relationship was found to exist between STEP and NPV with a correlation coefficient of 0.97 (Figure 5.20a). As the reservoir permeability is increased, NPV and STEP increase (Figure 5.20b). A vertical permeability of 0.625 Darcy seems too low for an efficient SAGD process for this type of reservoir as STEP (0.3) is lower than 1.
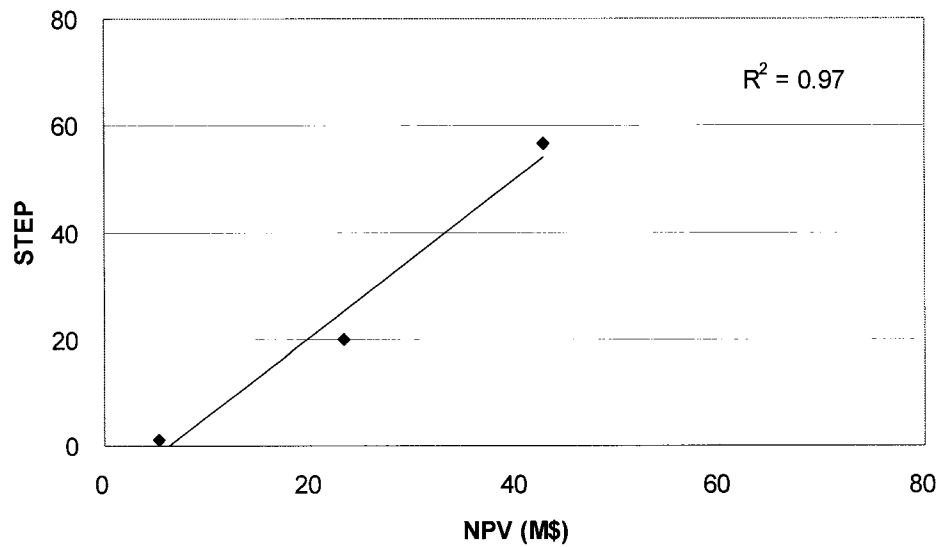
Figure 5.20a: Correlation of NPV and STEP

161
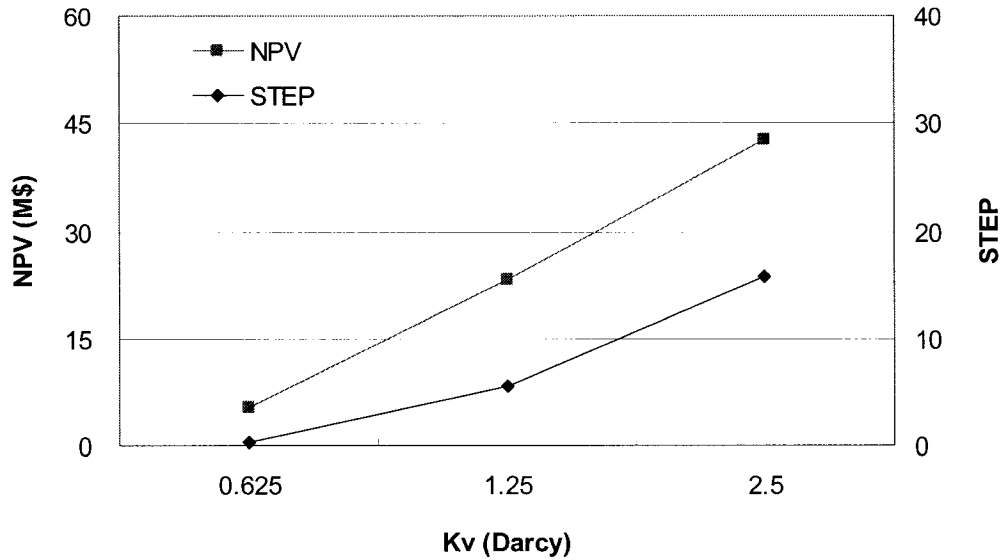
Figure 5.20b: Effect of reservoir permeability on NPV and STEP

5.4.2 Cold Lake-type reservoirs

The reservoir parameters for the base case simulation are: permeability (K_v) of 1.25 Darcy, reservoir thickness of 20 m, and bitumen viscosity of 60,000 cp. The operating conditions are an I/P spacing of 10 m and a maximum injection pressure of 3,100 kPa. Table 5.8 shows the sensitivity of the simulation results for Cold Lake-type reservoir cases where two reservoir parameters, thickness and permeability, are modified.

Table 5.8: SAGD simulation results for Cold Lake-type reservoir

Case	CSOR	CDOR (m^3/d/m)	RF	NPV (M$)	STEP
1) Reservoir thickness (well pattern spacing 100 m)					
15 m	2.76	0.098	0.25	2.7	0.6
20 m	2.61	0.118	0.42	5.9	1.0
25 m	2.72	0.120	0.69	9.9	1.6
30 m	2.49	0.137	0.73	14.0	2.4
2) Reservoir permeability (K_v)					
0.625 D	3.45	0.066	0.38	1.9	0.3
1.25 D	2.74	0.114	0.46	5.8	1.2
2.5 D	2.91	0.146	0.72	8.3	2.0

162

5.4.2.1 Reservoir thickness

A linear relationship was found to exist between STEP and NPV with a correlation coefficient of 1.00 (Figure 5.21a). As the reservoir thickness is increased, NPV and STEP increase (Figure 5.21b). At least 20 m of reservoir thickness is required for an economic SAGD process in Cold Lake resulting in a STEP value of 1.

5.4.2.2 Reservoir permeability

A linear relationship was found to exist between STEP and NPV with a correlation coefficient of 0.98 (Figure 5.22a). As the reservoir permeability is increased, NPV and STEP increase (Figure 5.22b). A vertical permeability of 0.625 Darcy seems too low for an efficient SAGD process for this type of reservoir as STEP (0.3) is lower than 1.
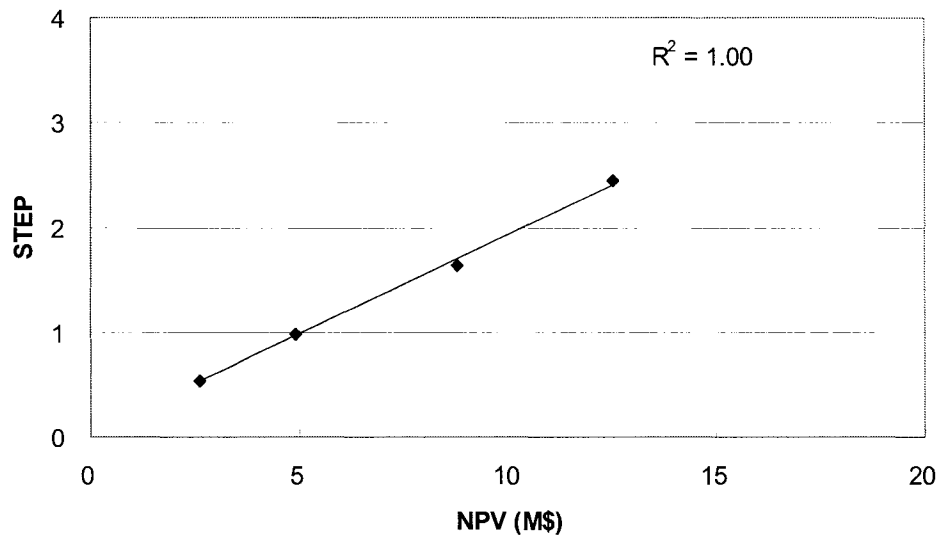
Figure 5.21a: Correlation of NPV and STEP
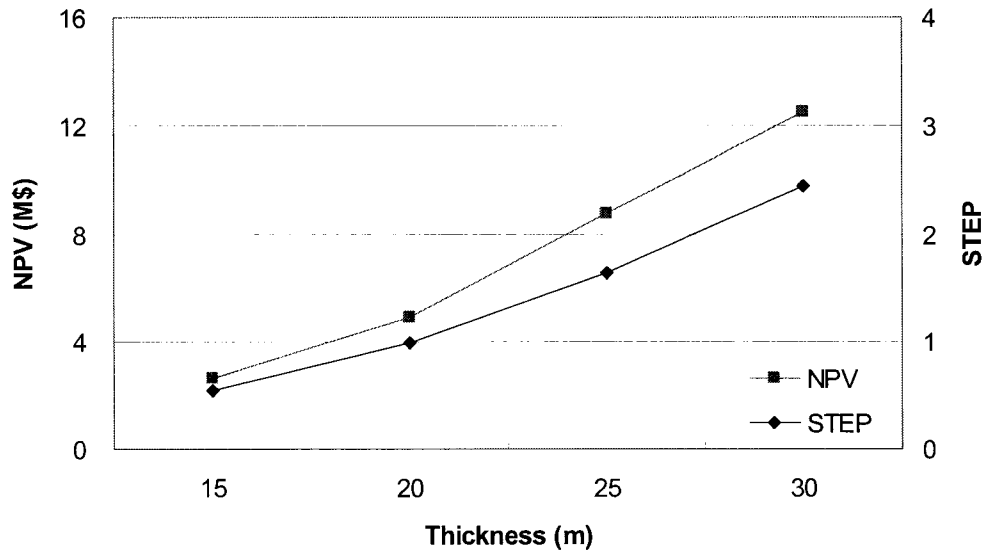
Figure 5.21b: Effect of reservoir thickness on NPV and STEP
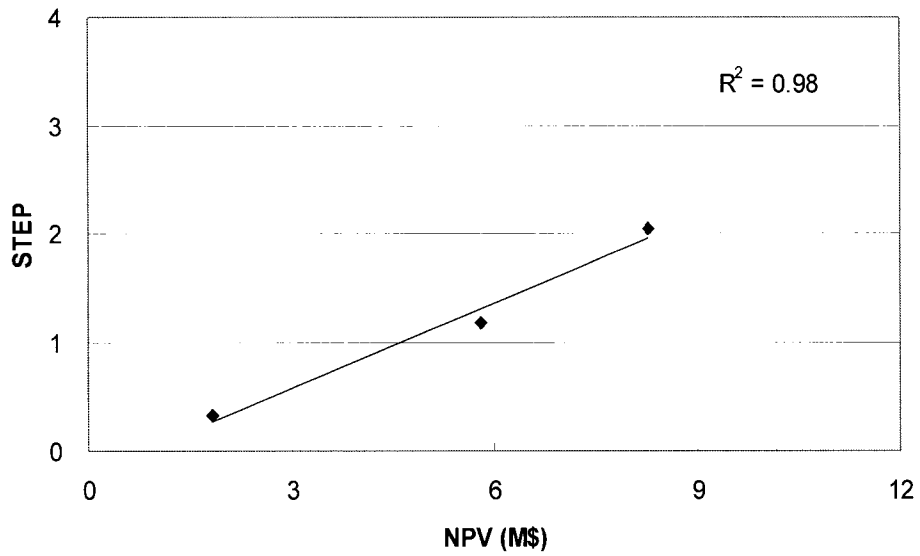
Figure 5.22a: Correlation of NPV and STEP

164
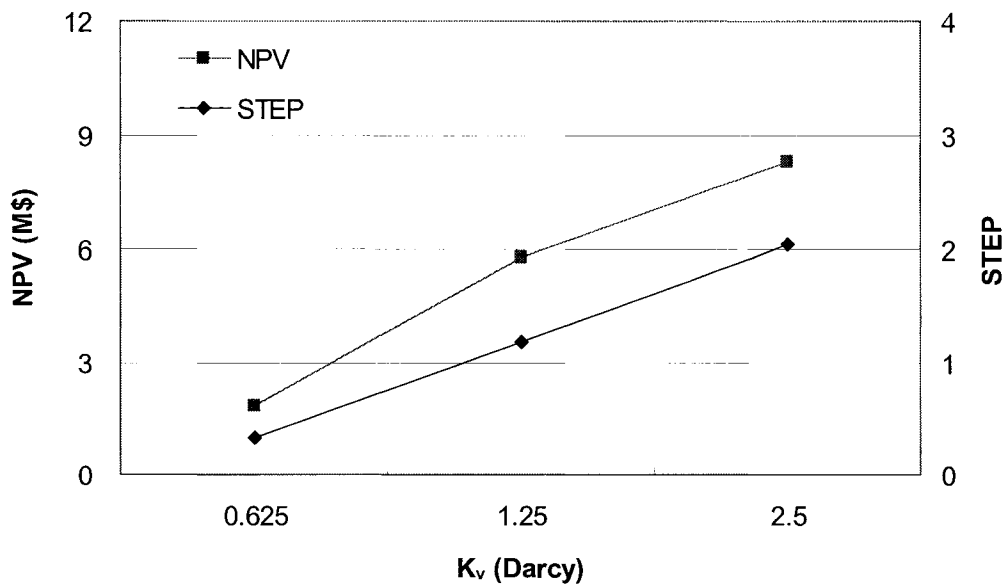
Figure 5.22b: Effect of reservoir permeability on NPV and STEP

5.4.3 Peace River-type reservoirs

The reservoir parameters for the base case simulation are: permeability (K_v) of 0.65 Darcy, reservoir thickness of 25 m, and bitumen viscosity of 200,000 cp. The operating conditions are an I/P spacing of 10 m and a maximum injection pressure of 4,500 kPa. Table 5.9 shows the sensitivity of the simulation results for Peace River-type reservoir cases where two reservoir parameters, thickness and permeability, are modified.

Table 5.9: SAGD simulation results for Peace River-type reservoir

Case	CSOR	CDOR (m³/d/m)	RF	NPV (M$)	STEP
1) Reservoir thickness (well pattern spacing 100 m)					
15 m	3.34	0.117	0.20	1.1	0.3
20 m	2.98	0.138	0.27	2.1	0.4
25 m	3.33	0.154	0.38	3.6	0.7
30 m	3.03	0.165	0.51	5.4	1.0
2) Reservoir permeability (K_v)					
0.65 D	3.00	0.158	0.31	5.0	0.9
1.25 D	2.81	0.237	0.37	7.6	1.9
2.5 D	3.12	0.246	0.71	10.6	2.9

165

5.4.3.1 Reservoir thickness

A linear relationship was found to exist between STEP and NPV with a correlation coefficient of 1.00 (Figure 5.23a). As the reservoir thickness is increased, NPV and STEP increase (Figure 5.23b). The reservoir thickness should be at least thicker than 30 m for an economic SAGD process in Peace River-type reservoir as STEP value is 1 at the reservoir thickness of 30 m (Table 5.8).

5.4.3.2 Reservoir permeability

A linear relationship was found to exist between STEP and NPV with a correlation coefficient of 1.00 (Figure 5.24a). As the reservoir permeability is increased, NPV and STEP increase (Figure 5.24b). A vertical permeability of 0.65 Darcy seems too low for an efficient SAGD process for this type of reservoir: STEP (0.9) is lower than 1.
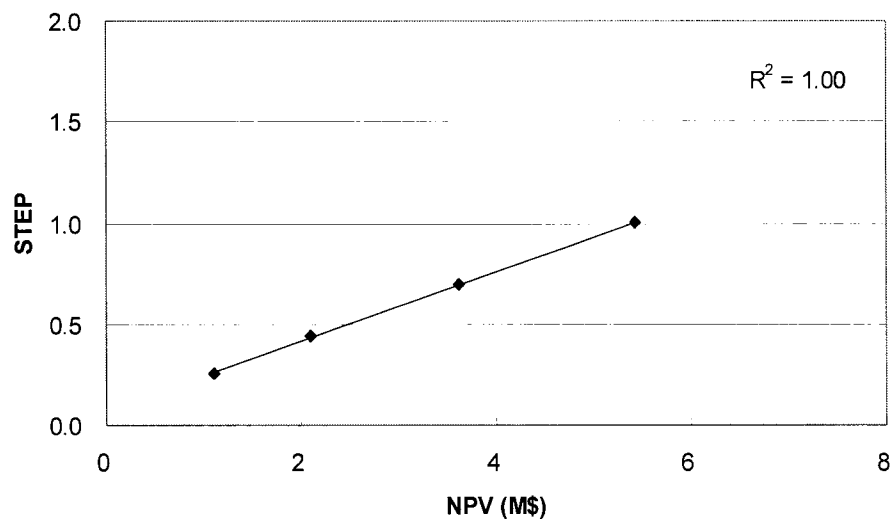
Figure 5.23a: Correlation of NPV and STEP

166
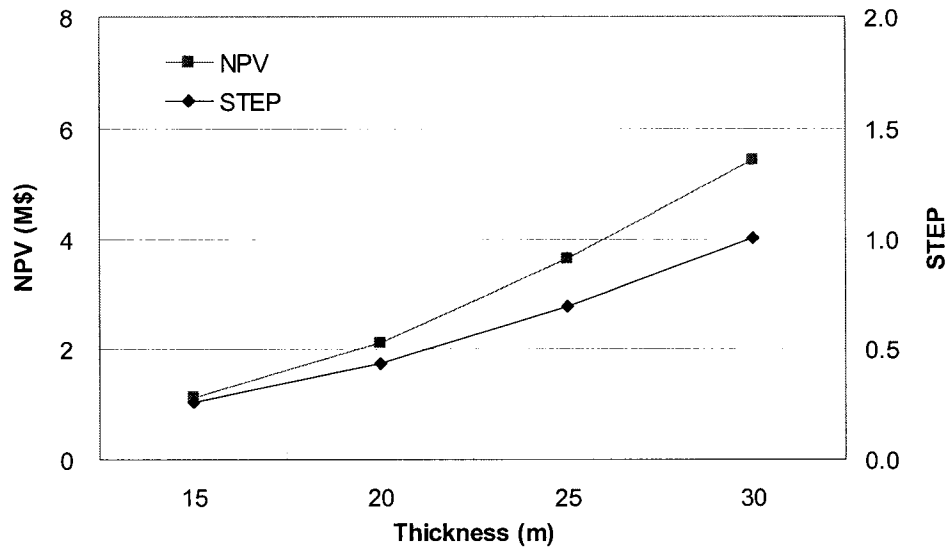
Figure 5.23b: Correlation of NPV and STEP
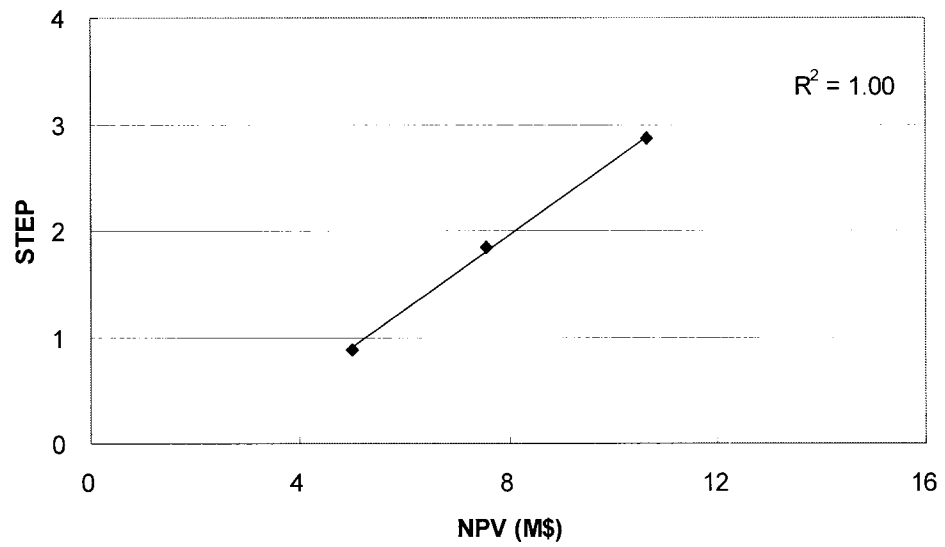
Figure 5.24a: Correlation of NPV and STEP

167
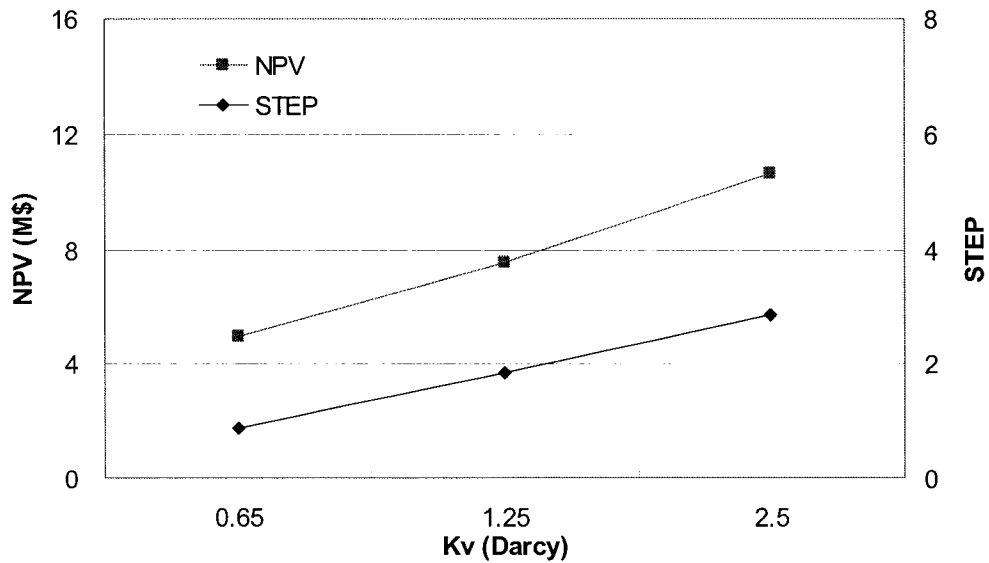
Figure 5.24b: Effect of reservoir permeability on NPV and STEP

5.4.4 Correlation of NPV and STEP for all three reservoir types

The relationship between NPV and STEP for all three areas has been analyzed. There is a linear relationship between NPV and STEP with a correlation coefficient 0.97 (Figure 5.25) for all the cases of reservoir parameters studied in the three Alberta oil sands areas.

The reservoir parameters required for an economic SAGD performance leading to a STEP greater than 1 are different for each oil sands reservoir. Athabasca-type reservoirs, which can have an average permeability of 2.5 Darcy, show that STEP is greater than 3 for a 15m thick reservoir. On the other hand, Peace River-type reservoirs, which have a lower permeability such as 0.65 Darcy, show that STEP is 1 for a 30 m thick reservoir. Cold Lake-type reservoirs, which have a permeability of 1.25 Darcy, show that STEP is higher than 1 for a 20 m thick reservoir. Reservoir permeability should be higher than 1.25 Darcy for an economic SAGD process in the three typical oil sands.

168

This study looked at the most favourable permeability/thickness combination for a given reservoir for determining the highest STEP value. Although Edmunds and Chhina (2001) considered much higher permeability values (2.8 and 5.6 Darcies) and different thicknesses (10 and 25 m) than our study, their results could still be analyzed using the economic indicator developed here.

In this research, an instantaneous SOR of 4 was assumed as a cut off for an economic SAGD operation to calculate STEP. However, the magnitude of the SOR value as an economic criterion will change depending on the bitumen price and steam cost. If SOR = 3 is assumed as an economic cut off, a higher STEP value will be required as an economic criterion for a successful SAGD process.
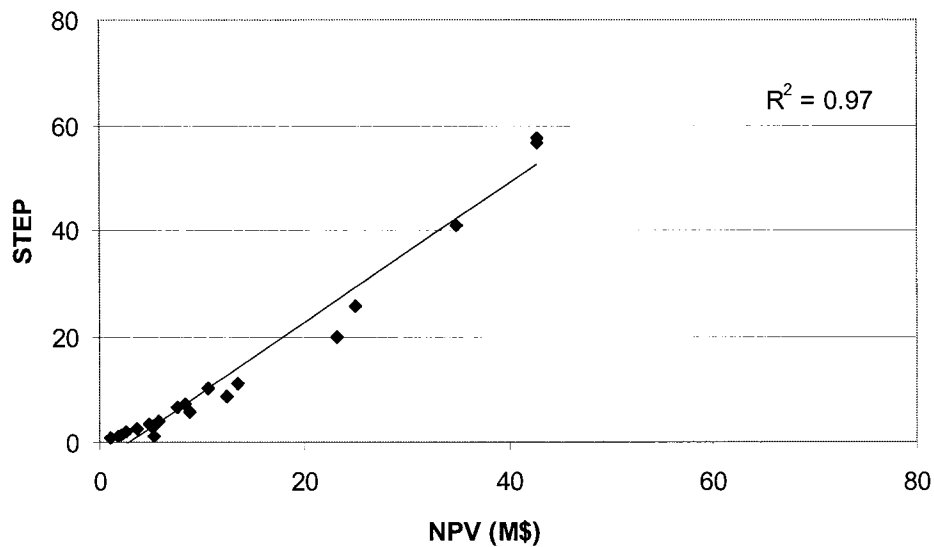
Figure 5.25: Correlation of NPV and STEP for the all cases of reservoir parameters

169

5.5 Evaluating Fast-SAGD performance using STEP

The following STEP equation was used for evaluating Fast-SAGD performance quantitatively as well as qualitatively:

$$STEP = \frac{(RF/0.5) \times (CDOR/0.111)}{(CSOR/3)^{2.4}}$$ (Equation 5.2)

It was suggested that STEP should have the highest value when the case is the best and that the STEP value be higher than 1 for an economical SAGD project in the previous section. In this section, NPV or C-NPV (only for offset well location case) and STEP were used for evaluating the Fast-SAGD process.

5.5.1 Athabasca-type reservoir

The simulations were conducted under the following conditions: I/P spacing of 5 m, reservoir permeability (Kv) of 2.5 Darcy, and reservoir thickness of 30 m. Table 5.10 shows simulation results for the shallow Athabasca-type reservoir cases related to three operating conditions and a reservoir parameter.

5.5.1.1 Offset Well Location

To choose the proper distance between the offset well and the SAGD well pair, the simulations were conducted with a maximum offset well pressure of 4,500 kPa, a maximum steam injection rate of 1,600 m^3/d at the offset well, and additional steam injection of 600 m^3/d into the SAGD injector. The economics measured by C-NPV were best in the case of a distance of 50 m with the CSS startup time of 1.5 years: the STEP value is also highest (Figure 5.26a). A linear relationship was found to exist between STEP and C-NPV with a correlation coefficient of 0.89 (Figure 5.26b).

170

Table 5.10: Fast-SAGD simulation results for Athabsca-type reservoirs

Case	CSOR	CDOR (m³/d/m)	RF	NPV (M$)	STEP
1) Offset well location					
40 m	1.49	0.274	0.83	44.4	22.1
50 m	1.41	0.260	0.85	55.7	24.4
60 m	1.44	0.252	0.86	61.0	22.5
70 m	1.54	0.263	0.86	66.6	20.1
2) CSS startup time at the offset well					
1 yr	1.41	0.208	0.86	51.2	19.7
1.5 yrs	1.41	0.260	0.85	55.7	24.4
2 yrs	1.51	0.267	0.84	52.7	20.8
2.5 yrs	1.54	0.277	0.85	53.0	21.0
3) Steam injection pressure at the offset well					
3000 kPa	1.44	0.192	0.87	49.8	17.6
4500 kPa	1.41	0.260	0.85	55.7	24.4
6000 kPa	1.46	0.274	0.84	55.1	23.3
4) Reservoir thickness					
15 m	2.51	0.161	0.38	15.6	1.7
20 m	2.03	0.224	0.81	29.7	8.4
25 m	1.69	0.267	0.81	41.6	15.4
30 m	1.52	0.287	0.83	53.9	22.0
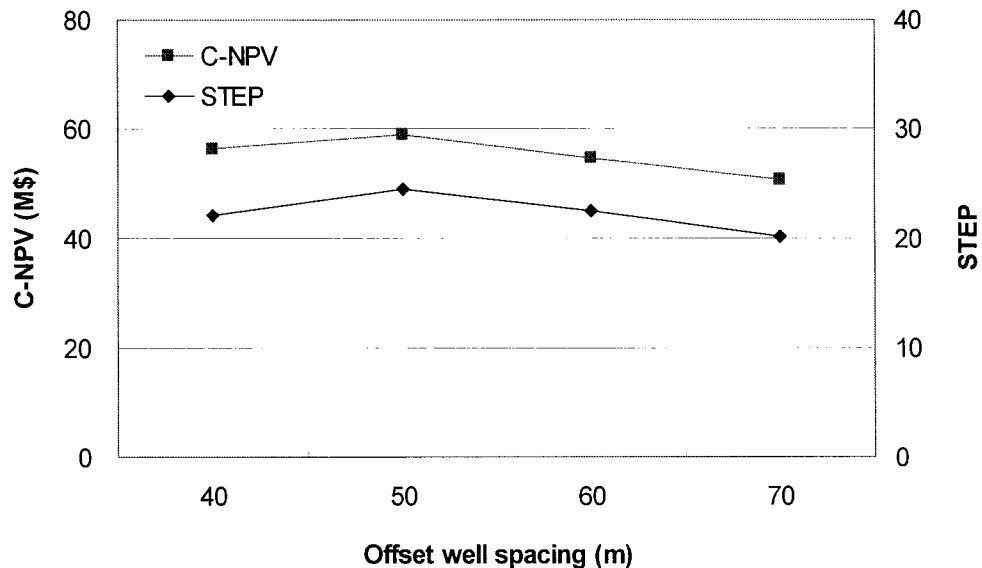
Figure 5.26a: Effect of offset well spacing on C-NPV and STEP in Athabasca-type reservoir

171
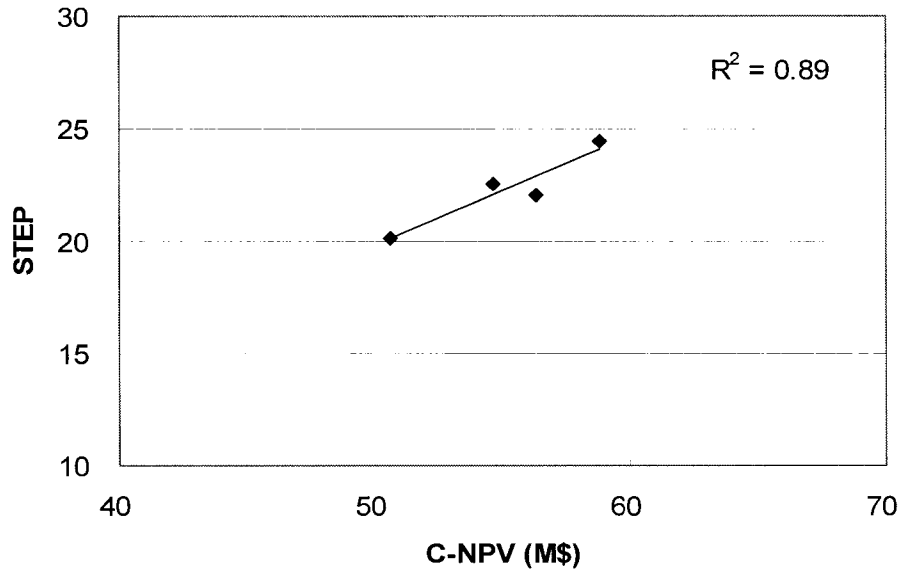
Figure 5.26b: Correlation of C-NPV and STEP

5.5.1.2 CSS startup time at the Offset Well

The proper CSS startup time at the offset well is important during the Fast-SAGD process. This startup time will be changed depending on the offset well distance. Simulations were conducted with the offset well spacing of 50 m and the steam injection pressure of 4,500 kPa. The results showed that NPV and STEP were highest in the case of 1.5 years with lowest CSOR (Figure 5.27a). The CSS startup time of 1.5 years is the proper one for this reservoir type. A linear relationship was found to exist between STEP and C-NPV with a correlation coefficient of 0.97 (Figure 5.27b).

172
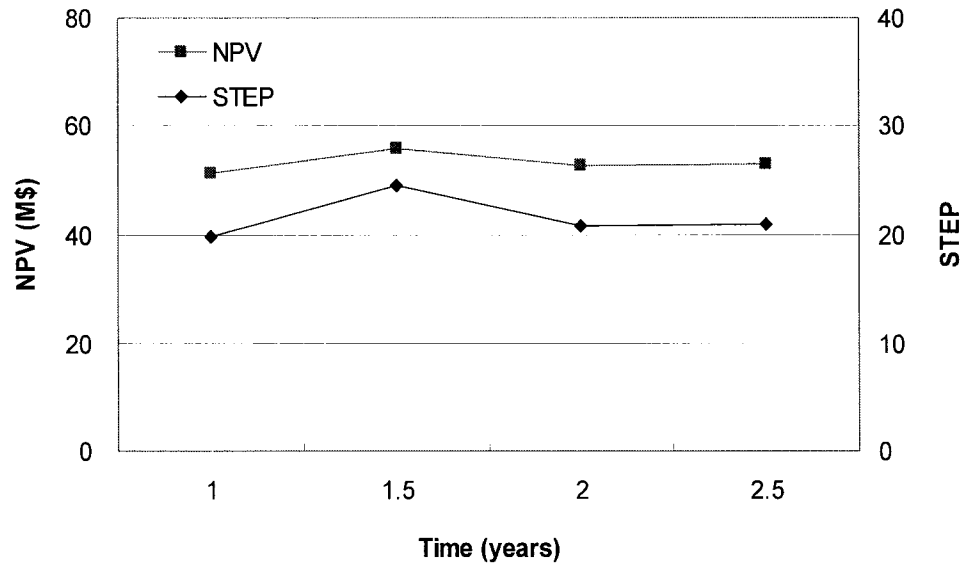
Figure 5.27a: Effect of CSS startup time on NPV and STEP in Athabasca-type reservoir
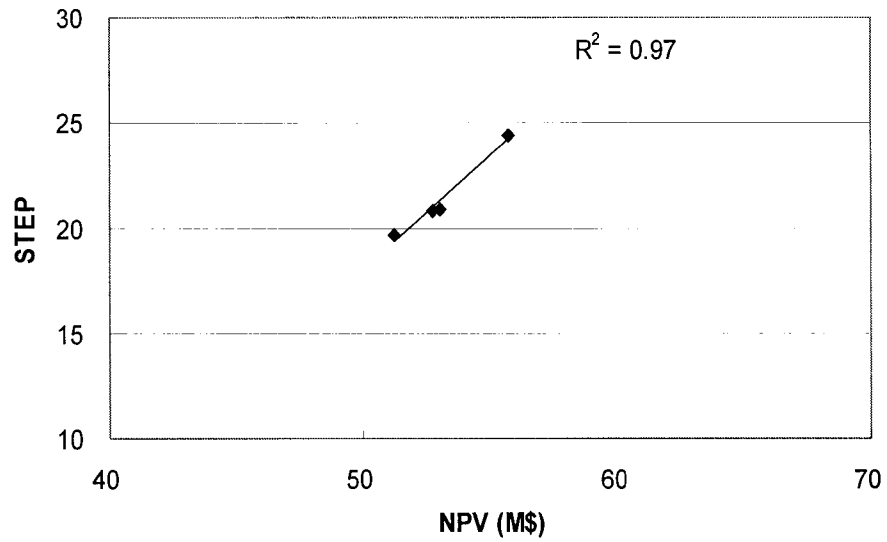
Figure 5.27b: Correlation of NPV and STEP

173

5.5.1.3 Steam Injection Pressure at the Offset Well

Simulations were conducted to determine the proper steam injection pressure at the offset well. With the offset well spacing of 50 m, the simulation results showed that both NPV and STEP values were highest at 4,500 kPa due to the highest CDOR (Figure 5.28a). The injection pressure of 4,500 kPa at the offset well is adequate in this type reservoir. A linear relationship was found to exist between STEP and C-NPV with a correlation coefficient of 1.00 (Figure 5.28b).
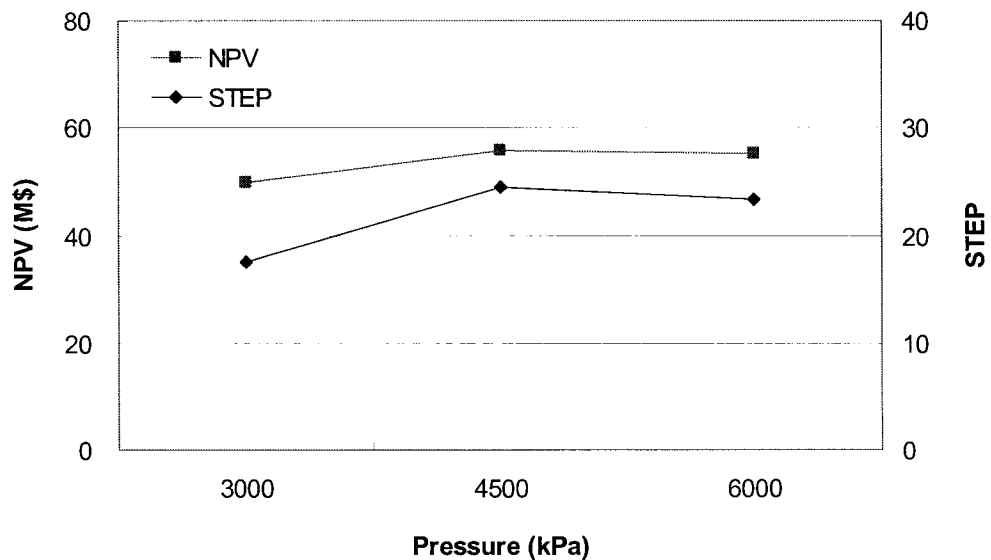
Figure 5.28a: Effect of steam injection pressure at the offset well on NPV and STEP in Athabasca-type reservoir

174
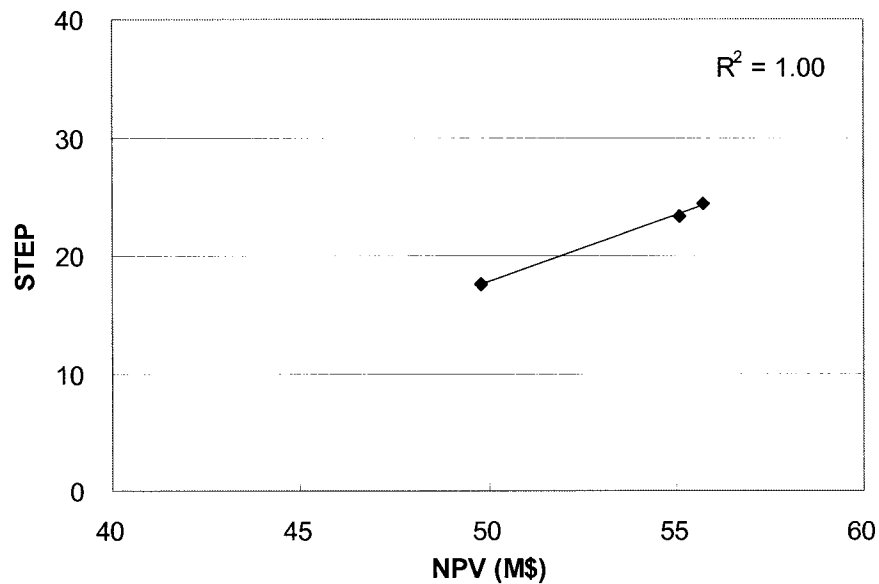
Figure 5.28b: Correlation of NPV and STEP

5.5.1.4 Reservoir Thickness

One can definitely predict that the thicker the reservoir, the better the thermal efficiency and the higher the productivity in the Fast-SAGD process. The simulations were conducted to evaluate the effect of reservoir thickness on the Fast-SAGD performance. As the thickness is increased, CSOR decreases and both CDOR and RF increase. Even if the pay thickness is as thin as 15 m, the Fast-SAGD seems to be an economical operation: NPV is higher than 10 M$ (Figure 5.29a)

A linear relationship was found to exist between STEP and NPV with a correlation coefficient of 1.00 (Figure 5.29b).

175
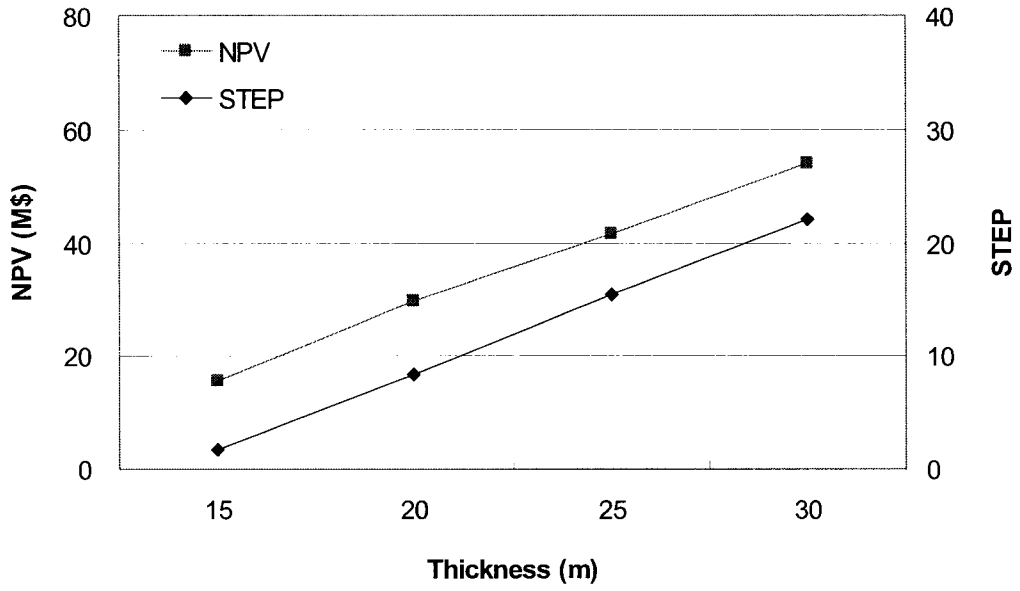
Figure 5.29a: Effect of reservoir thickness on NPV and STEP in Athabasca-type reservoir
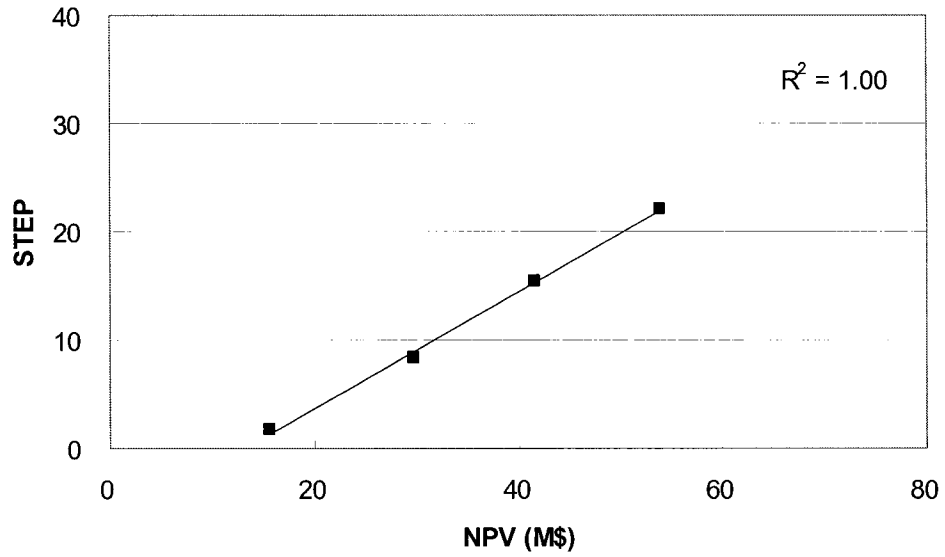
Figure 5.29b: Correlation of NPV and STEP

176

5.5.1.5 Best operating conditions

Simulation results for a shallow Athabasca-type reservoir, which is thick and highly permeable reservoir, give the following most favourable operating conditions: offset well spacing of 50 m, CSS startup time of 1.5 years, and steam injection pressure of 4,500 kPa at the offset well. A linear relationship was found to exist between STEP and NPV with a correlation coefficient in excess of 0.89 for most of the cases.

5.5.2 Cold Lake-type reservoir

This reservoir type has the thinnest pay and lowest bitumen viscosity. The simulations were conducted under the following conditions: I/P spacing of 10 m, reservoir permeability (Kv) of 1.25 Darcy, and reservoir thickness of 20 m. Table 5.11 shows simulation results for the Cold Lake-type reservoir cases related to three operating conditions and a reservoir parameter.

5.5.2.1 Offset Well Location

To choose the proper distance between the offset well and the SAGD well pair, the simulations were conducted with a maximum offset well pressure of 8,000 kPa, a maximum steam injection rate of 800 m^3/d at the offset well, and additional steam injection of 400 m^3/d into the SAGD injector.

NPV was highest at the offset well spacing of 50 m (Table 11), however C-NPV was highest in the case of a distance of 40 m with the CSS startup time of 1.5 years: the STEP value is also highest (Figure 5.30a). It might be said that less than 50 m of offset well spacing is adequate for the thin reservoirs.

A linear relationship was found to exist between STEP and C-NPV with a correlation coefficient of 0.99 (Figure 5.30b).

177

Table 5.11: Fast-SAGD simulation results for Cold Lake-type reservoirs

Case	CSOR	CDOR $(m^3/d/m)$	RF	NPV (M$)	STEP
1) Offset well location					
40 m	2.40	0.135	0.74	13.7	3.1
50 m	2.31	0.121	0.67	15.3	2.7
60 m	2.65	0.106	0.64	12.9	1.7
70 m	2.82	0.102	0.61	11.8	1.3
2) CSS startup time at the offset well					
1 year	2.52	0.084	0.69	11.6	1.6
1.5 years	2.31	0.121	0.67	15.3	2.7
2 years	2.52	0.123	0.71	14.6	2.4
2.5 years	2.69	0.118	0.73	12.8	2.0
3) Steam injection pressure at the offset well					
4500 kPa	3.07	0.060	0.65	7.7	0.7
6000 kPa	2.45	0.101	0.65	13.2	1.9
8000 kPa	2.31	0.121	0.67	15.3	2.7
4) Reservoir thickness					
15 m	3.03	0.117	0.61	5.6	1.2
20 m	2.31	0.121	0.67	15.3	2.7
25 m	2.22	0.130	0.73	20.8	3.5
30 m	2.09	0.138	0.75	26.2	4.5
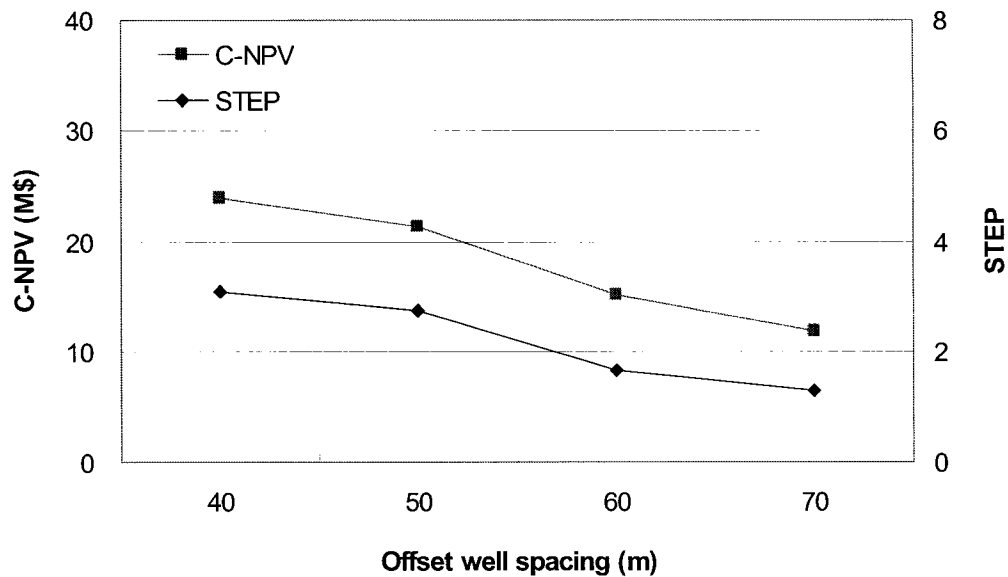
Figure 5.30a: Effect of offset well spacing on C-NPV and STEP in Cold Lake-type reservoir

178
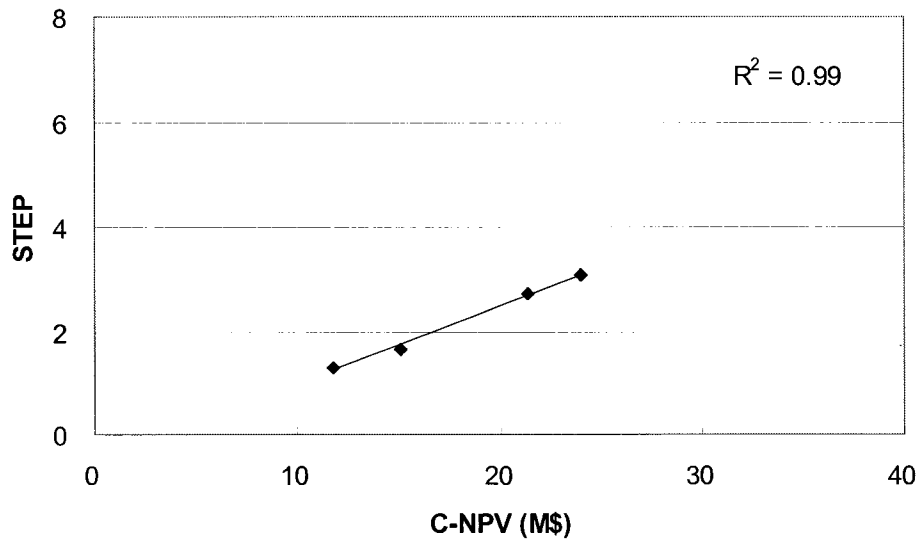
Figure 5.30b: Correlation of C-NPV and STEP

5.5.2.2 CSS startup time at the Offset Well

Simulations were conducted with the offset well spacing of 50 m and the steam injection pressure of 8,000 kPa. The results showed that NPV and STEP were highest in the case of 1.5 years with the lowest CSOR and high CDOR (Figure 5.31a).

A linear relationship was found to exist between STEP and NPV with a correlation coefficient of 0.99 (Figure 5.31b).

5.5.2.3 Steam Injection Pressure at the Offset Well

With the offset well spacing of 50 m, the simulation results showed that the NPV and STEP values were highest at 8,000 kPa due to the highest CDOR and lowest CSOR (Figure 5.32a). The injection pressure of 8,000 kPa at the offset well is adequate in this reservoir type.

179

A linear relationship was found to exist between STEP and NPV with a correlation coefficient of 0.99 (Figure 5.32b).
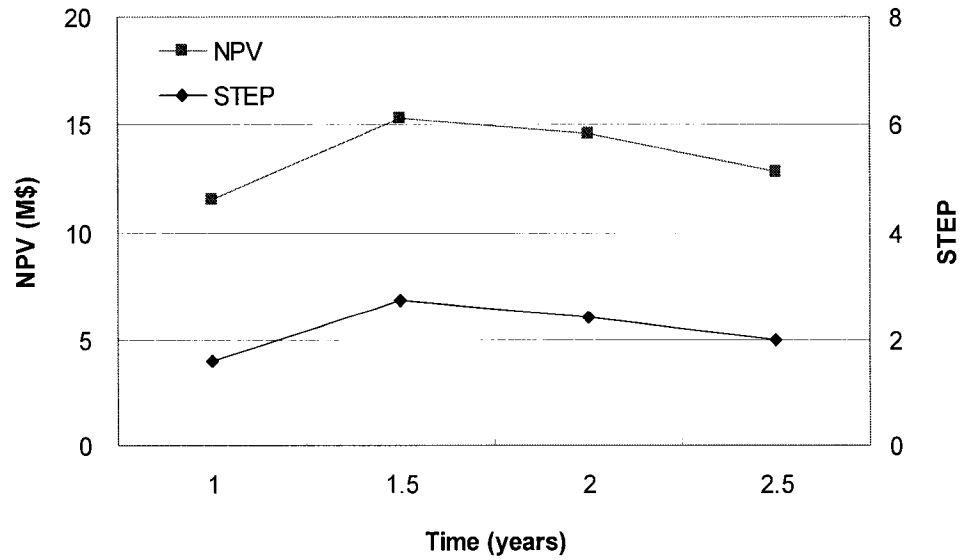
Figure 5.31a: Effect of CSS startup time on NPV and STEP in Cold Lake-type reservoir
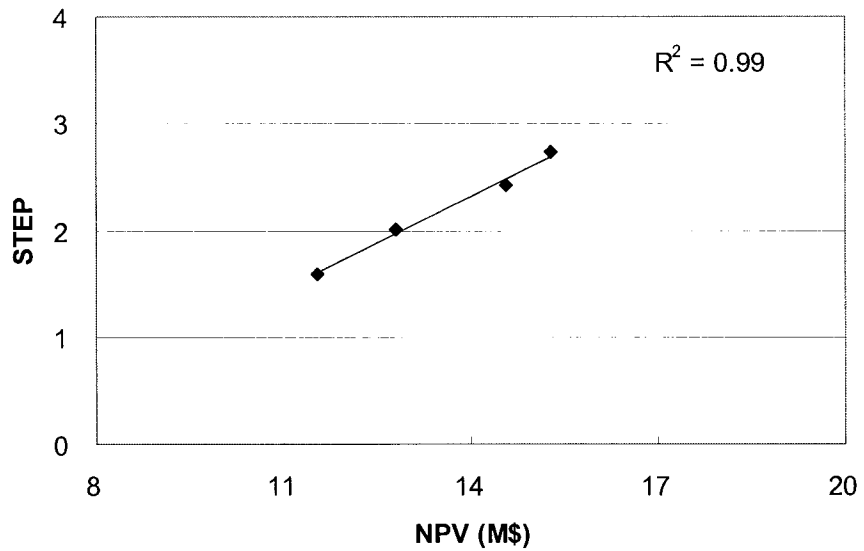
Figure 5.31b: Correlation of NPV and STEP

180
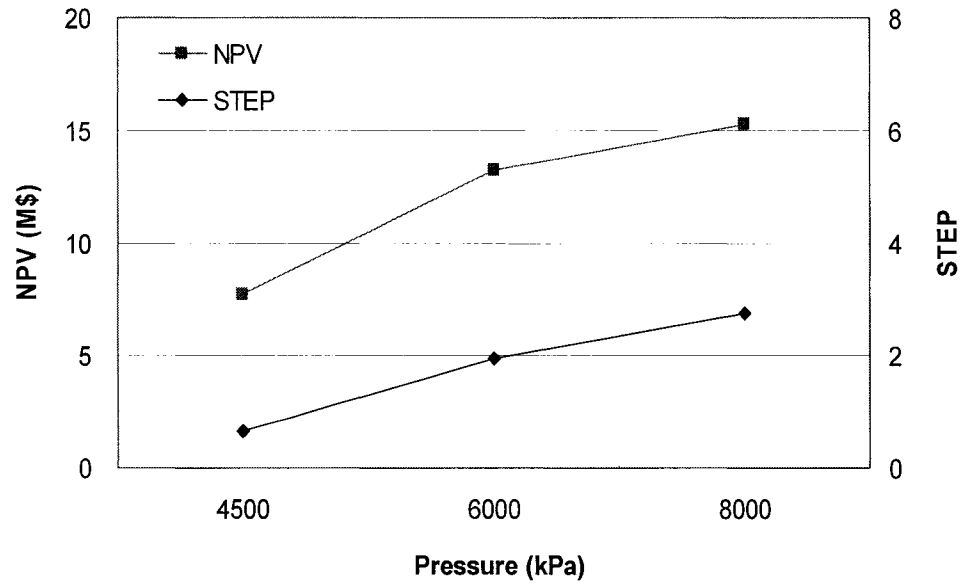
Figure 5.32a: Effect of steam injection pressure at the offset well on NPV and STEP in Cold Lake-type reservoir
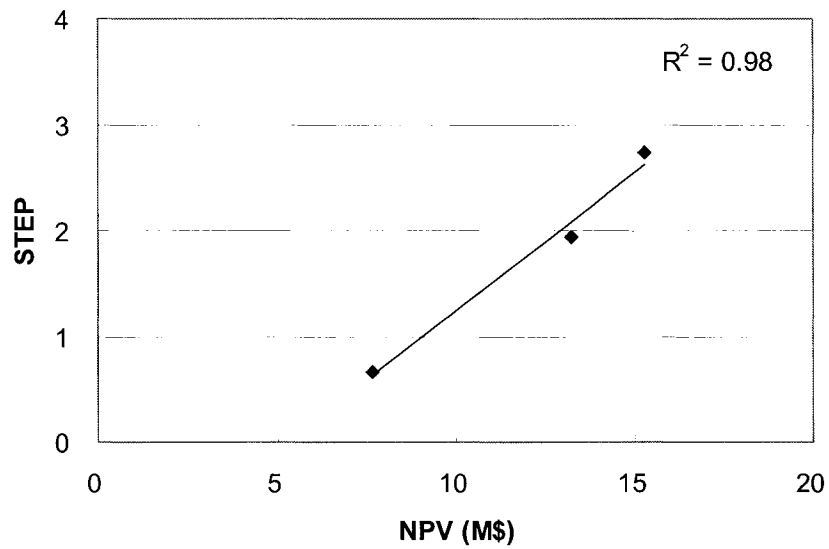
Figure 5.32b: Correlation of NPV and STEP

181

5.5.2.4 Reservoir thickness

The simulations were conducted to evaluate the effect of reservoir thickness on the Fast-SAGD performance. As the thickness is increased, CSOR decreases and both CDOR and RF increase. At least the pay thickness should be thicker than 20 m for an economical Fast-SAGD operation: NPV is higher than 10.3 M$ (Figure 5.33a).

A linear relationship was found to exist between STEP and NPV with a correlation coefficient of 0.99 (Figure 5.33b).
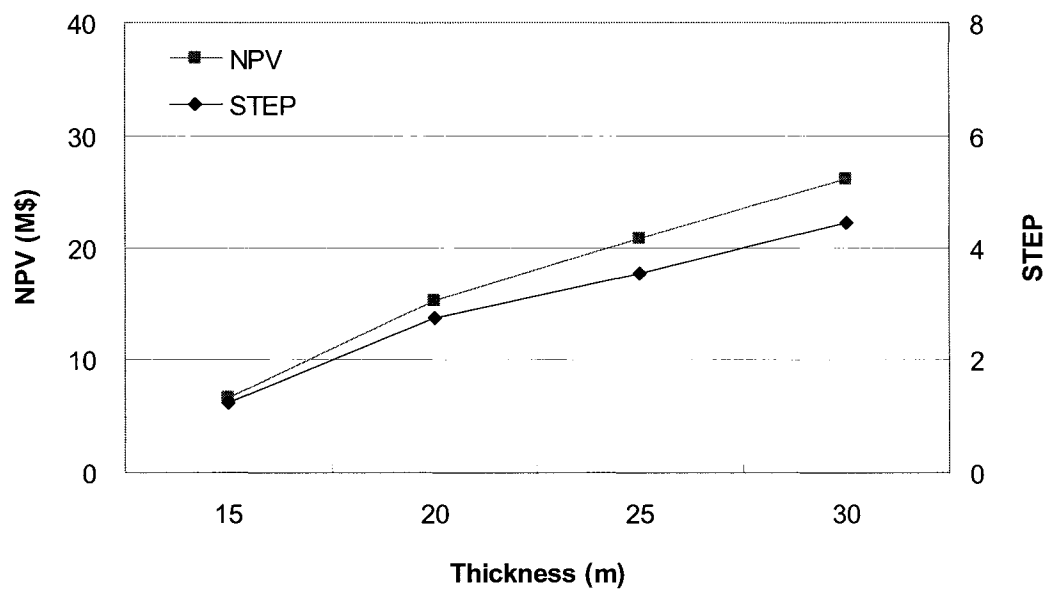
Figure 5.33a: Effect of reservoir thickness on NPV and STEP in Cold Lake-type reservoir

182
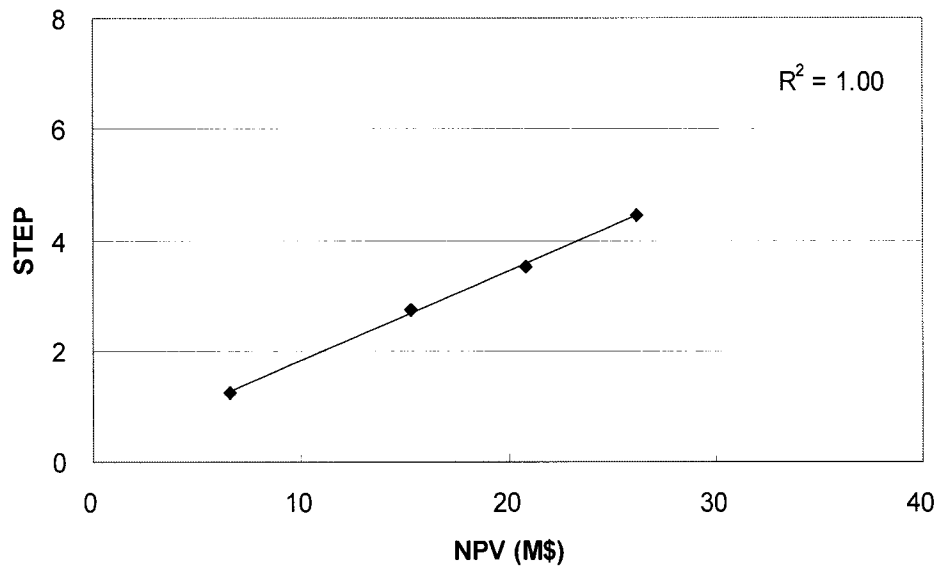
Figure 5.33b: Correlation of NPV and STEP

5.5.2.5 Best operating conditions

Simulation results for a Cold Lake-type reservoir, which is thin and moderately permeable, give the following most favourable operating conditions: offset well spacing of 40 m, CSS startup time of 1.5 years, and steam injection pressure of 8,000 kPa at the offset well.

A linear relationship was found to exist between STEP and NPV with a correlation coefficient in excess of 0.98 for most of the cases.

5.5.3 Peace River-type reservoir

This reservoir type represents the deepest, lowest permeability reservoir with middle range bitumen viscosity in the Alberta oil sands. The simulations were conducted under the following conditions: I/P spacing of 10 m, reservoir permeability (Kv) of 0.65 Darcy, and reservoir thickness of 25 m. Table 5.12 shows simulation results for the Peace River-type reservoir cases related to three operating conditions and a reservoir parameter.

183

Table 5.12: Fast-SAGD simulation results for Peace River-type reservoirs

Case	CSOR	CDOR (m³/d/m)	RF	NPV (M$)	STEP
1) Offset well location					
40 m	3.00	0.131	0.67	9.7	1.6
50 m	2.90	0.138	0.57	10.8	1.5
60 m	3.01	0.134	0.54	10.6	1.3
70 m	3.25	0.118	0.54	8.5	1.0
2) CSS startup time at the offset well					
1 year	3.02	0.123	0.62	10.3	1.4
1.5 years	2.90	0.138	0.57	10.8	1.5
2 years	3.20	0.128	0.64	8.9	1.3
2.5 years	3.02	0.138	0.55	9.3	1.4
3) Steam injection pressure at the offset well					
6000 kPa	3.04	0.119	0.55	9.1	1.1
7000 kPa	2.97	0.128	0.56	10.0	1.3
8000 kPa	2.90	0.138	0.57	10.8	1.5
4) Reservoir thickness					
15 m	3.85	0.106	0.43	-0.3	0.5
20 m	3.27	0.128	0.49	5.3	0.9
25 m	2.90	0.138	0.57	10.8	1.5
30 m	2.88	0.132	0.66	14.3	1.7

5.5.3.1 Offset Well Location

Simulations were conducted with a maximum offset well pressure of 8,000 kPa, a maximum steam injection rate of 800 m³/d at the offset well, and additional steam injection of 400 m³/d into the SAGD injector.

NPV was highest at the offset well spacing of 50 m (Table 5.12), however C-NPV was highest in the case of a distance of 40 m with the CSS startup time of 1.5 years: the STEP value is also highest (Figure 5.34a). It might be said that around 50 m of offset well spacing is adequate for this reservoir type.

A linear relationship was found to exist between STEP and NPV with a correlation coefficient of 0.93 (Figure 5.34b).

184
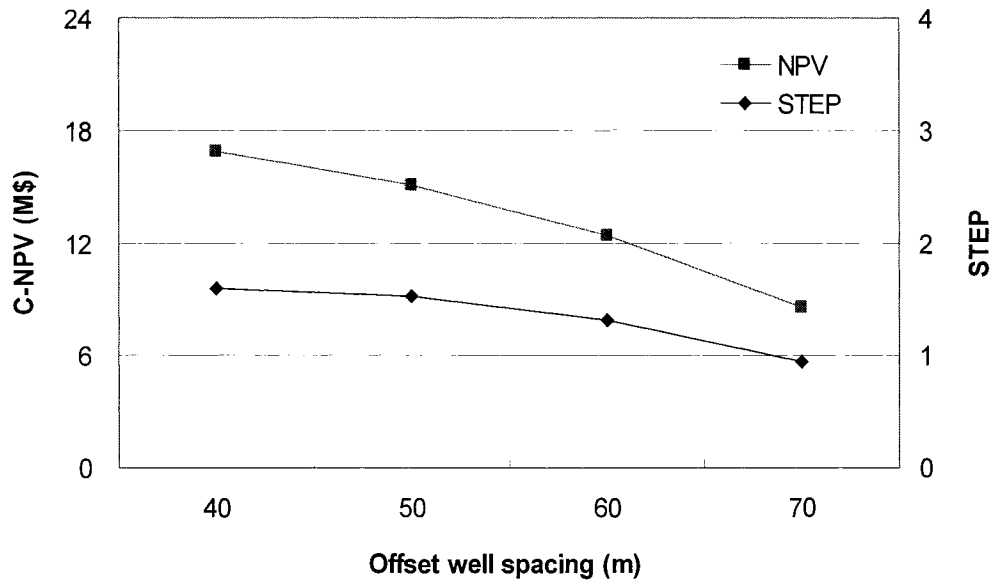
Figure 5.34a: Effect of offset well spacing on C-NPV and STEP in Peace River-type reservoir
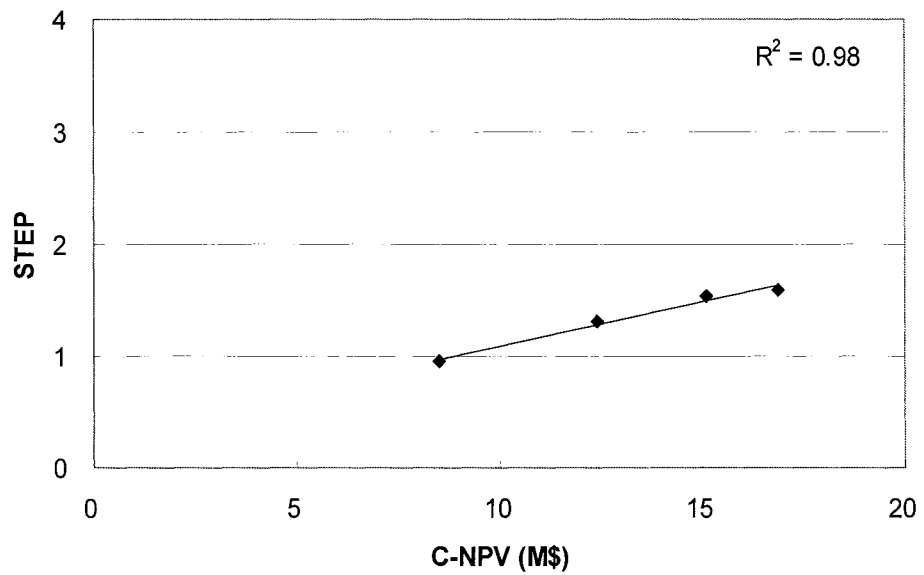
Figure 5.34b: Correlation of C-NPV and STEP

185

5.5.3.2 CSS startup time at the Offset Well

Simulations were conducted with the offset well spacing of 50 m and the steam injection pressure of 8,000 kPa. The results showed that NPV and STEP were highest in the case of 1.5 years with the lowest CSOR (Figure 5.35a).

A linear relationship was found to exist between STEP and NPV with a correlation coefficient of 0.79 (Figure 5.35b).

5.5.3.3 Steam Injection Pressure at the Offset Well

With the offset well spacing of 50 m, the simulation results showed that the NPV and STEP values were highest at 8,000 kPa due to the highest CDOR and lowest CSOR (Figure 5.36a). The injection pressure of 8,000 kPa at the offset well is adequate in this reservoir type.

A linear relationship was found to exist between STEP and NPV with a correlation coefficient of 1.00 (Figure 5.36b).
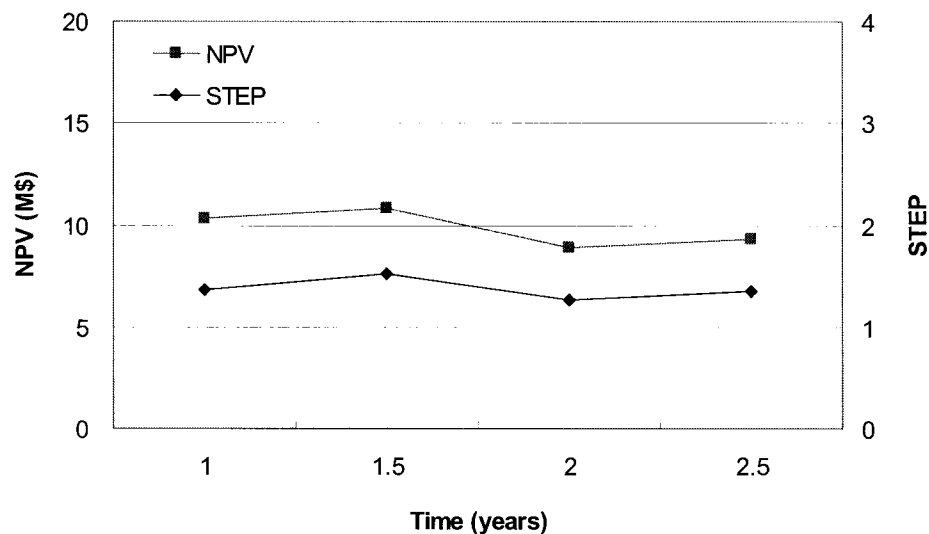
Figure 5.35a: Effect of CSS startup time on NPV and STEP in Peace River-type reservoir

186
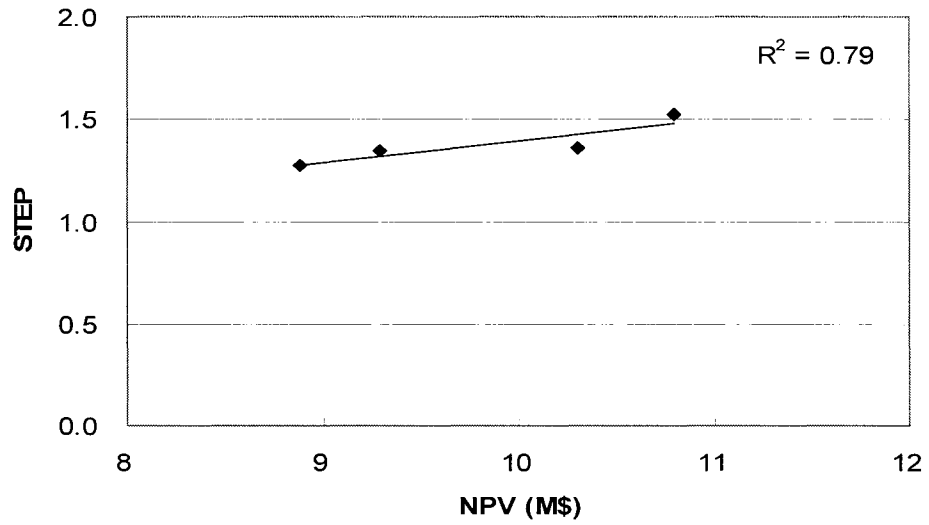
Figure 5.35b: Correlation of NPV and STEP
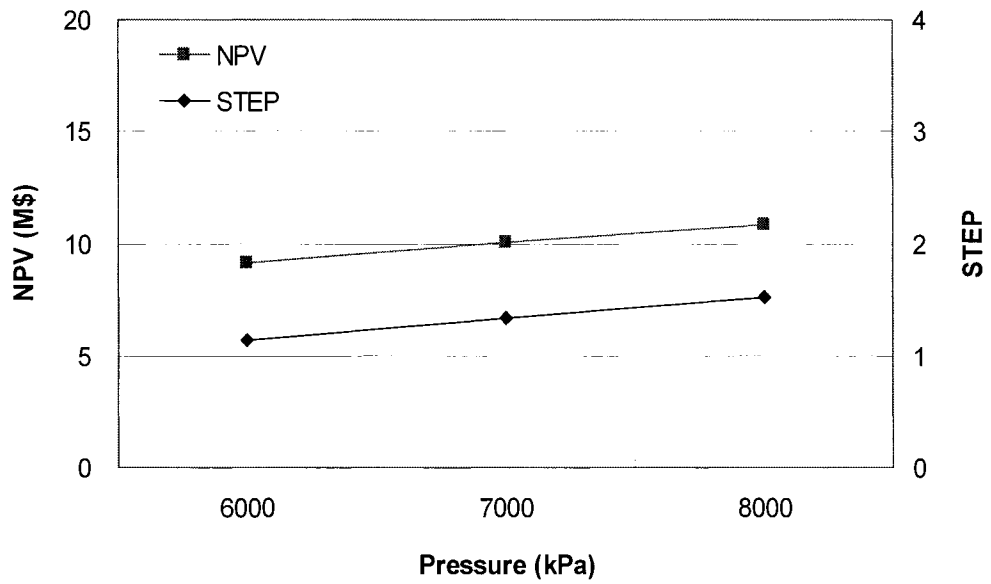
Figure 5.36a: Effect of steam injection pressure at the offset well on NPV and STEP in Peace River-type reservoir

187
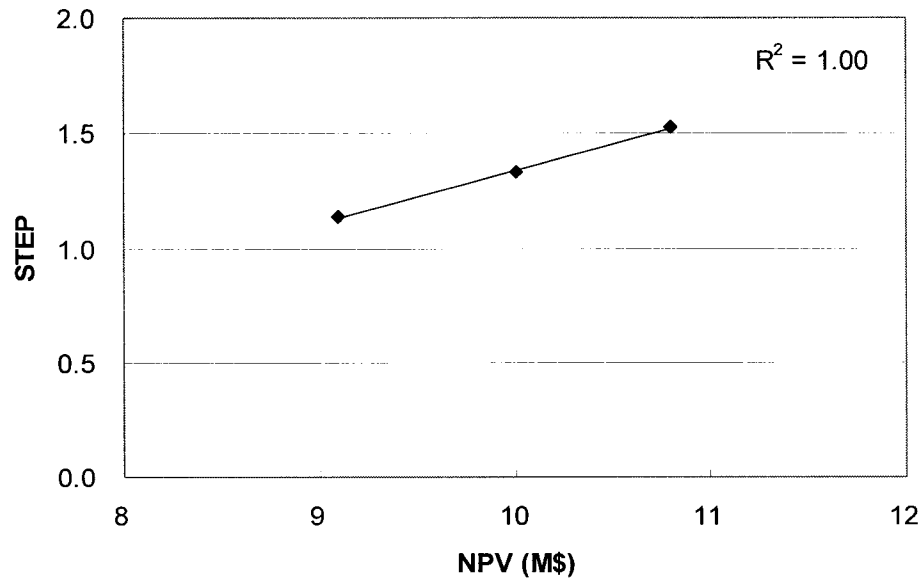
Figure 5.36b: Correlation of NPV and STEP

5.5.3.4 Reservoir thickness

The simulations were conducted to evaluate the effect of reservoir thickness on the Fast-SAGD performance. As the thickness is increased, CSOR decreases and both CDOR and RF increase. At least the pay thickness should be thicker than 25 m for an economical Fast-SAGD operation: NPV is higher than 5.8 M$ (Figure 5.37a).

A linear relationship was found to exist between STEP and NPV with a correlation coefficient of 0.99 (Figure 5.37b).

188
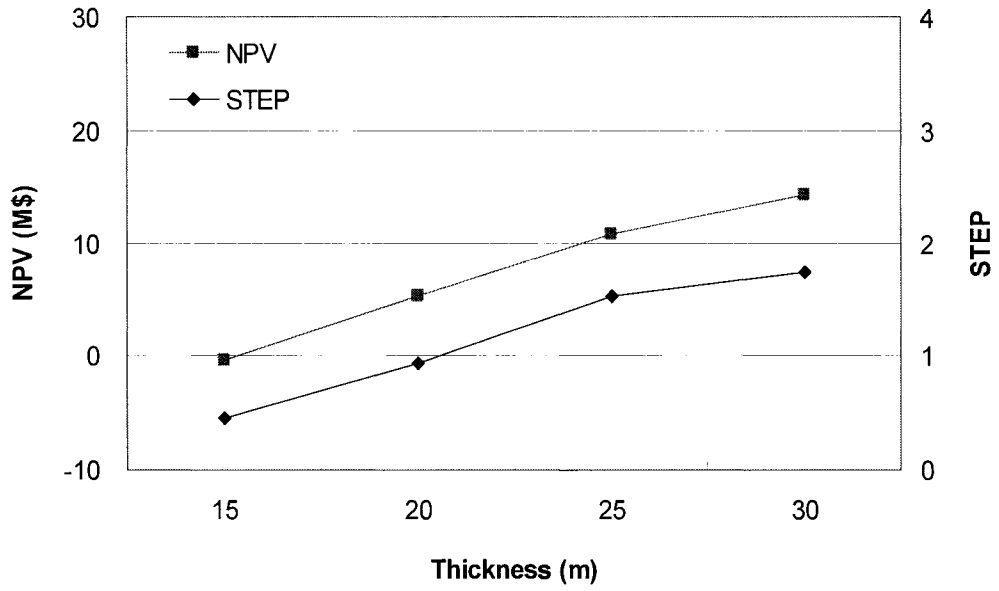
Figure 5.37a: Effect of reservoir thickness on NPV and STEP in Peace River-type reservoir
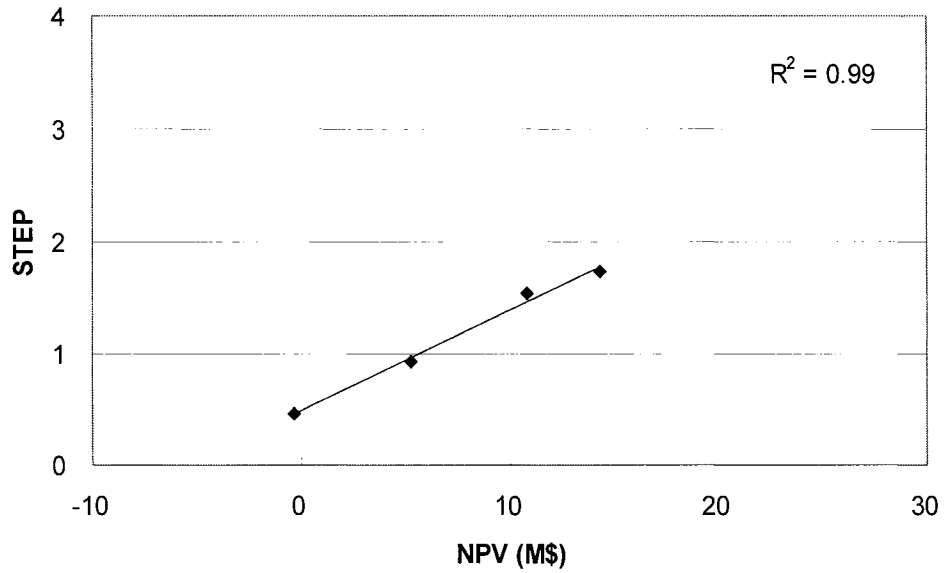
Figure 5.37b: Correlation of NPV and STEP

189

5.5.3.5 Best operating conditions

Simulation results for a Peace River-type reservoir, which is moderately thick with low permeability, give the following optimal operating conditions: offset well spacing of 40 m, CSS startup time of 1.5 years, and steam injection pressure of 8,000 kPa at the offset well.

A linear relationship was found to exist between STEP and NPV with a correlation coefficient in excess of 0.83 for most of the cases.

5.5.4 STEP as an economic indicator for Fast-SAGD

STEP has already been validated to use as an economic indicator for evaluating SAGD performance. In this section, STEP was used for evaluating the Fast-SAGD process. STEP always has the highest value when the case is best. A linear relationship was found to exist between STEP and NPV, with a correlation coefficient in excess of 0.89 for most of the individual cases (Table 5.13), and 0.95 overall for all the cases (Figure 5.38).

Table 5.13: Correlation coefficients between NPV and STEP

Best case	Correlation coefficient (R^2)		
	AB	CL	PR
Offset well location	0.89	0.99	0.98
CSS startup time at the offset well	0.97	0.99	0.79
Steam injection pressure at the offset well	1.00	0.98	1.00
Reservoir thickness	1.00	1.00	0.99

Comparing the best cases for three typical reservoirs, there is a good linear relationship between STEP and NPV with a correlation coefficient of 1.00 (Figure 5.39). As STEP values of three best cases are higher than 1, it may be said that Fast-SAGD process is economical for all three typical cases.

190
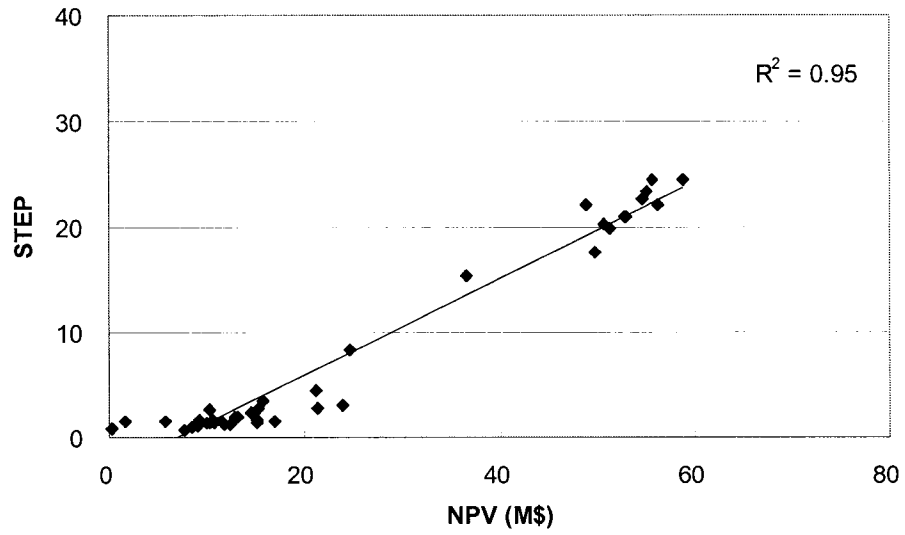
Figure 5.38: Correlation of NPV and STEP for all cases
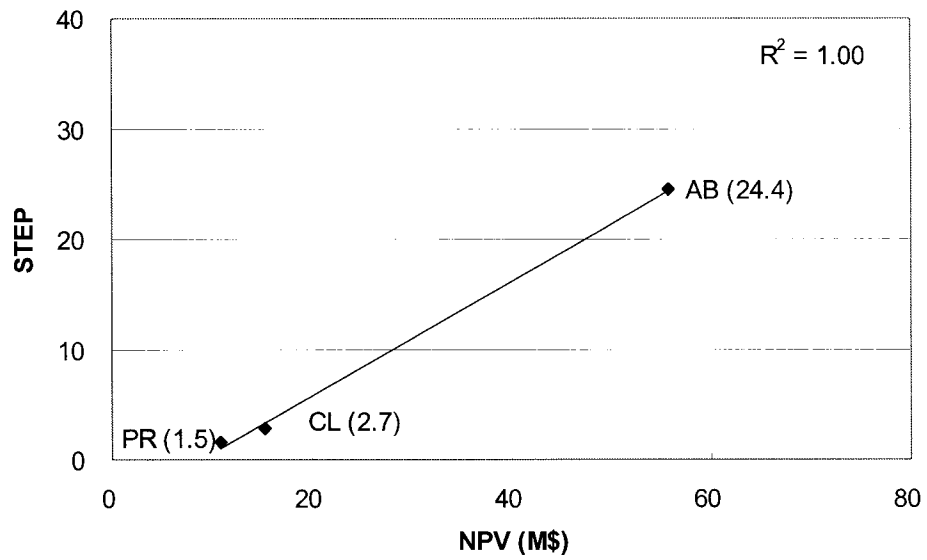
Figure 5.39: Correlation of NPV and STEP for the best cases

191

6 EXPERIMENTAL STUDIES

6.1 Experimental Apparatus using the Automated Process Control System

The high temperature and high pressure SAGD experiments were operated using the process control software, Emerson's DeltaV automation system (Emerson$_{TM}$, 2004). The DeltaV I/O cards are connected to the experimental panel for control and monitoring. The thermocouple panel, which monitors the model conditions, is connected to the DeltaV system via Foundation Fieldbus. The DeltaV controller and the ProfessionalPlus (Engineering) station communicate via redundant ethernet (Figure 6.1). Control system configuration and data archiving are done at the ProfessionalPlus station.

This new automated process control system controls various parameters such as temperature, pressure, and flow rate, all at the same time. With this advanced system, steam quality, and water and oil production can be analyzed. For safety reasons, the control system is programmed to shut down automatically if any operating condition exceeds the design range.
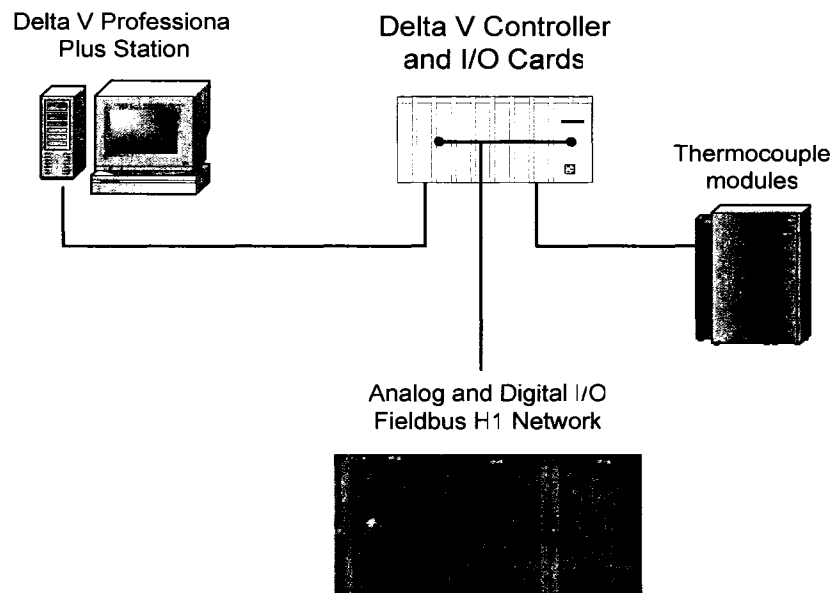
Figure 6.1: Delta V Process Control Architecture

192

There are five main interfaces in a SAGD experiment with the DeltaV control system as shown in Figure 6.2. The panels and the schematic of the experimental apparatus are shown in Figure 6.3 and Figure 6.4. The SAGD experimental procedures can be summarized with the following steps:

- the pump feeds demineralized water to the electric heat exchanger
- the electric heat exchanger generates the required steam for each experiment
- the steam is injected into the SAGD model through the steam distribution lines
- the produced hot oil and water from the SAGD model pass though a cooler
- the cooled production is measured and collected in production sample cylinders

High pressure and high temperature model experiments are difficult to perform as many variables such as steam quality, injection rate and pressure need to be controlled continuously and in a real time. An advanced automated process control system has been commissioned to overcome operating complexities in steam injection and production wells for the SAGD process. The automated system will continuously control the most critical operational parameters during the experiment, which are pressure, temperature, and flow rate. The system also includes advanced control functions, which allow steam quality, and water and oil production rates to be analyzed and optimized.

Figure 6.2: SAGD Experiment Interfaces

193

Figure 6.3: Panels of the experimental apparatus (designed and manufactured by Spartan Controls Ltd., Edmonton, Canada)

194

Figure 6.4: Schematic diagram of the experimental apparatus

195

6.1.1 Steam quality measurement

To develop the steam quality measurement system, the heater drive (UY101, heater net energy for flashing water, as a percent) is increased, from a low value which is not enough to generate steam to a high value which is enough to generate superheated steam, at a rate of 1 % per 10 minutes. There are a total of five locations for measuring the water or steam temperatures including three locations inside the heater (Figure 6.5). An electronic heating element is installed inside the tubing and submerged into the fluid inside the tubing, which gives an efficient heating system.

Figure 6.5: Schematic diagram of the steam quality measurement system

196

TE101 measures the feed water temperature and TE201, which measures directly the fluid temperature inside the tubing, gives the steam temperature leaving the heater. If the heater drive is increased, temperatures at the four locations above TE101 increase until steam is generated at TE201. Once steam starts being generated from the heater, this point represents 0 % steam quality, and the temperature at TE201 has reached a constant value. The temperatures at TE153 and TE152 will reach this constant value, one after the other, as shown in Figure 6.6. Finally, the temperature at TE201 will start increasing again when the steam is superheated. This point is the 100 % steam quality stage and at this moment TE151 still has not reached the constant steam temperature value. This feature can be used to calculate the steam quality, because there is a linear increasing trend of temperature at TE151 throughout the steam generating process, from 0 to 100% steam quality.

Figure 6.6: Main parameter trends of the steam quality measurement system

197

As the two steam quality points of 0 and 100 % depend on the temperature, pressure and flow rate which all vary during the experiment, it is impossible to measure the steam quality directly. Another complexity is the possibility for the water in the heater to be in the two-phase region. Thus, it is difficult to predict the parameters using thermodynamics. A neural network in the DeltaV system (DeltaV, 2004) makes it possible to calculate the steam quality by using experimental runs to learn the behavior of the important monitored parameters at different steam qualities. The neural network uses a multivariable correlation function resulting from temperature (TE151), flow rate (FT100), steam pressure (PT201), and heater drive (UY101) to calculate the steam quality ranging between 0 and 100 %. To apply this system to various flow rates and injection pressures, it is necessary to generate several data sets of TE151, FT100, PT201 and UY101 from 0 to 100 % steam quality. Some external manipulation of the data had to be done to find the 0 and 100 % points based on the TE201 trend.

The flow rate controller (FIC100), using a proportional-integral-derivative (PID) function block, is a continuous controller which gives a rapid response and exhibits no offset (Murrill, 1981). It controls the feed water rate as close as possible to a set point value by adjusting the FV100 valve position.

However, the steam quality measurement system can only predict the steam quality leaving the heater. Therefore, the steam injection line has to be insulated perfectly and the heater has to be located close to the experimental model so that heat losses from the steam to be injected can be minimized.

6.1.2 Steam distribution line

This kind of steam distribution system is needed for a multi-injection well operation. In the case of a Fast-SAGD operation, steam needs to be injected into both a SAGD injection well and an offset well. The flow ratio controller (FIC202-3) controls the proportion of steam injection into two wells by using PID function blocks (Figure 6.7). Once the set point for the flow ratio between two injection lines is entered, FIC202-3 tries to keep controlling the flow ratio as close as possible to a set point value by adjusting the valve position of PV201A and PV201B.
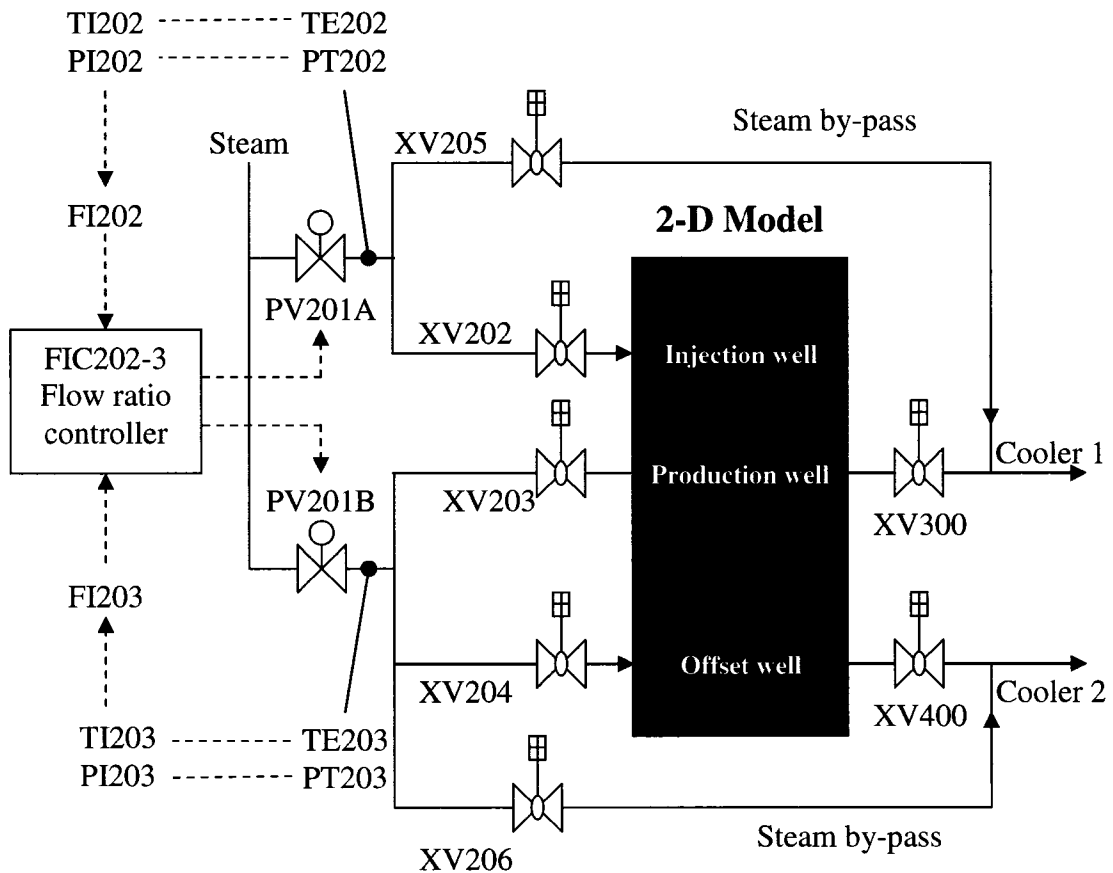
Figure 6.7: Schematic diagram of the steam distribution system

199

6.1.3 Production cooling system

The temperature of the production fluid OUT (TE301) is controlled by the controller TIC301, a PID with feed forward control function block, adjusting the valve position of TV301. TIC301 will open the cooling water valve (TV301) widely if the production fluid OUT (TE301) is higher than the set point temperature, and then will partially close the valve if the TE301 is lower than the set point temperature (Figure 6.8). The feed forward aspect of the controller allows the temperature controller (typically slow acting) to respond faster. Here, the cooler inlet stream temperature TE300 allows the controller to act earlier on a disturbance in the production feed temperature. This greatly facilitates obtaining better control performance and more stable temperature control, which is crucial for the steam-to-oil ratio measurement.
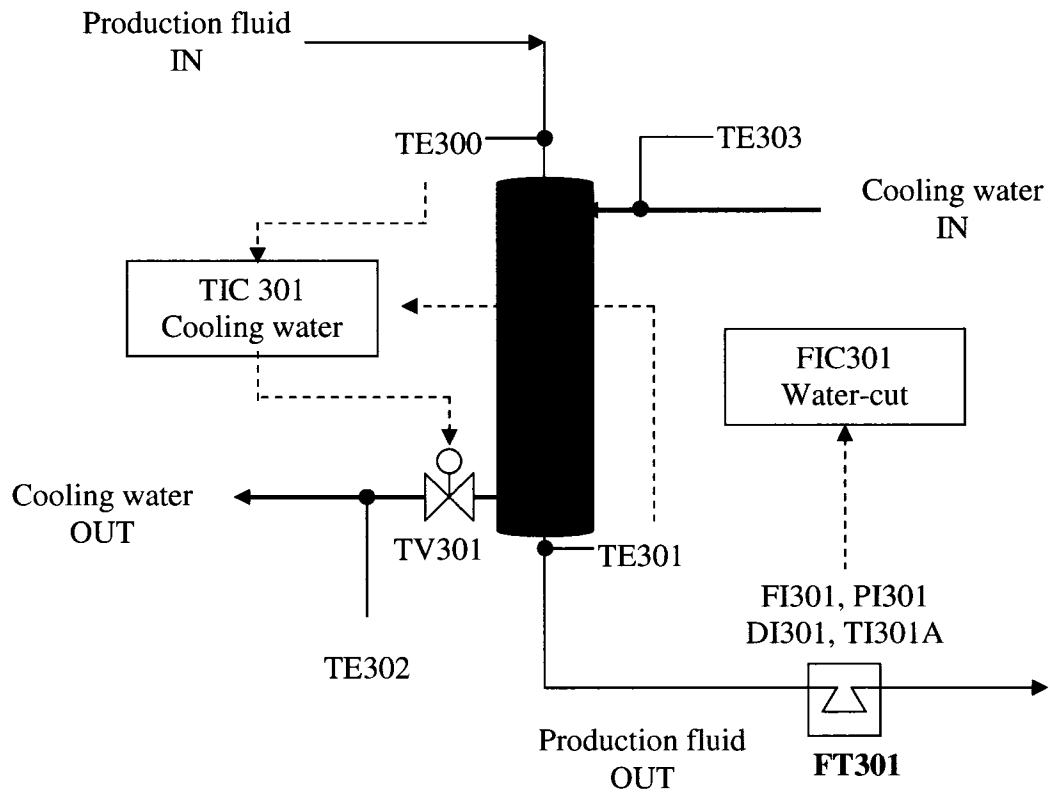
Figure 6.8: Schematic diagram of the production cooling system

200

The density difference of the two fluids (water and heavy oil) is dependent on the temperature of the produced fluids because the densities of these fluids vary with temperature (Figure 6.9). For heavy oil with a 15° API gravity, a temperature range of 60 to 100 °C gives the maximum density difference. In the validation experiment (described in chapter 6.2), the production cooling system controls the temperature of the produced fluids at 60 °C in order to achieve a significant difference in density between water and heavy oil.
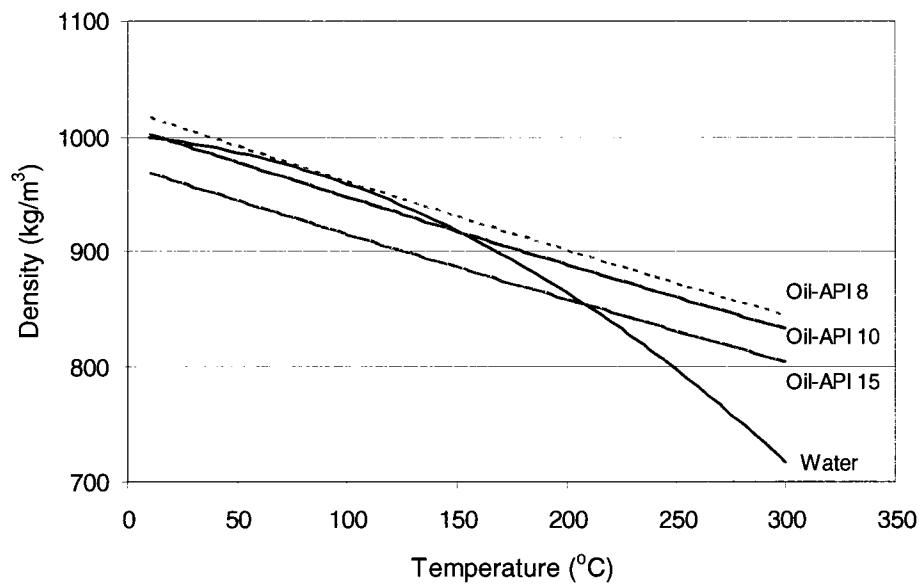
Figure 6.9: Density curves of water and oils versus temperature

Experiments have been conducted to tune and validate this production cooling system. Figure 6.10 shows the results of one of the experiments. The temperature of the production fluid IN (TE300) is 234 °C and the temperature of the cooling water IN (TE303) is 16 °C. As a result, the production fluid OUT temperature (TE301) and cooling water OUT (TE302) both show 60 °C. TE301 temperature has a very constant value around the set point temperature (Figure 6.10).

201
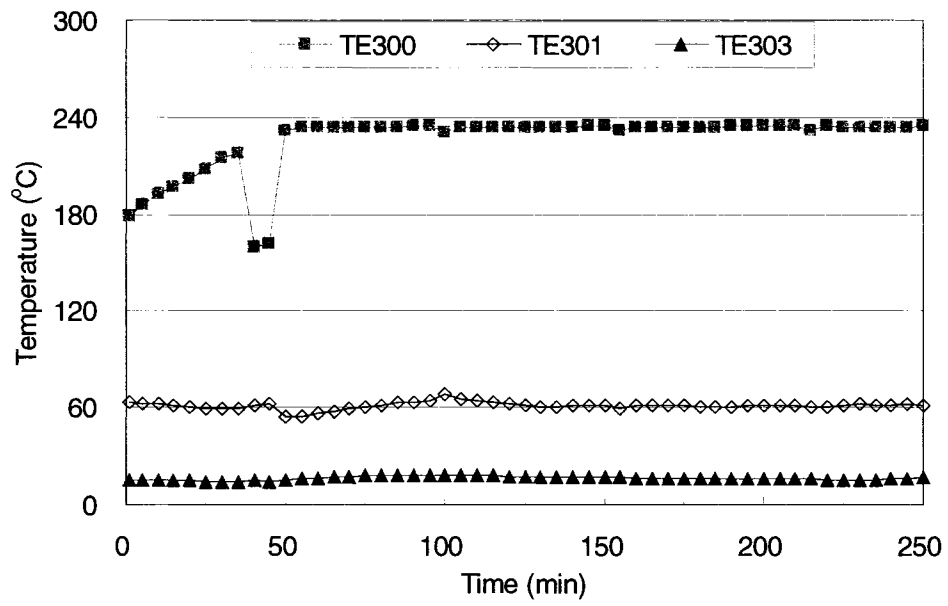
Figure 6.10: Main parameter trends of the production cooling system

202

6.1.4 Oil-cut determination

As the water and oil densities are known at the controlled temperature, the oil-cut can be determined by measuring the combined density of the produced fluids (water + heavy oil) with a coriolis flow meter, FT301 (Figure 6.8).

The coriolis flow meter (FT301) gives information on temperature (TI301A), flow rate and density of the fluid. Maximum density difference of the production fluids is achieved as they have already passed through the production cooling system. Calculation procedures for the oil-cut determination are summarized in Figure 6.11.
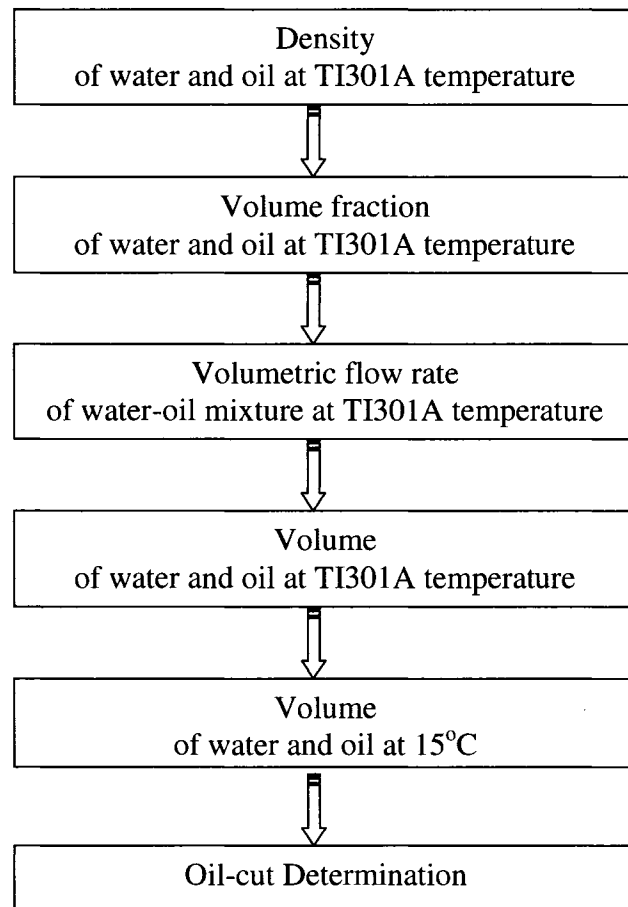
Figure 6.11: Flow chart for oil-cut determination using a coriolis flow meter

6.1.5 Production pressure control system

As gravity drainage is the main recovery mechanism in the SAGD process, the pressure difference between the injection and the production wells has to be kept small in order not to produce live steam. Steam trap control is used to prevent a production well from producing live steam, which is a very important concept for a successful SAGD operation. It is therefore very important to control the production cylinder pressure because this pressure is used as the production well pressure in this facility. The production fluids temperature and pressure need to be known accurately to properly use the steam trap control.

In applying the steam trap control to this experimental facility, the production pressure will be kept 10 kPa lower than the injection pressure. A PID block, PIC350 (Figure 6.12), will control the production pressure (PT350) by opening and closing two shut-down valves, XV350A and XV350B so that it remains close to the set point pressure.

Experiments have been conducted to tune and validate this production pressure control system. Figure 6.13 shows one of the experimental results. The production pressure was set at 3,100 kPa, which is a typical reservoir pressure for the Cold Lake heavy oil reservoirs. This loop was tuned using the proportional and integral tuning constants of the PID controller and a manual needle valve at the pressure vent. The results show that a PID block at PIC350 controls this production pressure very well (Figure 6.13).

204
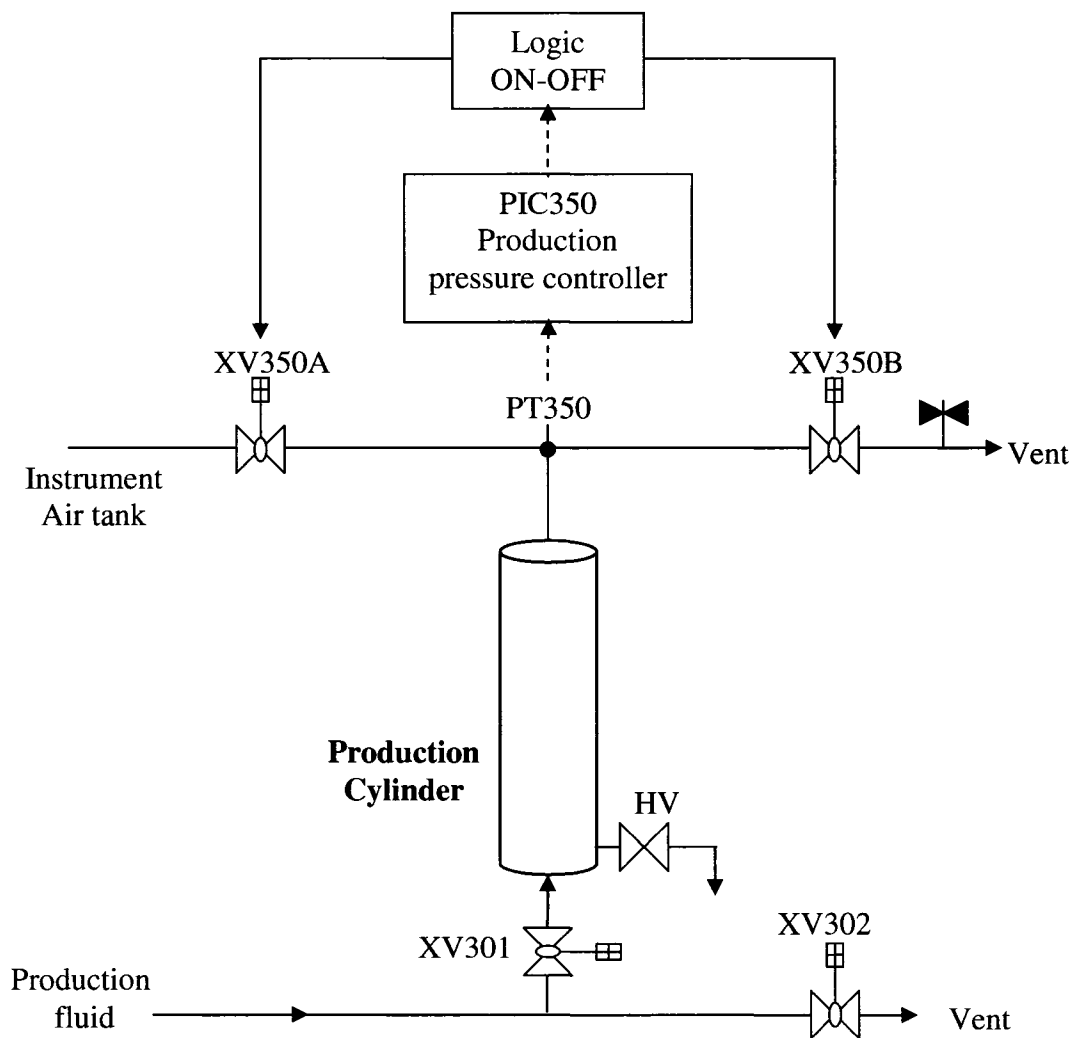
Figure 6.12: Schematic diagram of the production pressure control system

205
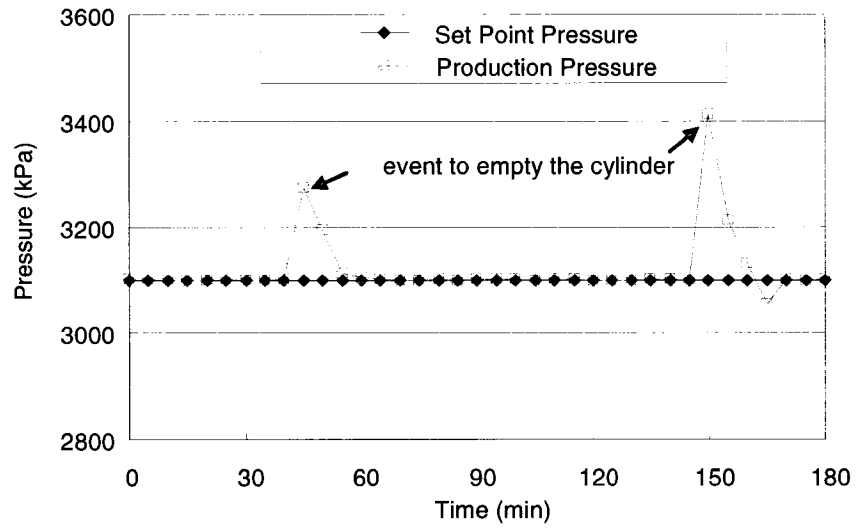
Figure 6.13: Main parameter trends of the production pressure control system

206

6.2 Validation Experiment for Oil-cut Determination

6.2.1 Cylindrical model experiment

An experiment was conducted using a simple model to validate the oil-cut determination system. As this experiment was designed for oil-cut determination, the conception of an experimental model is not as critical. A cylindrical model, 60 cm in length and 7.6 cm in diameter, was packed with glass beads, 2.8 mm in diameter. The calculated porosity is about 33%, and the expected permeability calculated from the Kozeny-Carman equation (Plitt, 2004) is 4,000 Darcy. The model was saturated with Lloydminster oil having a viscosity of 10,000 cp and a density of 963.6 kg/m^3 at 15°C. The initial oil saturation of the sand pack was 0.98. The experimental apparatus for this model is shown in Figures 6.14 and 6.15.

A thermocouple is installed 10 cm above the injection port inside the model to measure the steam temperature. Steam is injected through the injection well which is located 10 cm above the bottom of the cylinder. Fluids are produced from the production port at the center of the base of the cylindrical model (Figure 6.14).

The cylindrical model, steam injection and production lines are wrapped with a wrap tracer (fiber glass tape) for insulation. All the injection and production lines used in the experiment are stainless steel tubing having a diameter of 6.35 mm.

Demineralized water was injected with a pump, and the injection rate was set at 3 kg/hr during the experiment. The steam by-passes the model before it is injected into the model. The heater generated superheated steam at 270 °C at the heater outlet, and the steam temperature dropped to around 230 °C inside the model. The steam injection pressure was between 3,100 and 3,400 kPa, depending on the steam temperature and quality. The production pressure at the production cylinder was set at 3,100 kPa.

207
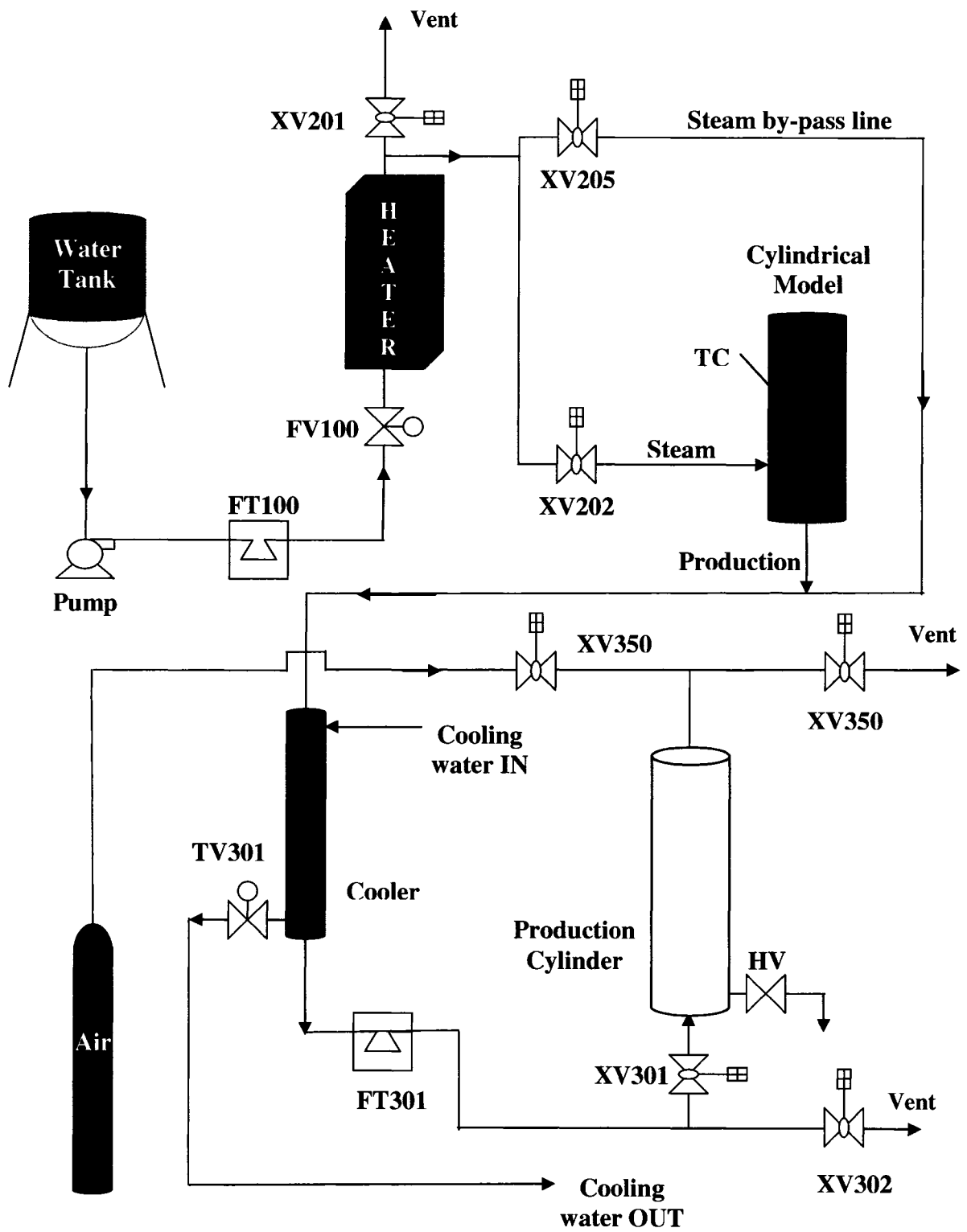
Figure 6.14: Schematic diagram of the cylindrical model experimental apparatus

208
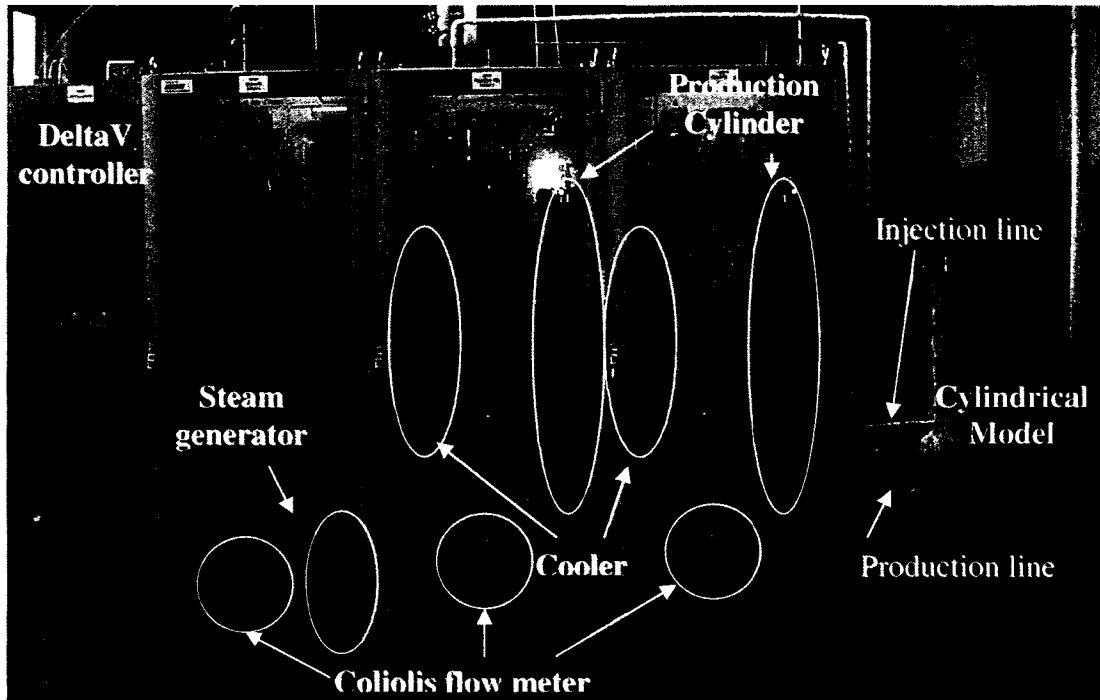
Figure 6.15: Experimental apparatus using automated control system for the cylindrical model

209

6.2.2 Experimental results for oil-cut determination

The trends of several parameters of the experiment to determine oil-cut during a four-hour run are shown in Figures 6.16, 6.17 and 6.18. The steam injection rate varied between 2.5 and 3.5 kg/hr, but was kept close to 3 kg/hr which is the set point (Figure 6.16).

The steam quality changed from 30 to 100 %; however, it was kept as close as possible to 100 % quality (Figure 6.17). The oil-cut fraction shows a range of 0 to 0.33, and the cumulative oil production reached 900 cm^3 after three hours of operation (Figure 6.18). As the coriolis flow meter gives a systematic error during this experiment, an oil-cut fraction value of 0.14, which is the reading during the steam by-pass period, was subtracted from initial data as correction. With this correction, the total oil production from the cylindrical model matches the amount of oil in the model.

This experiment was designed for investigating a steam injection process. The oil-cut trend seems to be related to the steam quality: higher steam quality results in higher oil-cuts (Figure 6.17).
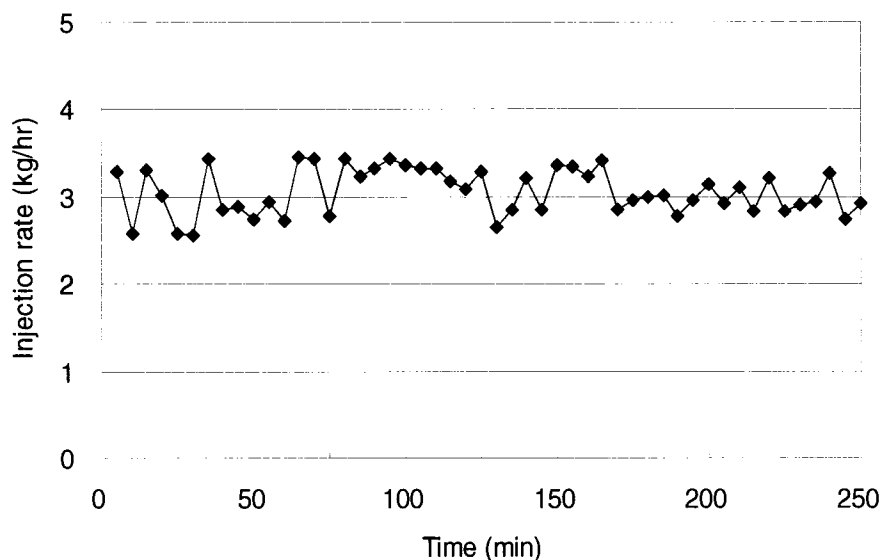
Figure 6.16: Steam injection rate trend

210
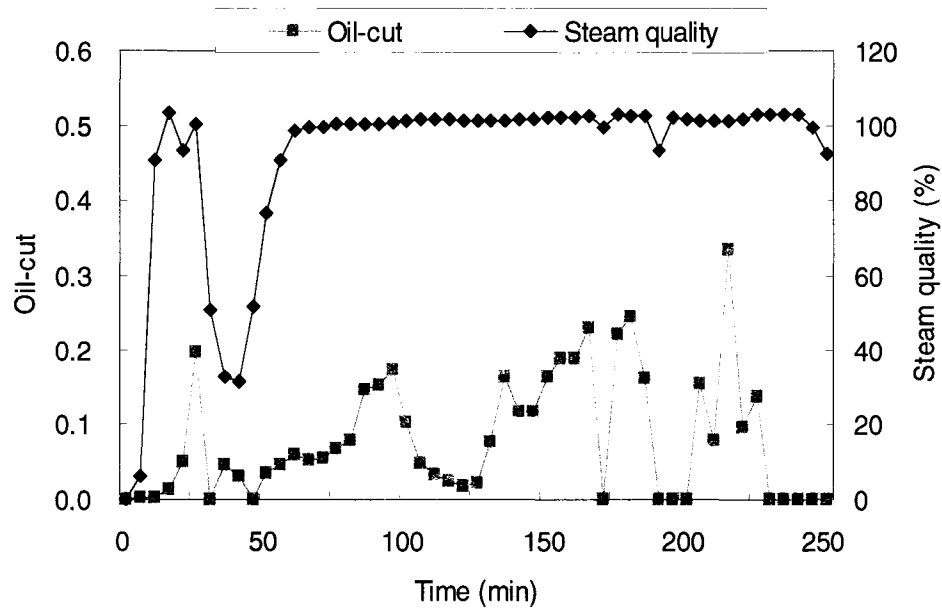
Figure 6.17: Steam quality and oil-cut trends
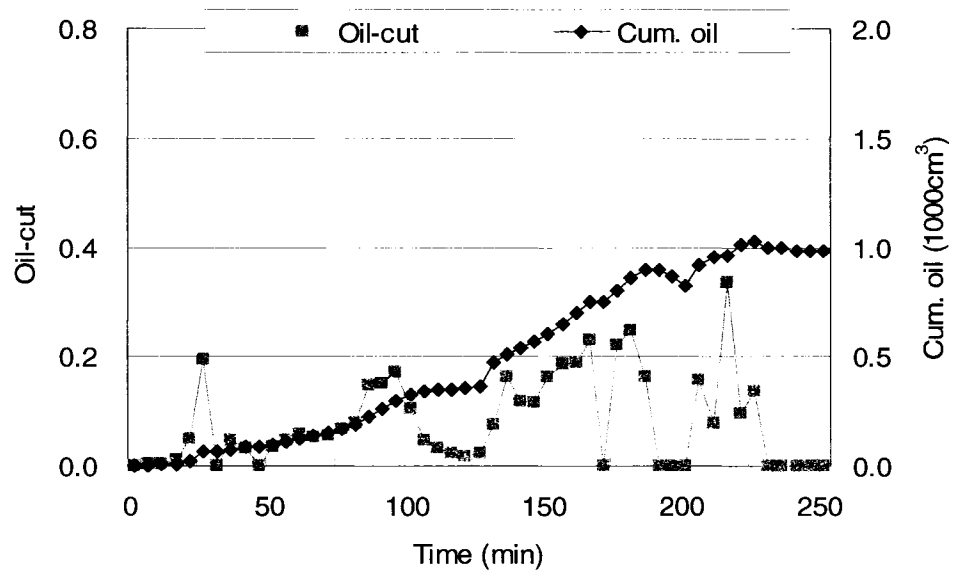
Figure 6.18. Oil-cut and cumulative oil production trends

211

6.3 High Pressure and High Temperature Scaled Physical Model Experiments

6.3.1 Scaling Parameters

A two-dimensional scaled model can not represent a field reservoir prototype because there are no perfect scaling methods. The heat loss aspect is different; only over- and under-burden heat loss in the field, but heat loss to the over- and under-burden and the sides of the scaled model. The main objective of these experiments is to compare the SAGD and Fast-SAGD processes, therefore this semi-scaled model would be a valuable tool. Numerical simulation results of a prototype were used for scaling the model.

The scaled model has been designed according to the Pujol and Boberg criteria (1972), which are suitable for steam processes, especially if gravitational effects are dominant. In this scaling procedure, the same fluids and different porous media will be used in the laboratory as compared to the field.

As the numerical simulations showed that the Fast-SAGD process resulted in enhanced performance compared to the SAGD process in Cold-Lake-type reservoirs, a permeability of 1.25 Darcy was chosen for the prototype. Key scaling parameters are shown in Table 6.1.

Table 6.1: Scaling parameters for Prototype and Model (scaling factor: 150)

Scaling parameters	Prototype	Model
Reservoir thickness	34 m	22.7cm
Horizontal well length	7.5 m	5 cm
Reservoir width	131 m	87.4 cm
Permeability	1.25 Darcy	187 Darcy
Injection rate (SAGD injection well)	6.5 m^3/d	33 cm^3/min
Injector/Producer spacing	8 m	5.3 cm
Time	1 yr	0.38 hr

212

The scaling factor, geometry ratio (R), is the basic parameter used in designing the scaled model,

$$R = (\text{prototype reservoir thickness/model reservoir thickness})$$

$$= H_p/H_m$$

$$= 34 \text{ m}/22.7 \text{ cm}$$

$$= 150$$

Permeability in model will be increased by "R":

$$K_m = R * K_p$$

$$= 150 * 1.25 \text{ Darcy} = 187 \text{ Darcy}$$

Time in the model will be decreased by "R^2", therefore 1 yr in the prototype will be:

$$t_m = (1/R^2) * t_p$$

$$= (1/150^2) * 1 \text{ yr} = 0.38 \text{ hr in the model.}$$

The injection rate will be decreased by "R": therefore 6 m^3/d in the prototype will be:

$$q_m = (1/R) * q_p$$

$$= (1/150) * 6.5 \text{ m}^3/\text{d} = 33 \text{ cm}^3/\text{min}$$

6.3.2 Two-Dimensional Scaled Model Design

Based on the above scaling parameters, two-dimensional scaled models were designed (Figures 6.19 and 6.20). The size of these models is 87.4 cm x 22.7 cm x 5 cm (width x height x thickness). The spacing between injection and production wells is 5.3 cm, and the production well is located 2.7 cm above the bottom of the model. For a SAGD model, well pairs are located at the center line of the model, 43.7 cm away from both ends. For a Fast-SAGD model, the SAGD well pairs are located 27 cm away from one end and an offset well is located 27 cm away from the other end. The distance between the SAGD well pairs and the offset well is 33.4 cm. A drain port is located at the very bottom of the side wall, and two ports are on the top lid for saturating the model. Two O-ring grooves are located at the top of the model for providing a good seal (Figure D.2).

213

A total of forty thermocouple points, five J-type multi thermocouple strings with 8 points in each string (3.175 mm in OD), are installed inside the model to monitor the steam chamber shape and its propagation (Figures 6.19 and 6.20). The distance between thermocouple strings is 4.4 cm and the distance between thermocouple points is 11 cm.
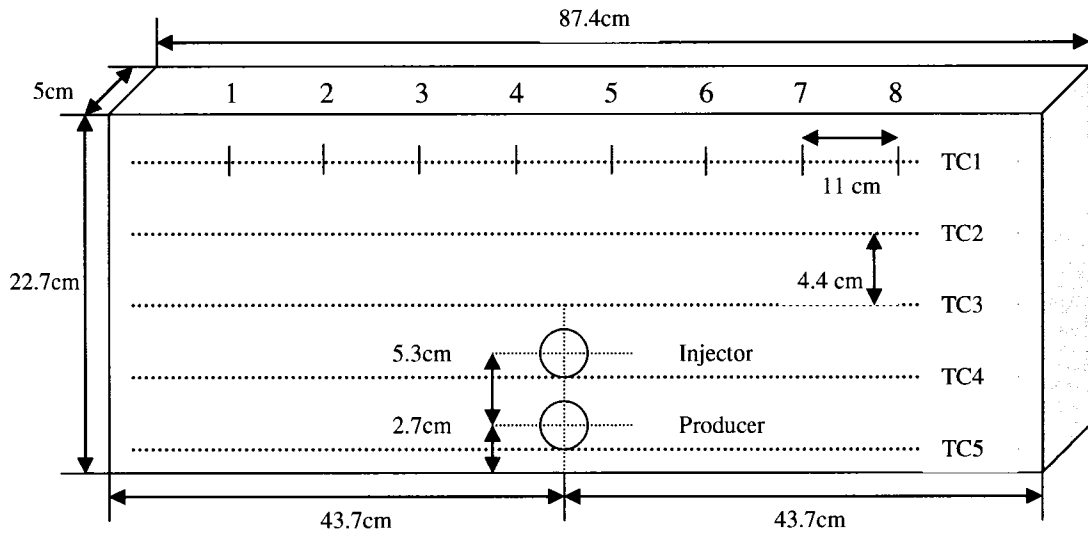
Figure 6.19: Well positions in the SAGD model.
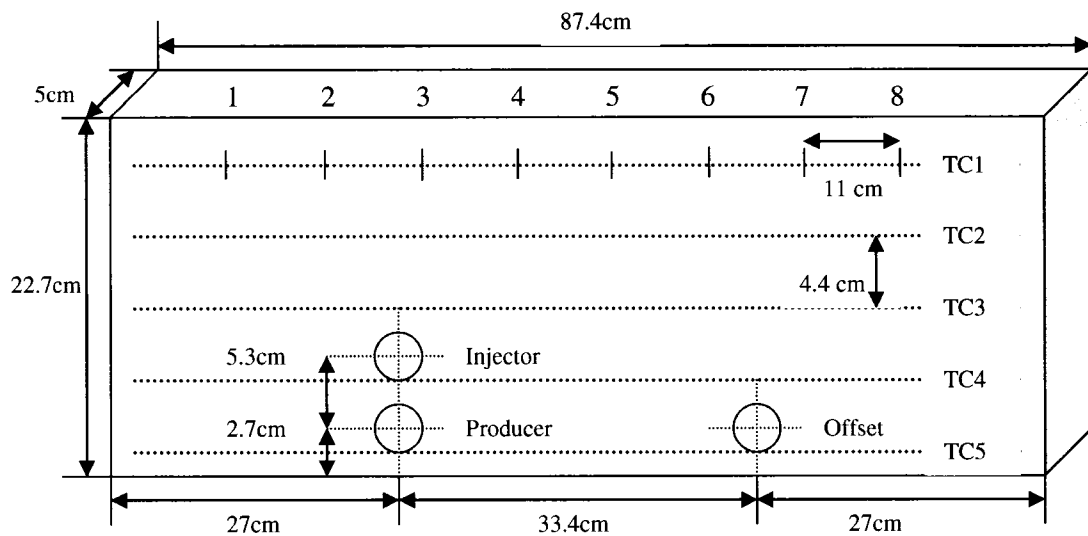
Figure 6.20: Well positions in the Fast-SAGD model.

214

The well radius will not be scaled for these two-dimensional physical models, as it is not a serious problem in a two-dimensional model. Also, the calculated well radius (3 cm for the model versus 11 cm for the prototype) is too large to use in such a small-scaled model. Small stainless tubing (6.35 mm OD and 3.175 mm ID) is used for injection and production wells.

The injection and production wells were designed with holes small enough for preventing the glass beads' outflow into the wells (Figure 6.21). For a glass beads size of 0.6 to 0.8 mm (20 to 30 mesh), holes having 0.4 mm diameter were selected. The injection well has a total of 24 holes (6 holes in each pattern with 4 patterns, 1 cm pattern spacing), and the production well has 30 holes (6 holes in each pattern with 5 patterns, 1 cm pattern spacing). To help prevent live steam entering a production well, patterns are located alternatively between injection well and production well as shown in Figure 6.21.
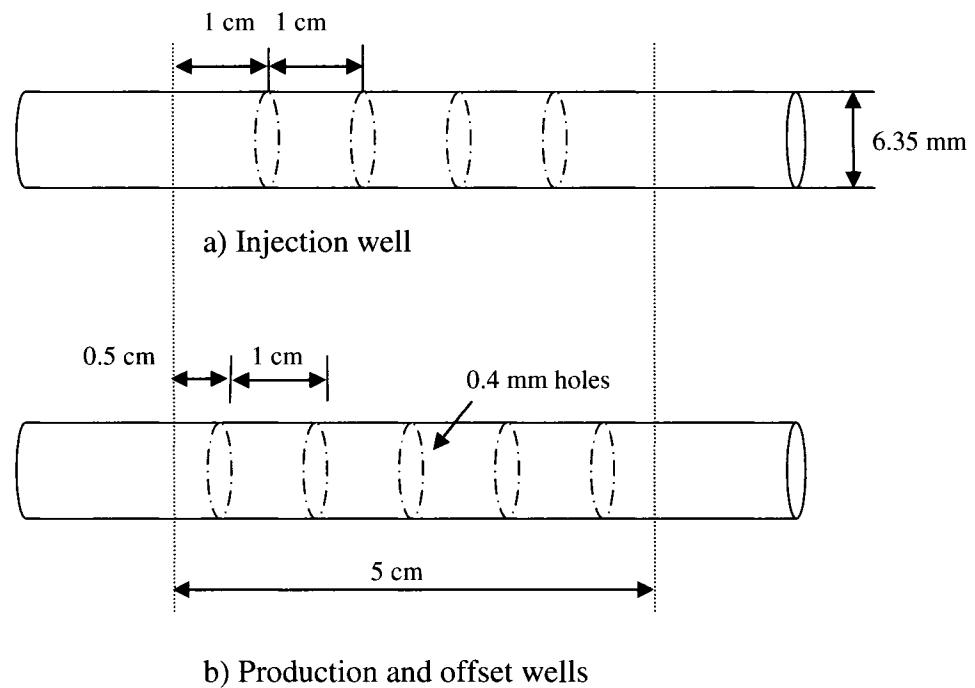
Figure 6.21: Schematic diagram of injection and production wells

215

The pressure vessel, which contains the scaled model described earlier, is designed with seamless carbon steel pipe (SA 106) for high pressure and high temperature operation conditions up to 8,200 kPa at 204 °C. The dimensions of the pressure vessel are: an outside diameter of 45.7 cm, an inside diameter of 43.2 cm and a length of 109 cm (Figure 6.22). There are five ports at the one end of the vessel for connecting the five strings of multi-thermocouples, and five pairs of ports on both sides of the vessel walls for the injection and production wells. There are five ports at the top of the vessel for the nitrogen gas blanket system; two are for pressure relief valves, one for a pressure gauge, another for nitrogen gas inlet, and the other for the pressure transmitter (PT250). The support of the pressure vessel is designed so that the vessel could be used at various inclinations, from horizontal to vertical.
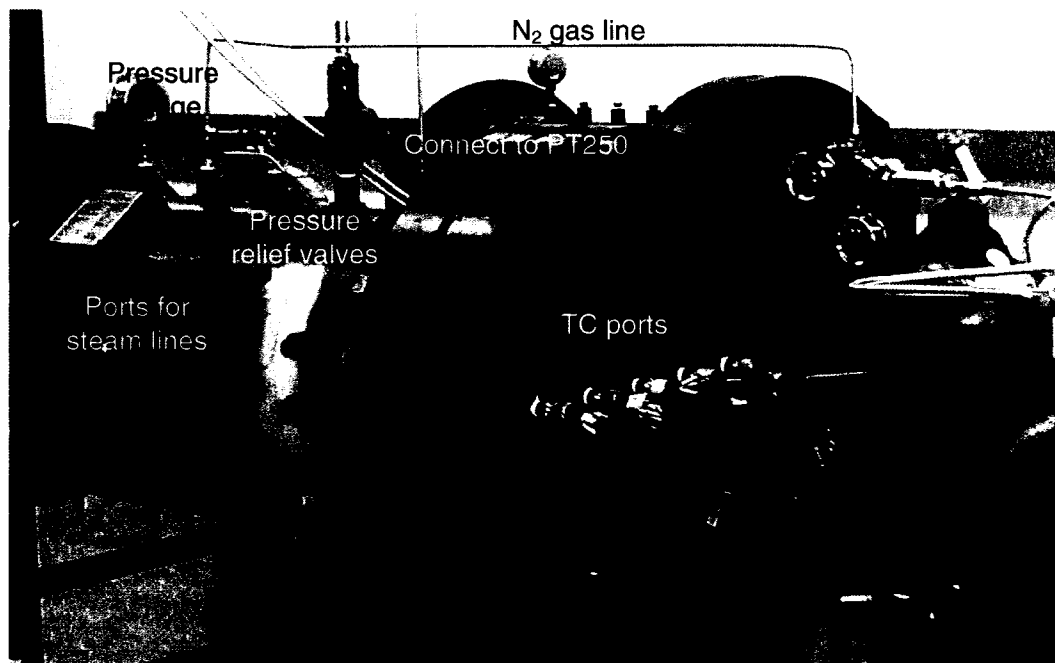
Figure 6.22: Pressure vessel (manufactured by ECO Technica, Edmonton, Canada) and nitrogen gas blanket system

216

6.3.3 Preparation of the Experiments

After installing wells and thermocouples, the scaled model is packed with glass beads, -20 to +30 mesh, to obtain the target design permeability for the experiments. To minimize the effect of the thermocouple strings and wells, the packing process is carried on slowly (see Appendix D for details). The calculated porosity is about 33 % for both the SAGD and Fast-SAGD models. The expected permeability is around 170 Darcy. In fact, it is difficult to measure exactly the permeability of a rectangular model. In this study, two indirect methods for calculating and measuring the permeability of a model were considered: calculation from the Kozeny-Carman equation and measurement with a cylindrical model. The equation gives a range of permeabilities between 180 and 340 Darcy depending on the average grain size 0.6 to 0.8 mm, but the measured permeability from a cylindrical model, 30.5 cm in length and 3.8 cm in diameter, gave 170 Darcy.

The model is saturated with Lloydminster oil having a viscosity of 10,000 cp and a density of 963.6 kg/m^3 at 15°C. During the saturation procedure, the heavy oil is heated up to 50 °C with a banding heater to increase its mobility. The initial oil saturation is about 0.95. The total oil volume in a model is about 3,100 cm^3, but the expected recoverable oil from these models is about 2,740 cm^3 because the oil located below the production well cannot be produced during the conventional SAGD process, in which the gravity is the main recovery mechanism.

The saturated models are insulated with a mineral fibre board of 2.5 cm thickness except for the bottom exposure (Figure 6.23). All the steam injection and fluid production lines, made of stainless steel tubing having a diameter 6.35 mm, are wrapped with a wrap tracer for insulation.

The scaled model is then installed inside the pressure vessel, and connected to the thermocouple panel (TC panel), which communicates with the DeltaV controller. Finally, the nitrogen gas blanket system is connected to the pressure vessel for applying overburden pressure (Figure 6.24).

217
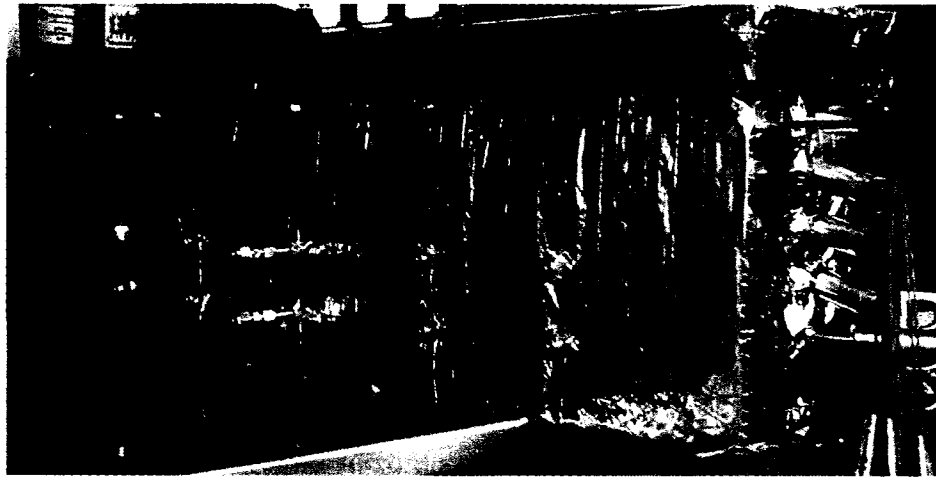
Figure 6.23: Model insulated with a mineral fibre board
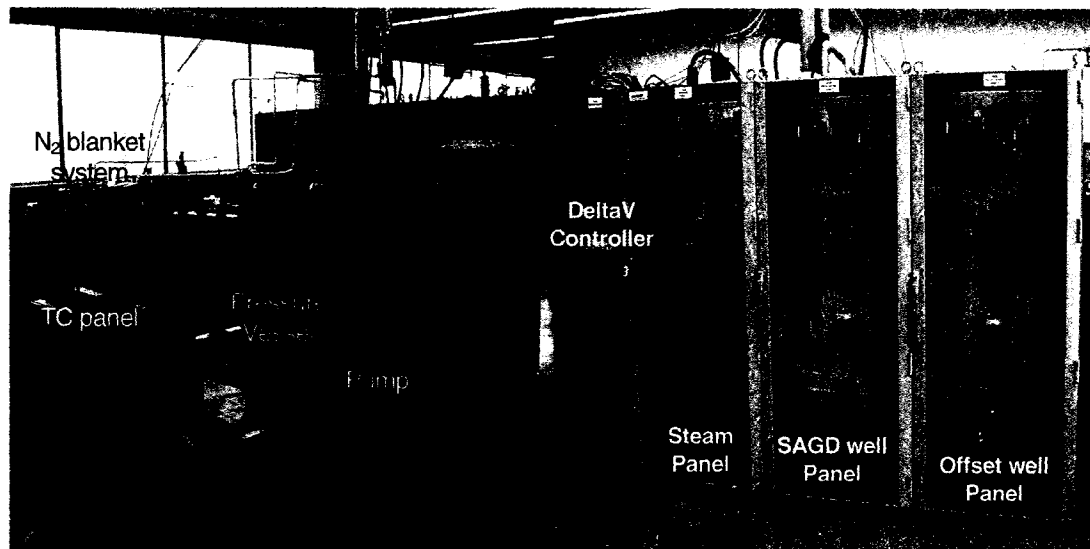
Figure 6.24 shows SAGD experiment panel

218

6.3.4 Experimental procedures

The SAGD experiments are operated with two programmed Sequential Function Charts: a startup sequence and a shutdown sequence, as shown in Figures 6.25 and 6.26. The startup sequence has two options, one for the SAGD operation and the other for the Fast-SAGD operation, in which the CSS operation from the offset well is included. The shutdown sequence, designed for a safe shutdown of the experiments, will be activated automatically when any operating condition exceeds its range. The reason for the shutdown will be indicated at the shutdown sequence interface.

Once a scaled model is installed inside the pressure vessel and connected to the injection and production lines, the first step is to pressurize the model and the pressure vessel. During this procedure, the pressure is increased from 290 to 1,500 kPa, and the differential pressure between the inside and the outside of model is kept as small as 25 kPa in order not to cause the model to collapse: the overburden pressure always kept higher than the injection pressure. Flowing water through the production well by opening XV203 and XV300 will pressurize the inside of the model. The overburden pressure is set at around 1,700 kPa by the nitrogen gas blanket system.

Demineralized water is injected with a pump, and the injection rate is set at 2 kg/hr during the SAGD experiment. The heater generates superheated steam at 265 °C at the heater outlet, and the steam temperature drops to between 205 and 209 °C inside the model due to heat losses through steam lines and valves. The pressure of the steam injected into the model is between 1,740 and 1,790 kPa. The stress due to thermal expansion of a packed model is not considered. The production pressure at the cylinder is set at 1,700 kPa, corresponding to the overburden pressure, which can not be controlled during the experiment. If the production pressure were to change during the experiment, it would be automatically controlled back to its set value of 1,700 kPa.

The produced oil and water are collected in a production cylinder of 5-litre capacity after passing through a cooling system. This cylinder is emptied several times during the experiment.

```
┌──────────────────┐                    ┌─────────────────────────┐
│      SET UP       │                    │     SAGD INJECTION      │
└────────┬─────────┘                    └───────────┬─────────────┘
         │
┌────────┴─────────┐
│    START PUMP     │
└────────┬─────────┘                    ┌─────────────────────────┐
         │                              │      CSS OPERATION       │
┌────────┴─────────┐                    │     AT OFFSET WELL       │
│    RAMP HEATER    │                    │                          │
└────────┬─────────┘                    │  1)  INJECTION           │
         │                              │  2)  SOAK                │
┌────────┴─────────┐                    │  3)  PRODUCTION          │
│   UIC* TO AUTO    │                    └───────────┬─────────────┘
└────────┬─────────┘
         │
┌────────┴─────────┐
│  STEAM TO MODEL   │
└────────┬─────────┘
         │          F-SAGD Mode ──────────►
SAGD Mode │
┌────────┴─────────┐
│  SAGD INJECTION   │
└────────┬─────────┘
```

```
┌──────────────────┐
│    WIND DOWN      │
└────────┬─────────┘
         │
┌────────┴─────────┐
│    CLEAN UP       │
└──────────────────┘
```
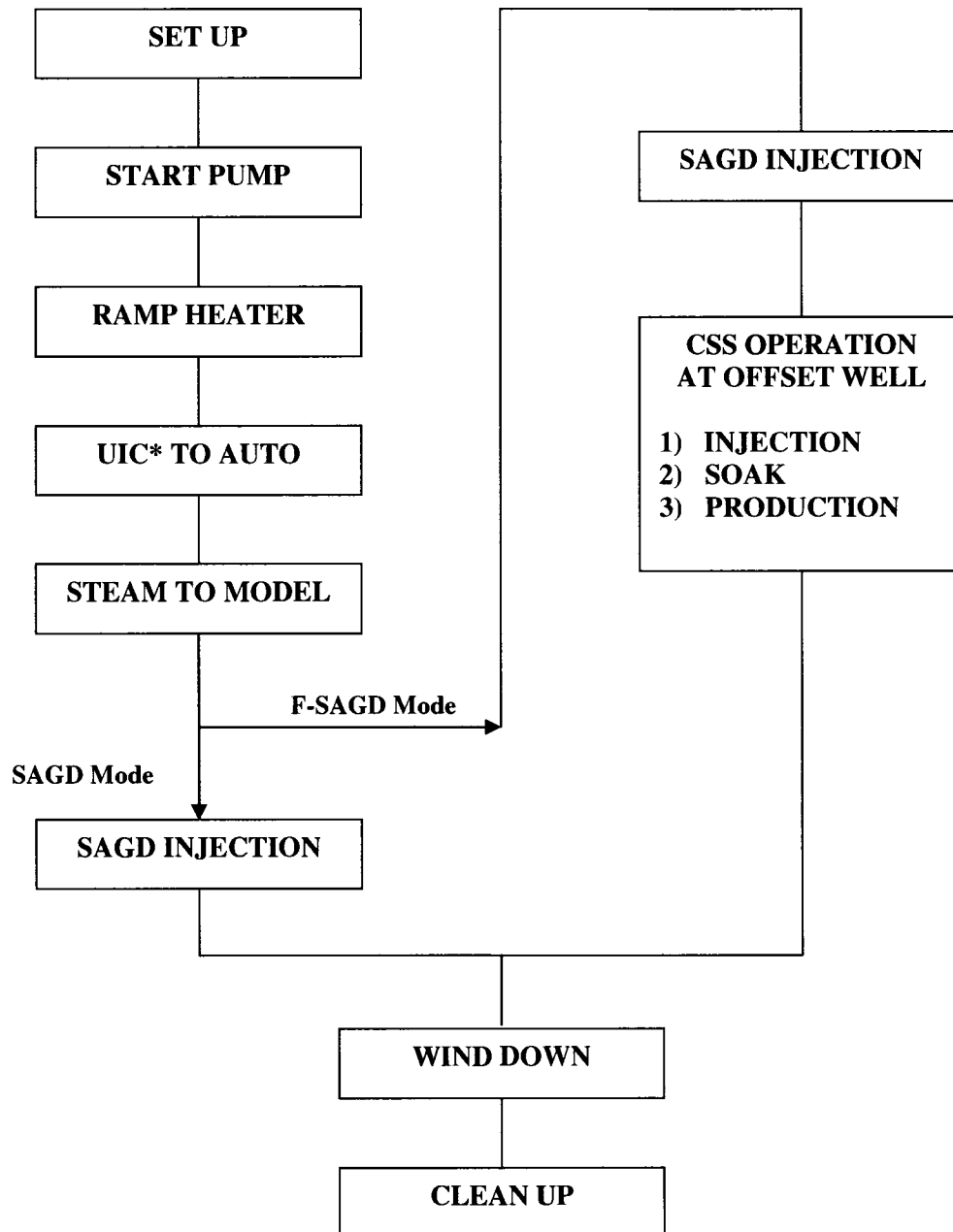
UIC*: Steam Quality Controller

Figure 6.25: Startup Sequence for SAGD experiment operation

220

```
┌─────────────────────┐
│    HEATER OFF       │
└─────────────────────┘
          │
┌─────────────────────┐
│    VENT STEAM       │
└─────────────────────┘
          │
┌─────────────────────┐
│    COOL DOWN        │
└─────────────────────┘
          │
┌─────────────────────┐
│   SAFE SHUTDOWN     │
└─────────────────────┘
          │
┌─────────────────────┐
│    PUMP OFF         │
└─────────────────────┘
```
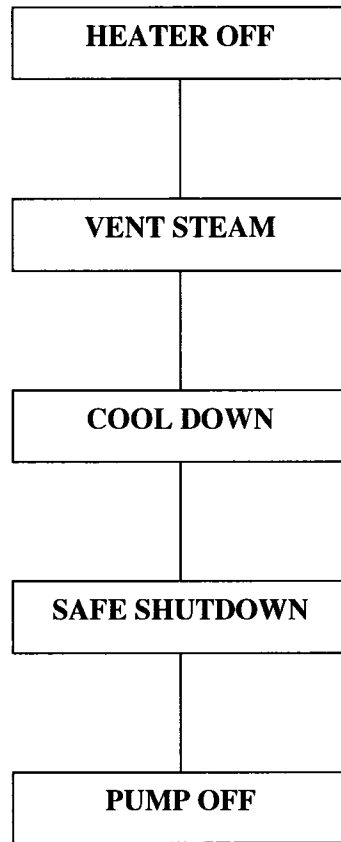
Figure 6.26: Shutdown Sequence for SAGD experiment operation

221

6.4 Experimental Results

The type of experiments described in the thesis has never been performed before with such a complex experimental apparatus using an automated process control system. For that reason, the nature of the experimental work is exploratory, and involves a great deal of commissioning effort. Therefore, the results of these experiments have to be considered as preliminary. They will not provide a definitive answer of their performance and comparison in the laboratory but will serve for determining the conditions required in order to perform definitive and predictive experiments.

6.4.1 SAGD experimental results

A SAGD experiment was conducted for four hours after steam injection into the model was started. The main experimental data are shown in Table F.1. Steam was injected into the SAGD model 40 minutes after starting the steam generation at the heater. While the steam being generated was reaching the injection conditions, it by-passed the model (it took 40 minutes in the case of this experiment). The generated steam temperature (TE201) was between 254 and 276 °C, and controlled to be kept close to 265 °C; the generated pressure (PT201) was between 1,800 and 1,900 kPa (Figure 6.27). The pressure inside the SAGD model is expected to be as low as 1,750 kPa, which is an average value of PT202 (Figure 6.7) and PI301 (Figure 6.8) because of pressure losses in the steam injection line.

The steam injection rate (FT100) varied between 1.9 and 2.1 kg/hr, but was kept close to 2 kg/hr which is the set point. As a result, the heater drive (UY101) stayed around a value of 25 % (Figure 6.28). The production pressure, PT350 (Figure 6.12) varied between 1,620 and 1,750 kPa, and was kept close to 1,700 kPa which is the set point (Figure 6.29). The production pressure was kept 25 kPa lower than overburden pressure applied by the nitrogen gas blanket system, which can not be controlled. The PI301 trend is expected to stay as close as possible to the overburden pressure, and the steam injection pressure is between PT202 (Figure 6.7) and PI301 (Figure 6.8), but closer to PI301.

222
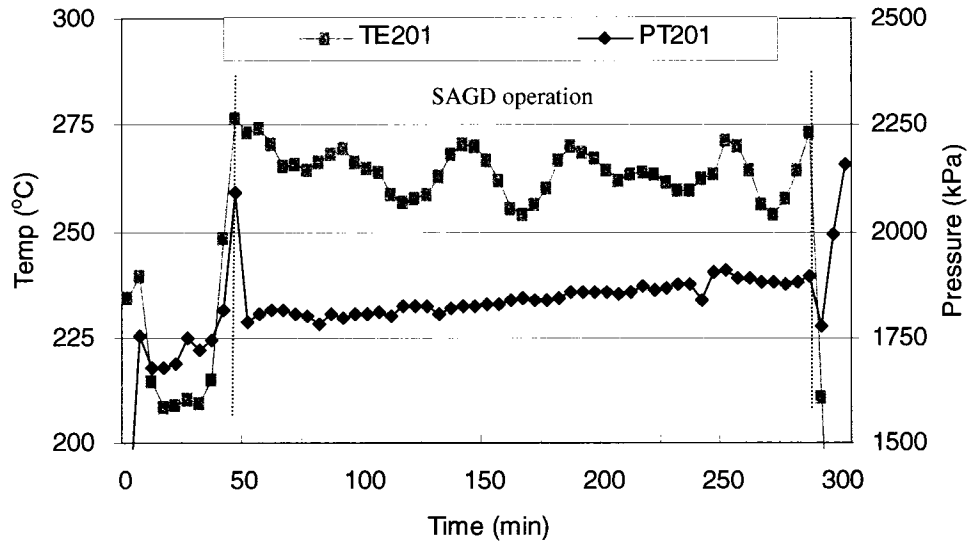
Figure 6.27: Steam temperature and pressure trends (SAGD experiment)
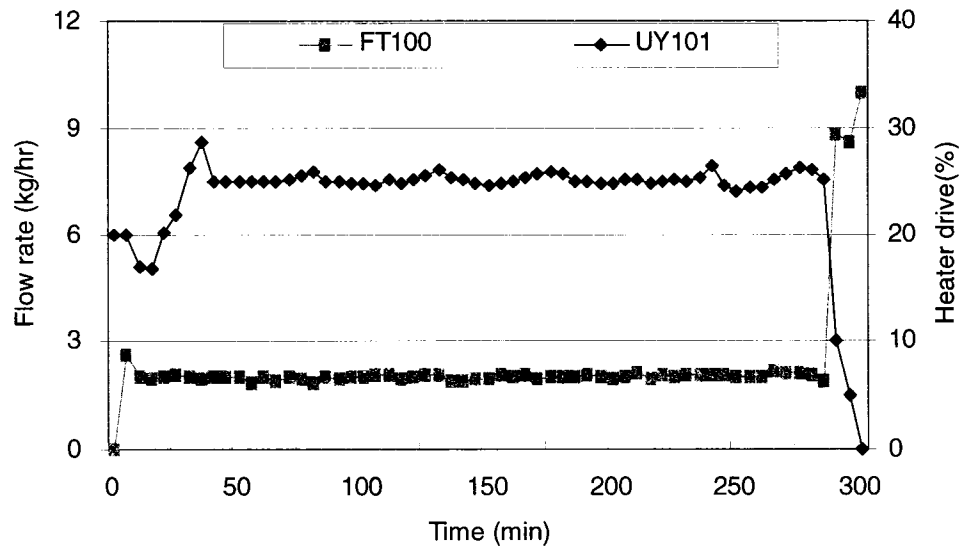
Figure 6.28: Steam injection rate and heater drive trends (SAGD experiment)

223
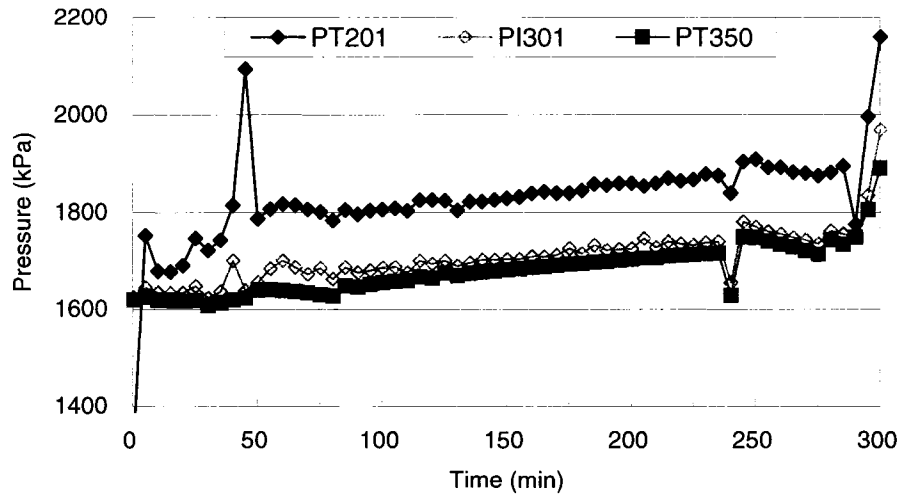
Figure 6.29: Injection and production pressure trends (SAGD experiment)

The temperature of the production fluids IN (TE300) during the SAGD operation was around $80^{\circ}C$, and the temperature of the cooling water IN (TE303) was $16\,^{\circ}C$. As a result, the production fluid OUT (TE301) was kept around $55\,^{\circ}C$, in the range of 45 to 60 $^{\circ}C$. The cooling water OUT (TE302) showed a value between 20 to 45 $^{\circ}C$ (Figure 6.30). The TE301 temperature had a very constant value around the set point temperature of 60 $^{\circ}C$.

A thermocouple was installed between the scaled model wall and the insulation board just below the injection well for investigating the temperature trend on the surface of the model. The model skin temperature (T-skin) increased from 20 $^{\circ}C$ to 70 $^{\circ}C$ during the experiment (Figure 6.31). Considering the steam temperature of 265 $^{\circ}C$ at the heater (TE201) and the expected steam temperature of 210 $^{\circ}C$ inside the scaled model, the model skin temperature seems to be quite low. Therefore, it is expected that the heat transfer from the injected steam line to the model wall is small. Furthermore, the heat transfer from the model wall to the inside of model should be even smaller as the thermocouple data showed low temperatures in the areas away from the injection well.
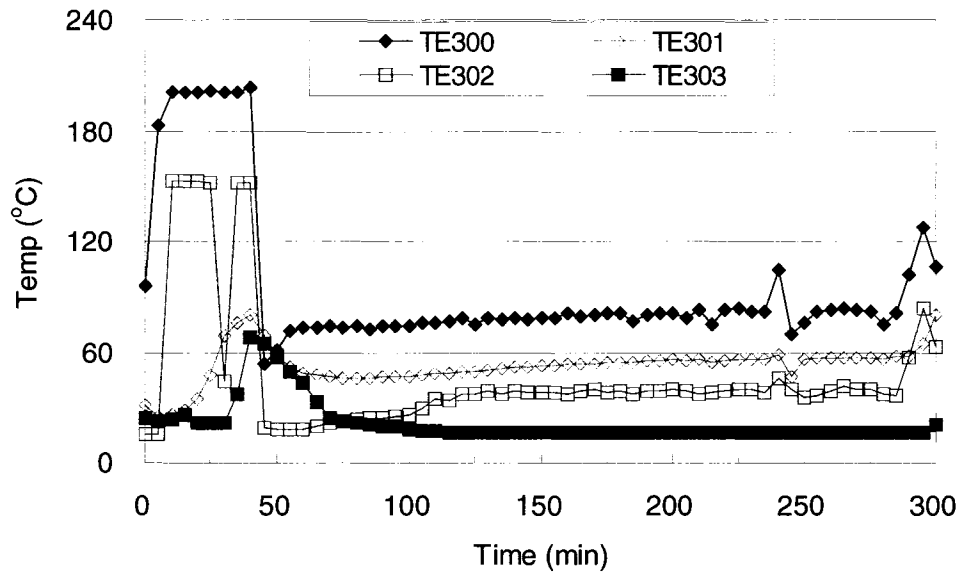
Figure 6.30: Main temperature trends of the production cooling system (SAGD experiment)
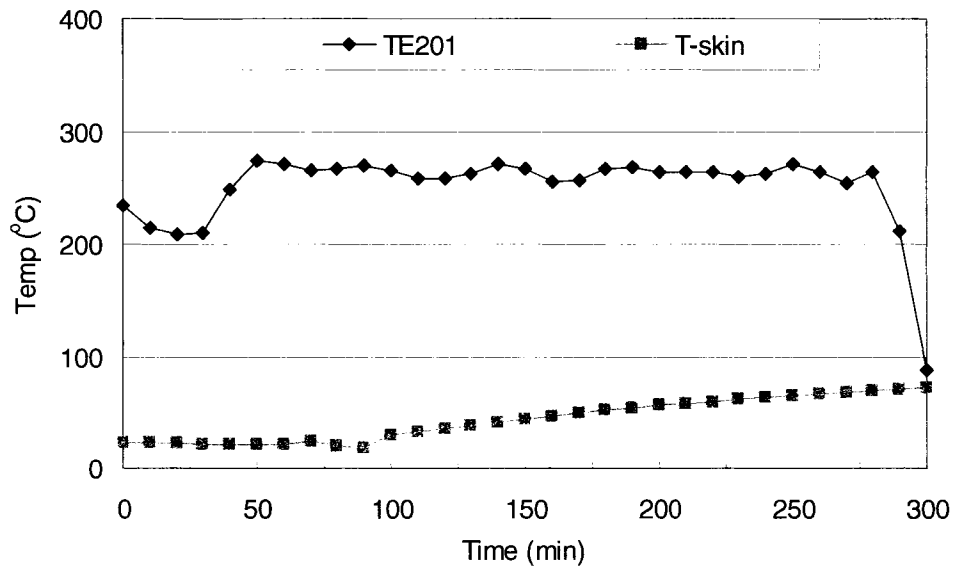
Figure 6.31: Temperature trends of the steam and the model wall (SAGD experiment)

225

The oil-cut trend, as determined with a coriolis flow meter, is shown in Figure 6.32. The average oil-cut is 0.17, with a maximum value of 0.24. The oil-cut value increased in the early stages of the SAGD operation and then dropped until the operating time had reached 100 minutes. After this point, the oil-cut increased again slightly until the operating time of 200 minutes, and then decreased again for the remaining portion of experiment. Although the oil-cut trend was mainly related to the SAGD process mechanism itself, it also seemed to be affected by the steam temperature (or steam quality): a higher steam temperature resulted in higher oil-cuts (Figure 6.32).
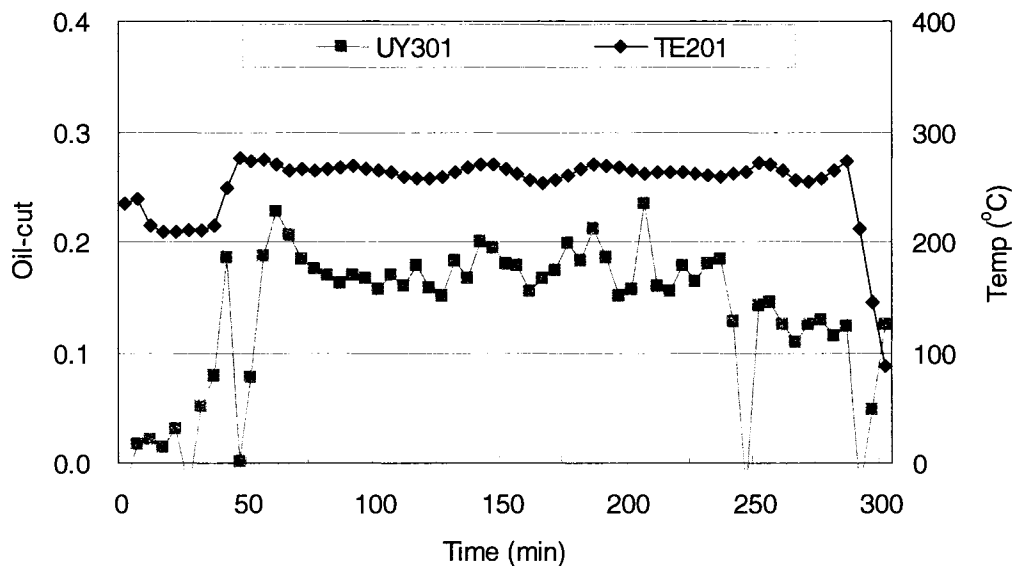
Figure 6.32: Steam temperature and oil-cut trends (SAGD experiment)

Cumulative oil production was 1,503 cm^3 (including 130 cm^3 for the 15 minutes wind-down period), which is close to the 1,530 cm^3 of oil collected from the production cylinder. This represented a cumulative steam-oil ratio (CSOR) of 5.99 after four hours of operation (Figure 6.33). The lowest CSOR was 5.43 at the operating time of 75 minutes. The final recovery factor was 0.55. During the SAGD process, 8,210 cm^3 of steam were injected and 8,370 cm^3 of a mixture of oil and water were produced. A quite

226

large pressure difference between injection and production wells was suspected and may have resulted in additional production. There could be an error in calculating the injected steam quantity by taking an average flow rate every 5 minutes.
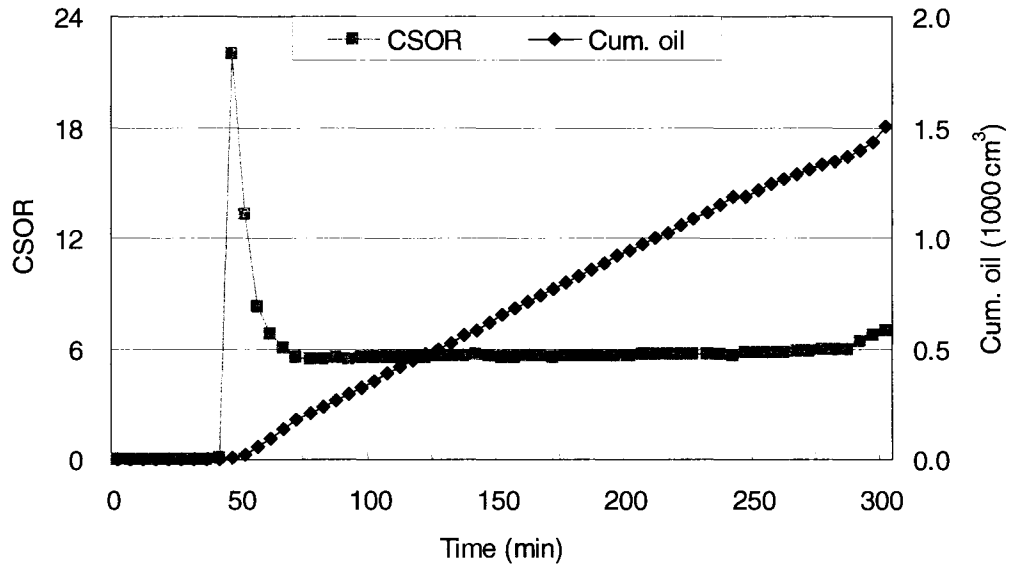
Figure 6.33: Cumulative oil production and CSOR trends (SAGD experiment)

Thirty-seven thermocouples data points out of forty (three were broken) collected the temperatures inside the model. They were analyzed using a contour software (Surfer) to investigate the steam chamber propagation during the SAGD process (Table F.3). Initially, the steam chamber grew in a vertical direction, and then started to propagate laterally (Figure 6.34). This was the typical trend expected from a SAGD operation. Due to the loss of a thermocouple point at the position TC2-6, the steam chamber did not show exact symmetry (Figure 6.34).

227
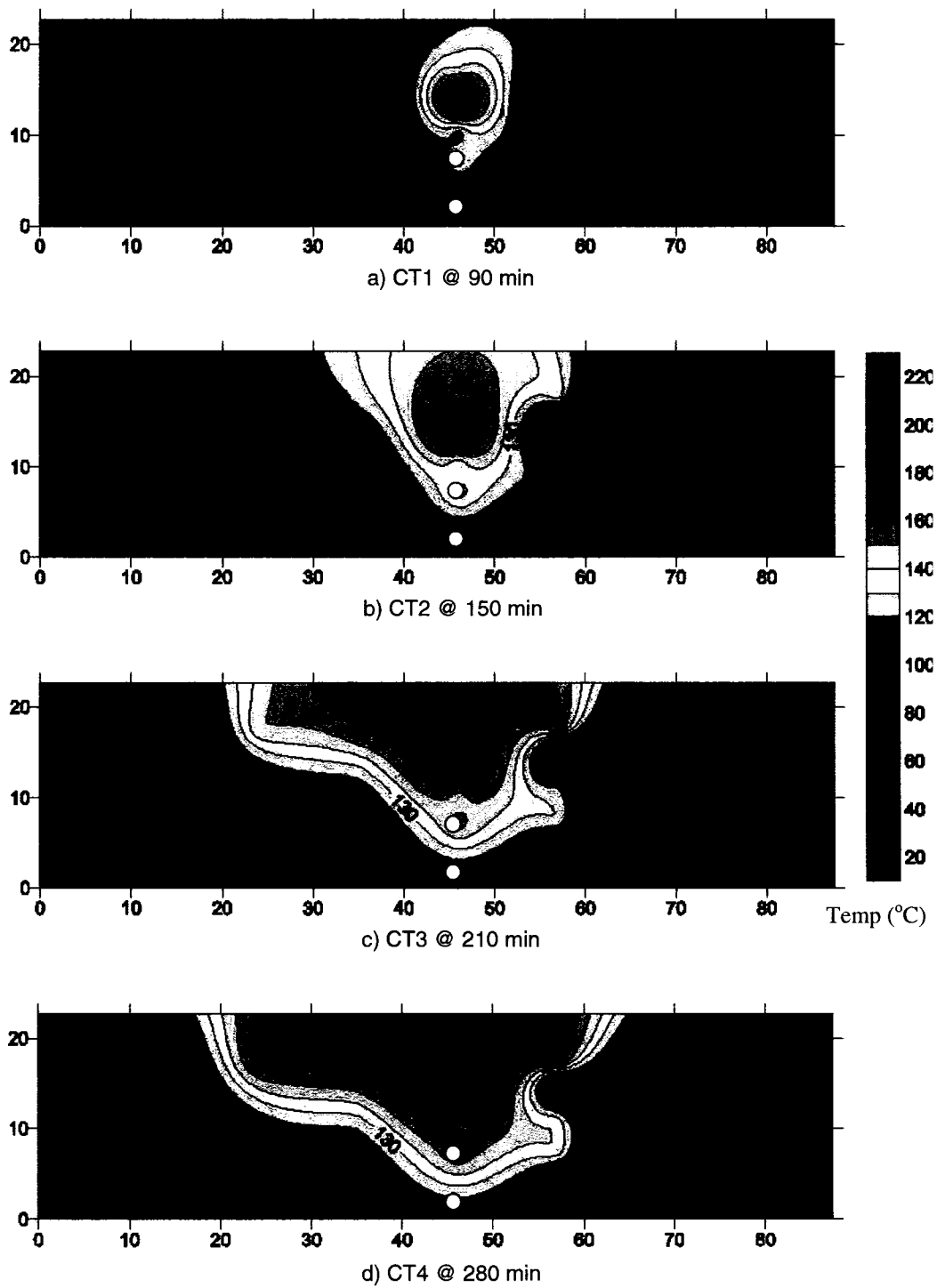
Figure 6.34: Steam chamber profiles for SAGD experiment

228

6.4.2 Fast-SAGD experimental results

A Fast-SAGD experiment was conducted for three hours after steam injection into the model. The main experimental data are shown in Table F.2. Steam was injected into the SAGD model 45 minutes after starting steam generation at the heater. The generated steam temperature (TE201) was between 210 and 255 °C, and depended on the steam flow rate and pressure. As shown in Figure 6.35, the steam temperature after starting the CSS operation from the offset well did not reach as high a degree of superheat as that of the SAGD experiment because the flow rates were increased suddenly from 2 to 6 kg/hr to meet the CSS operating requirements. The same heater was used for generating the entire amount of steam required for both wells. A sudden increase of its throughput associated with a simultaneous splitting of the flow into the SAGD injector (about 2 kg/hr) and the offset well (about 4 kg/hr) caused the steam quality to decrease. This caused the steam chamber to collapse and affected the overall performance of the Fast-SAGD operation negatively.

The generated pressure (PT201) was between 1,750 and 2,090 kPa (Figure 6.35). The pressure inside the Fast-SAGD model was expected to be as low as 1,750 kPa, which is an average value of PT202 (Figure 6.7) and PI301 (Figure 6.8) because of pressure losses in the steam injection line.

The steam injection rate (FT100) varied between 1.9 and 6.9 kg/hr, but was kept close to 2 and 6 kg/hr, which are the set points for the SAGD and Fast-SAGD operating periods, respectively. The steam injection rate was increased from 2 to 6 kg/hr after the CSS operation at the offset well. The heater drive (UY101) changed between 25 and 40 % depending on the steam flow rate; if the flow rate was increased, the heater drive would increase, with a time delay, to keep the steam temperature as close as possible to the set point value (Figure 6.36).

229
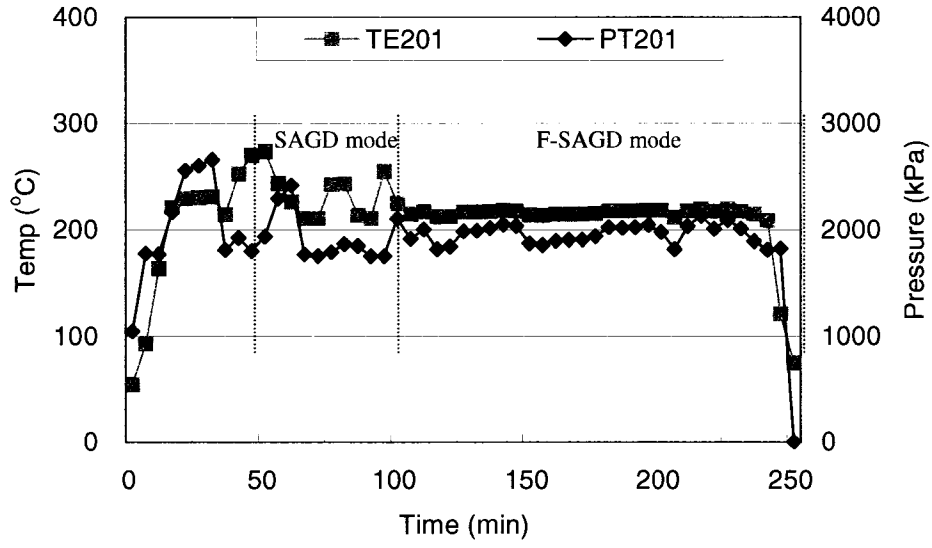
Figure 6.35: Steam temperature and pressure trends (Fast-SAGD experiment)
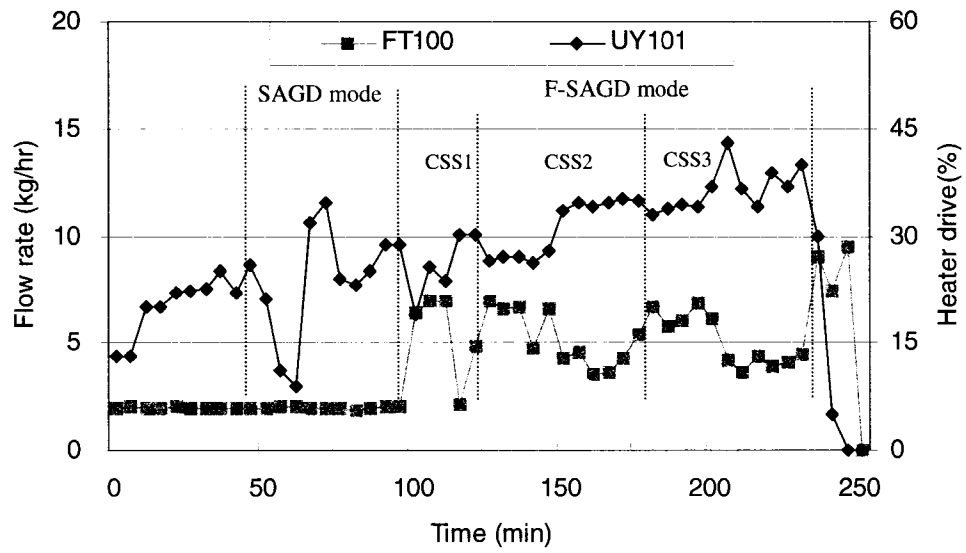
Figure 6.36: Steam injection rate and heater drive trends (Fast-SAGD experiment)

230

Initially, two cycles of the CSS operation were planned. After monitoring the steam chamber and its collapse during the first two cycles, one more cycle was operated to re-establish the steam chamber. Three cycles of cyclic steam injection were conducted during the Fast-SAGD experiment: the first CSS cycle started at the 45 minutes after steam injection into the model and lasted 20 minutes (12 minutes of injection, 1 minute of soak, and 7 minutes of production), the second CSS cycle started at the operating time of 60 minutes and lasted 60 minutes (30 minutes of injection, 2 minutes of soak, and 28 minutes of production), and the third CSS cycle started at the operating time of 120 minutes until the end of experiment (25 minutes of injection, 7 minutes of soak).

The production pressure (PT350) varied between 1,600 and 1,740 kPa, and was kept close to 1,700 kPa, which is the set point (Figure 6.37). The production pressure was kept 25 kPa lower than the overburden pressure applied by the nitrogen gas blanket system, which can not be controlled. The PI301 trend was expected to stay as close as possible to the overburden pressure, and the steam injection pressure is between PT201 and PI301, but closer to PI301.
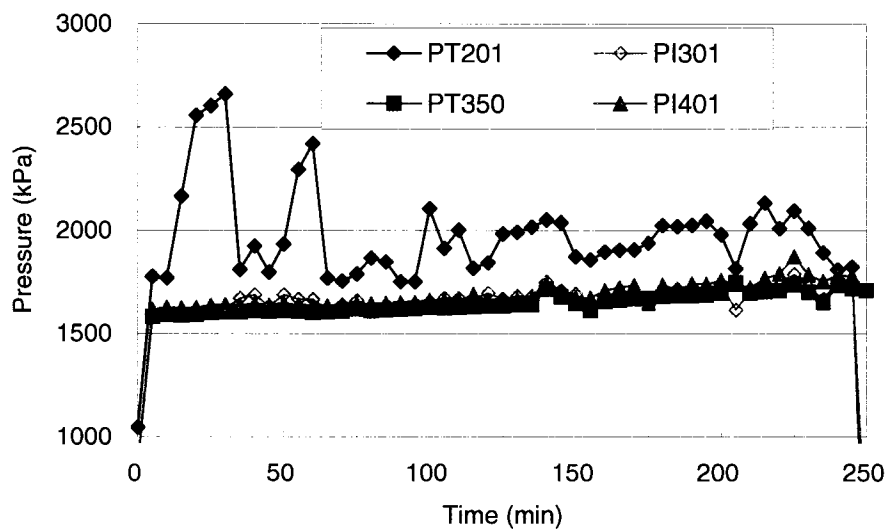
Figure 6.37: Injection and production pressure trends (Fast-SAGD experiment)

231

The temperature of the production fluids IN (TE300) during the SAGD operating period varied between 65 to 110 °C, and the temperature of the cooling water IN (TE303) was 22 °C. As a result, the production fluid OUT (TE301) was kept around 55 °C, in the range of 45 to 60 °C. The cooling water OUT (TE302) showed a value between 25 to 55 °C (Figure 6.38). The TE301 temperature had a very constant value around the set point temperature of 60°C.

In this experiment and in order to investigate the heat loss, a thermocouple was installed in the annulus filled with nitrogen gas, on top of the insulation of the scaled model. The annulus temperature (T-annu) increased from 20 °C to 50 °C during the experiment (Figure 6.39). Considering the high steam temperature of between 210 and 255 °C at the heater (TE201) and the expected average steam temperature of 205 °C inside the scaled model, the annulus temperature is low. This is due to the fact that the insulation board has a high thermal efficiency of 93 % and the nitrogen gas has a thermal conductivity as low as 0.02828 W/m-K at 2MPa (Stephan et al., 1987).
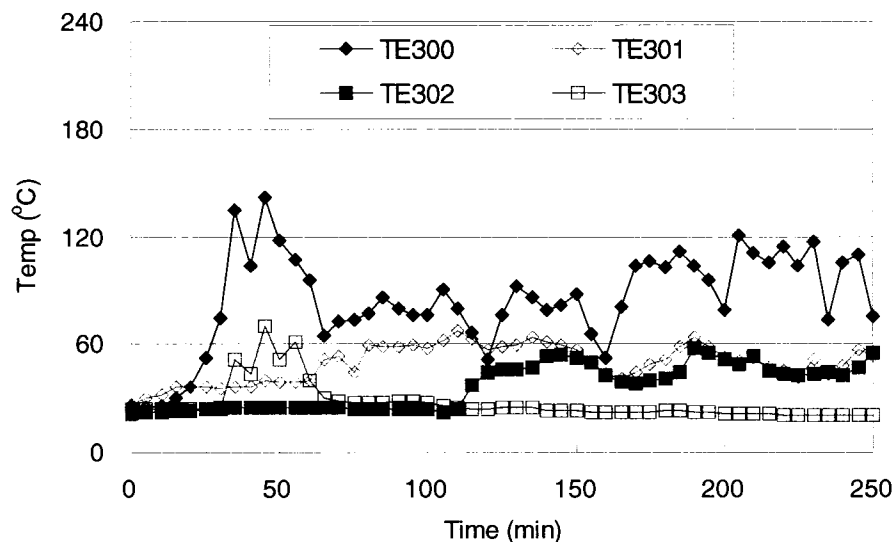
Figure 6.38: Main temperature trends of the production cooling system (Fast-SAGD experiment)

232
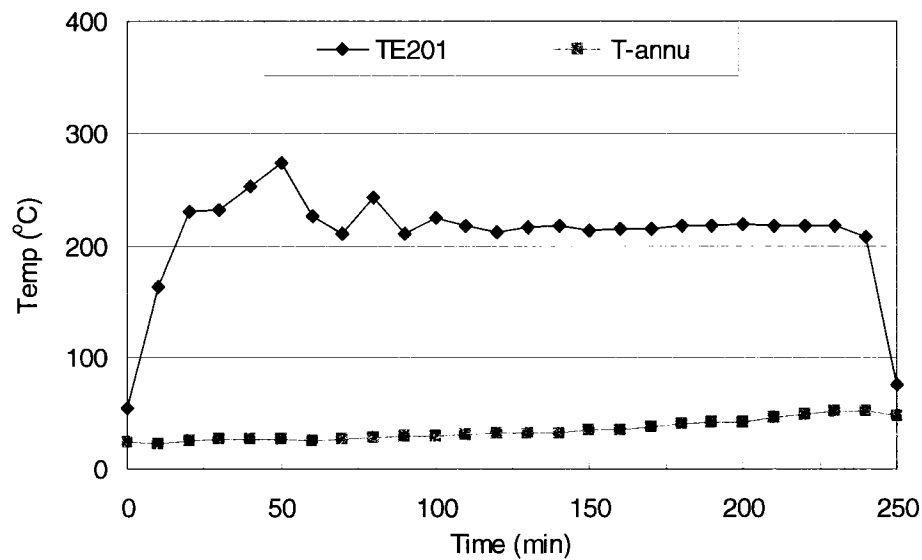
Figure 6.39: Temperature trends of the steam and the annulus (Fast-SAGD experiment)

After the first CSS cycle, the offset well production line became obstructed after exiting the model. Therefore, the oil-cut analysis was done only for the SAGD production well (UY301).

The oil-cut trend (UY301), as determined with a coriolis flow meter, is shown in Figure 6.40. The average oil-cut is 0.14 with a maximum value of 0.54. The oil-cut value increased in the early stages and then dropped until the operating time reached 100 minutes, which was the time when the first CSS operation was started at the offset well. After this point, the oil-cut varied according to the cyclic operation. The oil-cut value reached a maximum value during the second CSS period. After the third CSS operation, the oil-cut values dropped for the remaining portion of the experiment. During the SAGD operating period (45 to 90 minutes), although the oil-cut trend was mainly related to the SAGD process mechanism itself, it also seemed to be affected by the steam temperature (or steam quality): a higher steam temperature resulted in higher oil-cuts (Figure 6.40). However, for the Fast-SAGD period (90 to 230 minutes) the oil-cut seemed to be mainly related to the CSS operation at the offset well.

233
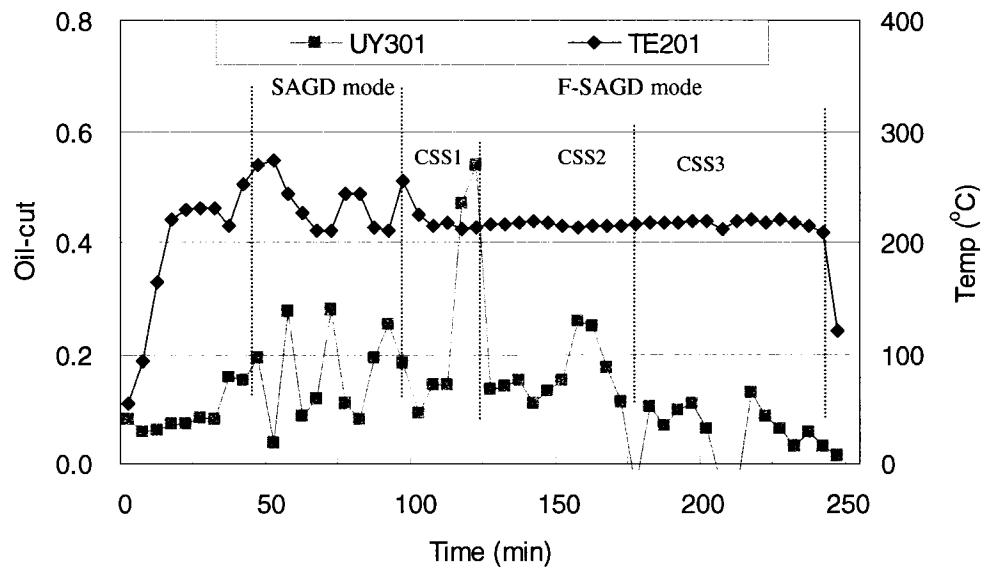
Figure 6.40: Steam temperature and oil-cut trends (Fast-SAGD experiment)

Cumulative oil production was 1,540 cm³ (including 30 cm³ for the 20 minutes wind-down period) and the cumulative steam-oil ratio (CSOR) was 8.76 after three hours of operation (Figure 6.41). The lowest CSOR was 4.87 at the operating time of 75 minutes, while operating in SAGD mode and before the steam chamber collapsed. The final recovery factor was 0.56. During the Fast-SAGD process, 13,390 cm³ of steam were injected and 13,670 cm³ of mixture of oil and water was produced. A quite large pressure difference between the injection and production wells, as well as the CSS operation at the offset well may have resulted in additional production. There would be an error in calculating the injected steam quantity by taking an average flow rate every 5 minutes.

234
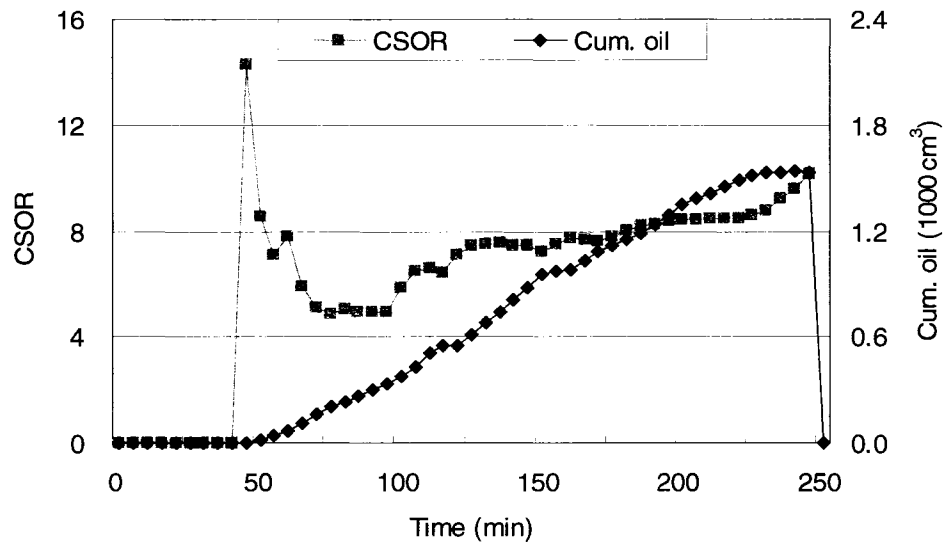
Figure 6.41: Cumulative oil production and CSOR trends (Fast-SAGD experiment)

The steam chamber profiles (Figure 6.45) during the Fast-SAGD process were larger than those of the SAGD process due to the CSS operation at the offset well. The CSS operation during the Fast-SAGD process helped the steam chamber expand laterally. The steam chamber could not propagate to the left side of the offset well: there was no production from the offset well due to a blockage in the production line outside of the model. Therefore, one would expect to have more oil produced from the SAGD well due to the steam drive effect. Figure 6.42 shows the steam chamber collapse at the SAGD well pair, just after CSS operation at the offset well, because the heater could not provide enough energy to deal with the increased injection rate in a short time.

235
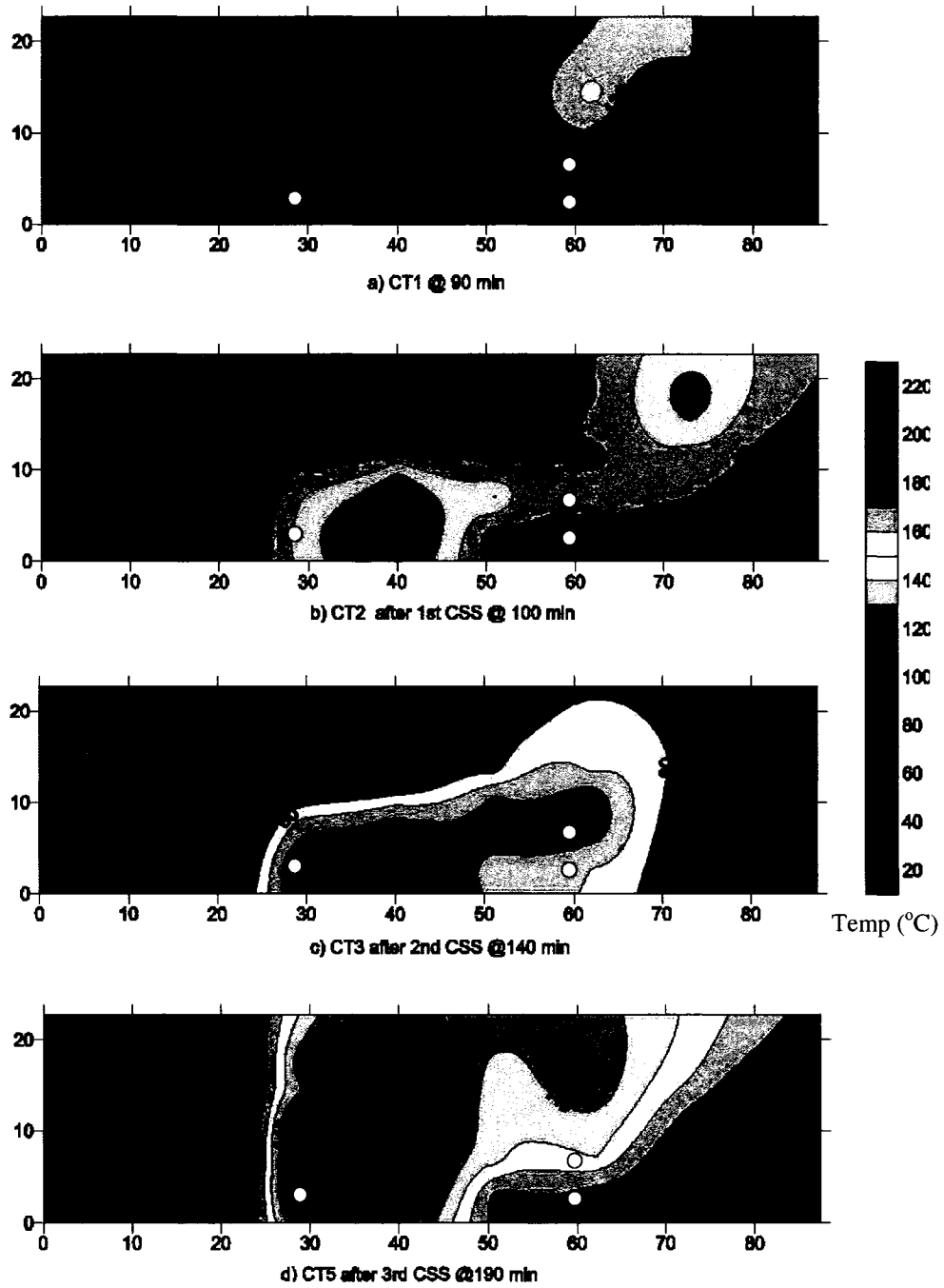
Figure 6.42: Steam chamber profiles during the CSS periods for Fast-SAGD experiment

236

6.4.3 Comparison of SAGD and Fast-SAGD experiments

These preliminary experiments were conducted to assess the capability of the facility for high temperature and high pressure steam injection processes with an automated process control system. It is valuable to compare the experimental results for understanding these processes.

The two experiments were compared with respect to thermal efficiency and productivity. The overall cumulative oil production was larger in the Fast-SAGD case (Figure 6.43), but the end-point CSOR was lower in the SAGD case (Figure 6.44). At 60 minutes after starting steam injection, when SAGD and Fast-SAGD have the same CSOR value of 5.53, Fast-SAGD gave higher cumulative oil production by 6 % (376 versus 355 cm^3). The SAGD experiment produced 1,370 cm^3 of oil with a CSOR of 5.99 (excluding wind-down) in 245 minutes and the Fast-SAGD experiment produced the same amount of oil in 165 minutes with a CSOR of 8.44. In these experiments, the Fast-SAGD process produced the same amount of oil in a much shorter time (165 versus 245 minutes) with a higher CSOR. In all these cases, the CSOR has been calculated with the assumption that 100 % quality steam was injected at all times into the model.
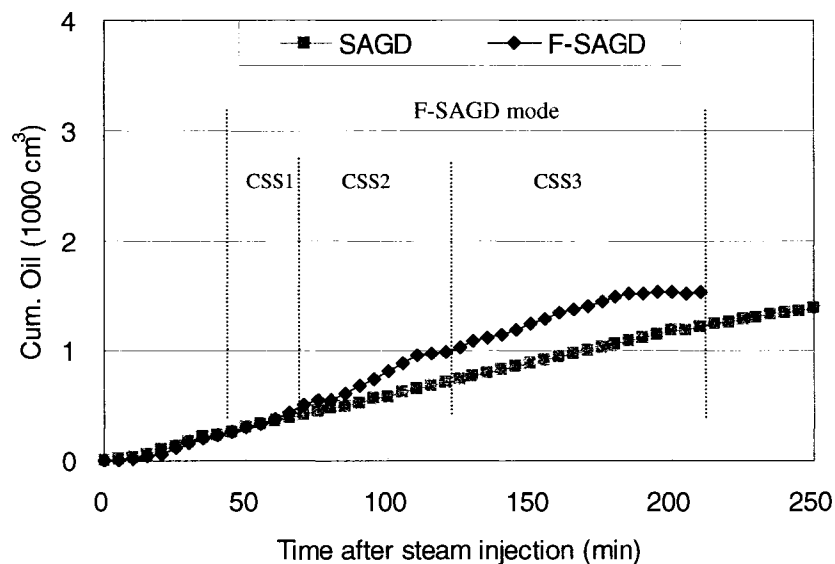
Figure 6.43: Comparison of cumulative oil production trends for SAGD and Fast-SAGD

237
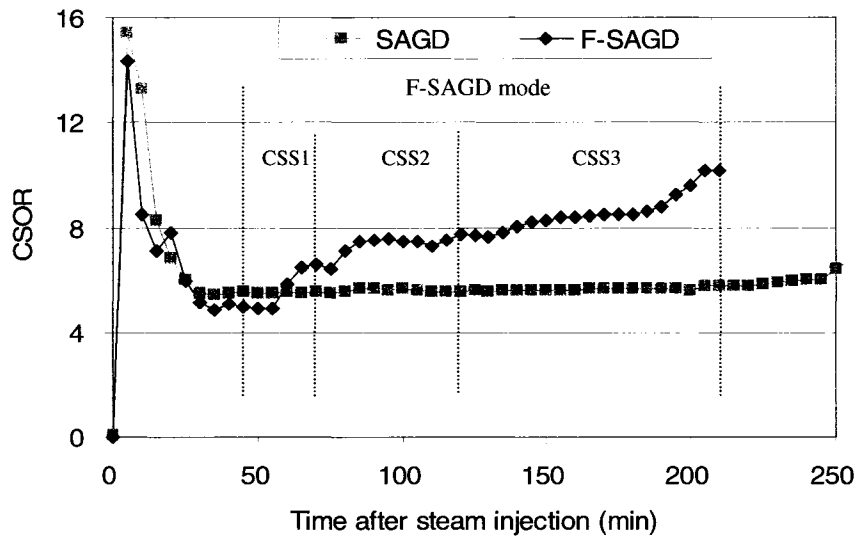
Figure 6.44: Comparison of cumulative steam-oil ratio trends for SAGD and Fast-SAGD

Both experiments were not optimized with respect to the amount of injected steam, and duration of the injection. Therefore, the results given above should only be looked at qualitatively, and not quantitatively.

Figure 6.45 shows the steam chamber shapes at the same time for both experiments. The steam chambers of the Fast-SAGD experiment are larger than the ones of the SAGD experiment. The heater was not working for a while during the SAGD period of the Fast-SAGD experiment, so the Fast-SAGD case shows a lower temperature profile in the steam chamber (Figure 6.45 B-a). During the first two CSS operations at the offset well, the steam chamber collapsed because the heater could not generate the proper amount and quality of steam in a short time due to the sudden increase of the flow rate from 2 to 6 kg/hr for the offset well operation.

238

(A) SAGD

(B) Fast-SAGD

a) CT1 @ 90 min

a) CT1 @ 90 min

b) CT2 @ 150 min

b) CT4 @ 150 min

c) CT3 @ 210 min

c) CT6 @ 210 min

Temp (°C)

d) CT4 @ 280 min

d) CT7 @ 240 min
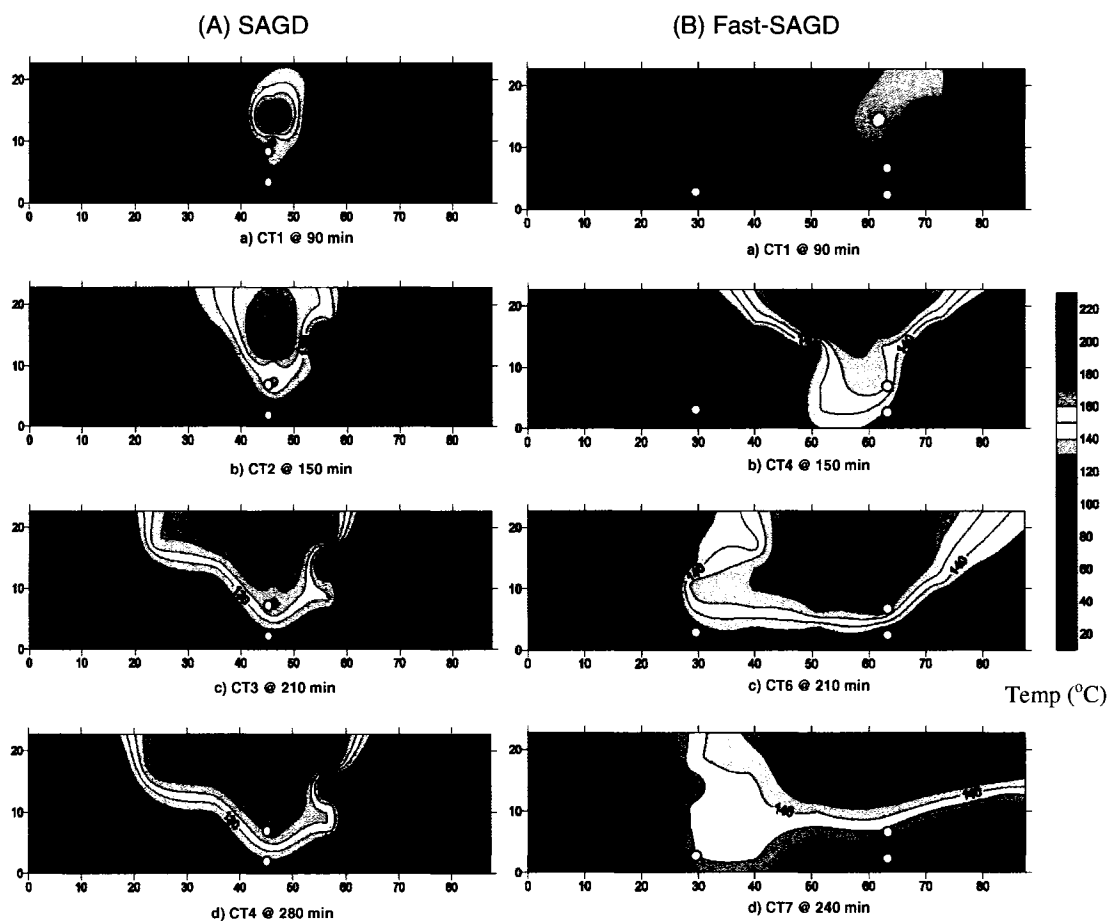
Figure 6.45: Comparison of steam chamber profiles for SAGD and Fast-SAGD experiments

239

6.5 Comparison of Experimental and Numerical Results

Numerical simulation results of the scaled physical models for SAGD and Fast-SAGD are compared with the experimental results. Even though superheated steam was generated from the heater in the experiments, the steam quality inside the model may be less than 100 %. For the SAGD case, the injected steam temperature inside model was between 202 and 209 °C and the pressure was expected as 1,750 kPa. The saturated steam temperature at this pressure is 206 °C. Then, steam quality could vary from 0 % to 100 %. In the experiments, steam quality varies depending on the injected steam temperature. An average steam quality for the SAGD and Fast-SAGD experiments can be predicted based on history matching. Even though this predicted value might not be the exact value, it is valuable to compare the average steam qualities of the SAGD and Fast-SAGD experiments.

Beside steam quality, the relative permeability would be a critical factor for a laboratory scale numerical simulation because different porous media and fluid properties were used in the experiment and the simulation.

Two-dimensional numerical simulations were performed with CMG's STARS based on the experimental geometry and parameters. The numerical grid size for the scaled model is 0.67 cm in the i and k directions, respectively, and 5 cm along the horizontal well (j direction). The total grid number is 131 x 1 x 34 (i, j, k).

6.5.1 SAGD case

A sensitivity analysis was conducted to investigate the effect of steam quality on the SAGD experiment. As the steam quality increases, cumulative oil production increases and CSOR decreases (Figures 6.46 and 6.47). A steam quality of 0.3 (NUM-SQ 0.3) was found to be close to the experimental results in the cumulative oil production case, and also in the CSOR case. As a result, the case of NUM-SQ 0.3 seems to give the best history match with the experimental results in both cumulative oil production and CSOR.

240

These results imply that the steam quality inside the scaled model was around 0.3, and that this steam quality information will be very valuable for the heat balance calculation.
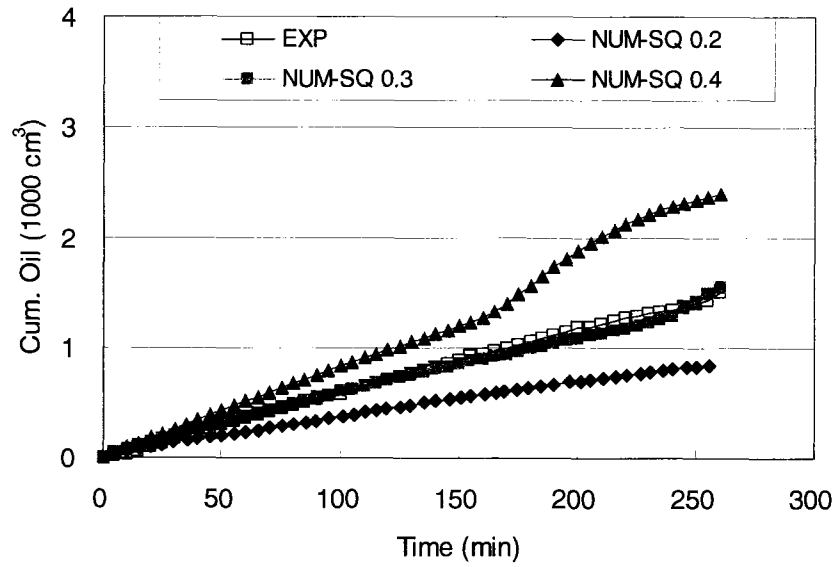
Figure 6.46: Steam quality effect on cumulative oil production for SAGD
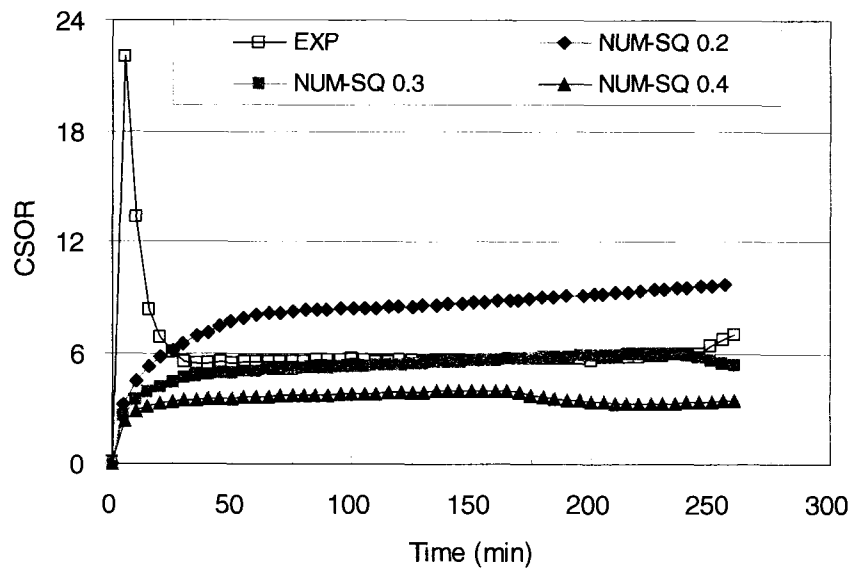
Figure 6.47: Steam quality effect on CSOR for SAGD

241

There is a difference in the preheating of the reservoir between the experiment and the numerical simulation. The electric heater option, which means no steam injection during the preheating period, is used for STARS, and steam passing through the model for the experiment. Therefore, the CSOR is higher for the experiment at early times as shown in Figure 6.47.

Two different types of relative permeability curves (Appendix A) were used for history matching. One is the Athabasca-type (NUM-AB) for a dead oil case and the other is the Lloydminster-type (NUM-LM) for a live oil case. These simulations considered a steam quality of 0.3. The simulation results show that the Athabasca-type curves give a better match with the experimental results for both cumulative oil production (Figure 6.48) and the CSOR (Figure 6.49). Relative permeability curves which can represent a dead oil case had to be used for the simulation of the experimental scaled models because the Lloydminster-type oil, which is a dead oil at laboratory condition, was used for the experiments, even though this type of oil is a live oil at field conditions. Beside this, as the oil saturation and permeability of the experimental modes are different from those of the field, the relative permeability curves had to be selected properly for a laboratory scale numerical simulation.
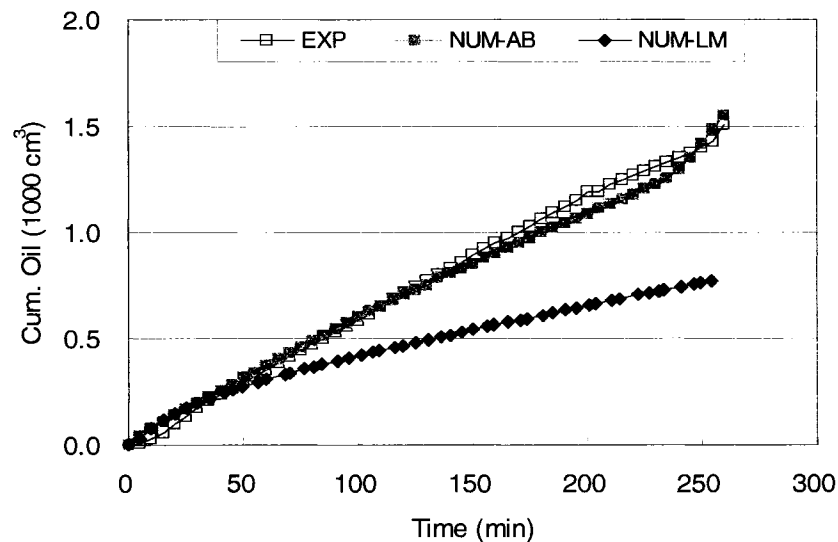
Figure 6.48: Relative permeability effect on cumulative oil production

242

24

CSOR

18

12

6

0

—□— EXP   ■ NUM-AB   ◆ NUM-LM

0   50   100   150   200   250   300

Time (min)
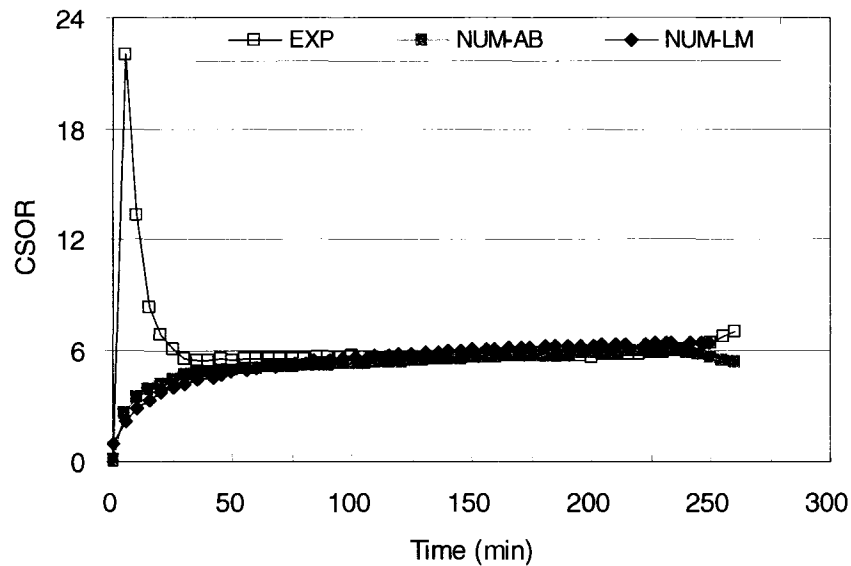
Figure 6.49: Relative permeability effect on CSOR

6.5.2 Fast-SAGD case

The Fast-SAGD experiment, unlike the SAGD one, requires a flexible steam injection system due to the CSS operation at the offset well. There are two important factors that can affect the Fast-SAGD experimental results; steam quality and injection rate at both the SAGD injector and the offset well.

As it is difficult to know the flow rate of steam into both injection wells and as the steam quality changes during the experiment, the history match for the Fast-SAGD experiment is more complicated than that of the SAGD experiment. Based on the numerical simulation results of the field scale case, the Fast-SAGD operating parameters for the experiment have been set-up as shown in Table 6.2.

For the first two cycles of the CSS operation, a steam chamber could not be developed because the steam quality of the injected steam decreased due to the splitting of the injected steam into the SAGD and offset wells. Also, the steam injection rate ratio

243

between the SAGD injection well and the offset well could not be controlled as desired. To overcome these shortcomings for the third cycle, the total injection rate was increased gradually instead of in one time step.

Table 6.2: Operating parameters for Fast-SAGD experiment

Operating parameter		Field scale	Scaled model
Injection pressure	SAGD well	1,710 kPa	
	Offset well	4,500 kPa	1,720 kPa
Production pressure (all wells)		1,700 kPa	
Injection rate	SAGD well	600 m³/d	2 kg/hr
	Offset well	1,200 m³/d	4 kg/hr
CSS start-up time		1.5 yr	35 min

CSS cycle period
  - Injection
  - Soak
  - Production
		9 month
		0.5 month
		2.5 month
			18 min
			1 min
			5 min

A sensitivity analysis was conducted to investigate the effect of steam quality on the Fast-SAGD experiment. As the steam quality increases, cumulative oil production increases and CSOR decreases (Figures 6.50 and 6.51). A steam quality of 0.2 (NUM-SQ 0.2) is close to the experimental results, both in the cumulative oil production case and the CSOR case. The cumulative oil production trends show that there is a good match between NUM-SQ 0.3 and the experimental results during the early times (SAGD mode). After that period (after starting the Fast-SAGD mode), the experimental results are close to NUM-SQ 0.2. This could imply that there might be a change in the steam quality after the start of the CSS operation at the offset well. During the Fast-SAGD experiment, there was a temperature drop just after starting the CSS operation at the offset well due to the sudden increase of steam flow rate. Compared to the SAGD case in which a constant steam injection rate is applied, the Fast-SAGD case proves more difficult to history match the steam quality due to the change of the steam flow rate.

244
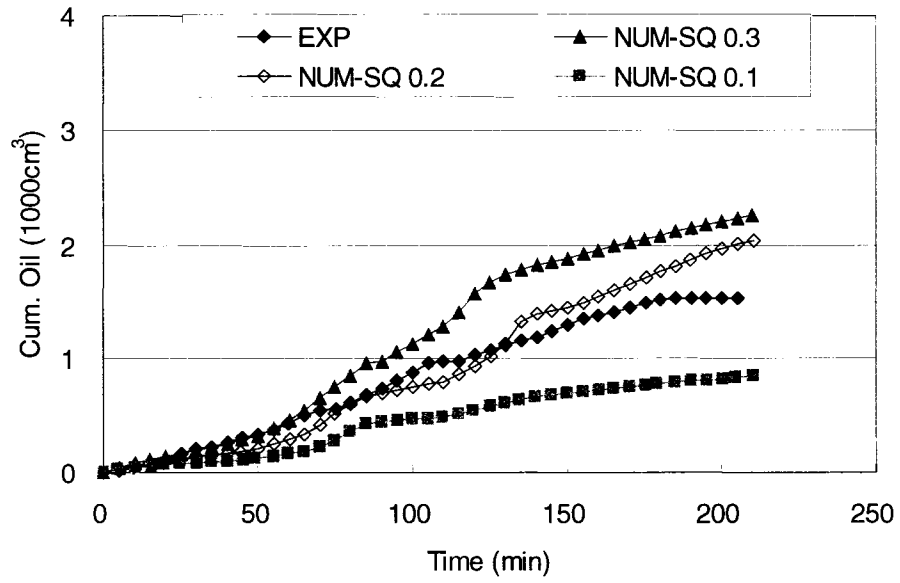
Figure 6.50: Steam quality effect on cumulative oil production for Fast-SAGD
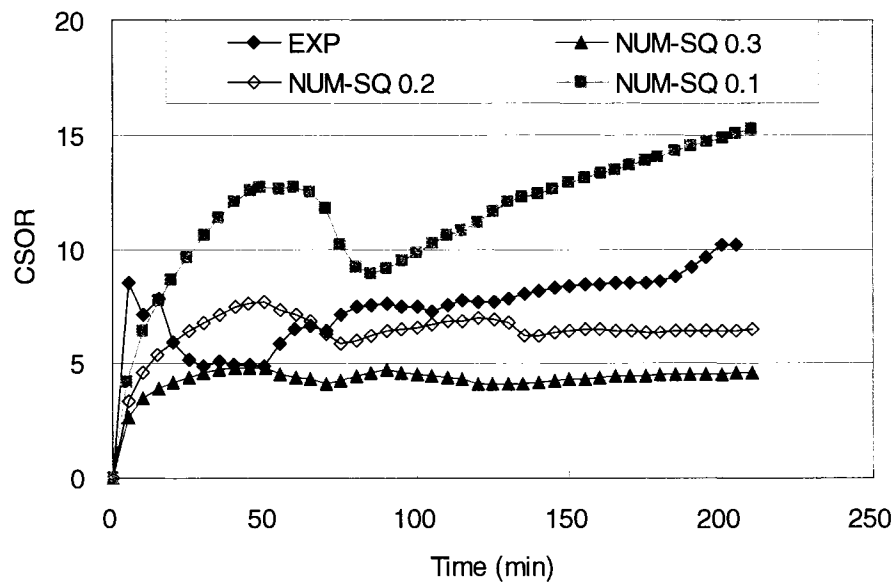
Figure 6.51: Steam quality effect on CSOR for Fast-SAGD

245

For a detailed history match of the Fast-SAGD experiment, follow-up simulations were conducted by changing the steam quality during the Fast-SAGD mode only. Both of the NUM-SQ 0.3-0.15 (steam quality is changed from 0.3 to 0.15 after starting the CSS) and NUM-SQ 0.3-0.2 cases are close to the experimental results of the cumulative oil production (Figures 6.52), but NUM-SQ 0.3-0.15 provides a closer match in the CSOR case (Figure 6.53). As a result, the case of NUM-SQ 0.3-1.5 seems to give a better history match with the experimental results in both cumulative oil production and CSOR.

If the same quality of steam were injected into the Fast-SAGD model as in the SAGD case, the experimental results of the Fast-SAGD case would be improved as shown in Figures 6.54 and 6.55. For these simulations, it was assumed that the offset wells worked properly. Simulation results show that the NUM-SQ 0.3F case increases the cumulative oil production by 70 % (2,600 cm^3 versus 1,490 cm^3) and decreases the CSOR by 52 % (4.29 versus 9.01).
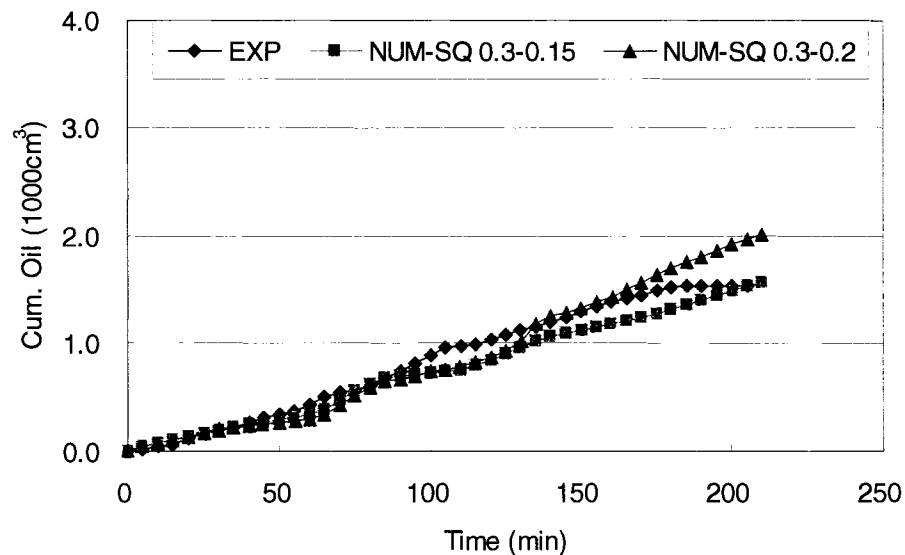
Figure 6.52: Steam quality change effect on cumulative oil production for Fast-SAGD

246
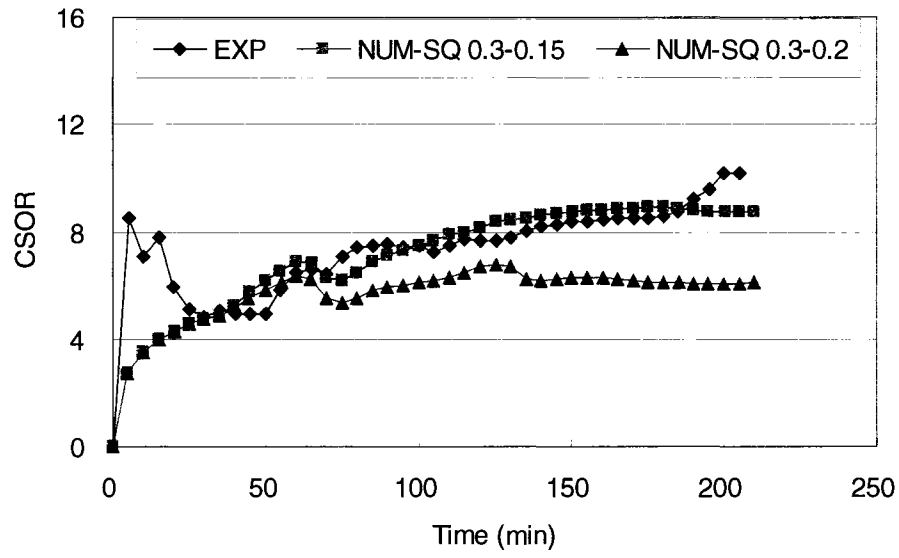
Figure 6.53: Steam quality change effect on CSOR for Fast-SAGD
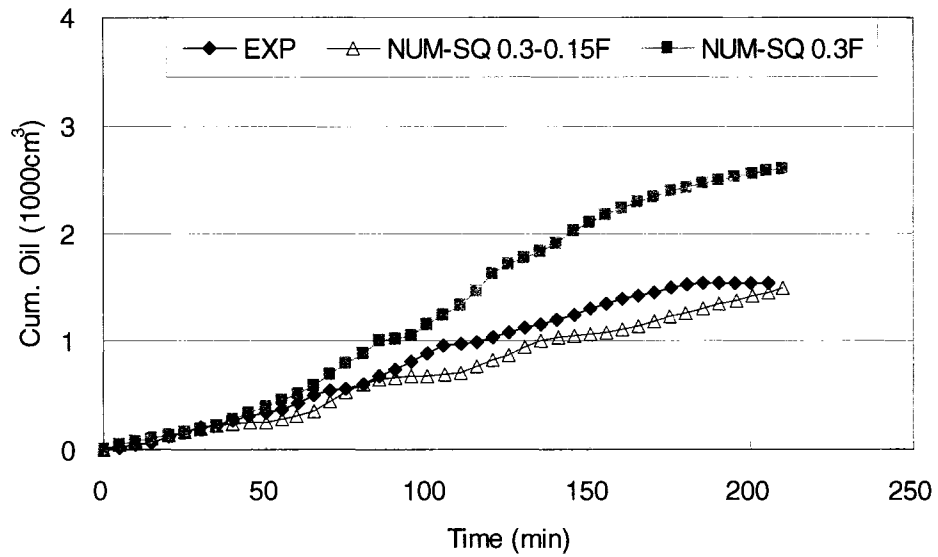
Figure 6.54: Steam quality effect on cumulative oil production for Fast-SAGD

247
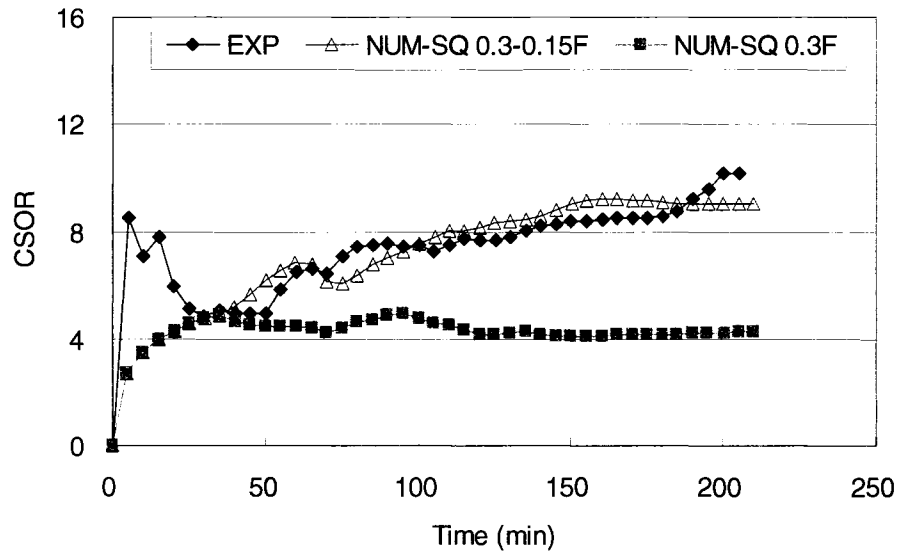
Figure 6.55: Steam quality effect on CSOR for Fast-SAGD

6.5.3 Heat balance for the experiments

The history match results using the numerical simulations give good information for investigating the heat balance through the experiments. The overall heat balance was calculated with a simple equation, $Q_{gn} = Q_{ac} + Q_{pd} + Q_{ls}$, based on the flow rate, temperature and steam quality of both the injected steam and produced fluids (Appendix F).

Q_{gn}, the heat generated at the heater, is calculated using the steam temperature (TE201), steam pressure (PT201), and steam injection rate (FI100).

Q_{pd}, the heat produced from the model, is calculated using the flow rate (FT301) and temperature (TE301) of the production fluid.

248

Q_{ac}, the heat accumulated in the model, is calculated using the temperature profile of thermocouple data (Table F.3) and saturation profile inside model.

Q_{ls} is the heat loss through steam injection (Q_{ls-in}), production lines (Q_{ls-pd}), stainless steel model (Q_{ls-md}), and annulus between model and pressure vessel (Q_{ls-an}). Q_{ls-in} is calculated from the following relationship, $Q_{ls-in} = Q_{gn} - Q_{md}$. Q_{ls-pd} is calculated from the following relationship, $Q_{ls-pd} = Q_{md} - Q_{ls-ms} - Q_{ls-an} - Q_{pd}$. Due to the limitation of thermocouple availability, Q_{ls-ms} is calculated for the SAGD experiment and Q_{ls-an} is calculated for the Fast-SAGD experiment.

Q_{md}, the heat injected into the model, is calculated using the steam quality estimated from the numerical history matching results (see Appendix F for detailed calculations). Steam temperature was assumed as 210 $^{\circ}$C and 205 $^{\circ}$C for the SAGD and Fast-SAGD experiments, respectively. The numerical history matching results suggest to use a steam quality of the injected steam of 0.3 for the SAGD mode and 0.15 for the Fast-SAGD mode. In other words, for the Fast-SAGD experiment, the steam quality is changed from 0.3 to 0.15 after starting the CSS operation at the offset well.

For the SAGD experiment (Table F.4), the total heat generated is 23,725 kJ, and the heat loss through the injection line (Q_{ls-in}) is 48 % of the generated heat, resulting in 12,243 kJ of heat injected into the model (Figure 6.56). The produced heat (Q_{pd}) is 2,705 kJ, and the heat accumulated in the model (Q_{ac}) is 1,656 kJ which is 14 % of the heat injected into the model. The heat loss through stainless steel model (Q_{ls-ms}) is 769 kJ which is overestimated because there is only one thermocouple, which is located just below injection well and gives a higher temperature of the skin than the average, to measure the skin temperature on the model wall. As Q_{ls-an} is very small in the Fast-SAGD experiment (0.3 % of heat injected into the model), if the same thermal efficiency is assumed for the SAGD experiment, then Q_{ls-an} is 35 kJ. Therefore the heat loss through the production line (Q_{ls-pd}) is 7,064 kJ.

249

For the Fast-SAGD experiment (Table F.5), the total heat generated is 39,016 kJ and the heat loss through the injection line (Q_{ls-in}) is 54 % of the generated heat, resulting in 17,768 kJ of heat injected into the model (Figure 6.57). The produced heat (Q_{pd}) is 5,812 kJ, and the heat accumulated in the model (Q_{ac}) is 2,185 kJ which is 12 % of the heat injected into the model. The heat loss through the stainless steel model (Q_{ls-ms}) is estimated to be as high as 1,166 kJ if the same thermal efficiency (6.56% of heat injected into the model in the SAGD experiment) is assumed. Q_{ls-an} is 58 kJ, which is 0.3 % of heat injected into the model. Then the heat loss through the production line (Q_{ls-pd}) is 8,547 kJ.

The heat accumulated in the model is very small for both of experiments; 14 % for SAGD and 12% for Fast-SAGD. As the pressure and temperature conditions inside the SAGD model do not vary much and could be quite similar between the injection and production wells, this may cause direct steam flow into the producer, and may result in the small heat accumulated inside the model.

For the thermal efficiency evaluation, the injected energy per the unit produced oil (kJ/cm^3) has been calculated. The total heat injected of 12,243 kJ has produced 1,530 cm^3 of oil for the SAGD experiment, therefore the energy per unit produced oil is 8.00 kJ/cm^3. In the Fast-SAGD experiment case, the total heat injected of 17,768 kJ has produced 1,540 cm^3 of oil, then the energy per unit produced oil is 11.54 kJ/cm^3. These results are matched with the CSORs of SAGD and Fast-SAGD; 5.99 for SAGD and 8.76 for Fast-SAGD experiments.

The SAGD experiment gave a better energy efficiency than Fast-SAGD by 46% in CSOR and by 44 % in energy per unit produced oil. Therefore, the overall energy balance calculation including steam quality estimation seems to be reasonable.

250
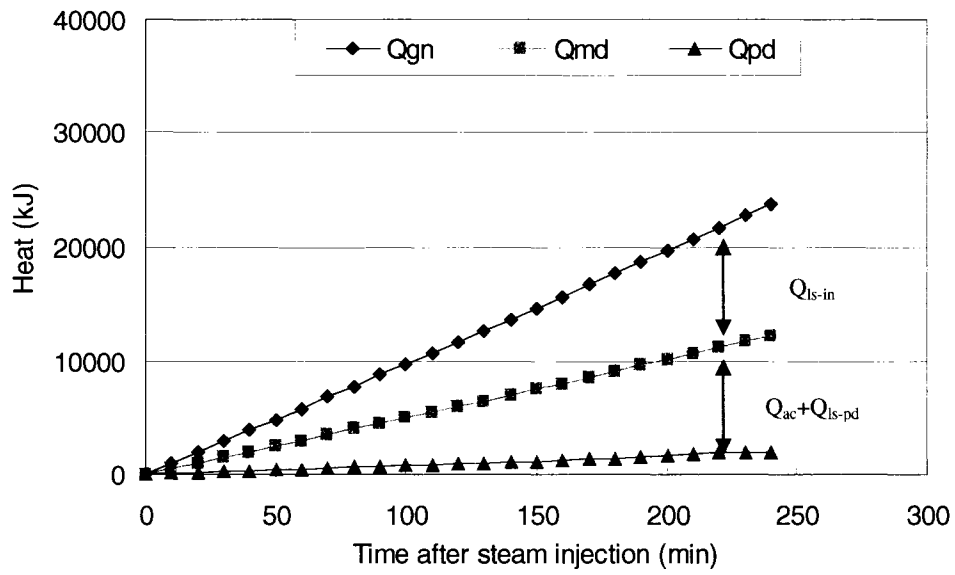
Figure 6.56: Heat distribution trends for the SAGD experiment
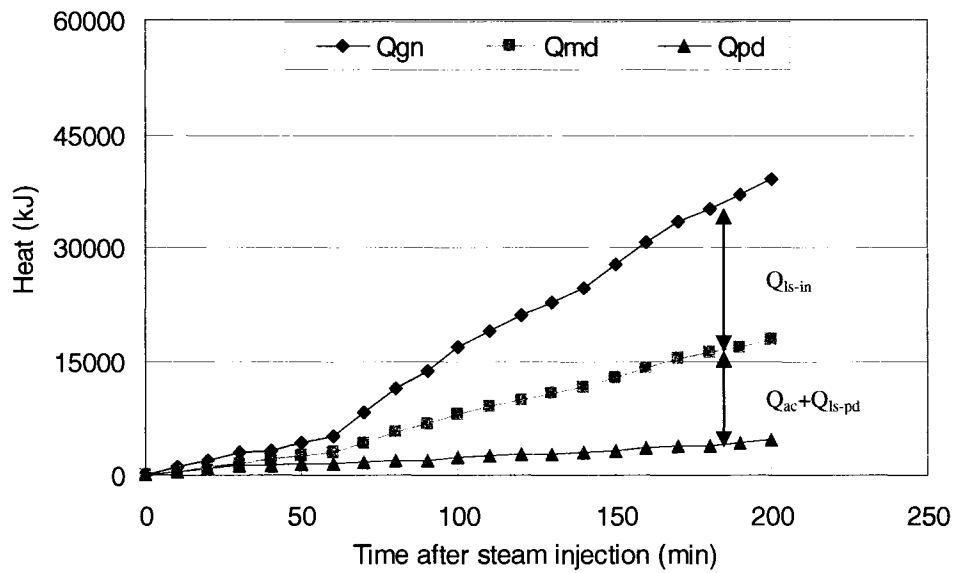
Figure 6.57: Heat distribution trends for the Fast-SAGD experiment

251

7 CONCLUSIONS AND RECOMMENDATIONS

7.1 Conclusions

The SAGD process has been tested in the field, and is now in a commercial stage in Western Canadian oil sands areas. Recent research studies that not only reduce the steam production costs but also enhance heat efficiency of the SAGD process have been conducted.

The Fast-SAGD method can partly solve the drilling difficulty and reduce cost in a SAGD operation requiring paired parallel wells one above the other, and also enhances the thermal efficiency in the reservoir (Polikar et al., 2000). Simulation results have shown that the Fast-SAGD process can achieve lower cumulative steam oil ratio (CSOR) due to higher thermal efficiency (less heat loss), and higher calendar day oil rate (CDOR), which means higher productivity. In other words, the Fast-SAGD process can produce the same amount of bitumen with less steam in a shorter time compared to the conventional SAGD process.

In this research, the reservoir conditions and most suitable operating conditions for the SAGD and the Fast-SAGD processes are investigated by numerical simulation in the three oil sands areas. In addition, preliminary scaled physical model experiments, which are operated by an automated process control system, are conducted under the high temperature and high pressure conditions. The following conclusions are derived from this study:

1) shallow Athabasca-type reservoirs show that a net pay thickness of 15 m is still economic for the SAGD process because of the high permeability of this type of reservoir.

2) for Cold Lake-type reservoirs, a net pay thickness of at least 20 m is required for an economic SAGD implementation.

252

3) in Peace River-type reservoirs, net pay thicker than 30 m is recommended for a successful SAGD performance due to the low permeability of this type of reservoir.

4) the shallow Athabasca-type reservoir, which is thick with high permeability (high k x h), is a good candidate for SAGD application, whereas Cold Lake- and Peace River-type reservoirs, which are thin with low permeability, are not as good candidates for conventional SAGD implementation.

5) the Fast-SAGD process showed better performance than SAGD for reservoirs having low permeability (1 Darcy or less) and thin pay (25 m or less). Therefore, both Cold Lake- and Peace River-type reservoirs are good candidates for a Fast-SAGD application.

6) a new economic indicator, STEP, was developed as a useful economic indicator qualitatively as well as quantitatively for the evaluation of SAGD and Fast-SAGD performance. The highest values of NPV and STEP indicated the best SAGD operating conditions for each simulated case and a linear relationship was found to exist between STEP and NPV with a high correlation coefficient value.

7) a high temperature and high pressure experimental facility for steam injection processes was developed and commissioned. Its several features were validated by using an automated process control system. These are: steam quality measurement, production cooling system, oil-cut determination, and production pressure control system.

8) the preliminary experimental results showed the overall cumulative oil production to be larger in the Fast-SAGD case, but end-point CSOR lower in the SAGD case. If SAGD and Fast-SAGD would have the same CSOR value, Fast-SAGD would give higher cumulative oil production by 6 %.

253

9) the steam chamber collapsed during the Fast-SAGD operation because the heater could not generate the proper amount and quality of steam. The steam chamber was later restored by modifying the experimental procedure.

10) numerical simulation results of the scaled physical model for SAGD showed that steam quality of 0.3 gave the best history match with experimental results in both cumulative oil production and CSOR. For the Fast-SAGD case, history matching results implied that steam quality of 0.3 should be changed to 0.15 after starting the CSS. This result showed a good match with the fact that the steam chamber was lost during the Fast-SAGD experiment.

11) if the same quality of steam were injected into the Fast-SAGD model as in the SAGD case, the experimental results of the Fast-SAGD case would be improved, cumulative production by 70 % and the CSOR by 52%.

7.2 Recommendations

This study focuses on a sensitivity study of the SAGD and Fast-SAGD processes through numerical simulations and scaled model experiments of SAGD and Fast-SAGD with an automated process control system. Based on this preliminary work, more in-depth investigations are proposed as follows:

7.2.1 Numerical Simulation Aspect

1) investigation of the Fast-SAGD process under the conditions of reservoir heterogeneity: shale barrier, bottom water, and top gas.

2) multi-offset wells operating strategies in the Fast-SAGD process gave a good result. This result requires more investigation about various multi-offset well strategies including non-condensable gas injection strategy as a gas blanket to reduce heat loss, carbon dioxide injection as a gas blanket as well as for sequestration purposes.

254

3) three-dimensional investigation will provide a better understanding of the Fast-SAGD process.

7.2.2 Experimental Aspect

1) Measuring the steam temperatures inside the injection tubing, instead of surface temperature, for the more accurate and better control in automated process control system.

2) having a thermocouple inside the injection well for providing an exact steam temperature in the model.

3) for multi-injection scenarios, separate steam generator and steam injection lines are essential.

4) a water-oil separator after the production line is recommended to improve operation of the experiment.

5) conducting more experiments to define the most favourable conditions for the Fast-SAGD process: I/P spacing, offset well spacing, and multi-offset wells operation.

255

REFERENCES

AEUB, Alberta's Reserves 2003 and Supply/Demand Outlook 2004-2013, Statistical Series 2004-98, 2004

Batycky, J., An Assessment of In Situ Oil Sands Recovery Processes, Journal of Can. Pet. Tech., Vol.36, No.9, pp. 15-19, 1997

Beattie, C.I., Boberg, T.C., and McNab, G.S., Reservoir Simulation of Cyclic Steam Stimulation in the Cold Lake Oil Sands, SPERE, Vol.6, No.2, 1991

Boyle, T.B., Gittins, S.D., and Chakrabarty, C., The Evolution of SAGD Technology at East Senlac, Journal of Can. Pet. Tech., Vol.42, No.1, pp. 58-61, 2003

Butler, R.M., Progress in the In Situ Recovery of Heavy Oils and Bitumen, Journal of Can. Pet. Tech., Vol.41, No.1, pp. 31-40, 2002

Butler, R.M., Some Recent Developments in SAGD, Journal of Can. Pet. Tech., Vol.40, No.1, pp. 18-22, 2001

Butler, R. M., "Thermal Recovery of Oil and Bitumen", published by Prentice-Hall Inc. 1997.

Butler, R.M., A New Approach to the Modelling of Steam-Assisted Gravity Drainage; Journal of Can. Pet. Tech., Vol.24, No.3, pp. 42-51, 1985

Butler, R.M., Jiang, Q., and Yee, C.T., The Steam and Gas Push (SAGP) – 4: Recent Theoretical Developments and Laboratory Results Using Layered Models, Journal of Can. Pet. Tech., Vol.40, No.1, pp. 54-61, 2001

Butler, R.M., Jiang, Q., and Yee, C.T., The Steam and Gas Push (SAGP) – 2: Mechanism Analysis and Physical Model Testing, Journal of Can. Pet. Tech., Vol.39, No.4, pp. 52-61, 2000

Butler, R.M. and Stephens, D.J., The Gravity Drainage of Steam- Heated Heavy Oil to Parallel Horizontal Wells, Journal of Can. Pet. Tech., Vol.20, No.2, pp. 90-95, 1981a

Butler, R.M., McNab, G.S., and Lo, H.Y., Theoretical Studies on the Gravity Drainage of Heavy Oil During In-Situ Steam Heating, Canadian Journal of Chemical Engineering, Vol.59, No.4, pp. 455-460, 1981b

Chung, K.H. and Butler, R.M., A Theoretical And Experimental Study of Steam-Assisted Gravity Drainage Process, proceedings of the 4TH UNITAR International Conference On Heavy Oil and Tar Sands, Vol.4, pp.191-210, Edmonton, August 7-12, 1989

Chung, K.H. and Butler, R.M., Geometrical effect of Steam injection on the formation of

256

emulsions in the steam-assisted gravity drainage process, Journal of Can. Pet. Tech., Vol.27, No.1, pp. 36-42, 1988

DeltaV$_{TM}$, DeltaV Books Online, Emerson Process Management, 2004

Doan, L.T., Baird, H., Doan, Q.T., and Farouq Ali, S.M., Performance of the SAGD Process in the Presence of a Water Sand - A Preliminary Investigation; paper 99-40, presented at 50th Annual Technical Meeting of the Petroleum Society in Calgary, Canada, 1999

Donnelly, J.K., Hilda Lake a Gravity Drainage Success, SPE 54093, presented at the 1999 SPE International Thermal Operations and Heavy Oil Symposium, Bakersfield, California, USA, March 17-19, 1999

Donnelly, J.K., Application of Steam Assisted Gravity Drainage (SAGD) to Cold Lake, paper 97-192, presented at the Joint SPE-Petroleum Society of CIM 6th One-Day Conference on Horizontal Well Technology, Calgary, Canada, November 1997

Edmunds, N.R., and Chhina, H., Economic Optimum Operating Pressure for SAGD Projects in Alberta, Journal of Can. Pet. Tech., Vol.40, No.12, pp. 13-17, 2001

Edmunds, N.R., Investigation of SAGD Steam Trap Control in Two and Three Dimensions, Journal of Can. Pet. Tech., Vol.39, No.1, pp. 30-40, 2000

Edmunds, N.R., and Gittins, S.D., Effective Application of Steam Assisted Gravity Drainage of Bitumen to Long Horizontal Well Pairs, Journal of Can. Pet. Tech., Vol.32, No.6, pp. 49-55, 1993

Edmunds, N.R., Haston, J.A., and Best, D.A., Analysis and Implementation of the SAGD Process at the AOSTRA UTF, proceedings of the 4th UNITAR/UNDP International Conference on Heavy Crude and Tar Sands, Vol.4, pp. 223-238, Edmonton, August 7-12, 1989

Emerson$_{TM}$ Process Management, DeltaV control system, version 7, 2004

Farouq-Ali, S.M. and Redford, D.A., Physical Modeling of In Situ Recovery Methods for Oil Sands, Canada-Venezuela Oil Sands Symposium, Edmonton, Canada, CIM Special Volume No. 17, pp. 319-326, 1977

Gao, Y. et. al.: "Implementing Steam Assisted Gravity Drainage Through Combination of Vertical and Horizontal Wells in a Super-heavy Crude Reservoir With Top-Water," paper SPE 77798, presented at the SPE Asia Pacific Oil and Gas Conference and Exhibition, Melbourne, Australia, 8-10 October 2002.

Glandt, C.A. and Malcolm, J.D., Numerical Simulation of Peace River Recovery Process, SPE 22645, presented at the 66th Annual Technical Conference and Exhibition of the SPE, Dallas, Texas, USA, October 6-9, 1991

Gong, J., Polikar, M., and Chalaturnyk, R.J., Fast-SAGD and Geomechanical Mechanisms, paper 2002-163, presented at the 2002 CIPC Conference, Calgary, Alberta, Canada, June 11-13, 2002

Good, W.K., Rezk, C. and Felty, B.D., Other Criteria Affecting SAGD Performance in the Athabasca McMurray Formation, Alberta Department of Energy, April 1997

Hamm, R.A. and Ong, T.S., Enhanced Steam Assisted Gravity Drainage: A New Horizontal Well Recovery Process for Peace River, Canada, Journal of Can. Pet. Tech., Vol.34, No.4, pp. 33-40, 1995

Ito, Y., and Singhal, A.K., Reinterpretation of Performance of Horizontal Well Pilot No.1 (HWPI) 1980-1989, Journal of Can. Pet. Tech., Vol.38, No.13, pp. 1-9, 1999

Ito, Y., Suzuki, S., and Yamada, H., Effect of Reservoir Parameter on Oil rates and Steam Oil Ratios in SAGD Projects, presented at the 7th UNITAR International Conference on Heavy Crude and Tar Sands, Beijing, China, Oct 27-30, 1998

Ito, Y., and Suzuki, S., Numerical Simulation of the SAGD Process in the Hangingstone Oil Sands Reservoir, paper CIM 96-57, presented at CIM 1996 Annual Technical Conference, Calgary, Alberta, June 1996

Jacobsen, R.,T., Stewart, R.B., and Jahangiri, M., Thermodynamic Properties of Nitrogen from the Freezing Line to 2000 K at Pressure to 1000 MPa, J. Phys. Chem. Ref. Data, Vol.15, No.2, pp. 735-846, 1986

Kimber, K.D., Farouq Ali, S.M., and Puttagunta, V.R., New scaling criteria and their relative merits for steam recovery experiments, Journal of Can. Pet. Tech., Vol.27, No.4, pp. 86-94, 1988

Kisman, K.E., Artificial Lift - A Major Unresolved Issue for SAGD, Journal of Can. Pet. Tech., Vol.42, No.8, pp. 39-45, 2003

Kisman, K.E. and Yeung, K.C., Numerical Study of the SAGD Process in the Burnt Lake Oil Sand Lease; SPE 30276, presented at the International Heavy Oil Symposium, Calgary, Canada, June 19-21, 1995

Kisman, K.E. and Ruitenbeek, H.J., A new performance indicator for thermal recovery based on a practical economic model, paper 86-37-45 presented at the 37th Annual Technical Meeting of the Petroleum Society of CIM held in Calgary, June 8-11, 1986.

Law, D.H., Nasr, T.N., and Good, W.K., Field-Scale Numerical Simulation of SAGD Process With Top-Water Thief Zone, SPE 65522, presented at the 2000 SPE/Petroleum

258

Society of CIM International Conference on Horizontal Well Technology, Calgary, Canada, November 2000.

McCormack, M., Fitzgibbon, J., and Horbachewski, N., Review of Single Well SAGD Field Operating Experience, presented at Canadian Section/SPE Petroleum Society 6th International One Day Conference on Horizontal Well Technology, Calgary, Alberta, Canada, November 1997

Mossop, G.D., Kramers, J.W., Flach, P.D., and Rottenfusser, B.A, Geology of Alberta's Oil Sands and Heavy Oil Deposits, 1st UNITAR Conference on the Future of Heavy Crude Oils and Tar Sands, 1981

Mossop,G.D., Geology of Athabasca Oil Sands, Science, Vol.207, No. 4427, pp. 145-152, Jan.11, 1980

Murill, P.W., Fundamentals of process control theory, published by ISA, 1981

Nasr, T.N., Beaulieu, G., Golbeck, H., and Heck, G., Novel Expanding Solvent-SAGD Process "ES-SAGD", Journal of Can. Pet. Tech., Vol.42, No.1, pp. 13-16, 2003

Oballa, V. and Buchanan, W. L., Single Horizontal Well in Thermal Recovery Processes, SPE 37115, presented at the SPE International Conference on Horizontal Well Technology held in Calgary, Canada, November 1996

O'Rourke, J.C., Begley, A.G., Boyle, H.A., Yee, C.T., Chambers, J.I., Luhning, R.W., UTF Project Status Update May 1997, paper 97-08, presented at the Petroleum Society in Calgary, Alberta, Canada, June 8-11, 1997

Plitt, L.R., Personal communication, July 2004

Polikar, M., Cyr, T.J., and Coates, R.M., Fast-SAGD: Half the Wells and 30% Less Steam, SPE 65509, presented at the 2000 SPE/Petroleum Society of CIM International Conference on Horizontal Well Technology, Calgary, Alberta, Canada, November 2000.

Pujol, L., and Boberg, T.C., Scaling accuracy of laboratory steam flooding models, SPE 4191, 43rd Annual California Regional Meeting, Bakersfield, California, 1972

Qi, J.X., Optimal solvent and well geometry for production of heavy oil by cyclic solvent injection, MSc. thesis, University of Alberta, Edmonton, Canada, 2005

Shin, H. and Polikar, M., Review of reservoir parameters to optimize SAGD and Fast-SAGD operating conditions, paper 2004-221, presented at the CIPC Conference 2004, Calgary, Canada, June 2004

Singhal, A.K., Das, S., Goldman, J., and Turta, A.T., A Mechanistic study of Single-Well Steam Assisted Gravity Drainage, presented at the 2000 SPE/DOE Improved Oil Recovery Symposium, Tulsa, Oklahoma, April 3-5, 2000

Singhal, A.K., Das, S.K., Leggitt, S.M. and Kasraie, M., Screening of Reservoirs For Exploitation by Application of SAGD/Vapex Process, SPE 37144, presented at the 1996 International Conference on Horizontal Well Technology, Calgary, Alberta, Canada, 1996

Spirax Sarco, www.spiraxsarco.com, 2005

Stegemeier, G.L., Laumbach, D.D., and Volek, C.W., Representing steam processes with vacuum models, SPE Journal, pp. 151-174, June 1980

Stephan, K., Krauss, R., and Laesecke, A., Viscosity and Thermal Conductivity of Nitrogen for a Wide Range of Fluid States, J. Phys. Chem. Ref. Data, Vol.16, No.4, pp. 993-1023, 1987

Sugianto, S. and Butler, R.M., The Production of Conventional Heavy Oil Reservoirs with Bottom Water Using SAGD, Journal of Can. Pet. Tech., Vol.29, No.2, pp. 78-86, 1990

Takamura, K., Physico-chemical Characterization of Athabasca Oil Sand and its Significance to Bitumen Recovery, AOSTRA Jouranl of Research, Vol.2, No.1, pp. 1-10, 1985

Venuto, P.B., Tailoring EOR Process to Geologic Environments, World Oil, pp. 61-68, November 1989

Wightman, D., Rottenfusser, B., Kramers, J., and Harrison, R., Geology of Alberta Oil Sands Deposits, AOSTRA Technical Handbook on Oil Sands, Bitumens and Heavy Oils, 1989

Zhao, L., Law, D.H., and Coates, R., Numerical Study and Economic Evaluation of SAGD Wind-Down Methods, Journal of Can. Pet. Tech., Vol.42, No.1, pp. 53-57, 2003

APPENDIX A: Relative Permeability Curves
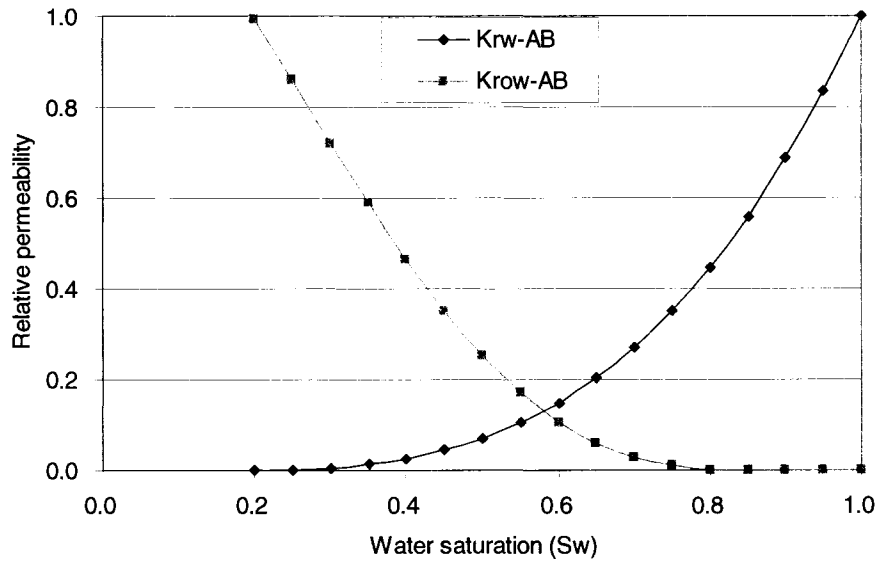
Figure A.1: Water-oil relative permeability curves of Athabasca-type oil (Law et al., 2000)
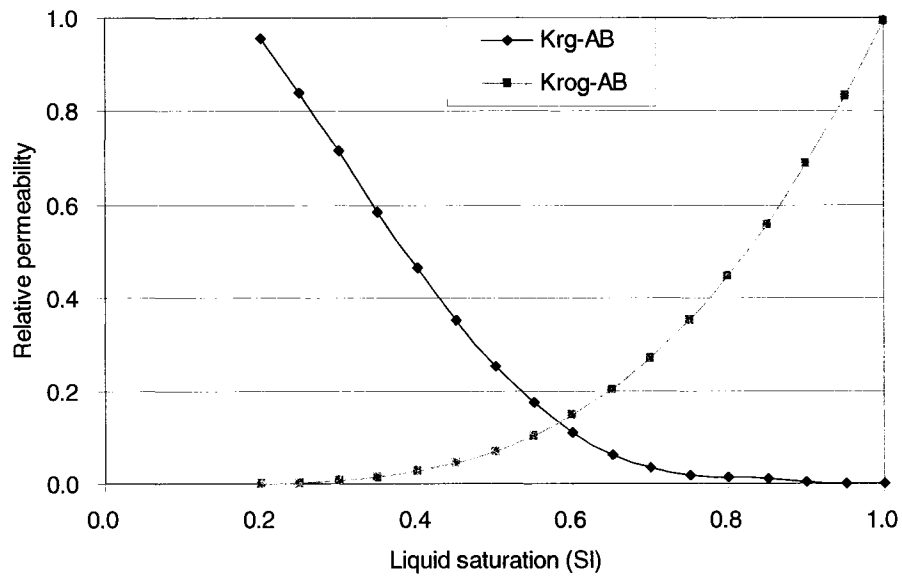
Figure A.2: Liquid-gas relative permeability curves of Athabasca-type oil (Law et al., 2000)

261
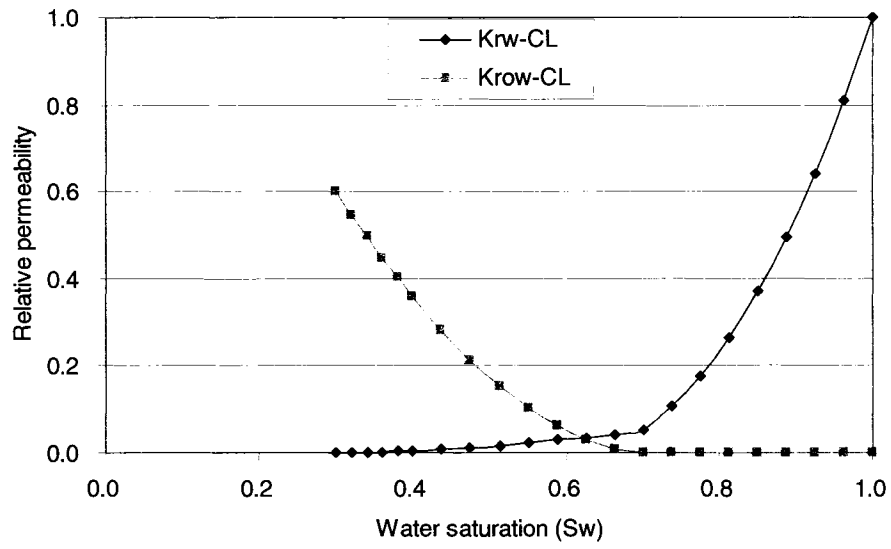
Figure A.3: Water-oil relative permeability curves of Cold Lake-type oil (Gong et al., 2002)
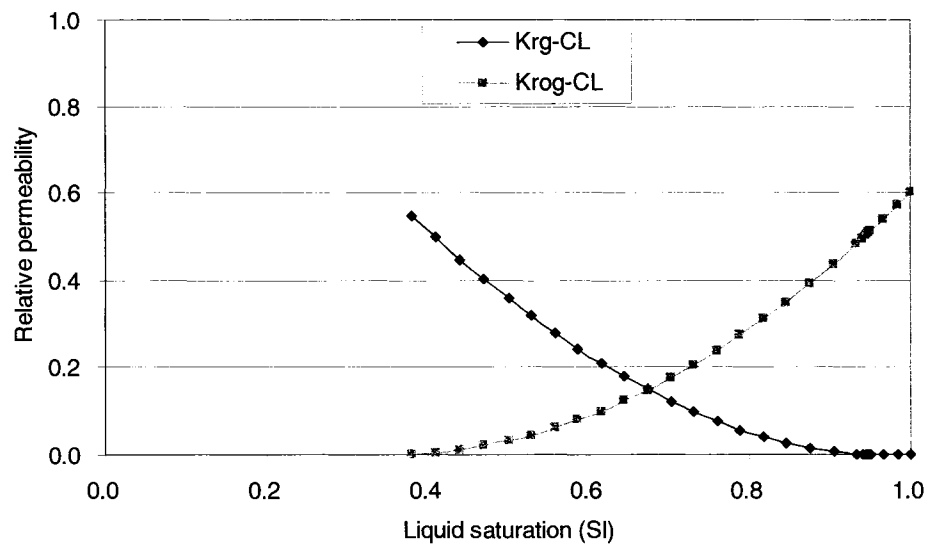
Figure A.4: Liquid-gas relative permeability curves of Cold Lake-type oil (Gong et al., 2002)

262
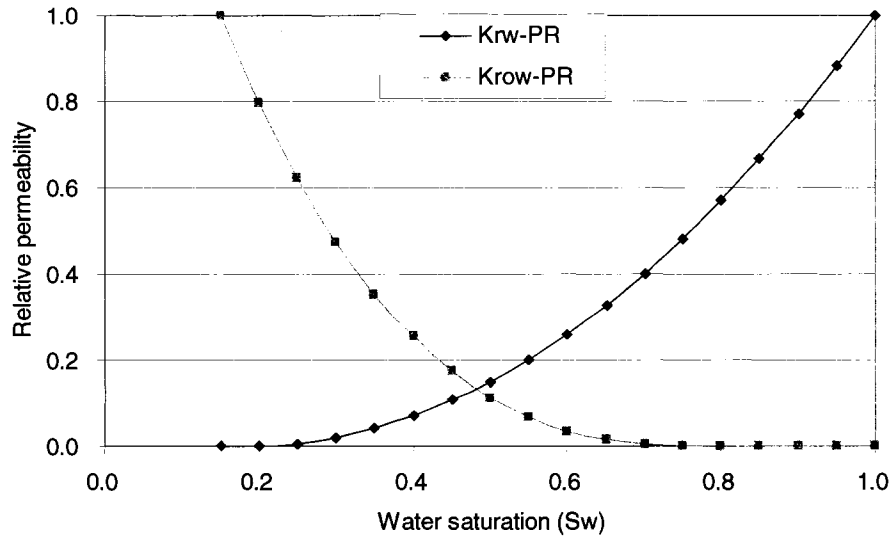
Figure A.5: Water-oil relative permeability curves of Peace River-type oil (generated using the data from Glandt and Malcolm,1991)
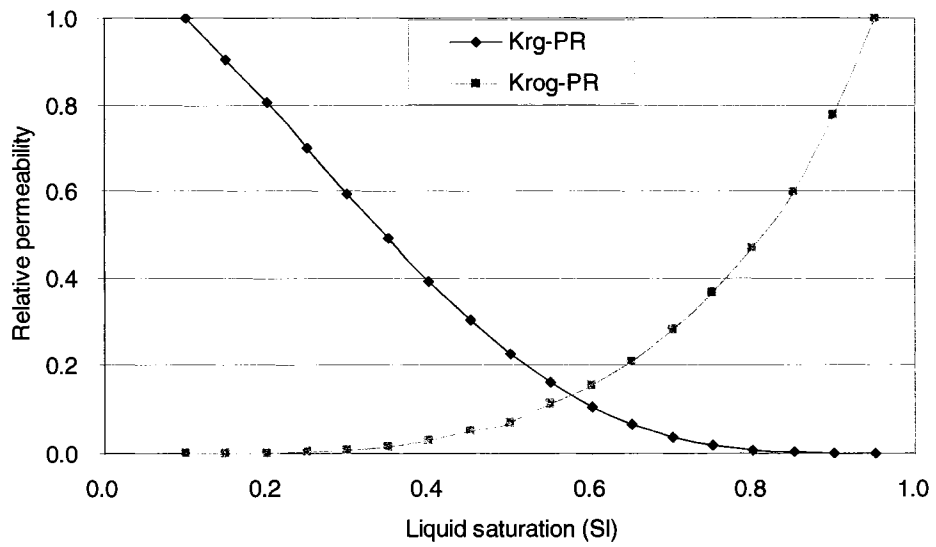
Figure A.6: Liquid-gas relative permeability curves of Peace River-type oil (generated using the data from Glandt and Malcolm, 1991)

263
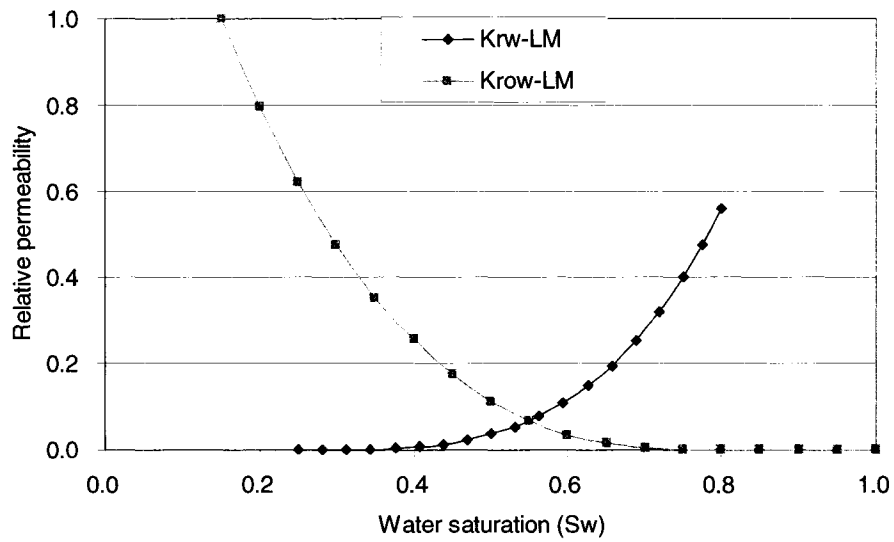
Figure A.7: Water-oil relative permeability curves of Lloydminster-type oil (Qi, 2005)
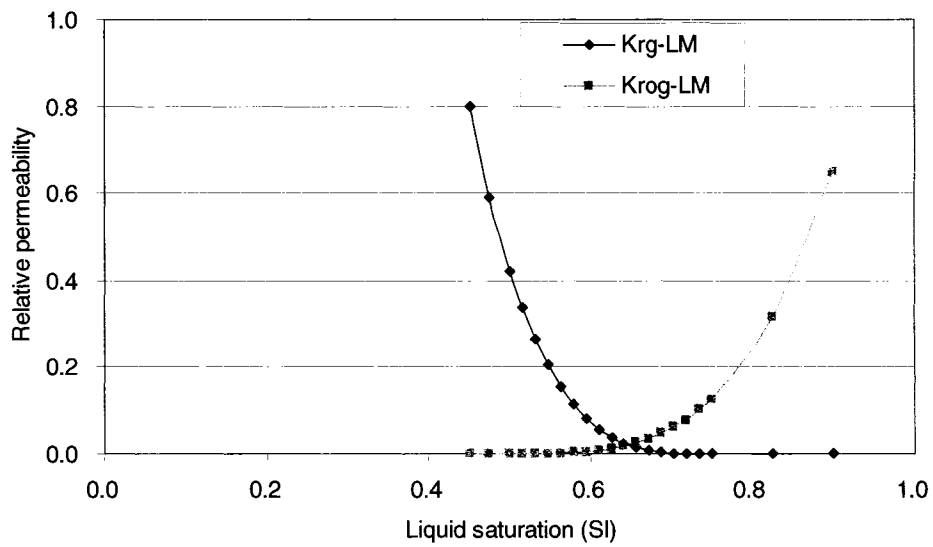
Figure A.8: Liquid-gas relative permeability curves of Lloydminster-type oil (Qi, 2005)

264

APPENDIX B: STARS data files for numerical simulations

B.1 Data file for SAGD field scale simulation

```
**=========INPUT/OUTPUT CONTROL=====================
TITLE1 'COLD_LAKE'
TITLE2 '2-D SAGD with Horizontal Wells'
TITLE3 'Data file: CL-SAGD-BASE'
CASEID '10-year'
INUNIT *SI EXCEPT 6 1 **$ darcy instead of md
OUTUNIT *SI EXCEPT 6 1 **$ darcy instead of md
WRST *TIME    **RESTART OPTION FOR FUTURE
OUTPRN *GRID *NONE
OUTPRN *ITER *BRIEF
OUTSRF *WELL *DOWNHOLE *LAYER *ALL
OUTSRF *GRID *PRES *SW *SO *SG *TEMP *X *Y *VPOROS
PRNTORIEN 2 0


**=========RESERVOIR DESCRIPTIONS=============
GRID CART 101 1 15
KDIR UP
DI CON 1.
DJ CON 900.
DK CON 1.


** Half well along axis of symmetry (Gridblock size = 0.5 m 0.5 m)
VAMOD 2 0.5 1.0 0.5 0.5 1.0 0.5 0.5  **9p 1.0 1.0 just for ninepoint
VATYPE *CON  1
      *MOD  1 1 1:15 = 2
            101 11:15 = 2
```

265

DTOP 101*402.

NINEPOINT IK

POR CON 0.32

PERMI CON 2.5

PERMJ EQUALSI

PERMK CON 1.25

END-GRID

ROCKTYPE 1

  PRPOR 3100.

  CPOR 9.6E-06

  ROCKCP 2.35E+06

  THCONR 6.6E+05

  THCONW 5.3496E+04

  THCONO 1.15E+04

  THCONG 139.97

  THCONMIX SIMPLE

  HLOSST 18.

  HLOSSTDIFF 0.1

  HLOSSPROP OVERBUR 2.35E+06 1.469E+05

    UNDERBUR 2.35E+06 1.469E+05

**========COMPONENT PROPERTIES===========

MODEL   3 3 3 1

** Standard water properties

COMPNAME 'WATER' 'OIL' 'METHANE'

KV1   0.E+00 0.E+00 3.1914E+04

KV4   0.E+00 0.E+00 -3.3067E+01

KV5   0.E+00 0.E+00 -2.771E+01

CMM   0 0.5 0.01604

PCRIT   0.0E+0 1.360E+3 4.600E+3

TCRIT   0.0E+0 6.2465E+2 -8.255E+1

266

CPG1   0.0E+0 8.41E+2 3.52E+1

CPL1   0.0E+0 1.060E+3 6.72E+1

HVAPR   0 1346 1770

SURFLASH W O G

PRSR   101.325

TEMR   20

PSURF   1.01325E+2

TSURF   2.0E+1

MOLDEN   0.0E+0 1.848E+3 1.87509E+4

CP   0.0E+0 5.5E-7 5.5E-7

CT1   0.0E+0 8.0E-4 8.0E-4

CT2   0.0E+0 0.0E+0 0.0E+0

VISCTABLE

**Temp(C)   Water   Oil   CH4   **Live oil

** --

Temp(C)	Water	Oil	CH4
12	0	60590	450
20	0	21540	211.3
30	0	7000	46.08
40	0	2261	30
50	0	1153	13.76
60	0	558	8.16
70	0	296.4	4.8
80	0	170.3	4
100	0	68.14	3.4
120	0	33.25	2.9
140	0	18.83	2.5
160	0	11.94	2.15
180	0	8.256	1.85
200	0	6.106	1.45
220	0	4.761	1.16
240	0	3.815	0.95
260	0	3.257	0.79
280	0	2.815	0.68
300	0	2.488	0.548

** =============== ROCK-FLUID PROPERTIES ===============

ROCKFLUID

RPT 1

SWT

** Sw	Krw	Krow	Pcow
0.300000	0.0000000	0.6000000	6.6102490
0.320000	0.0002276	0.5470836	5.8107371
0.340000	0.0007924	0.4963496	5.1559744
0.360000	0.0016441	0.4478219	4.6196809
0.380000	0.0027595	0.4015256	4.1803331
0.400000	0.0041235	0.3574881	3.8202991
0.437500	0.0073149	0.2811098	3.3106978
0.475000	0.0112909	0.2129961	2.9585462
0.512500	0.0160143	0.1534072	2.7137392
0.550000	0.0214563	0.1026615	2.5414460
0.587500	0.0275937	0.0611671	2.4171529
0.625000	0.0344074	0.0294817	2.3231745
0.662500	0.0418810	0.0084664	2.2461400
0.700000	0.0500000	0.0000000	2.1750901
0.737500	0.1050487	0.0000000	2.0999134
0.775000	0.1754919	0.0000000	2.0099154
0.812500	0.2627652	0.0000000	1.8922905
0.850000	0.3682758	0.0000000	1.7303030
0.887500	0.4934058	0.0000000	1.5009053
0.925000	0.6395141	0.0000000	1.1714581
0.962500	0.8079394	0.0000000	0.6950878
1.000000	1.0000000	0.0000000	0.0000000

*SLT

** Sl	Krg	Krog	Pcgo
0.3800000	0.5470837	0.0012781	7.2870235
0.4100000	0.4963497	0.0051124	6.1564059
0.4400000	0.4478219	0.0115030	5.3175530
0.4700000	0.4015256	0.0204497	4.6943998
0.5000000	0.3574880	0.0319527	4.2304420
0.5288554	0.3172891	0.0454285	3.8950956
0.5577109	0.2792353	0.0612693	3.6399288
0.5865663	0.2433573	0.0794750	3.4435489
0.6154218	0.2096886	0.1000455	3.2894900
0.6442772	0.1782663	0.1229809	3.1648359
0.6731327	0.1491311	0.1482812	3.0591342
0.7019881	0.1223291	0.1759464	2.9635236

268

```
0.7308435  0.0979122  0.2059765  2.8699872
0.7596990  0.0759404  0.2383715  2.7706833
0.7885544  0.0564841  0.2731314  2.6572852
0.8174099  0.0396277  0.3102561  2.5202856
0.8462653  0.0254766  0.3497457  2.3481982
0.8751208  0.0141687  0.3916002  2.1265948
0.9039762  0.0058999  0.4358196  1.8368946
0.9328316  0.0010000  0.4824039  1.4548093
0.9400771  0.0003728  0.4944725  1.3407885
0.9442649  0.0001389  0.5015159  1.2710992
0.9466853  0.0000518  0.5056095  1.2294959
0.9480842  0.0000193  0.5079830  1.2049950
0.9488927  0.0000072  0.5093574  1.1906799
0.9493600  0.0000027  0.5101526  1.1823543
0.9500000  0.0000000  0.5112426  1.1708897
0.9666666  0.0000000  0.5400394  0.8453855
0.9833333  0.0000000  0.5696252  0.4615968
1.0000000  0.0000000  0.6000000  0.0000000
```

**$ RESULTS PROP KRTYPE Units: Dimensionless

KRTYPE CON 1.

RESULTS SECTION INIT

**=============== INITIAL CONDITIONS ===============

INITIAL

VERTICAL *ON

INITREGION 1

REFDEPTH 417

REFPRES 3100

SW CON 0.3

SO CON 0.7

PRES CON 3100

TEMP CON 18

SG CON 0

MFRAC_OIL 'OIL' CON 0.89

MFRAC_OIL 'METHANE' CON 0.11

**=========== NUMERICAL CONTROL ===============

NUMERICAL

CONVERGE *TOTRES *TIGHTER

**==========WELL AND RECURRENT DATA============

RUN

TIME 0

DTWELL 0.0001

UHTR IJK

      1:1   1:1 6:6   1950000000

      1:1   1:1 1:1   1950000000

  101:101 1:1 6:6   1950000000

  101:101 1:1 1:1   1950000000

TMPSET IJK

      1:1   1:1 6:6   265

      1:1   1:1 1:1   265

  101:101 1:1 6:6 265

  101:101 1:1 1:1 265

WELL 1 'Injector1' FRAC 0.5

INJECTOR MOBWEIGHT 'Injector1'

TINJW 235.

QUAL 0.95

INCOMP WATER 1.0 0.0 0.0

OPERATE MAX BHP 3110 CONT REPEAT

OPERATE MAX STW 500 CONT REPEAT

270

GEOMETRY J 0.11 0.249 1. 0.

PERF GEO 'Injector1'

    1 1 6 1

WELL 2 'Producer1' FRAC 0.5

PRODUCER 'Producer1'

OPERATE MIN BHP 3100 CONT REPEAT

OPERATE MIN STEAMTRAP 5 CONT REPEAT

GEOMETRY J 0.11 0.249 1. 0.

PERF GEO 'Producer1'

    1 1 1 1

WELL 3 'Injector2' FRAC 0.5

INJECTOR MOBWEIGHT 'Injector2'

TINJW 235

QUAL 0.95

INCOMP WATER 1.0 0 0

OPERATE MAX BHP 3110 CONT REPEAT

OPERATE MAX STW 500 CONT REPEAT

GEOMETRY J 0.11 0.249 1 0

PERF GEO 'Injector2'

    101 1 6 1

WELL 4 'Producer2' FRAC 0.5

PRODUCER 'Producer2'

OPERATE MIN BHP 3100 CONT REPEAT

OPERATE MIN STEAMTRAP 5 CONT REPEAT

GEOMETRY J 0.11 0.249 1. 0.

PERF GEO 'Producer2'

    101 1 1 1

271

TIME 50

DTWELL 0.001

UHTR CON 0

TIME 91.5

TIME 121.5

TIME 151.75

TIME 182.5

TIME 212.75

TIME 243

TIME 273.75

TIME 365

TIME 548

TIME 730

TIME 913

TIME 1095

TIME 1278

TIME 1460

TIME 1643

TIME 1825

TIME 2008

TIME 2190

TIME 2373

TIME 2555

TIME 2738

TIME 2920

TIME 3103

TIME 3285

TIME 3468

TIME 3650

STOP

272

B.2 Data file for Fast-SAGD field scale simulation

```
**=========INPUT/OUTPUT CONTROL=======================
TITLE1  'COLD_LAKE'
TITLE2  '2-D Fast-SAGD with Horizontal Wells'
TITLE3  'Data file: CL-F-SAGD-BASE'
CASEID  '10-year'
INUNIT *SI EXCEPT 6 1 **$ darcy instead of md
OUTUNIT *SI EXCEPT 6 1 **$ darcy instead of md
WRST *TIME    **RESTART OPTION FOR FUTURE
OUTPRN *GRID *NONE
OUTPRN *ITER *BRIEF
OUTSRF *WELL *DOWNHOLE *LAYER *ALL
OUTSRF *GRID *PRES *SW *SO *SG *TEMP *X *Y *VPOROS
PRNTORIEN 2 0


**=========RESERVOIR DESCRIPTIONS=============
GRID CART 151 1 20
KDIR UP
DI CON 1.
DJ CON 900.
DK CON 1.


** Half well along axis of symmetry (Gridblock size = 0.5 m 0.5 m)
VAMOD 2 0.5 1.0 0.5 0.5 1.0 0.5 0.5  **9p 1.0 1.0 just for ninepoint
VATYPE *CON  1
     *MOD  1 1 1:20 = 2
          151 1 1:20 = 2
DTOP 151*402.
NINEPOINT IK
```

273

POR CON 0.32

PERMI CON 2.5

PERMJ EQUALSI

PERMK CON 1.25

END-GRID

ROCKTYPE 1

  PRPOR 3100

  CPOR 9.6E-06

  ROCKCP 2.35E+06

  THCONR 6.6E+05

  THCONW 5.3496E+04

  THCONO 1.15E+04

  THCONG 139.97

  THCONMIX SIMPLE

  HLOSST 18

  HLOSSTDIFF 0.1

  HLOSSPROP OVERBUR 2.35E+06 1.469E+05

           UNDERBUR 2.35E+06 1.469E+05

**=========COMPONENT PROPERTIES===========

MODEL   3 3 3 1

**Standard water properties

COMPNAME 'WATER' 'OIL' 'METHANE'

KV1   0.E+00 0.E+00 3.1914E+04

KV4   0.E+00 0.E+00 -3.3067E+01

KV5   0.E+00 0.E+00 -2.771E+01

CMM   0 0.5 0.01604

PCRIT   0.0E+0 1.360E+3 4.600E+3

TCRIT   0.0E+0 6.2465E+2 -8.255E+1

CPG1   0.0E+0 8.41E+2 3.52E+1

CPL1   0.0E+0 1.060E+3 6.72E+1

HVAPR   0 1346 1770

SURFLASH W O G

PRSR   101.325

TEMR   20

PSURF   1.01325E+2

TSURF   2.0E+1

MOLDEN   0.0E+0 1.848E+3 1.87509E+4

CP   0.0E+0 5.5E-7 5.5E-7

CT1   0.0E+0 8.0E-4 8.0E-4

CT2   0.0E+0 0.0E+0 0.0E+0

*VISCTABLE

**Temp(C)	Water	Oil	CH4	**Live oil
12	0	60590	450	
20	0	21540	211.3	
30	0	7000	46.08	
40	0	2261	30	
50	0	1153	13.76	
60	0	558	8.16	
70	0	296.4	4.8	
80	0	170.3	4	
100	0	68.14	3.4	
120	0	33.25	2.9	
140	0	18.83	2.5	
160	0	11.94	2.15	
180	0	8.256	1.85	
200	0	6.106	1.45	
220	0	4.761	1.16	
240	0	3.815	0.95	
260	0	3.257	0.79	
280	0	2.815	0.68	
300	0	2.488	0.548	

275

** =============== ROCK-FLUID PROPERTIES ===============

ROCKFLUID

RPT 1

SWT

** Sw	Krw	Krow	Pcow
0.300000	0.0000000	0.6000000	6.6102490
0.320000	0.0002276	0.5470836	5.8107371
0.340000	0.0007924	0.4963496	5.1559744
0.360000	0.0016441	0.4478219	4.6196809
0.380000	0.0027595	0.4015256	4.1803331
0.400000	0.0041235	0.3574881	3.8202991
0.437500	0.0073149	0.2811098	3.3106978
0.475000	0.0112909	0.2129961	2.9585462
0.512500	0.0160143	0.1534072	2.7137392
0.550000	0.0214563	0.1026615	2.5414460
0.587500	0.0275937	0.0611671	2.4171529
0.625000	0.0344074	0.0294817	2.3231745
0.662500	0.0418810	0.0084664	2.2461400
0.700000	0.0500000	0.0000000	2.1750901
0.737500	0.1050487	0.0000000	2.0999134
0.775000	0.1754919	0.0000000	2.0099154
0.812500	0.2627652	0.0000000	1.8922905
0.850000	0.3682758	0.0000000	1.7303030
0.887500	0.4934058	0.0000000	1.5009053
0.925000	0.6395141	0.0000000	1.1714581
0.962500	0.8079394	0.0000000	0.6950878
1.000000	1.0000000	0.0000000	0.0000000

*SLT

** Sl	Krg	Krog	Pcgo
0.3800000	0.5470837	0.0012781	7.2870235
0.4100000	0.4963497	0.0051124	6.1564059
0.4400000	0.4478219	0.0115030	5.3175530
0.4700000	0.4015256	0.0204497	4.6943998
0.5000000	0.3574880	0.0319527	4.2304420
0.5288554	0.3172891	0.0454285	3.8950956
0.5577109	0.2792353	0.0612693	3.6399288
0.5865663	0.2433573	0.0794750	3.4435489
0.6154218	0.2096886	0.1000455	3.2894900
0.6442772	0.1782663	0.1229809	3.1648359
0.6731327	0.1491311	0.1482812	3.0591342
0.7019881	0.1223291	0.1759464	2.9635236

276

```
0.7308435  0.0979122  0.2059765  2.8699872
0.7596990  0.0759404  0.2383715  2.7706833
0.7885544  0.0564841  0.2731314  2.6572852
0.8174099  0.0396277  0.3102561  2.5202856
0.8462653  0.0254766  0.3497457  2.3481982
0.8751208  0.0141687  0.3916002  2.1265948
0.9039762  0.0058999  0.4358196  1.8368946
0.9328316  0.0010000  0.4824039  1.4548093
0.9400771  0.0003728  0.4944725  1.3407885
0.9442649  0.0001389  0.5015159  1.2710992
0.9466853  0.0000518  0.5056095  1.2294959
0.9480842  0.0000193  0.5079830  1.2049950
0.9488927  0.0000072  0.5093574  1.1906799
0.9493600  0.0000027  0.5101526  1.1823543
0.9500000  0.0000000  0.5112426  1.1708897
0.9666666  0.0000000  0.5400394  0.8453855
0.9833333  0.0000000  0.5696252  0.4615968
1.0000000  0.0000000  0.6000000  0.000000 0
```

**$ RESULTS PROP KRTYPE Units: Dimensionless

KRTYPE CON 1.

**============== INITIAL CONDITIONS ===============

INITIAL

VERTICAL *ON

INITREGION 1

REFDEPTH 422

REFPRES 3100

SW CON 0.3

PRES CON 3100

SO CON 0.7

TEMP CON 18

SG CON 0

MFRAC_OIL 'OIL' CON 0.89

MFRAC_OIL 'METHANE' CON 0.11

277

**=========== Numerical Control ===============

NUMERICAL

**==========WELL AND RECURRENT DATA===========

RUN

TIME 0

DTWELL 0.0001

UHTR IJK

1:1	1:1	11:11	1950000000
1:1	1:1	1:1	1950000000
151:151	1:1	11:11	1950000000
151:151	1:1	1:1	1950000000

TMPSET IJK

1:1	1:1	11:11	265
1:1	1:1	1:1	265
151:151	1:1	11:11	265
151:151	1:1	1:1	265

WELL 1 'Injector1' FRAC 0.5

INJECTOR MOBWEIGHT 'Injector1'

TINJW 235

QUAL 0.95

INCOMP WATER 1.0 0.0 0.0

OPERATE MAX BHP 3110 CONT REPEAT

OPERATE MAX STW 500 CONT REPEAT

GEOMETRY J 0.11 0.249 1. 0.

PERF GEO 'Injector1'

          1 1 11 1.

WELL 2 'Producer1' FRAC 0.5

PRODUCER 'Producer1'

278

OPERATE MIN BHP 3100. CONT REPEAT

OPERATE MIN STEAMTRAP 5. CONT REPEAT

GEOMETRY J 0.11 0.249 1. 0

PERF GEO 'Producer1'

     1 1 1 1

WELL 3 'Injector2' FRAC 0.5

INJECTOR MOBWEIGHT 'Injector2'

TINJW 235.

QUAL 0.95

INCOMP WATER 1.0 0.0 0.0

OPERATE MAX BHP 3110 CONT REPEAT

OPERATE MAX STW 500 CONT REPEAT

GEOMETRY J 0.11 0.249 1. 0

PERF GEO 'Injector2'

     151 1 11 1

WELL 4 'Producer2' FRAC 0.5

PRODUCER 'Producer2'

OPERATE MIN BHP 3100 CONT REPEAT

OPERATE MIN STEAMTRAP 5 CONT REPEAT

GEOMETRY J 0.11 0.249 1. 0

PERF GEO 'Producer2'

     151 1 1 1

WELL 5 'Injector_OFFS1' FRAC 1

INJECTOR MOBWEIGHT 'Injector_OFFS1'

TINJW 295

QUAL 0.95

INCOMP WATER 1.0 0.0 0.0

OPERATE MAX BHP 8000 CONT REPEAT

279

OPERATE MAX STW 800 CONT REPEAT

GEOMETRY J 0.11 0.249 1. 0

PERF GEO   'Injector_OFFS1'

     51 1 1 1

WELL 6 'Producer_OFFS1' FRAC 1

PRODUCER 'Producer_OFFS1'

OPERATE MIN BHP 3100. CONT REPEAT

OPERATE MIN STEAMTRAP 5 CONT REPEAT

GEOMETRY J 0.11 0.249 1. 0.

PERF GEO   'Producer_OFFS1'

     51 1 1 1

WELL 7 'Injector_OFFS2' FRAC 1

INJECTOR MOBWEIGHT 'Injector_OFFS2'

TINJW 295.

QUAL 0.95

INCOMP WATER 1.0 0.0 0.0

OPERATE MAX BHP 8000 CONT REPEAT

OPERATE MAX STW 800 CONT REPEAT

GEOMETRY J 0.11 0.249 1. 0

PERF GEO   'Injector_OFFS2'

     101 1 1 1

WELL 8 'Producer_OFFS2' FRAC 1

PRODUCER 'Producer_OFFS2'

OPERATE MIN BHP 3100. CONT REPEAT

OPERATE MIN STEAMTRAP 5. CONT REPEAT

GEOMETRY J 0.11 0.249 1. 0

PERF GEO   'Producer_OFFS2'

     101 1 1 1

280

```
SHUTIN 5 6 7 8

TIME 180

DTWELL 0.001

UHTR CON 0


TIME 182.5

TIME 212.75

TIME 243

TIME 273.75

TIME 365


TIME 547                    **1st OFFSET WELLS (1st CSS)

OPEN 5 7


TIME 730

TIME 822

SHUTIN 5 7


TIME 836

OPEN 6 8


TIME 912

SHUTIN 6 8

OPEN 5 7


TIME 1095                   **1st Offset WELLS (2nd CSS)

SHUTIN 5 7


INJECTOR MOBWEIGHT 'Injector1'

INCOMP WATER  1.0 0.0 0.0

OPERATE MAX BHP  3110 CONT REPEAT
```

281

OPERATE MAX STW 800 CONT REPEAT

INJECTOR MOBWEIGHT 'Injector2'

INCOMP WATER 1.0 0.0 0.0

OPERATE MAX BHP 3110 CONT REPEAT

OPERATE MAX STW 800 CONT REPEAT

TIME 1109

OPEN 6 8

TIME 1278

TIME 1460

TIME 1643

TIME 1825

TIME 2008

TIME 2190

TIME 2373

TIME 2555

TIME 2738

TIME 2920

TIME 3103

TIME 3285

TIME 3468

TIME 3650

STOP

282

B.3 Data file for SAGD lab scale simulation

**=========INPUT/OUTPUT CONTROL========================

TITLE1 'SCALED-MODEL'

TITLE2 '2-D SAGD Lab'

TITLE3 'Data file: 'SAGD-LAB-BASE'

CASEID '4-hours'

INUNIT *LAB EXCEPT 6 1 **$ darcy instead of md

OUTUNIT *LAB EXCEPT 6 1 **$ darcy instead of md

INTERRUPT *INTERACTIVE

RANGECHECK

WRST *TIME

OUTPRN *GRID *NONE

OUTPRN *ITER *BRIEF

OUTSRF *WELL *DOWNHOLE *LAYER *ALL

OUTSRF *GRID *PRES *SW *SO *SG *TEMP *X *Y *VPOROS

PRNTORIEN 2 0

**=========RESERVOIR DESCRIPTIONS============

GRID CART 131 1 34

KDIR UP

DI CON 0.67

DJ CON 5

DK CON 0.67

DTOP

      131*268

NINEPOINT IK

POR CON 0.33

PERMI CON 170

PERMJ EQUALSI

283

PERMK CON 170

END-GRID

ROCKTYPE 1

  PRPOR 1700.

  CPOR 9.6E-06

  ROCKCP 2.35

  THCONR 4.58333

  THCONW 0.3715

  THCONO 0.0798611

  THCONG 0.000972014

  THCONMIX SIMPLE

  HLOSST 18.

  HLOSSTDIFF 0.1

  HLOSSPROP OVERBUR 2.35 1.020139

             UNDERBUR 2.35 1.020139

MODEL   3 3 3 1

** Standard water properties

COMPNAME 'WATER' 'OIL' 'METHANE'

KV1   0.E+00 0.E+00 3.1914E+04

KV4   0.E+00 0.E+00 -3.3067E+01

KV5   0.E+00 0.E+00 -2.771E+01

CMM   0 0.5 0.01604

PCRIT   0.0E+0 1.360E+3 4.600E+3

TCRIT   0.0E+0 6.2465E+2 -8.255E+1

CPG1   0.0E+0 8.41E+2 3.52E+1

CPL1   0.0E+0 1.060E+3 6.72E+1

HVAPR   0 1346 1770

SURFLASH W O G

PRSR   101.325

TEMR   20

PSURF   1.01325E+2

TSURF   2.0E+1

MOLDEN   0.0E+0 1.848E-3 1.87509E-2

CP   0.0E+0 5.5E-7 5.5E-7

CT1   0.0E+0 8.0E-4 8.0E-4

CT2   0.0E+0 0.0E+0 0.0E+0

VISCTABLE

**Temp(C)	Water	Oil	CH4	**Live oil

12	0	20000	450
20	0	10000	211.3
30	0	3500	46.08
40	0	1200	30
50	0	520	13.76
60	0	350	8.16
70	0	200	4.8
80	0	120	4
100	0	48	3.4
120	0	24	2.9
140	0	15.0	2.5
160	0	10.0	2.15
180	0	7.1	1.85
200	0	5.2	1.45
220	0	4.2	1.16
240	0	3.4	0.95
260	0	3.0	0.79
280	0	2.6	0.68
300	0	2.3	0.548

** =============== ROCK-FLUID PROPERTIES ===============

ROCKFLUID

RPT 1

285

SWT

```
** Sw       Krw        Krow       Pcow
**-----------------------------------------------------
0.200000  0.000000  0.994200  0.000000
0.250000  0.001400  0.858200  0.000000
0.300000  0.005200  0.721000  0.000000
0.350000  0.012900  0.588000  0.000000
0.400000  0.025500  0.463400  0.000000
0.450000  0.044100  0.350900  0.000000
0.500000  0.070000  0.252900  0.000000
0.550000  0.104300  0.171300  0.000000
0.600000  0.148400  0.106700  0.000000
0.650000  0.203500  0.059000  0.000000
0.700000  0.270800  0.027100  0.000000
0.750000  0.351700  0.009100  0.000000
0.800000  0.447300  0.000000  0.000000
0.850000  0.558800  0.000000  0.000000
0.900000  0.687400  0.000000  0.000000
0.950000  0.834100  0.000000  0.000000
1.000000  1.000000  0.000000  0.000000
```

*SLT

```
** Sl       Krg
** -----------------------------------------------
0.200000  0.956700  0.000000  0.000000
0.250000  0.840000  0.001400  0.000000
0.300000  0.714300  0.005500  0.000000
0.350000  0.587200  0.013200  0.000000
0.400000  0.465200  0.025700  0.000000
0.450000  0.353100  0.044100  0.000000
0.500000  0.254900  0.069700  0.000000
0.550000  0.173100  0.103900  0.000000
0.600000  0.109000  0.147900  0.000000
0.650000  0.062600  0.203200  0.000000
0.700000  0.033000  0.270800  0.000000
0.750000  0.017600  0.352100  0.000000
0.800000  0.013000  0.448100  0.000000
0.850000  0.008700  0.559600  0.000000
0.900000  0.004300  0.687300  0.000000
0.950000  0.000000  0.831700  0.000000
1.000000  0.000000  0.994200  0.000000
```

286

KRTYPE CON 1

RESULTS SECTION INIT

**============== INITIAL CONDITIONS ===============

INITIAL

VERTICAL *ON

**$ Data for PVT Region 1

**$ ------------------------------------

INITREGION 1

REFDEPTH 288

REFPRES 1700.

SW CON 0.05

PRES CON 1700

SO CON 0.95

TEMP CON 18.

SG CON 0

MFRAC_OIL 'OIL' CON 0.99

MFRAC_OIL 'METHANE' CON 0.01

**============ NUMERICAL CONTROL ===============

NUMERICAL

RUN

TIME 0

DTWELL 0.001

287

**$ RESULTS PROP UHTR Units: J/min-C
UHTR IJK

      66:66 1:1 12:12 90

      66:66 1:1 4:4 90

TMPSET IJK

      66:66 1:1 12:12 210

      66:66 1:1 4:4 210

WELL 1 'InjectorB1' FRAC 1

INJECTOR MOBWEIGHT 'InjectorB1'

TINJW 210

QUAL 0.30

INCOMP WATER 1.0 0.0 0.0

OPERATE MAX BHP 1710 CONT REPEAT

OPERATE MAX STW 32.0 CONT REPEAT

GEOMETRY J 0.12 0.249 1. 0

PERF GEO 'InjectorB1'

      66 1 12 1

WELL 2 'ProducerB1' FRAC 1

PRODUCER 'ProducerB1'

OPERATE MIN BHP 1700. CONT REPEAT

OPERATE MIN STEAMTRAP 0.5 CONT REPEAT

GEOMETRY J 0.12 0.249 1. 0

PERF GEO 'ProducerB1'

      66 1 4 1.

TIME 3.328

DTWELL 0.001

288

UHTR CON 0

TIME 11.648

TIME 23.36

TIME 46.72

TIME 70.08

TIME 93.44

TIME 116.8

TIME 140.16

TIME 163.52

TIME 186.88

TIME 210.24

TIME 233.6

TIME 256.96

STOP

APPENDIX C: SAGD Experimental Interfaces in the DeltaV control system using DeltaV software (Emerson_{TM}, 2004)
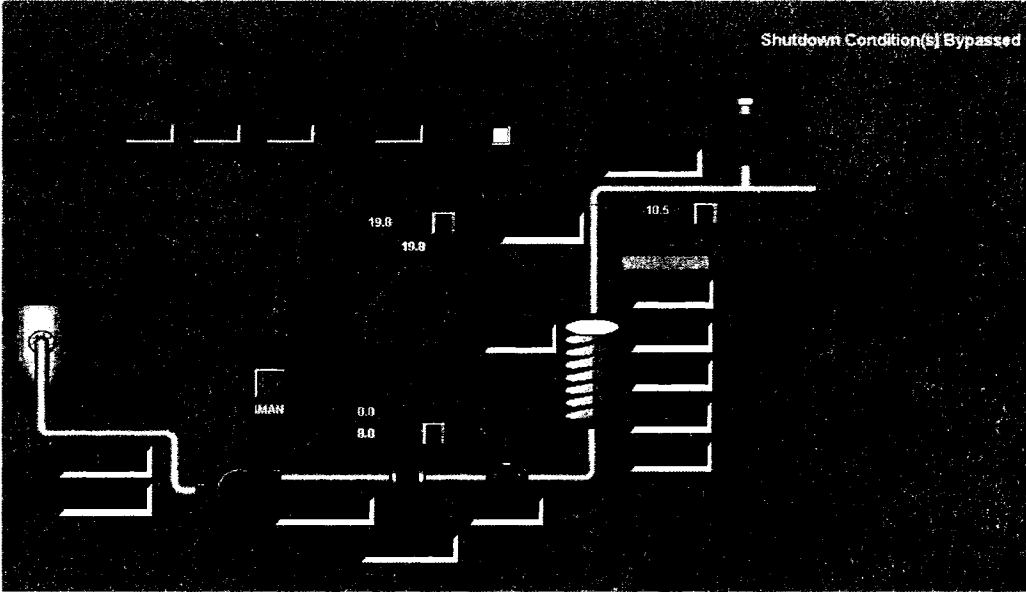
Figure C.1: Steam Generator Interface
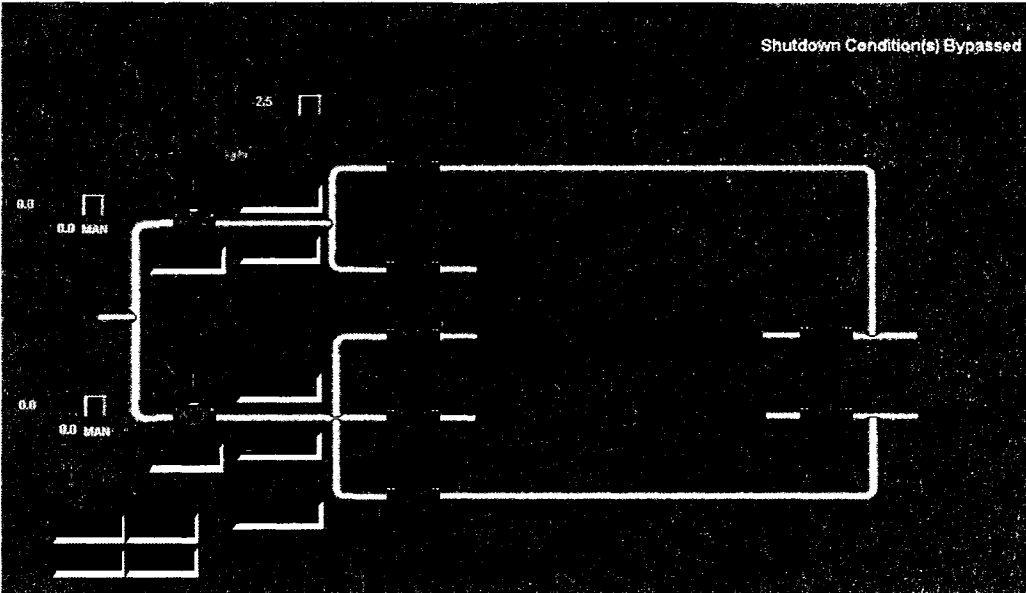
Figure C.2: Steam Distribution Interface
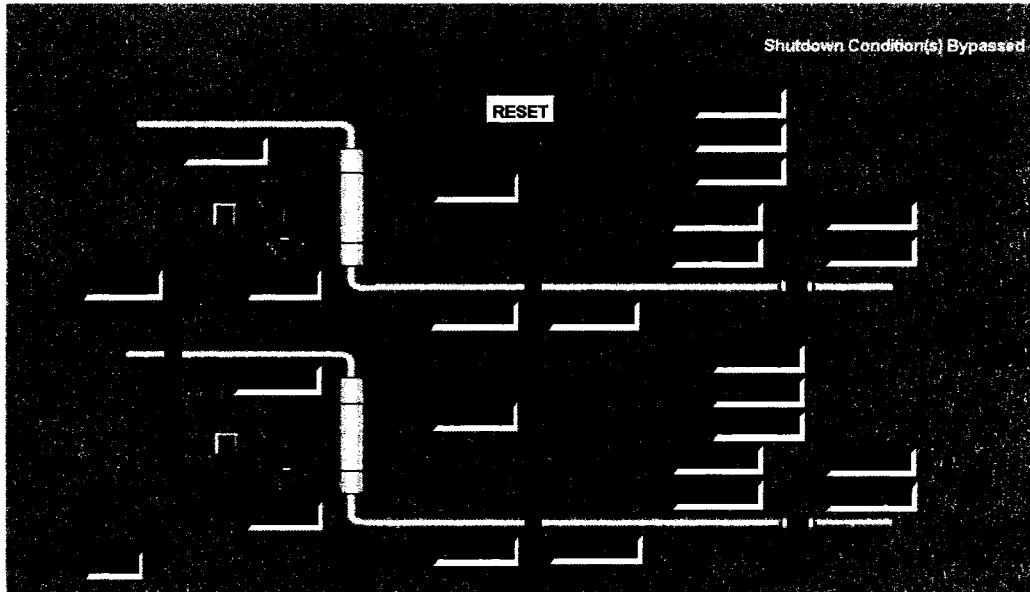
Figure C.3: Production Cooling Interface
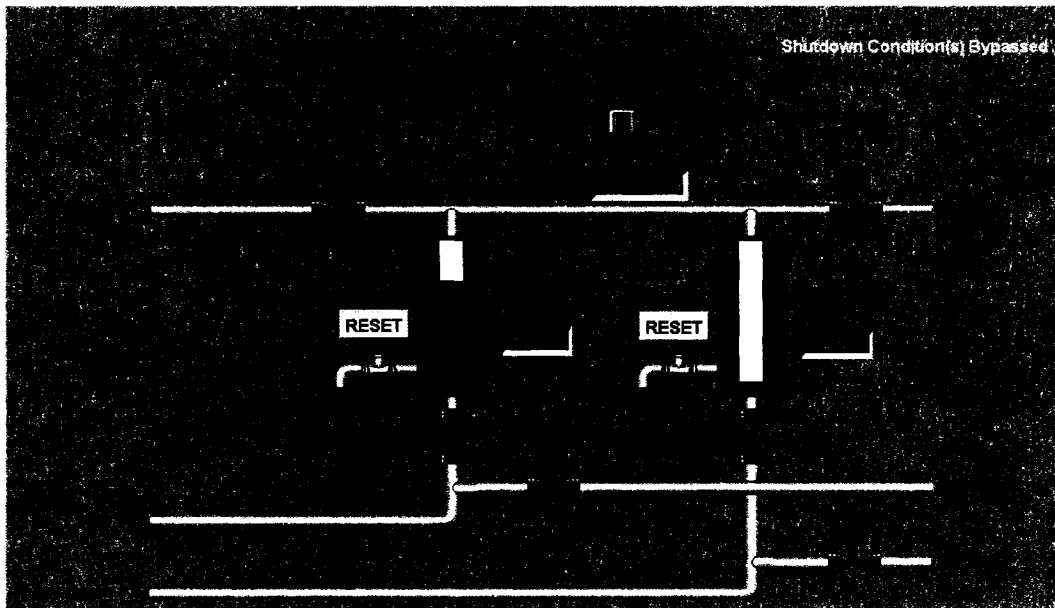
Figure C.4: Production Recovery Interface

291

APPENDIX D: Scaled Model Packing and Saturation

Glass beads of the sizes between 14 to 50 mesh (300 to 1400 µm) were sieved with 20 and 30 mesh screens to get the range of grain size of 600 to 850 µm. A scaled model required about 15 kg of glass beads for packing. Glass beads were washed several times before packing, and poured into the model which was already installed with muti-thermocouples and wells. The scaled model had a hydraulic head hat on the top, and an air vibrator was attached to help proper packing (Figure D.1). As the glass beads size is large, round, and homogeneous, it did not take long for the compaction. After two hours of vibration, glass beads which were on the top of the model were removed (Figure D.2). The model was then sealed with a lid which has two ports on the top. The water was drained from the bottom end port for the porosity calculation. For the oil saturation procedure, heavy oil was heated to 50 °C using a banding heater (Figure D.3). The oil viscosity is expected to be reduced from 10,000 cp to 500 cp at that temperature.
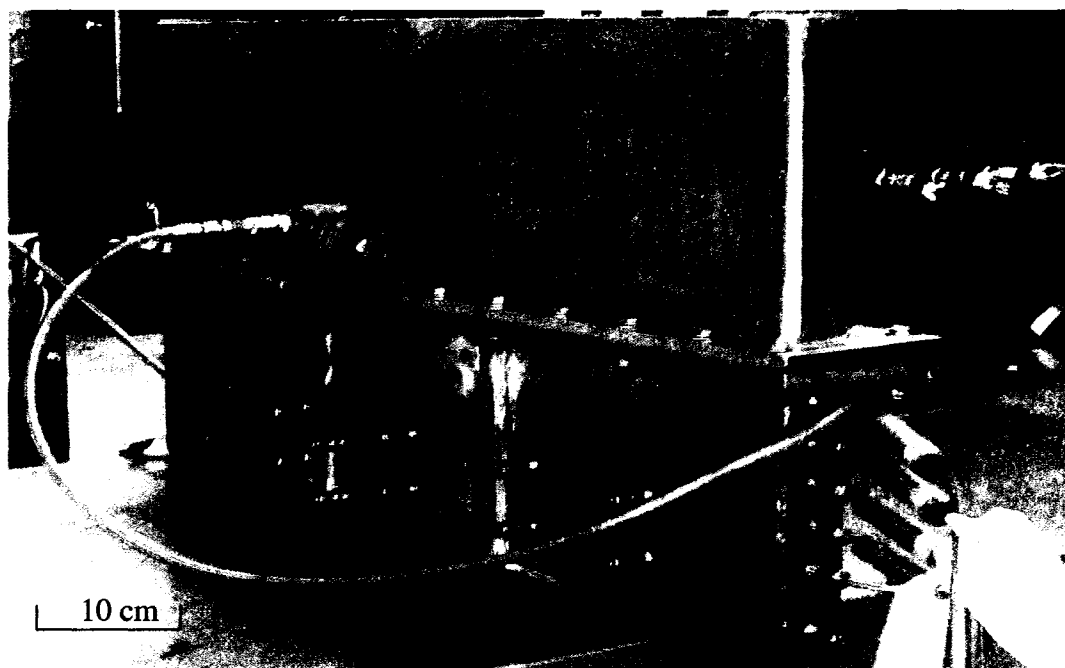
Figure D.1: A scaled model with an air vibrator

292

Figure D.2: Top view of a model before sealing with a lid
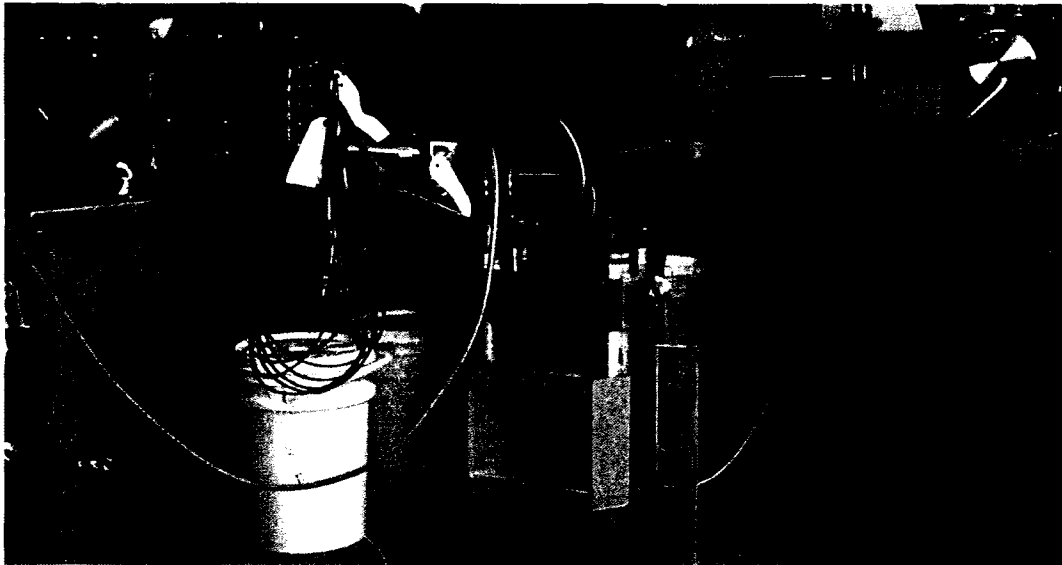
Figure D.3: Apparatus for oil saturation procedure

293

APPENDIX E: Permeability of the scaled model

E.1 Permeability calculation

The permeability of a model packed with glass beads was calculated by using a modified Kozeny-Carman equation (Equation E.2). With the assumption of c = 4.16 , the original Kozeny-Carman equation, Equation E.1, becomes Equation E.2 (Plitt, 2004).

$$D = \sqrt{\frac{36 \times c \times (1-\phi)^2 \times K}{\phi^3}}$$ (Equation E.1)

where, D = average particle diameter (cm)

c = Kozeny constant

ϕ = porosity

K = permeability (cm^2)

$$K = \frac{1013250 \times \phi^3 \times D^2}{10000^2 \left[1.5 \times (1-\phi)^2\right]}$$ (Equation E.2)

where, D = average particle diameter (μm)

ϕ = porosity

K = permeability (cm^2)

In this experiment, the glass beads used for packing the model are between 20 and 30 mesh sizes, which is in the range of between 600 to 850 μm. This size of glass beads gives a permeability of 135 - 390 Darcy depending on the model porosity (Figure E.1). If the model porosity is 0.33 and the average grain size is 710 μm, the model will have a permeability of about 273 Darcy.

294
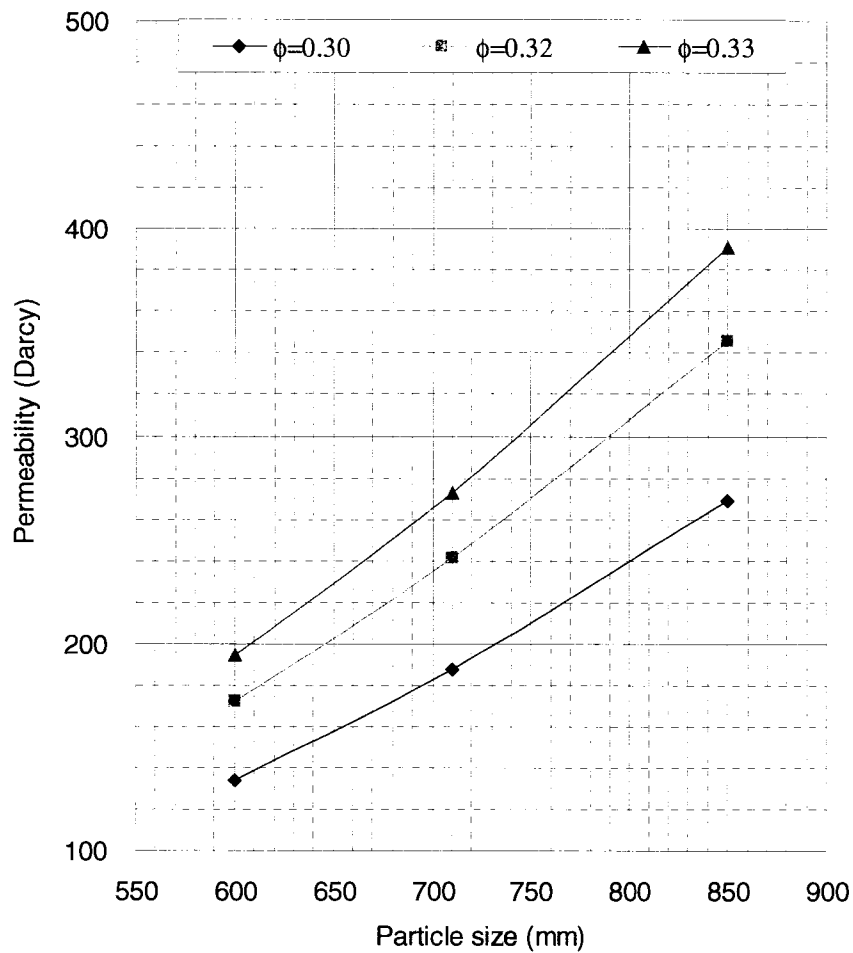
Figure E.1: Particle size and permeability relationship from Equation E.2

E.2 Permeability measurement

The permeability of a scaled model was estimated by measurement from a cylindrical model packed with the same glass beads size which was used for a scaled model. A cylindrical model, having a diameter of 3.1 cm and a length of 16 cm, was saturated with water. For the measurement of pressure drop, the water flow rate was kept at a constant value. An absolute permeability can be calculated from the Darcy equation (Equation E.3). The permeability calculation performed for four different water flow rates gives around 170 Darcy (Figure E.2). At the range of low water flow rates (less than 30 kg/hr),

295

the pressure drop was quite small, which may result in error. Therefore, the higher flow rate cases were used as they will give more accurate value.

$$K(darcy) = 28.14583 \frac{q(kg/hr) \times \mu(cp) \times \Delta L(cm)}{A(cm^2) \times \Delta P(kPa)}$$ (Equation E.3)

where, q = flow rate

μ = fluid viscosity

ΔL= distance between pressure measurement ports

A = cross sectional area

ΔP = pressure drop
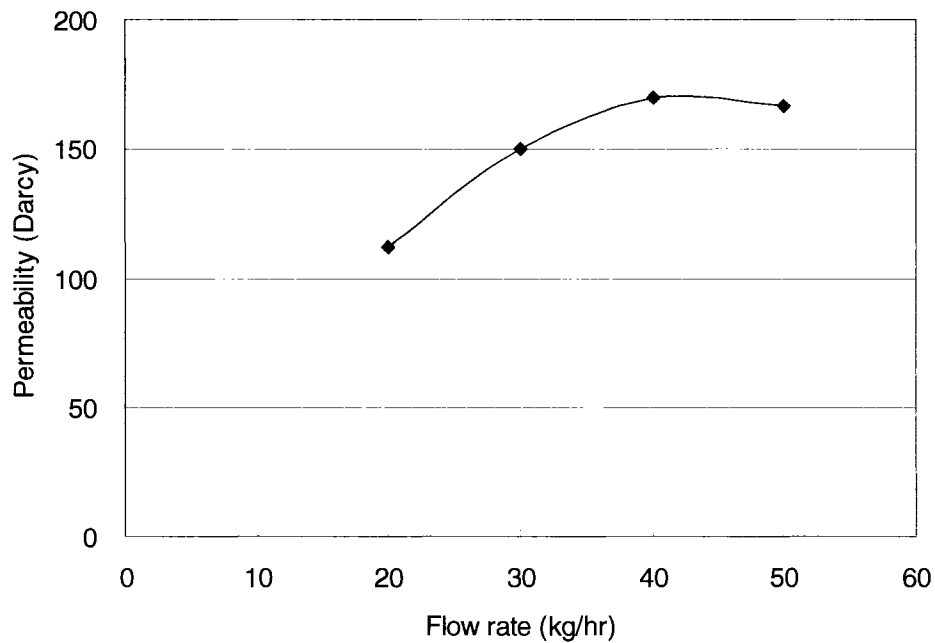
Figure E.2: Permeability measurement for different flow rates

296

APPENDIX F: Heat Balance Calculations

A heat balance is very important to understand the thermal process. The following Equation F.1 gives a basic concept for heat balance calculations. Specific equations for enthalpy, heat capacity, and density are summarized in Butler (1997)

$$Q_{gn} = Q_{ac} + Q_{pd} + Q_{ls} \qquad \text{(Equation F.1)}$$

Where, Q_{gn} = heat generated at the heater (kJ)

Q_{pd} = heat produced (kJ)

Q_{ls} = heat lost (kJ)

Q_{ac} = heat accumulated in the model (kJ)

Q_{gn} is the heat generated at the heater, and is calculated using the specific enthalpy of superheated steam (Spirax Sarco, 2005), with knowledge of steam flow rate, steam temperature, and steam pressure at the heater.

Q_{md} is the heat injected into the model, and is calculated using Equation F.2, with knowledge of steam flow rate, steam temperature, and steam quality estimated from the numerical history matching results.

$$Q_{md} = q_s \{ H_L + f_s (H_v - H_L) \} t \qquad \text{(Equation F.2)}$$
$$H_L = -14.54 + 4.5196\ T - 0.002771\ T^2 + 0.00000922\ T^3$$
$$H_v = 2523.43 + 1.3556\ T + 0.003561\ T^2 - 0.00001824\ T^3$$

Where, q_s = steam injection rate (kg/hr)

H_L = enthalpy of water (kJ/kg)

H_v = enthalpy of vapor (kJ/kg)

f_s = steam quality (ratio)

t = injection time (hr)

Q_{pd} is the heat produced from the model through production lines, and calculated with Equation F.3 using the production rates of water and oil.

$$Q_{pd} = (V_o \times C_o \times \rho_o + V_w \times C_w \times \rho_w)(T_{pd}-T_m)$$

(Equation F.3)

$$C_o = 1.605 + 0.04361\,T - 4.046 \times 10^{-4}\,T^2$$

$$C_w = 4.182 - 1.5 \times 10^{-4}\,T + 3.44 \times 10^{-7}\,T^2 + 4.26 \times 10^{-8}\,T^3$$

$$\rho_o = \rho_{15}\{1 - 0.06285\,[(T-15)/100] + 0.001426\,[(T-15)/100]^2\}$$

$$\rho_w = 1001.7 - 0.1616\,T - 0.00262\,T^2$$

Where, V_o = produced volume of oil (m^3)

V_w = produced volume of water (m^3)

C_o = heat capacity of oil (kJ/kg ^{o}C)

C_w = heat capacity of water (kJ/kg ^{o}C)

ρ_o = density of oil at temperature T (kg/m^3)

ρ_w = density of water at temperature T (kg/m^3)

T_{pd} = temperature of production fluids (^{o}C)

T_m = initial model temperature (20 ^{o}C)

Q_{ac}, the heat accumulated in the model, is calculated with Equation F.4 using the volume of oil, water, and glass beads (Table F.1)

$$Q_{ac} = V_{cn}\{\phi \times S_o \times C_o \times \rho_o + \phi \times S_w \times C_w \times \rho_w + (1-\phi) \times C_{gl} \times \rho_{gl}\} \times (T_{cn}-T_m)$$

(Equation F.4)

Where, V_{cn} = volume in contour at temperature T_{cn} (m^3)

ϕ = porosity

S_o = oil saturation in contour at temperature T_{cn}

S_w = water saturation in contour at temperature T_{cn}

C_{gl} = heat capacity of glass bead (0.8 kJ/kg ^{o}C)

298

ρ_{gl} = density of glass bead (2,400 kg/m³)

T_{cn}= temperature in contour (°C)

T_m = initial model temperature (20 °C)

The contour volume, V_{cn}, for each temperature range is calculated using thermocouple data assuming that each thermocouple represents the temperature of the same area inside the model. The oil saturations of each contour inside the model are estimated based on the temperature profile and the cumulative production. The calculated oil production from the oil saturation profile, which is estimated from temperature profile, is compared to the cumulative production from the experiments (Figure F.1).
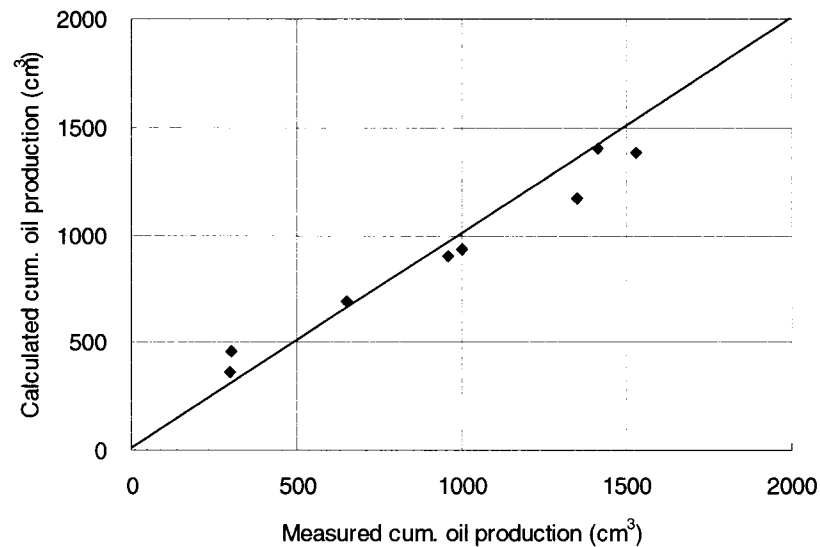
Figure F.1: Comparison of the calculated and measured cumulative oil productions

Q_{ls} is the heat lost through the steam injection (Q_{ls-in}) and production lines (Q_{ls-pd}), the stainless steel model (Q_{ls-ms}), and the annulus between the model and the pressure vessel (Q_{ls-an}) (Equation F.5).

$$Q_{ls} = Q_{ls-in} + Q_{ls-pd} + Q_{ls-ms} + Q_{ls-an} \qquad \text{(Equation F.5)}$$

299

Q_{ls-in} is calculated from the following relationship, $Q_{ls-in} = Q_{gn} - Q_{md}$. The heat injected into the model (Q_{md}) is calculated with Equation F.2 using the steam temperature, which is estimated from the thermocouple data inside the model, and the steam quality, which is estimated from history matching results.

Q_{ls-pd} is calculated from the following relationship, $Q_{ls-pd} = Q_{md} - Q_{ls-ms} - Q_{ls-an} - Q_{pd}$. The heat loss of the model skin, Q_{ls-ms}, is calculated with Equation F.6 using the model skin temperature (T_{skin}). However, as only one thermocouple data was available for the model skin temperature, the calculated Q_{ls-ms} will be the maximum estimation of heat loss of the model skin.

$$Q_{ls-ms} = (V_{st} \times C_{st} \times \rho_{st}) \times (T_{skin} - T_m) \qquad \text{(Equation F.6)}$$

Where, V_{st} = volume of stainless steel (m^3)

$\quad\quad$ C_{st} = heat capacity of stainless steel (0.5 kJ/kg °C)

$\quad\quad$ ρ_{st} = density of stainless steel (7,990 kg/m^3)

$\quad\quad$ T_{skin} = model skin temperature (°C)

$\quad\quad$ T_m = initial model temperature (20 °C)

The heat loss into the annulus, Q_{ls-an} is calculated with Equation F.7 using the annulus temperature.

$$Q_{ls-an} = (V_{an} \times C_{n2} \times \rho_{n2}) \times (T_{an} - T_m) \qquad \text{(Equation F.7)}$$

Where, V_{an} = volume of annulus (0.144 m^3)

$\quad\quad$ C_{n2} = heat capacity of nitrogen gas (kJ/kg °C)

$\quad\quad\quad$ = 0.98 + 0.000149 (273 + T)

$\quad\quad$ ρ_{n2} = density of nitrogen gas (kg/m^3)

$\quad\quad\quad$ = -0.0512 T + 18.271 (at 1.75 MPa, generated from Jacobsen et al., 1986)

$\quad\quad$ T_{an} = temperature in annulus (°C)

$\quad\quad$ T_m = initial model temperature (20 °C)

300

Q_{ls} is the heat lost mainly through the steam injection and fluid production lines. The heat loss into the annulus, which is filled with nitrogen gas, is neglected because it will be very small due to the low thermal conductivity of nitrogen gas as well as the high efficiency of the insulation board wrapped around the scaled model.

301

Table F.1: Main SAGD experimental data

| Time* (min) | FT100 (kg/hr) | TE201 (oC) | PT201 (kPa) | PT301 (kPa) | PT350 (kPa) | TE300 (oC) | T-skin (oC) | FT301 (kg/hr) | UY301 | Cumulative | | CSOR |
										oil prod (liter)	water inj (liter)	
0	2.00	248.5	1814	1700	1619	203.7	22.0	3.11	0.19	0.00	0.00	0.05
5	2.00	276.6	2093	1639	1623	53.7		5.05	0.00	0.01	0.17	21.99
10	2.00	273.2	1787	1655	1639	61.7	21.9	2.77	0.08	0.03	0.33	13.30
15	1.87	274.1	1807	1683	1640	71.9		2.32	0.19	0.06	0.49	8.26
20	2.00	270.6	1817	1700	1638	73.6	21.5	2.18	0.23	0.10	0.66	6.79
25	1.91	265.2	1814	1686	1636	73.5		2.36	0.21	0.14	0.82	6.02
30	2.01	265.6	1806	1672	1634	73.8	23.5	2.94	0.18	0.18	0.98	5.49
35	1.98	264.5	1800	1684	1629	73.5		1.36	0.18	0.21	1.15	5.44
40	1.84	266.4	1783	1662	1627	74.3	20.3	2.10	0.17	0.24	1.30	5.47
45	2.03	268.1	1805	1686	1648	72.7		2.59	0.16	0.27	1.47	5.52
50	1.93	269.6	1796	1676	1645	74.5	17.8	2.17	0.17	0.30	1.63	5.47
55	2.01	266.1	1803	1680	1651	74.3		2.47	0.17	0.33	1.80	5.50
60	2.01	264.8	1806	1686	1655	74.4	29.4	2.39	0.16	0.36	1.97	5.53
65	2.05	263.6	1808	1687	1658	75.7		2.59	0.17	0.39	2.14	5.50
70	2.04	258.8	1803	1675	1659	76.2	33.0	2.70	0.16	0.42	2.31	5.55
75	1.95	257.0	1825	1700	1667	76.9		2.83	0.18	0.45	2.47	5.50
80	2.01	257.9	1824	1693	1664	78.7	36.0	2.63	0.16	0.48	2.64	5.54
85	2.06	258.5	1823	1700	1675	75.0		2.80	0.15	0.50	2.81	5.64
90	2.07	263.0	1804	1689	1668	78.5	39.0	2.15	0.18	0.53	2.98	5.64
95	1.92	268.3	1821	1696	1674	77.5		2.12	0.17	0.56	3.14	5.61
100	1.92	270.6	1822	1701	1676	78.2	41.8	1.65	0.20	0.58	3.30	5.66
105	1.97	270.0	1824	1701	1678	77.6		2.08	0.19	0.62	3.47	5.63
110	1.93	266.6	1828	1702	1681	78.6	44.5	2.32	0.18	0.65	3.63	5.56
115	2.04	262.2	1831	1702	1683	78.3		2.07	0.18	0.68	3.80	5.54
120	2.00	255.6	1839	1709	1686	81.5	47.1	2.38	0.15	0.71	3.96	5.57
125	2.07	253.8	1842	1709	1688	79.4		2.41	0.17	0.74	4.14	5.58
130	1.98	256.2	1839	1712	1691	80.4	49.5	1.79	0.17	0.77	4.30	5.57
135	2.03	260.2	1839	1725	1693	81.1		1.46	0.20	0.80	4.47	5.60
140	2.03	266.6	1844	1715	1694	81.3	51.9	2.37	0.18	0.83	4.64	5.60
145	2.00	270.0	1858	1732	1697	77.2		2.30	0.21	0.85	4.81	5.63
150	2.05	268.5	1855	1722	1698	80.4	54.2	2.39	0.19	0.89	4.98	5.61
155	2.01	267.1	1859	1723	1701	81.2		2.36	0.15	0.92	5.15	5.59
160	1.98	264.2	1859	1725	1703	81.3	56.3	2.11	0.16	0.95	5.31	5.62
165	2.00	261.7	1853	1746	1705	78.4		0.24	0.24	0.97	5.48	5.66
170	2.13	263.4	1859	1728	1705	82.7	58.3	2.31	0.16	1.00	5.65	5.66
175	1.95	263.6	1869	1739	1709	75.5		2.42	0.16	1.02	5.82	5.68
180	2.09	263.5	1864	1734	1711	82.8	60.2	1.45	0.18	1.06	5.99	5.66
185	1.99	261.5	1866	1732	1712	83.4		2.08	0.16	1.09	6.16	5.66
190	2.06	259.8	1878	1738	1715	82.2	62.0	2.12	0.18	1.12	6.33	5.67
195	2.09	259.4	1875	1740	1716	82.1		2.05	0.18	1.15	6.50	5.67
200	2.05	262.3	1839	1655	1628	104.2	63.7	4.76	0.13	1.19	6.67	5.63
205	2.06	263.5	1903	1780	1749	69.5		0.00	0.00	1.19	6.85	5.77
210	2.00	271.4	1908	1770	1748	75.8	65.3	2.27	0.14	1.22	7.01	5.75
215	1.99	269.8	1892	1760	1741	81.8		2.21	0.14	1.24	7.18	5.77
220	2.02	264.4	1892	1756	1734	82.8	66.8	2.25	0.12	1.27	7.35	5.80
225	2.17	256.4	1882	1748	1728	83.7		2.33	0.11	1.29	7.53	5.84
230	2.15	254.2	1880	1743	1721	83.3	68.3	1.78	0.12	1.31	7.70	5.88
235	2.13	257.6	1874	1734	1713	82.3		1.97	0.13	1.33	7.88	5.92
240	2.06	264.2	1881	1762	1742	75.5	69.7	1.52	0.12	1.35	8.05	5.98
245	1.88	273.5	1894	1755	1734	81.1		2.41	0.12	1.37	8.21	6.00
250	8.84	211.0	1775	1751	1748	102.0	71.0	0.00	0.00	1.40	8.95	6.40
255	8.59	145.3	1995	1834	1805	128.0		7.93	0.05	1.43	9.66	6.75
260	9.98	87.4	2159	1969	1889	106.4	71.9	8.34	0.13	1.50	10.49	6.98

* time: after steam injection into the model

302

Table F.2: Main Fast-SAGD experimental data

Time* (min)	FT100 (kg/hr)	TE201 (oC)	PT201 (kPa)	PT301 (kPa)	PT350 (kPa)	TE300 (oC)	T-annu (oC)	FT301 (kg/hr)	UY301	Cumulative oil prod (liter)	Cumulative water inj (liter)	CSOR
0	2.00	269.6	1796	1632	1605	141.3	24.1	3.30	0.19	0.00	0.00	14.30
5	1.99	273.4	1933	1687	1610	117.7		9.16	0.04	0.02	0.17	8.52
10	2.03	243.5	2292	1666	1605	106.9	21.9	3.71	0.28	0.05	0.33	7.09
15	2.03	226.1	2417	1664	1599	95.8		5.64	0.09	0.06	0.50	7.78
20	1.97	210.6	1767	1618	1603	64.4	25.2	3.25	0.12	0.11	0.67	5.93
25	1.96	210.5	1754	1636	1607	72.4		2.67	0.28	0.16	0.83	5.13
30	1.99	242.5	1788	1658	1618	73.2	25.8	5.19	0.11	0.21	1.00	4.85
35	1.89	243.0	1864	1626	1608	76.9		4.01	0.08	0.23	1.15	5.06
40	1.98	213.6	1847	1636	1613	86.1	26.7	4.06	0.19	0.27	1.32	4.96
45	2.05	210.5	1751	1638	1618	79.4		2.26	0.25	0.30	1.49	4.92
50	2.03	254.9	1750	1642	1621	76.0	26.1	2.68	0.19	0.34	1.66	4.91
55	6.42	224.6	2103	1655	1626	76.5		7.21	0.09	0.38	2.19	5.83
60	6.97	214.6	1913	1672	1625	90.5	25.7	5.59	0.14	0.43	2.78	6.46
65	6.95	216.9	2001	1671	1625	79.3		6.22	0.14	0.51	3.35	6.60
70	2.17	212.1	1816	1667	1628	66.5	26.8	0.23	0.47	0.55	3.54	6.43
75	4.83	212.4	1841	1696	1632	51.3		0.33	0.54	0.55	3.94	7.10
80	7.02	216.5	1982	1668	1634	76.2	28.1	5.34	0.14	0.61	4.52	7.46
85	6.63	216.5	1990	1680	1638	92.4		6.12	0.14	0.68	5.08	7.51
90	6.66	217.1	2015	1680	1638	85.6	29.2	6.01	0.15	0.74	5.63	7.58
95	4.71	218.1	2049	1750	1716	78.5		6.48	0.11	0.81	6.02	7.44
100	6.63	217.6	2036	1706	1676	81.7	29.9	6.47	0.13	0.88	6.58	7.48
105	4.24	213.8	1871	1691	1644	88.1		5.80	0.15	0.96	6.93	7.25
110	4.55	213.3	1856	1639	1611	65.8	30.2	0.41	0.26	0.97	7.31	7.50
115	3.52	214.4	1894	1681	1654	52.0		0.25	0.25	0.98	7.60	7.74
120	3.60	214.6	1903	1696	1660	80.8	31.4	3.87	0.18	1.03	7.90	7.68
125	4.28	214.7	1906	1693	1667	103.8		4.27	0.11	1.08	8.26	7.65
130	5.42	215.1	1938	1661	1668	106.3	31.8	-3.92	-0.05	1.12	8.71	7.79
135	6.67	217.5	2023	1704	1678	102.9		5.66	0.10	1.15	9.27	8.04
140	5.75	217.4	2018	1715	1681	111.3	32.2	6.47	0.07	1.19	9.74	8.19
145	6.02	217.8	2024	1721	1683	103.6		6.61	0.10	1.24	10.25	8.26
150	6.85	218.1	2045	1717	1684	95.6	34.2	6.22	0.11	1.29	10.82	8.36
155	6.13	218.1	1979	1736	1695	79.1		8.12	0.06	1.35	11.33	8.40
160	4.21	211.7	1814	1614	1745	120.4	35.5	0.00	-0.05	1.38	11.68	8.45
165	3.59	218.0	2032	1708	1695	110.4		0.00	-0.05	1.41	11.98	8.49
170	4.42	219.7	2130	1731	1703	105.5	38.2	4.05	0.13	1.45	12.35	8.51
175	3.91	217.2	2009	1732	1707	114.0		5.92	0.09	1.49	12.67	8.49
180	4.11	219.5	2092	1786	1736	103.4	40.8	14.48	0.06	1.51	13.02	8.59
185	4.46	217.2	2011	1724	1699	116.7		5.88	0.03	1.53	13.39	8.76
190	8.99	214.6	1891	1668	1651	73.9	42.3	8.69	0.06	1.53	14.14	9.22
195	7.47	208.3	1808	1753	1733	105.1		7.28	0.03	1.54	14.76	9.60
200	9.50	121.1	1821	1739	1717	110.2	42.0	7.65	0.01	1.53	15.55	10.18

* time: after steam injection into the model

303

Table F.3: Temperature data of the scaled model for contouring

	SAGD				Fast-SAGD			
	CT1 @90 min	CT2 @150 min	CT3 @210 min	CT4 @280 min	CT1 @90 min	CT4 @150 min	CT6 @210 min	CT7 @240 min
TC1-1	21.7	26.6	46.7	68.1	23.2	25.2	30.9	41.9
TC1-2	21.5	27.2	47.9	70.0	n/a			
TC1-3	37.8	101.9	149.0	166.5	22.6	102.1	127.1	138.9
TC1-4	50.9	122.1	159.4	173.3	22.7	137.3	134.8	141.3
TC1-5	141.5	159.6	177.9	188.0	97.0	207.9	210.3	178.3
TC1-6	104.8	136.0	164.8	179.9	133.9	207.8	210.3	183.7
TC1-7	20.0	31.6	52.7	75.3	130.1	140.5	158.9	187.7
TC1-8	n/a				94.0	108.3	133.7	183.2
TC2-1	21.1	25.4	39.5	56.9	22.8	25.1	33.2	44.7
TC2-2	21.0	26.3	42.5	61.1	22.7	25.4	35.7	50.2
TC2-3	34.7	80.0	118.1	137.2	22.4	38.5	127.2	115.5
TC2-4	45.4	97.9	130.4	146.0	23.4	67.5	159.6	138.4
TC2-5	209.4	207.1	208.2	208.4	115.0	124.8	206.0	171.9
TC2-6	n/a				144.1	150.9	207.3	176.8
TC2-7	20.7	28.3	44.6	62.7	107.8	83.0	152.4	163.9
TC2-8	20.9	26.5	40.1	56.5	77.7	67.2	126.0	153.1
TC3-1	21.1	24.5	35.5	49.4	22.6	25.0	32.9	41.2
TC3-2	20.9	25.0	37.6	52.7	22.5	25.6	35.5	45.6
TC3-3	32.1	64.0	93.3	111.1	22.3	64.6	155.6	134.2
TC3-4	40.9	79.4	106.0	121.0	22.6	72.6	161.0	137.8
TC3-5	115.0	131.6	145.1	155.3	95.0	131.6	166.4	142.2
TC3-6	78.9	103.3	122.7	136.7	129.9	154.6	178.2	149.6
TC3-7	20.7	27.0	39.9	54.6	56.8	77.7	144.3	136.2
TC3-8	20.7	25.2	35.9	49.3	43.9	62.9	117.2	122.4
TC4-1	20.8	23.6	32.2	44.0	22.4	24.9	32.5	39.4
TC4-2	20.8	23.9	33.8	46.6	22.3	25.6	35.2	43.5
TC4-3	29.6	54.7	78.0	93.4	22.5	82.4	144.2	132.6
TC4-4	36.5	67.8	89.8	103.3	22.9	90.2	149.8	135.4
TC4-5	130.9	144.8	154.0	159.0	90.7	138.7	168.2	128.2
TC4-6	96.6	116.0	129.7	138.0	125.2	159.7	179.8	133.9
TC4-7	20.6	25.6	35.9	47.8	53.3	72.1	105.7	112.1
TC4-8	20.4	24.2	32.8	43.7	41.6	58.5	86.8	99.0
TC5-1	20.9	23.1	30.1	39.9	n/a			
TC5-2	20.8	23.4	31.4	42.0	22.1	28.6	40.0	48.9
TC5-3	27.2	46.9	65.0	77.8	22.5	89.1	117.8	128.9
TC5-4	32.0	56.8	74.5	86.0	22.8	93.0	123.4	131.7
TC5-5	n/a				58.4	139.1	119.2	104.5
TC5-6	26.7	49.5	66.3	77.7	77.5	133.3	119.1	105.0
TC5-7	20.5	25.2	33.8	43.5	48.0	66.5	84.0	74.3
TC5-8	20.2	23.5	30.7	39.7	n/a			

Table F.4: Heat balance calculation results for the SAGD experiment

Time* (min)	Q_{gn} (kJ)	Q_{md} (kJ)	Q_{ac} (kJ)	Q_{pd} (kJ)	Q_{ls-in} (kJ)	Q_{ls-ms} (kJ)
0	0	0		0	0	0
10	991	507		110	424	0
20	1976	1013		204	847	45
30	2964	1522		335	1274	90
40	3867	1987		430	1664	141
50	4821	2476	586	528	2073	196
60	5809	2986		637	2501	242
70	6808	3503		763	2936	286
80	7789	4012		889	3365	329
90	8806	4537		991	3805	370
100	9752	5022		1068	4211	408
110	10702	5511	952	1178	4621	445
120	11675	6017		1296	5047	481
130	12638	6518		1383	5469	515
140	13638	7033		1499	5901	547
150	14648	7552		1614	6335	577
160	15619	8053		1719	6756	606
170	16663	8592	1355	1835	7209	632
180	17688	9121		1908	7653	659
190	18694	9643		2013	8092	683
200	19697	10161		2319	8527	706
210	20683	10668		2425	8951	727
220	21672	11179		2541	9380	749
230	22715	11722		2634	9837	769
240	23725	12243	1656	2705	10275	783

* time: after steam injection into the model

305

Table F.5: Heat balance calculation results for the Fast-SAGD experiment

Time * (min)	Q_{gn} (kJ)	Q_{md} (kJ)	Q_{ac} (kJ)	Q_{pd} (kJ)	$Q_{ls\text{-}in}$ (kJ)	$Q_{ls\text{-}annu}$ (kJ)
0	0	0		0	0	0
10	952	497		417	429	4
20	1932	995		1107	855	5
30	2896	1504		1446	1116	7
40	3214	1996		1554	1361	8
50	4127	2470	870	1749	1770	9
60	5084	2983		1851	2025	11
70	8128	4294		2197	3144	13
80	11377	5713		2498	4341	15
90	13632	6701		2506	5168	17
100	16740	8055		2850	6311	19
110	18940	9019	1500	3166	7125	21
120	20928	9885		3475	7852	24
130	22578	10603		3482	8456	27
140	24576	11477		3755	9191	30
150	27703	12840		4116	10342	34
160	30532	14071		4542	11381	38
170	33407	15323	2273	4951	12440	42
180	35093	16057		4951	13060	47
190	36926	16857		5372	13735	52
200	39016	17768	2185	5812	14504	58

* time: after steam injection into the model

306

Table F.6: Accumulated heat for the SAGD experiment CT4 (at 240 min after steam injection)

Temp (°C)	So	volume (cm³)				Accumulated heat (kJ)			
		contour	oil	water	matrix	in water	in oil	in matrix	total
25	0.95	0	0	0	0	0	0	0	0
35	0.95	1008	237	12	506	1	6	15	22
45	0.93	2016	541	41	1182	4	24	57	85
55	0.85	1008	283	50	675	7	18	45	70
65	0.70	756	291	125	844	23	24	73	120
75	0.60	1008	200	133	675	30	20	71	121
85	0.50	252	83	83	338	22	10	42	74
95	0.43	252	36	47	169	14	5	24	44
105	0.36	252	30	53	169	18	5	28	51
115	0.32	252	27	57	169	22	5	31	57
125	0.30	252	25	58	169	24	5	34	64
135	0.28	1008	70	180	506	82	16	112	210
145	0.25	252	21	62	169	31	5	41	77
155	0.23	504	38	128	338	68	10	88	166
165	0.22	252	18	65	169	37	5	47	89
175	0.21	504	35	131	338	80	11	100	191
185	0.20	252	17	67	169	43	6	53	102
195	0.20	0	0	0	0	0	0	0	0
205	0.20	252	17	67	169	48	6	60	114
total		10079	1967	1359	6753	555	181	921	1656

307

Table F.7: Accumulated heat for the Fast-SAGD experiment CT7 (at 200 min after steam injection)

Temp (°C)	So	volume (cm³)				Accumulated heat (kJ)			
		contour	oil	water	matrix	in water	in oil	in matrix	total
25	0.95	0	0	0	0	0	0	0	0
35	0.95	1008	316	17	675	1	8	19	29
45	0.93	1512	464	35	1013	4	20	49	73
55	0.90	0	0	0	0	0	0	0	0
65	0.85	0	0	0	0	0	0	0	0
75	0.75	252	62	21	169	5	6	18	29
85	0.68	252	57	27	169	7	7	21	35
95	0.60	252	50	33	169	10	7	24	41
105	0.55	504	91	75	338	26	15	55	96
115	0.50	504	83	83	338	32	15	62	108
125	0.45	756	112	137	506	58	23	102	183
135	0.40	2268	299	449	1519	205	68	335	608
145	0.35	756	87	162	506	80	22	122	223
155	0.30	252	25	58	169	31	7	44	82
165	0.27	252	22	61	169	35	7	47	88
175	0.23	756	57	192	506	117	18	151	285
185	0.21	756	52	197	506	127	18	160	305
195	0.20	0	0	0	0	0	0	0	0
205	0.20	0	0	0	0	0	0	0	0
total		10079	1779	1547	6753	737	240	1209	2185

308